Distributed Space-Time Block Coding in Cooperative Relay Networks with Application in Cognitive Radio

by

Faisal Thear Alotaibi

A Doctoral Thesis

Submitted in partial fulfilment of the requirements for the award of the degree of Doctor of Philosophy of Loughborough University

September 2012

Advanced Signal Processing Group
School of Electronic, Electrical and System Engineering
Loughborough University

Abstract

Spatial diversity is an effective technique to combat the effects of severe fading in wireless environments. Recently, cooperative communications has emerged as an attractive communications paradigm that can introduce a new form of spatial diversity which is known as cooperative diversity, that can enhance system reliability without sacrificing the scarce bandwidth resource or consuming more transmit power. It enables single-antenna terminals in a wireless relay network to share their antennas to form a virtual antenna array on the basis of their distributed locations. As such, the same diversity gains as in multi-input multi-output systems can be achieved without requiring multiple-antenna terminals.

In this thesis, a new approach to cooperative communications via distributed extended orthogonal space-time block coding (D-EO-STBC) based on limited partial feedback is proposed for cooperative relay networks with three and four relay nodes and then generalized for an arbitrary number of relay nodes. This scheme can achieve full cooperative diversity and full transmission rate in addition to array gain, and it has certain properties that make it alluring for practical systems such as orthogonality, flexibility, low computational complexity and decoding delay, and high robustness to node failure. Versions of the closed-loop D-EO-STBC scheme based on cooperative orthogonal frequency division multiplexing type transmission are also proposed for both flat and frequency-selective fading channels which can overcome imperfect synchronization in the network. As such, this proposed technique

can effectively cope with the effects of fading and timing errors. Moreover, to increase the end-to-end data rate, this scheme is extended for two-way relay networks through a three-time slot framework. On the other hand, to substantially reduce the feedback channel overhead, limited feedback approaches based on parameter quantization are proposed. In particular, an optimal one-bit partial feedback approach is proposed for the generalized D-EO-STBC scheme to maximize the array gain. To further enhance the end-to-end bit error rate performance of the cooperative relay system, a relay selection scheme based on D-EO-STBC is then proposed. Finally, to highlight the utility of the proposed D-EO-STBC scheme, an application to cognitive radio is studied.

I dedicate this thesis to

my parents, Thear and Najla,

my wife, Sultanah,

my son and daughter, Abdulaziz and Najla,

and my brother and sisters, Sultan, Abeer, Fauziah, Sultanah and Maram

Statement of Originality

The novelty of the work in this thesis can be summarized as follows: The contribution of Chapter 3 is a new low-complexity scheme for cooperative relay networks equipped with three or four relay nodes which is called the distributed extended orthogonal space-time block code (D-EO-STBC) scheme. The contributions within Chapter 4 are related to the extension of the D-EO-STBC scheme for operation with imperfect synchronization and over frequency-selective channels scenarios; new low-complexity feedback approaches; and a novel two-way cooperative transmission scheme based on D-EO-STBC. The contributions of Chapter 5 are new relay selection approaches based on the D-EO-STBC and the distributed Alamouti code. The contribution of Chapter 6 is the generalized D-EO-STBC approach; and for Chapter 7 the proposed application of D-EO-STBC within a cognitive radio system. The novelty of the work is supported by the following publications:

1. F. T. Alotaibi and J. A. Chambers, 'Extended Orthogonal Space-Time Block Code in Wireless Relay Networks', in Proc. IEEE Workshop SSP 2009, pp. 745-748, Cardiff, United Kingdom, Aug. 2009.

2. F. T. Alotaibi and J. A. Chambers, 'Robust Orthogonal Space-Time Block Coding Scheme for Use in Asynchronous Cooperative Relay Networks' in Proc. IEEE UKIWCWS 2009, pp. 1-4, Delhi, India, Dec. 2009.

3. F. T. Alotaibi and J. A. Chambers, 'Full-Rate and Full-Diversity Extended Orthogonal Space-Time Block Coding in Cooperative Relay

Networks with Imperfect Synchronization', in Proc. IEEE ICASSP 2010, pp. 2882-2885, Dallas, USA, Mar. 2010.

4. F. T. Alotaibi and J. A. Chambers, 'Extended Orthogonal Space-Time Block Coding Scheme for Asynchronous Cooperative Relay Networks over Frequency-Selective Channels', in Proc. IEEE SPAWC 2010, pp. 1-5, Marrakech, Morocco, Jun. 2010.

5. F. T. Alotaibi and J. A. Chambers, 'Relay Selection Scheme for Cooperative Relay Networks with Distributed Orthogonal Space-Time Block Coding', in Proc. IEEE UKIWCWS 2010, pp. 1-5, Delhi, India, Dec. 2010.

6. F. T. Alotaibi, F. Abdurahman, U. Mannai, and J. A. Chambers, 'Extended Orthogonal Space-Time Block Coding Scheme in Asynchronous Two-Way Cooperative Relay Networks over Frequency-Selective Fading Channels', in Proc. IEEE DSP 2011, pp. 1-5, Corfu, Greece, Jul. 2011.

7. F. T. Alotaibi and J. A. Chambers, 'Generalized Extended Orthogonal Space-Time Block Coding Schemes to Exploit Cooperative Diversity', submitted to IET Communication.

8. F. T. Alotaibi and J. A. Chambers, 'Outage Probability of Cooperative Cognitive Networks based on Distributed Orthogonal Space-Time Block Codes', accepted for publication in IEEE Trans. Vehicular Tech., Jun 2012.

Acknowledgements

First and foremost, I thank Allah Almighty for all His countless favours and guidance. Then, I would like to express my gratitude to my supervisor Prof. Jonathon Chambers for his continuous support and interest in my research. He provided support regardless of time and place. I am grateful to him for providing me with great motivation, enthusiasm, technical insight and encouragement during my PhD study. This work would not have been possible without his able guidance. I wish that I will have more opportunities to work with him in the future.

Also, I would like to thank my sponsor: the General Directorate of Telecommunications at the Ministry of Interior in Saudi Arabia for the scholarship to obtain PhD in communications engineering.

I am also grateful to all my friends in the Advanced Signal Processing Group for providing a stable and cooperative environment within the Advanced Signal Processing Group.

Finally, I really cannot find appropriate words or phrases to express my sincere heartfelt thanks, appreciations and gratefulness to all my family members, especially my grandfather, Dhawi, my father, Thear, and my mother, Najla, for their endless love, prayers, attention, constant encouragement and their support in innumerable ways throughout my PhD and before. I am really proud of all of them. May Allah save them and extend their ages with enjoying health and happiness.

Alotaibi, Faisal T.

June 2012

Contents

List of Acronyms

AF	Amplify-and-Forward
ADSL	Asymmetric Digital Subscriber Line
AWGN	Additive White Gaussian Noise
BER	Bit Error Rate
CDF	Cumulative Distribution Function
CDMA	Code-Division Multiple Access
CIR	Channel Impulse Response
CP	Cyclic Prefix
CSI	Channel State Information
DF	Decode-and-Forward
DFT	Discrete Fourier Transform
D-Alamouti	Distributed Alamouti
D-STBC	Distributed Space-Time Block Code
D-STC	Distributed Space-Time Code
DMT	Diversity-Multiplexing Tradeoff
DVB	Digital Video Broadcasting

FFT	Fast Fourier Transform
IDFT	Inverse Discrete Fourier Transform
IEEE	Institute of Electrical and Electronics Engineers
IFFT	Inverse Fast Fourier Transform
ISI	Inter-Symbol Interference
LTE	Long Term Evolution
MIMO	Multiple-Input Multiple-Output
ML	Maximum-Likelihood
OFDM	Orthogonal Frequency Division Multiplexing
PDF	Probability Density Function
PEP	Pairwise Error Probability
QPSK	Quadrature Phase-Shift Keying
SISO	Single-Input Single-Output
SNR	Signal-to-Noise Ratio
STBC	Space-Time Block Code
STC	Space-Time Code
STD	Space-Time Division
STTC	Space-Time Trellis Code
SVD	Singular Value Decomposition
TAS	Transmit Antenna Selection
TD	Time Division

TDMA	Time-Division Multiple Access
WCDMA	Wideband Code-Division Multiple Access
Wi-Fi	Wireless Fidelity
WiMAX	Worldwide Interoperability for Microwave Access
dB	Decibel
i.e.	'that is', 'in other words'
i.i.d.	Independent Identically Distributed
4G	4th Generation
3GPP	3rd Generation Partnership Project

List of Symbols

$\angle(.)$	Angle operator
$(\cdot)^*$	Complex conjugate
DFT(.)	Discrete Fourier transform operator
$\|.\|$	Euclidean distance
(.)!	Factorial operator
FFT(.)	Fast Fourier transform operator
$\|.\|_{\mathcal{F}}$	Frobenius norm
$\circ$	Hadamard product
$(\cdot)^H$	Hermitian transpose
IDFT(.)	Inverse discrete Fourier transform operator
IFFT(.)	Inverse fast Fourier transform operator
$\otimes$	Linear convolution operator
max(.)	Maximum value
min(.)	Minimum value
mod(.)	Modulo operator
Re{·}	Real part

$\mathrm{E}\{\cdot\}$	Statistical expectation
$\|.\|^2$	Squared modulus of a complex number
$\xi(.)$	Time-reversal operator
arg max	The argument which maximizes the expression
arg min	The argument which minimizes the expression
$(\cdot)^T$	Transpose operator
$\mathbf{I}_K$	$K \times K$ Identity matrix
$\mathbf{P}(.)$	The $N \times N$ reversed cyclic shift matrix
$\mathbf{Q}$	Normalized $N \times N$ DFT matrix
$\mathbf{Q}^*$	Normalized $N \times N$ IDFT matrix

List of Figures

List of Tables

Chapter 1

INTRODUCTION

Cooperative relay communications has recently gained much attention in academic and industrial advanced wireless research centers across the globe due to its potential to enable efficient solutions for challenging problems in wireless communications. In fact, this technique can through distributed transmission achieve the same diversity gain benefits of conventional point-to-point multiple-input multiple-output (MIMO) systems without requiring multiple-antenna terminals at a single terminal. In this chapter, conventional MIMO systems will firstly be presented and their main advantages and disadvantages will be highlighted. Then, the basic concepts and system features of cooperative relay systems will be introduced in detail. Moreover, various network architectures and transmission relaying protocols will be described.

The most common and efficient coding techniques to exploit spatial diversity within MIMO systems are space-time codes (STCs) which are also the origin for distributed STCs. A brief background for STCs is introduced and the milestone works in this field are described. Cooperative relays can also be exploited in cognitive radio, therefore, a quick introduction to this field and cooperative cognitive networks in particular is included.

1.1 Conventional MIMO Systems

In the past few decades, wireless communication technologies have witnessed an exponential growth and have become part of nowadays wireless applica-

tions. An important technology for wireless networks is multiple antenna systems which are also known as MIMO systems due to their ability to increase the system reliability and capacity without requiring additional bandwidth or transmit power [1]. The benefits of using multiple antennas result in MIMO wireless technology being exploited in many wireless communication standards such as the Wi-Fi (IEEE 802.11) standard, the WiMAX (IEEE 802.16) standard, and are a major focus for 4th generation (4G) and long-term evolution (LTE) cellular systems [2].

The three main advantages of a point-to-point MIMO system are multiplexing gain, diversity gain and array gain [1] and [2]. A MIMO system can offer linear increase in the capacity or transmission data rates proportional to the number of transmit-receive antennas pairs or the minimum number of transmit or receive antennas when the channels between all antennas are uncorrelated [3], [4] and [5], i.e. multiplexing gain. On the other hand, MIMO systems have the ability to obtain high diversity gain. Diversity gain is equal to the number of independent channels in the multiple antennas system [1]. The diversity gain indicates how fast the probability of error decreases with an increase in the signal strength [6]. Finally, MIMO systems can achieve an array gain which means the average increase in signal to noise ratio at the receiver [1]. The average increase in signal power is proportional to the number of receive antennas.

However, the requirement of multiple-antenna terminals increases the system complexity and the separation between the antennas increases the terminal size. Also, MIMO systems suffer from the effect of path loss and shadowing, where the path loss is referred to the signal attenuation between the source and destination nodes due to propagation distance, while the shadowing is the signal fading due to objects obstructing the propagation path between the source and destination nodes [7]. These different problems limit MIMO systems functionality and applicability which challenge

researchers to look for another innovative technology, and hence cooperative communications has emerged as a new paradigm that can offer effective solutions for the aforementioned problems.

1.2 Cooperative Relay Systems

Unlike traditional point-to-point MIMO systems, a cooperative relay system allows different nodes in a wireless network to share their antennas based on cooperation protocols [8] and [9]. Such cooperative nodes can be regarded as a distributed antenna array (i.e. virtual MIMO) where each node becomes part of this virtual array. This new communication paradigm has become a powerful technique that can achieve the same gain benefits of MIMO systems whilst avoiding some of their drawbacks. In fact, it promises significant improvements in the system reliability and capacity and in service coverage without additional bandwidth or transmit power [10]. It has recently been adopted for different new wireless systems such as 3GPP LTE-Advanced [11]. Also, it has been considered in different wireless system standards such as WiMAX standards (IEEE 802.16j and IEEE 802.16m) [12] and Wi-Fi standards (IEEE 802.11s and IEEE 802.11n) [13] and [14]. This new technology has been underpinned by Laneman's contributions in this area in 2000 and beyond [8] and [15] which specifically introduced different relaying protocols and proved that significant system performance and outage gains can be achieved.

A key feature of a cooperative relay system is its ability to obtain high spatial diversity gain. In fact, a cooperative relay system achieves a new form of spatial diversity which is known as cooperative diversity. This feature provides the ability to overcome the detrimental effects of severe fading in the wireless channel [8]. Thus by having several intermediate relays between the source and destination that forward copies of the same information in parallel

via independent channels with or without the information received from the direct path, will result in diversity gain. This gain comes from the fact that as the number of independent paths carrying the same information between the source and destination increases, the probability of all of them being in fade decreases [15], [16]. Therefore, diversity gain can be computed as the number of independent channels in the cooperative relay system, which depends on the number of the relay nodes and the environment [16]. So, in a frequency-flat channel, the maximum diversity gain equals $G_d = N_s \times N_r \times N_d$ where N_s, N_r and N_d are the number of single-antenna source nodes, relay nodes and destination nodes, respectively. In this thesis, N_s and N_d are unity. Increased diversity gain leads to improvements in the system performance such as the probability of error P_e or the outage probability P_{out}. The diversity gain indicates how fast the probability of error decreases with an increase in the signal strength typically measured by signal-to-noise ratio (SNR) [1], [6]. The diversity gain or diversity order, G_d, in terms of error probability is given by [7]

$$G_d = -\lim_{\mathrm{SNR}\to\infty} \frac{\log(P_e(\mathrm{SNR}))}{\log(\mathrm{SNR})} \tag{1.2.1}$$

The diversity gain, G_d, in terms of outage probability is given by [16]

$$G_d = -\lim_{\mathrm{SNR}\to\infty} \frac{\log(P_{out}(R))}{\log(\mathrm{SNR})} \tag{1.2.2}$$

where $\mathrm{P}_{out}(R)$ denotes the probability that the instantaneous system capacity R is lower than a particular transmission rate threshold R_{th} such that

$$\mathrm{P}_{out}(R) = \Pr\{R < R_{th}\} \tag{1.2.3}$$

Furthermore, cooperative relay systems provide the possibility to spatially multiplex the wireless communication system and thereby allow independent

data streams to be transmitted in parallel which result in improving capacity or transmission data rates. For example, for a source with one antenna and a destination with two antennas, using a single relay in addition to the direct path will establish another independent channel which results in doubling the multiplexing gain and hence doubling the transmission data rate if the SNR is kept constant [16]. The multiplexing gain, G_r, effectively equals the number of independent channels over which different information can be transmitted. The multiplexing gain as a function of SNR is given by

$$G_r = \lim_{\mathrm{SNR}\to\infty} \frac{R(\mathrm{SNR})}{\log(\mathrm{SNR})} \tag{1.2.4}$$

While the transmission rate of the system, R, at a given SNR can be computed by [7]

$$R = G_r \log_2(1 + \mathrm{SNR}) \tag{1.2.5}$$

In the literature, there are many cooperative schemes that were proposed for exploiting the multiplexing gain or the diversity gain among the available cooperative relay nodes. However, this thesis is focusing on diversity gain rather than multiplexing gain.

On the other hand, it is known that the wireless channel generally suffers from three fundamental problems which are fading, shadowing effects and pathloss attenuation [16]. Although the conventional point-to-point MIMO systems can efficiently mitigate the effects of fading in the wireless channel, they suffer unfavourably from the other two problems, i.e. shadowing effects and pathloss attenuation [17]. Both of them limit the transmission rate and service coverage for a wireless MIMO network. Fortunately, these shortcomings in MIMO networks can be effectively resolved by using cooperative relay networks. Cooperative strategies can significantly diminish the losses connected with the wireless channel by creating cooperative diversity and using different independent paths between the source and destination

nodes which can help in avoiding the shadowing problem. Also, using intermediate relay nodes helps in avoiding the pathloss problem because dividing the propagation path between the source and destination nodes into at least two parts yields transmit power gains because the total resultant pathloss of part of the whole path is less than the pathloss of the whole path [16]. This advantage of the cooperative relay network can be referred to as pathloss gain. It is known theoretically that the SNR is inversely proportional to the signal propagation distance, d, as given by [16]

$$\text{SNR} \propto \frac{1}{d^n} \ , \tag{1.2.6}$$

where d is the distance between the source and destination nodes and n is the pathloss exponent which typically fluctuates between 2 and 6 based on the type of the propagation environment. According to this relation, a cooperative relay system where the intermediate relay is half way between the source and destination and the power is divided equally between the source and the relay will result in the following gain as compared to the conventional point-to-point system

$$G_p = \frac{\frac{1/2}{(d/2)^n} + \frac{1/2}{(d/2)^n}}{\frac{1}{d^n}} = 2^n \ , \tag{1.2.7}$$

which means the cooperative system can achieve a transmit power saving of $(10 \log_{10} 2^n)$ dB. In fact, the power gains due to cooperative diversity and pathloss gain can be exploited to improve the system data rate R by increasing the cardinality of the signal constellation [16]. Therefore, cooperative relay systems potentially offer remarkable advantages for wireless communications [15], [16] and [18] in terms of the following:

1. High system reliability: A cooperative relay system can be extremely effective to combat the effects of channel fading by cooperative diver-

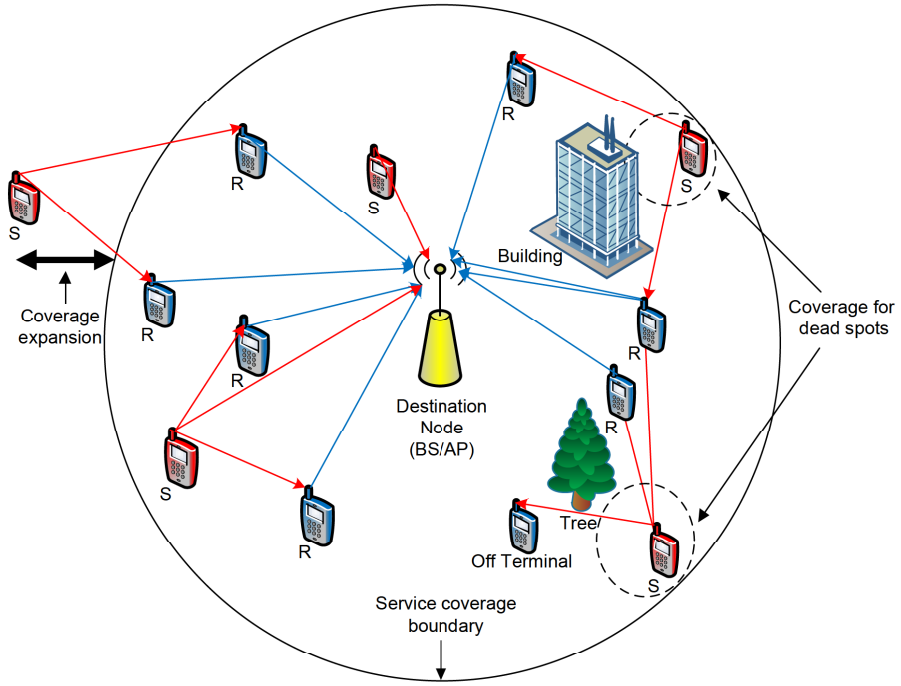

Figure 1.1. Service coverage and reliability of a cooperative relay system.

sity [15]. Also, it can effectively enhance the transmission robustness by guaranteeing the transmission between the source and destination even if the direct link is in fade or several of the system relays are off or lost as shown in Fig. 1.1.

2. High system coverage: The cooperative relay system can effectively expand the network coverage through the relaying capability. So, the transmitted signal can travel longer as compared to point-to-point systems. Also, it can expand the network coverage by covering dead holes or spots in the network such as shadowed terminals as shown in Fig. 1.1.

3. Increasing data rate: The cooperative system can effectively increase the system data rate through exploiting its multiplexing capability or by exploiting the power gains due to diversity and pathloss gains in increasing the cardinality of the signal constellation [16].

4. Interference mitigation: A cooperative relay system can exploit the cooperative diversity to overcome the effects of interference [16], [18], [19]. Also, it can exploit power gains to reduce the required transmit power which results in alleviating interference. Moreover, it can exploit an appropriate power allocation to control the transmit power. Furthermore, it can utilize an appropriate relay selection technique to avoid interference.

Next, different relay network architectures and transmission relaying protocols are considered.

1.3 Cooperative Relay Network Architectures and Transmission Relaying Protocols

A cooperative relay system consists basically of three parts which are the source node, relay nodes and destination node where the source broadcasts its information via one or a number of intermediate relays along with the direct source to destination transmission or without it. The destination combines the received multiple independent copies of the signal which results in cooperative diversity. So, the network architecture can typically be divided into two models which are a single-relay with direct-link transmission model and a multiple-relay transmission model [18]. In the following, the two cooperative relay network models will be described.

1. A single-relay with direct-link transmission model: In this model, the source node obtains benefits from the available single relay to convey

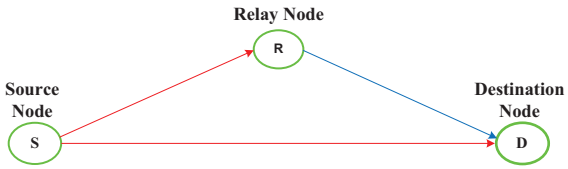

Figure 1.2. A single-relay with direct-link transmission model.

its information to the destination node in addition to the direct-link between the source and the destination which allows cooperative diversity as shown in Fig. 1.2. In fact, this model can achieve a maximum order-two cooperative diversity. This model requires two phases or two hops to complete the whole transmission. In the first phase, the source node broadcasts its information to the relay node and to the destination while in the second phase, the relay node relays its received signals to the destination. These two phases should be orthogonal to avoid detrimental interference through transmission [18].

2. A multiple-relay transmission model: In this model, the source node might send its information to the destination via a two-hop or multi-hop protocol with direct-link transmission or without it according to the network topology and direct-link transmission availability. So, this model can be categorized as follows [18]:

   (a) Serial topology with direct-link transmission: In this model, the multiple relays are connected in serial and hence the information received from the source should be transferred from one another in a multi-hop transmission to arrive at the destination node in addition to the direct-link transmission as shown in Fig. 1.3(a). The maximum spatial cooperative diversity order which can be

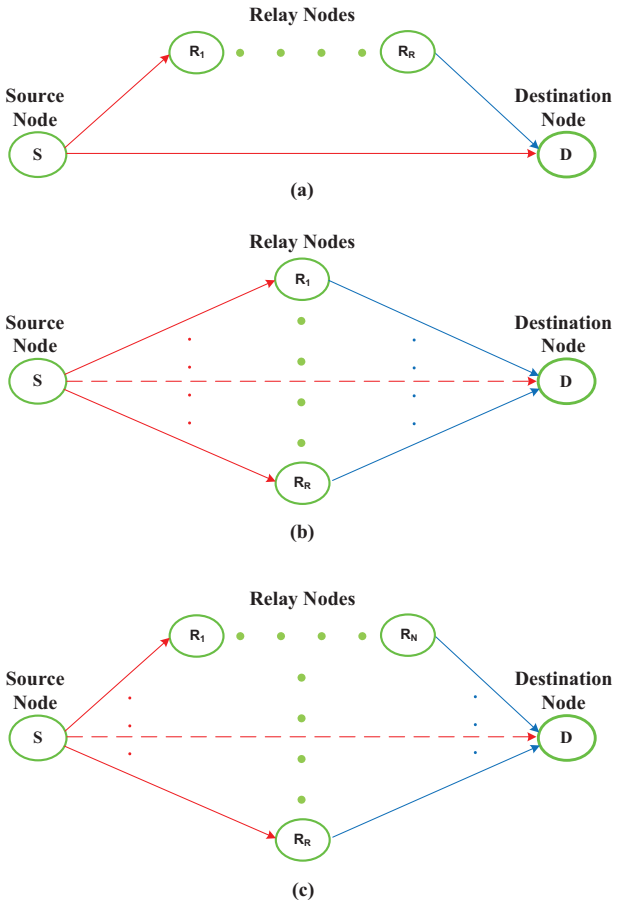

Figure 1.3. A multiple-relay transmission model (dash line pattern for direct link means it might be available or not available). (a) Serial topology with direct-link transmission. (b) Parallel topology. (c) Hybrid topology.

attained is two.

(b) Parallel topology: In this model, the system consists of parallel paths between the source and destination and each path passes through one relay so the transmission through relay nodes requires only two hops as shown in Fig. 1.3(b). This model might include direct-link transmission or not. This model can offer several features such as a high order cooperative diversity equal

to the number of available relay nodes plus one if the direct-link transmission is available, short-time transmission (only two-hops), ability to exploit the network resource efficiently, a way to extend the system coverage and a solution to the pathloss and shadowing effects.

(c) Hybrid topology: This model combines between the serial topology and the parallel topology as shown in Fig. 1.3(c). This model provides increased system complexity and decreased cooperative diversity as compared with the parallel topology.

In this thesis, the parallel cooperative relay model without direct-link is adopted, as shown in Fig. 1.3(b), in which the whole transmission requires only two hops or phases. In the first phase, which is named in this thesis as the broadcasting phase, the source node broadcasts its information signals to R number of relays, R_i; $i = 1, 2, ..., R$. In the second phase, which is named in this thesis as the relaying phase or cooperation phase, the relays in turn forward the processed signals towards the destination.

The relay nodes should be applied to an orthogonal transmission technique such as time-division multiple access (TDMA), code-division multiple access (CDMA) or space-time code (STC) to avoid interference between transmission. The relay nodes might operate in a full-duplex mode which can transmit and receive simultaneously at the same time or in a half-duplex mode wherein only transmission or reception can be performed at one time. However, to reduce hardware complexity, only half-duplex relays employing STC techniques are considered in this thesis.

Currently, several transmission relaying protocols have been proposed and can be generally divided into two main protocols: amplify-and-forward (AF) and decode-and-forward (DF) protocols [18]. In an AF protocol, the relay simply amplifies the received signal by an amplification factor and

forwards it to the destination. The amplification process is performed to combat the effect of channel fading between the source and relay [18]. The amplification factor which is also known as relaying gain is inversely proportional to the received power at the relay nodes and can be classified into two types which are variable relaying gain and fixed relaying gain [16], [18] and [20]. In a variable relaying gain type, the amplification factor is calculated based on the instantaneous channel state information (CSI) between the source and relay node, h_{SR_i}, [18] which can be expressed as

$$A_{VG} = \sqrt{\frac{P_r}{P_s|h_{SR_i}|^2 + N_0}} \tag{1.3.1}$$

where P_s is the average transmit power at the source node, P_r is the average transmit power at each relay node and N_0 is the additive white Gaussian noise (AWGN) variance at each relay node. On the other hand, a fixed relaying gain type does not need instantaneous CSI of the source-to-relay channel and instead it employs average values of channel gains [18] as follows

$$A_{FG} = \sqrt{\frac{P_r}{P_s E\{|h_{SR_i}|^2\} + N_0}} \tag{1.3.2}$$

where E{.} is the statistical expectation operator.

In practice, the AF scheme is more attractive due to its simplicity and low cost implementation since the relay nodes do not need to decode the received signals or perform any signal processing. However, in this protocol, the noise is also amplified which results in some performance degradation. In a DF protocol, the relay attempts to decode the received signals. If successful, signals will be forwarded after the encoding process. Otherwise, the signal will not be forwarded. So, this protocol has the capability to eliminate the noise from the received signal before transmitting it which represents the main advantage of the DF protocol. However, this protocol increases the system complexity and its performance is subjected to the decoding process

which might be incorrect. Particularly, it may not be realistic for the random relay node to decode the incoming signal from the source node, because the codebook is rarely available in most cases [21].

1.4 Space-Time Codes

Space-time coding (STC) [22] and [23] is an effective coding technique for conventional MIMO systems that has the potential to significantly exploit the MIMO offered gains. In the literature, there are many STC schemes which have been proposed. In particular, STCs can be categorized into two types based on the transmission structure of the signal symbols over the wireless channel which are space-time trellis codes (STTCs) and space-time block codes (STBCs). In STTCs, serial transmission of symbols is performed while block transmission of symbols is performed in STBCs. The STTCs were proposed by Tarokh, in [22], for two or four transmit antennas and provide a significant improvement in system performance due to diversity and coding gain especially in a slow-fading environment. However, they exhibit high system complexity. The STTCs system requires the Viterbi algorithm to be employed at the receiver for decoding the information symbols. The decoding complexity of STTC is measured by the number of trellis states at the decoder. In fact, the decoding complexity increases exponentially with transmission rate of the system [24].

On the contrary, STBCs are the most popular and attractive STC type for point-to-point MIMO systems due to their low decoding complexity. Different STBC schemes have been proposed in the last two decades for exploiting the spatial multiplexing or spatial diversity of MIMO systems. The most famous spatial multiplexing schemes are Bell laboratories layered space-time (BLAST) which was proposed by Foschini [3] and vertical BLAST (V-BLAST) which was introduced by Wolniansky and his coworkers [25]. In

fact, the V-BLAST scheme is an extension of the BLAST scheme that can be classified as the best STBC scheme in terms of multiplexing gain. On the other hand, the first space-time block code scheme using transmit diversity was proposed by Alamouti [23] which is designed for two transmit antennas. This scheme is significantly less complex than STTC for the same antenna configuration. The key feature of this scheme is the orthogonality property which results in very low decoder complexity. In fact, this scheme can be classified as the best STBC scheme in terms of diversity gain due to its ability to achieve full diversity from complex designs.

The excellent performance of the Alamouti code motivated Tarokh and his coworkers [26] to propose orthogonal STBCs (O-STBCs) for more than two transmit antennas which can achieve full diversity gain but at the expense of transmission data rate. In [26], the maximum data rate of complex orthogonal STBCs (O-STBCs), which achieve full diversity gain, was 3/4 for three and four transmit antennas and 1/2 for higher number of transmit antennas. On the contrary, a quasi-orthogonal STBC (QO-STBC) which was proposed in [27] for four transmit antennas achieves full data rate at the expense of loss in diversity gain and increasing the decoding complexity. In order to improve the system performance in terms of the bit error rate, variable-rate STBCs combined with an optimum power allocation scheme have been proposed for two, three and four transmit antenna systems [28].

However, the aforementioned schemes for more than two transmit antennas can not achieve full diversity and full rate at the same time. In fact, the only complex STBC scheme that achieves full data rate and full diversity gain was Alamouti's scheme as proved in [22] and [26]. So, much effort has been spent on developing the O-STBC or QO-STBC schemes for more than two antennas that can achieve full data rate and full diversity such as [29], [30], [31], [32], [33], [34], [35], and [36]. For example, from orthogonal designs, the group-coherent STBC (GC-STBC) scheme was proposed for

more than two transmit antennas [31] and the extended orthogonal STBC (EO-STBC) scheme was proposed for three and four transmit antennas [29]. Based on limited feedback, both of them can achieve full rate and full diversity with array gain. On the other hand, from quasi-orthogonal designs, the QO-STBC scheme which is also known as a generalized ABBA (GABBA) code in combination with a multi-group maximum-likelihood (ML) decoder was proposed for any number of transmit antennas [34], while a constellation rotation based QO-STBC scheme was proposed for any number of transmit antennas in [35]. Both of them can achieve full diversity and data rate but they also exhibited either long decoding delay or high system complexity.

The aforementioned schemes employed either an open-loop strategy or a closed-loop strategy where each strategy has a performance penalty. The open-loop strategy does not involve any feedback channels. However, this strategy introduces more system complexity due to the requirement of sophisticated signal processing on the source, relay nodes and destination such as signaling constellation rotation. On the contrary, the closed-loop strategy uses a feedback channel but the system complexity can be much less than that in the open-loop strategy because the relay nodes only require simple signal operations to exploit the feedback information. The closed-loop strategy also offers an array gain which provides further improvements in the system performance but at the expense of a small amount of feedback bandwidth.

In essence, STBC schemes exhibit excellent performance for MIMO systems with relatively low system complexity. Fortunately, they can be extended to cooperative relay systems in a distributed manner to form distributed STBC (D-STBC) schemes [8], [9] and [37]. In fact, the same gain benefits as in point-to-point MIMO systems can be extracted in addition to overcoming the drawback of point-to-point MIMO systems. In the next chapter, the state of the art works for D-STBC schemes as an efficient way

of exploiting cooperative diversity will be presented.

1.5 Cognitive Radio

The explosive growth in research for wireless communication systems in recent years has generated new wireless applications which result in increasing the demand for more radio spectrum. Most suitable frequency bands for wireless communications, i.e. below 3GHz, have already been assigned under the licensed bands for the existing wireless systems which result in increasing the complexity and difficulty to find available frequency bands for new wireless systems. Furthermore, spectrum allocation policy is inflexible to allow sharing of the licensed bands although several field measurements performed from leading spectrum regulatory commissions, such as the Federal Communications Commission (FCC) in the United States [38] or Ofcom in the United Kingdom [39], verified that there are licensed bands unoccupied most of time or partially occupied. Therefore, there are spectrum holes or white bands in certain time, frequency, and positions which result in reducing the spectrum efficiency.

These challenging problems of spectrum inefficiency motivated researchers to find efficient solutions which result in the concept of cognitive radio. It is a new communication paradigm that can effectively exploit the existence of spectrum holes by enabling unlicensed users to intelligently utilize these spectrum holes without causing harmful interference to the licensed users (primary users). Originally, the concept of cognitive radio is to sense the spectrum in order to find the unoccupied bands and then utilize them wisely at a certain time [40]. This concept has recently been developed to be fully aware of the surrounding environment and the primary users, and thereby further improve the efficiency of spectrum utilization [41]. Recently, several IEEE 802 standards for wireless systems have considered cognitive radio

systems such as IEEE 802.22 standard [42] and IEEE 802.18 standard [43].

In particular, the functions of cognitive radio can be categorized into three main functions which are spectrum sensing, spectrum sharing and spectrum management [18]. There are different approaches for spectrum sensing that have been proposed in the literature [41], [44] and [45]. However, the most common approaches are power energy detection, matched filtering detection, spectrum estimation and cyclostationary feature detection. On the other hand, there are three main spectrum sharing approaches which are underlay, overlay and interweave cognitive approaches [46]. In an underlay approach, cognitive users are allowed to access the spectrum at any time if the interference caused to primary users is below an acceptable limit. In an overlay approach, cognitive users forward the primary users traffic in addition to their own traffic provided that they do not cause undue interference to the primary users through exploiting interference cancelation techniques. In an interweave approach, cognitive users are opportunistically accessing the spectrum holes without causing interference to the primary users.

Cooperative communications has been proposed recently as an efficient approach for cognitive radio to improve substantially the performance of cognitive radio systems in terms of spectrum sensing and spectrum sharing. By this approach, cognitive users can cooperate with each other to sense the spectrum and detect the unused bands [47] and cooperate with each other to relay their traffic or primary users traffic and thereby promote the behaviour of cognitive radios [48]. In particular, the cooperative communications technique improves the ability of spectrum sensing by overcoming the problem of the hidden terminal and shadow effects, and helping in the detection process of unoccupied spectrum which results in minimizing the probability of false alarms and increasing the opportunity to utilize the spectrum for transmission. From the sharing spectrum side, the coopera-

tive communications technique improves the system reliability, transmission rate and spectrum efficiency. This combination of cooperative communications and cognitive radio techniques will enjoy the advantages offered from both techniques which potentially results in improving the service reliability, capacity and coverage extension.

At the end of this thesis, the combination between a cooperative relay network and cognitive radio where the intermediate relay nodes are equipped with cognitive radios will be presented. This network will be referred to as a cooperative cognitive relay network considering spectrum sharing and transmission robustness.

1.6 Challenges and Thesis Contributions

There are four main challenging problems related to conventional point-to-point MIMO systems. These are high system complexity due to the requirement of multiple antennas; large terminal size due to the requirement of positioning the multiple antennas apart from each other by a distance of at least half of the carrier frequency wave length, i.e. $\lambda/2$, otherwise the problem of correlated channels will affect adversely the system performance; signal attenuation due to path loss; and lastly severe fading due to shadowing. This thesis addresses the aforementioned challenging problems by exploiting different single-antenna terminals within a wireless network to cooperatively form a virtual antenna array that can achieve the same diversity gain benefits as a conventional MIMO systems. As such, the separation distance will no longer be an issue and the cooperative terminals are equipped with only a single antenna. Also, the relaying capability and the distributed nature of this cooperative relay system can cope with the effects of path loss and shadowing.

In fact, this potential solution has been adopted in the literature through

many different cooperative diversity schemes [16]. However, the existing schemes either lack the ability to achieve full cooperative diversity and full rate at the same time, for example, [49]; or they exhibit high computational complexity or high decoding delay, for example, [50] and [51]. The schemes with increased decoding delay require a very slow fading environment. The only low-complexity scheme that can achieve full diversity and full rate at the same time, and uses a very simple symbol-wise maximum-likelihood (ML) decoder is the distributed Alamouti code (D-Alamouti) [52]. However, the shortcoming of this scheme is that the scheme is designed for only two relay nodes. However, increasing the number of independent paths between the source and the destination nodes in a wireless relay network through increasing the number of relay nodes can give extra diversity performance. To enjoy increased diversity gain and preserve the same advantages of the D-Alamouti scheme, this thesis will initially propose a new cooperative diversity scheme for four relay nodes and thereafter for an arbitrary number of relay nodes.

On the other hand, the major issues in this field are the lack of synchronism problem and multipath fading effects due to the distributed nature of the relay nodes where each relay node has its own oscillator and the fading environment. In this thesis, these issues will be considered and an effective solution that can combat the timing errors problem and fading effects will be provided through exploiting cooperative orthogonal frequency division multiplexing (OFDM) type transmission. This solution will be developed to increase the end-to-end data rate. Moreover, due to the random nature of the wireless environment the channel gains between the source and destination nodes are different from one path to another which results in different signal attenuations at the destination. This phenomenon will cause a reduction in the overall system performance. In this thesis, the variation in channels gain will be exploited to add extra improvements to the system

through proposing new relay selection techniques. Finally, in this thesis a cognitive radio system will be used as an application to evaluate the functionality of the proposed scheme where the combination will also improve the spectrum efficiency.

In summary, the contributions of this thesis can be summarized into five main parts:

1. A new scheme for cooperative relay networks equipped with three or four relay nodes called the distributed extended orthogonal space-time block code (D-EO-STBC) scheme. This scheme based on partial limited feedback can achieve full diversity and full rate in addition to array gain.

2. An extension of the D-EO-STBC scheme for operation with imperfect synchronization and over frequency-selective channels scenarios with low-complexity partial feedback approaches. Also, to increase transmission rate a two-way cooperative transmission scenario is proposed.

3. A relay selection approach is proposed based on the D-EO-STBC scheme that can add dramatic gain in end-to-end bit error rate (BER) for cooperative relay networks.

4. A generalized D-EO-STBC scheme is presented for an arbitrary number of relay nodes. This generalized scheme can achieve at least full diversity and full rate. Furthermore, optimal one-bit feedback and two-relay selection approaches are proposed to enhance the overall system performance.

5. An application of the D-EO-STBC scheme to a cooperative cognitive network.

1.7 Structure of the Thesis

To simplify the understanding of this thesis and its contributions, its structure is summarized as follows: In Chapter 1, a basic introduction to cooperative relay systems is presented including the system advantages, the general system architecture and the transmission relaying protocols. Due to the similarity in the system implementation, a quick introduction to conventional MIMO systems is given highlighting their main benefits and shortcomings. Also, to facilitate understanding of the D-STBC schemes, which are the main focus of this thesis, a brief background to STCs as well as the key works in this area are provided. Moreover, since a cognitive radio system has been selected as an application for the proposed D-EO-STBC scheme, the main concept and functions of cognitive radio systems are presented. The importance of a cooperative cognitive network as a combination between two efficient techniques, cooperative communication and cognitive radio is emphasized.

Chapter 2 introduces a background and literature survey for D-STBCs. To evaluate the system performance of the D-STBC schemes, the distributed-Alamouti (D-Alamouti) code is studied and discussed highlighting that the maximum diversity that can be achieved is two without any array gain. Also, cooperative communication based on OFDM type transmission is briefly presented. In Chapter 3, the proposed D-EO-STBC scheme for cooperative relay networks is presented. The main scheme properties are introduced. The open-loop and closed-loop system implementations are explained in detail and the BER performance is evaluated through numerical simulation. On the other hand, the proposed D-EO-STBC scheme for cooperative relay networks under imperfect synchronization is studied in Chapter 4. The basic operations in the broadcasting and relaying phases are explained. Different feedback approaches based on a quantization criterion are proposed.

Simulation results that clarify the system performance are presented.

Chapter 5 presents two relay selection approaches based on the D-Alamouti and D-EO-STBC schemes for cooperative relay networks. The relay selection procedure for selecting the best relay paths is described. The performance of this system in terms of pairwise error probability (PEP) and BER is evaluated. In Chapter 6, a generalized approach based on a D-EO-STBC scheme for cooperative relay networks is proposed. The system implementation at the source, relays and destination for flat and frequency-selective Rayleigh channels under perfect and imperfect synchronization is presented. The optimal one-bit feedback and relay selection approaches are introduced. The BER performance of the proposed schemes is studied and discussed.

The proposed cooperation scheme based on D-EO-STBC combined with cognitive radio is investigated in Chapter 7. Two interference free schemes for cooperative cognitive networks are proposed as an application of the D-EO-STBC scheme that can combine the advantages of cooperative relay systems and cognitive radio systems. The outage probability as a performance metric is derived and evaluated. The system performance and the validation of the derived outage probabilities are studied and discussed through numerical simulation. Finally, in the last chapter which is Chapter 8, this thesis is concluded by summarizing its contributions and also suggesting some future possible research directions.

Chapter 2

BACKGROUND AND LITERATURE SURVEY

Cooperative communications via distributed space-time block codes (D-STBCs) has recently attracted much attention as an efficient technology that can provide considerable gains in fading wireless environments. In particular, this technology can form a virtual antenna array from a number of single-antenna nodes that are distributed in a wireless network without requiring multiple-antenna nodes as in MIMO systems. In fact, D-STBCs as powerful coding techniques can effectively exploit the gains of the distributed nature of relay nodes. As such, researchers have been encouraged to propose different schemes of D-STBCs for cooperative relay networks for various wireless scenarios in the last decade. However, this distributed nature of relay nodes opens up a number of new challenging problems in terms of coding, synchronization and environment fading. In this chapter, a historical background on wireless relay networks focusing on cooperative communications via D-STBCs is firstly given through summarizing the key works in this area. Throughout this literature survey, the encountered challenges are highlighted. Then, the system implementation and performance of the distributed-Alamouti (D-Alamouti) scheme is introduced and studied as a motivated and efficient example of D-STBCs for cooperative relay networks. At the end of this chapter, a cooperative communications system

based on orthogonal frequency division multiplexing (OFDM) type transmission is briefly presented clarifying the concept and implementation of the OFDM precoding technique.

2.1 D-STBC Developments in Cooperative Communications

Recent years have seen considerable progress in the wireless communications field. One of the potential candidates for next generation of wireless communications is cooperative communications due to its ability to extend the coverage range and enhance the system capacity and reliability without requiring additional bandwidth or transmit power. Cooperative communications is based on a cooperative relay network where the collection of distributed antennas belonging to multiple users is exploited. The concept of a cooperative relay network was presented in the pioneering works of Laneman [15], [53] wherein a simplified model of the cooperative relay network and cooperative transmission protocols was defined. This model is based on a three terminal model of a classical relay channel in addition to a direct link between source and destination. Also, the works of Sendonaris et al. [10], [54] added a significant contribution in cooperative communications. Their work on a cooperative relay was basically a quantum leap on the previous works on the classical relay network where the direct link between the source and destination is not available. The classical relay channel was initially investigated by Van der Meulen [55]. Then, Cover and El Gamal [56] studied the channel capacity of certain types of classical relay channels.

In general, research on cooperative communication can be divided into two categories which are research on multiplexing or capacity of a relay channel category and research on diversity of a cooperative channel category. Several valuable contributions have been proposed on relay channel capacity and achievable rate such as the work of Schein and Gallager [57], Gastpar and

Vetterli [58] and [59], Wang et al. [60] and Kramer et al. [61]. In parallel, cooperative diversity schemes have attracted much attention such as the work of Laneman [8] and Sendonaris et al. [10] using a single relay model and the work of Fan et al. [62] considering the operation of multiple-antenna relays in a cooperative environment. The central theme of this thesis focuses on cooperative diversity schemes that can achieve full diversity and full data rate at the same time. On the other hand, there are studies on the optimal diversity-multiplexing gain tradeoff for a single relay case and a multiple relay case as in [63] and [64].

Coding for wireless relay networks has developed greatly in the past decade. In [10], a cooperative transmission based on code division multiple access (CDMA) has been introduced while in [65] a constellation rotation scheme based on time-division multiple-access (TDMA) was proposed as a cooperative protocol for a decode-and-forward (DF) single relay model with a direct link. This protocol can achieve full diversity and full data rate with a relatively high complexity relay node. Cooperative transmission based on distributed space-time coding for a DF relay network was proposed in [8] and for an amplify-and-forward (AF) relay network was proposed in [66]. However, the excellent performance of D-STBCs with low decoding complexity has motivated researchers to investigate further schemes.

Jing and Hassibi in [67] proposed a two-stage transmission model for AF relay networks based on D-STBCs. In [68], D-STBCs achieving full cooperative diversity were constructed using division algebra. In [49], Jing and Jafarkhani proposed distributed orthogonal STBCs (D-OSTBCs) and distributed quasi O-STBCs (D-QO-STBCs) for more than two cooperative single-antenna nodes. In particular, D-OSTBCs can achieve full diversity at the expense of transmission rate while D-QO-STBCs can achieve full transmission rate at the expense of a loss in diversity gain and increasing the decoding complexity. In [63], D-STBCs based on different cooperative

transmission protocols for multiple-relay flat-fading channels have been proposed. However, these schemes can not achieve full diversity and full rate at the same time. In [50], limited feedback beamforming combined with D-OSTBCs considering multiple antennas at the receiver have been proposed for any number of relay nodes. Although this scheme can achieve full rate and full diversity, this approach increases the computational complexity and decoding delay. In [69], a D-QO-STBC scheme which is also known as a distributed GABBA (D-GABBA) code combined with a multi-group maximum-likelihood (ML) decoder was designed for any number of relay nodes. In this scheme, a feedback channel for transferring control information between the relays and destination node is required in the case of dynamic relay scenarios. Although this scheme can achieve full diversity and full rate, it also exhibited long time delay and requires relatively slow fading environments.

For non-coherent systems, distributed differential STBCs (D-DSTBCs) were proposed independently in [51], [70], [71] and [72]. In [70], the authors proposed D-DSTBCs based on unitary matrices. In [71], full diversity D-DSTBCs were constructed using circulant matrices in addition to proposing differential codes based on the Alamouti code, symplectic group $Sp(2)$ code and square real orthogonal codes for using in relay networks with a specific number of relays. In [51] and [72], D-DSTBC schemes were proposed for any number of relay nodes. They can achieve rate one with full diversity but at the expense of higher decoding delay and higher complexity in encoding and decoding especially in the case of more than four relay nodes. These non-coherent schemes require certain conditions on the STBC structure which make constructing the D-DSTBCs difficult and complex.

An important point to be noted about the aforementioned D-STBC schemes is that they either lack the ability to achieve full cooperative diversity, with full data rate, at the same time or they increase the computational

complexity, which makes them non cost-effective or even infeasible. In fact, the only low complexity D-STBC scheme that can achieve full cooperative diversity and full rate with very simple symbol-wise ML decoder is the D-Alamouti code [52]. However, this code was designed only for using two single-antenna nodes which limits its diversity order to two. In addition to that, this code can not achieve any array gain.

On the other hand, one of the major issues in wireless relay systems is synchronization. Most of the previous works on cooperative schemes have assumed exact synchronization among the relays. However, in practice, the relay nodes are allocated in different places and each one has its own local oscillator which makes synchronization between them difficult to achieve if not impossible. Such a lack of synchronization means the corresponding symbols of all relay nodes do not reach their destination node at the same time. Recently, several studies on coding schemes for asynchronous relay networks that employ DF protocol were proposed in [73], [74], [75], [76], [77], [78] and [79]. Also, asynchronous coding schemes for wireless relay networks that employ AF protocol were proposed in [21], [80], [81] and [82]. In [74], [75], [80] and [83], asynchronous transmission schemes that employ OFDM-type techniques at the relays were proposed. These schemes exhibited high computational complexity. In [81], a simple asynchronous scheme based on the D-Alamouti code that implements OFDM type transmission at the source node was proposed for flat fading channels. This scheme provided full diversity with simple ML decoder. This attractive scheme has been extended to frequency-selective fading channels in [21]. However, these two schemes [21] and [81] are limited to application over only two relay nodes which make the maximum diversity order that can be achieved two.

Feedback schemes or closed-loop systems are adopted in several realistic wireless application standards such as wideband code division multiple access (WCDMA) [84]. In particular, partial feedback schemes have attracted much

attention due to their high performance and low feedback overhead [85].

All the above schemes were designed for a one-way system scenarios. However, in practice it is important to consider a two-way scenario for cooperative relay systems where two terminal nodes exchange their information via intermediate relay nodes. Some studies have been recently presented for two-way relay networks [86], [87], [88] and [89]. Two way scenarios might contribute in enhancing the transmission data rate in addition to exploiting the spatial diversity gains [90]. In [86], the authors considered D-STBCs over flat fading channels while in [87] the authors considered D-STBCs over frequency-selective channels. Asynchronous coding schemes based on D-OSTBCs and D-QO-STBCs for a two way cooperative relay scenario were proposed in [90] to achieve full diversity whilst utilizing an ML decoder.

On the other hand, in wireless cooperative relay systems, the transmitted signal from the source node follows different paths passing through intermediate relay nodes to arrive at the destination node. Each path has different channel gain which results in different attenuation experiences and consequently reduces the overall system performance. So, to minimize the effect of heavy fade paths and effectively exploiting the distributed nature of the relay nodes, certain paths should be avoided by using selection techniques. In fact, the selection techniques offer the possibility to improve the system performance with certain bandwidth whilst reduce the system computational complexity. Recently, relay selection techniques for cooperative systems have been studied [91], [92], [93], [94], [95] and [96]. Most of the previous works on relay selection are based on selecting one relay to cooperate with the direct path between the source and the destination nodes. However, there are few works on relay selection considering multiple-relay selection scenarios [91], [97].

On the other hand, spectrum utilization is an important issue for wireless technologies, especially with the huge growth in wireless applications.

Cooperative communications contributes in improving spectrum efficiency. Also, spectrum utilization can be improved significantly by using cognitive radio technology [41] and [98]. The main concept of cognitive radio is allowing secondary users to access the frequency spectrum opportunistically or simultaneously with primary users [46]. Combining cooperative communication and cognitive radio in the form of cooperative cognitive schemes has recently gained much attention [14], [99], [100], [101], [102] and [103]. In [14] and [99], both cooperative sensing and cooperative transmission among secondary cognitive relays are considered and reliable transmission for the primary and secondary users can be attained. In [100], cooperative cognitive relay schemes to improve spatial and spectrum diversities have been developed. In [101], a cognitive cooperation scheme to select the optimal cognitive relay among many moving relays has been proposed. In [102] and [103], the primary and secondary transmission was studied based on a single secondary user that employs the DF or the AF relaying protocol, respectively, and the direct link between the source and destination nodes, where the secondary user can simultaneously transmit its own information using an overlay approach. As a result, a reliable transmission for primary and secondary users was obtained. Furthermore, the system performance of the cognitive relay schemes in terms of outage probability was also studied in some works [104], [105] and [106].

2.2 D-Alamouti Scheme

The D-Alamouti code is the distributed version of the Alamouti code [23] that can achieve the same diversity order without requiring multiple antenna systems, expansion in bandwidth or increasing transmit power. It is basically applied over any two single-antenna nodes forming a virtual antenna

array and the Alamouti code can be constructed at the receiver. In the following, the D-Alamouti scheme for a wireless relay system will be presented in detail. Also, the system performance of the D-Alamouti scheme will be shown through numerical simulation.

2.2.1 D-Alamouti scheme for wireless relay system

Consider a wireless relay system with one source node, one destination node and two relay nodes, as shown in Fig. 2.1. Every node in the system has only

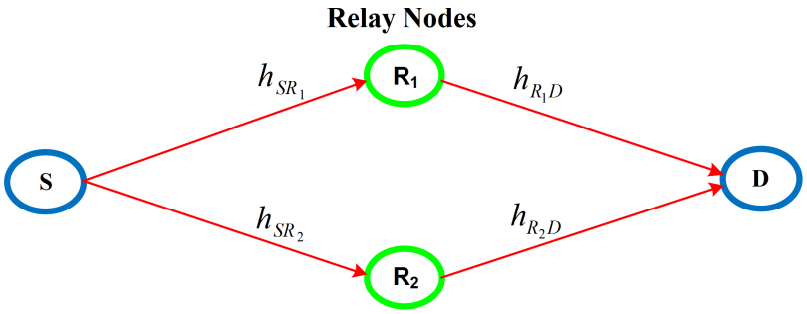

Figure 2.1. Wireless relay system architecture with single source and destination nodes and two relay nodes.

one antenna and there is no direct link between the source and destination. The system employs two-phase transmission protocol with two time periods for each phase. In the first phase, the source node transmits sequentially two different information symbols $\mathbf{s} = [s_1 \ s_2]^T$ towards the two relay nodes $R_i, i = 1, 2$. As a result, the relay nodes receive these information symbols attenuated by the fading channel h_{SR_i} and corrupted by the additive noise at each relay v_{ij} during time period j, $j = 1, 2$ as follows.

$$y_{ij} = \sqrt{P_s} s_j h_{SR_i} + v_{ij} \tag{2.2.1}$$

where P_s denotes the transmit power at the source node, the channel h_{SR_i} between the source node and the ith relay is assumed to be quasi-static flat Rayleigh fading with zero-mean and unit-variance and the noise v_{ij} is the corresponding zero mean additive white Gaussian noise (AWGN) at relay node i and time period j with zero-mean and unit-variance. In the second phase, in order to construct the Alamouti code distributively at the destination node, the received noisy signals will be simply processed according to the following encoding matrix and then forwarded to the destination node:

$$\begin{bmatrix} y_{11} & y_{22} \\ -y_{12}^* & y_{21}^* \end{bmatrix} \tag{2.2.2}$$

where $(.)^*$ denotes complex conjugation.

For the first time period during the second phase, the received signals y_{11} and y_{22} are transmitted simultaneously from R_1 and R_2, respectively. For the second time period, the received signals $-y_{12}^*$ and y_{21}^* are transmitted simultaneously from R_1 and R_2, respectively. The mean power of the received signal y_{ij} at a relay node is $P_s + 1$ due to the unit variance assumption of the additive noise v_{ij} and the channel coefficient from the source node to the relay node h_{SR_i} in (2.2.1). Let P_r denotes the average transmit power at every relay node. The optimum power allocation proposed in [67] is used in this scheme, which yields

$$P_s = RP_r = \frac{P}{2} \tag{2.2.3}$$

where P is the total transmit power in the whole scheme and R is the number of the relay nodes.

At the destination node, the received signals during the two time periods,

r_1 and r_2, can be written as

$$r_1 = \sqrt{\frac{P_r}{P_s+1}} y_{11} h_{R_1D} + \sqrt{\frac{P_r}{P_s+1}} y_{22} h_{R_2D} + w_1 \tag{2.2.4}$$

$$r_2 = -\sqrt{\frac{P_r}{P_s+1}} y_{12}^* h_{R_1D} + \sqrt{\frac{P_r}{P_s+1}} y_{21}^* h_{R_2D} + w_2 \tag{2.2.5}$$

where the channel h_{R_iD} between the ith relay and the destination node is assumed to be quasi-static flat Rayleigh fading with zero-mean and unit-variance and the noise w_j is the corresponding zero-mean unit-variance AWGN at the destination node during time period j.

The received signals at the destination can be expressed as

$$\begin{bmatrix} r_1 \\ r_2 \end{bmatrix} = \sqrt{\frac{P_r P_s}{P_s+1}} \underbrace{\begin{bmatrix} s_1 & s_2 \\ -s_2^* & s_1^* \end{bmatrix}}_{\text{Alamouti Code}} \begin{bmatrix} \hat{h}_{SR_1} h_{R_1D} \\ \hat{h}_{SR_2} h_{R_2D} \end{bmatrix} + \begin{bmatrix} n_1 \\ n_2 \end{bmatrix} \tag{2.2.6}$$

where $n_1 = \sqrt{\frac{P_r}{P_s+1}}(v_{11} h_{R_1D} + v_{22} h_{R_2D}) + w_1$, $n_2 = -\sqrt{\frac{P_r}{P_s+1}}(v_{12}^* h_{R_1D} + v_{21}^* h_{R_2D}) + w_2$, $\hat{h}_{SR_i} = h_{SR_i}$ for the received signal r_1 while $\hat{h}_{SR_i} = h_{SR_i}^*$ for the received signal r_2.

As shown in (2.2.6), the Alamouti code can be obtained at the destination. Since the Alamouti code is orthogonal, this property enables the receiver to decode s_1 and s_2 by a simple symbol-wise ML decoder. The received signals at the destination can be written in the following form

$$\begin{bmatrix} r_1 \\ r_2^* \end{bmatrix} = \sqrt{\frac{P_r P_s}{P_s+1}} \underbrace{\begin{bmatrix} h_{SR_1} h_{R_1D} & h_{SR_2} h_{R_2D} \\ h_{SR_2} h_{R_2D}^* & h_{SR_1} h_{R_1D}^* \end{bmatrix}}_{\mathbf{H}} \begin{bmatrix} s_1 \\ s_2 \end{bmatrix} + \begin{bmatrix} n_1 \\ n_2^* \end{bmatrix} \tag{2.2.7}$$

where $\mathbf{H}$ is the 2×2 equivalent channel matrix.

The channel gain can be obtained through computing the Gramian matrix

$\mathbf{G}$ as

$$\mathbf{G} = \mathbf{H}^H\mathbf{H} = \begin{bmatrix} \gamma & 0 \\ 0 & \gamma \end{bmatrix} \tag{2.2.8}$$

where $(.)^H$ denotes Hermitian transpose and γ represents the channel gain such that

$$\gamma = \sum_{i=1}^{2} |h_{SR_i} h_{R_i D}|^2 \tag{2.2.9}$$

Therefore, the resulting diversity order obtained by the D-Alamouti scheme is equal to two, which will be confirmed later from the numerical simulations. However, the D-Alamouti code has no array gain which limits the system reliability to the diversity gain only.

2.2.2 Simulation results

The performance of the D-Alamouti scheme using uncoded quadrature phase-shift keying (QPSK) symbols over a flat Rayleigh fading channel is shown in Fig. 2.2. It is assumed that the total transmit power for all schemes used in the comparison is the same. Also, it is assumed that the receiver has perfect knowledge of the channel. The BER performance of the D-Alamouti scheme is compared with a classical relay channel with one source, one relay, and one destination and a point-to-point Alamouti scheme that is applied over a system with two transmit antennas and one receive antenna.

As shown in Fig. 2.2, the D-Alamouti scheme has better BER performance compared with a classical relay model where the source node transmits its information via a single relay node to the destination node with no direct link between the source and the destination nodes. For example, the required transmit power to obtain the probability of BER of 10^{-4} for the uncoded classical relay model is approximately 47 dB (off figure) while by using the D-Alamouti scheme the required transmit power is 30 dB. So, it is clear that approximately 17 dB is needed to reach the same BER performance of the

D-Alamouti scheme. The D-Alamouti scheme shows a better performance because the order of diversity in this case is two while the classical relay model has no diversity.

From the BER curves of the D-Alamouti scheme and the point-to-point

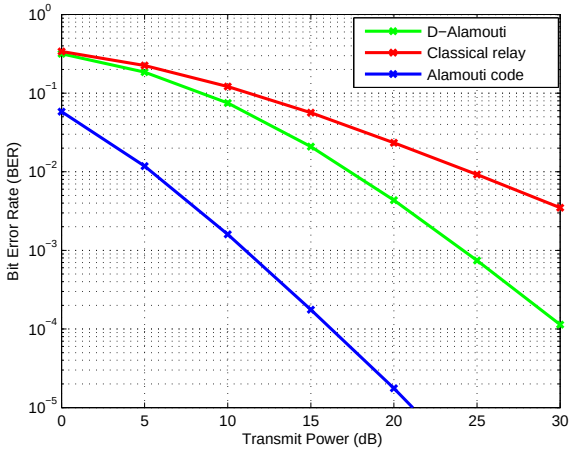

Figure 2.2. Comparison of BER performance of the D-Alamouti scheme with the classical relay model and the Alamouti scheme in a point-to-point MIMO system with two transmit antennas and one receive antenna.

Alamouti scheme, it is noticeable that they have parallel asymptotic lines which implies that they have the same diversity order of two. On the other hand, under the present assumptions, for the point-to-point scheme there is a 13 dB reduction in the transmit power for the D-Alamouti at a BER equal to 10^{-4} as compared to the point-to-point Alamouti code. However, in this simulation, the effects of correlated channels, pathloss and shadowing, which severely affect the behaviour of the point-to-point multiple antennas systems, are not considered in order to clarify the following two things; the advantage of cooperative relay channel model over the classical relay channel model and the capability of the D-Alamouti scheme to achieve the same diversity benefit (asymptotic slope of BER) as the point-to-point Alamouti scheme.

Next, cooperative communications based on OFDM type transmission is considered.

2.3 Cooperative Communications OFDM-Based Transmission

An OFDM-based transmission technique can be adopted in cooperative relay networks in different ways. The OFDM precoding modulator can be employed at the source node or at the relay nodes or at both of them. From a practical viewpoint, it is preferable to apply OFDM transmission only at the source node due to significant reduction in computational complexity. However, from a computational complexity side, if there is a necessity to employ OFDM over relay nodes, it will be better to limit this requirement to some relays instead of all relays deployed in the system. In the following, a brief introduction to the OFDM concept and implementation will be presented.

2.3.1 Basic concepts of OFDM

OFDM is a bandwidth efficient digital modulation technique [2], [107], [108] and [109] which forms the basis of many wireless standards such as the 802.11 Wi-Fi standard, 802.16 WiMAX standard, digital video broadcasting (DVB) standard and the asymmetric digital subscriber line (ADSL) standard. Also, it is adopted for fourth generation (4G) mobile wireless systems and 3GPP long-term evolution (LTE). Its basic concept is the division of the available bandwidth into a number of overlapping sub-carriers N, orthogonal to each other. The spacing between these subcarriers is selected to be the inverse of the symbol duration T, i.e., $1/T$ Hz, so that each subcarrier is orthogonal or in other words non-interfering.

It is an attractive approach for wireless systems especially for systems that suffer from multipath interference. OFDM has the capability to combat

completely inter-symbol interference (ISI) caused by such multipath channels because each sub-carrier is modulated at a very low symbol rate which makes the symbols much longer than the channel impulse response. A cyclic prefix (CP) is inserted between consecutive OFDM symbols as a guard interval [2] and [109]. Furthermore, OFDM converts a frequency selective channel into parallel frequency flat sub channels which results in reducing the complexity of the equalization. In addition, OFDM has the capability to exploit effectively the available bandwidth which results in increasing the spectral efficiency of the communications system.

2.3.2 OFDM implementation

OFDM is a block modulation technique where a block of N information symbols is modulated onto N parallel subcarriers having frequency separation $1/T$. An OFDM implementation is basically performed by using an inverse discrete Fourier transform (IDFT) at the modulator and a discrete Fourier transform (DFT) at the demodulator. Fortunately, the OFDM modulator and demodulator can be implemented as inverse fast Fourier transform (IFFT) and fast Fourier transform (FFT), respectively, which are fast signal processing transforms [2]. In fact, IFFT and FFT algorithms are efficient methods to compute the IDFT and DFT, respectively, in addition to providing further reductions in computation complexity especially when the transform size N is large and typically a power of two. For example, the FFT needs $N \log_2 N$ arithmetical operations compared with the DFT which requires N^2 arithmetical operations to achieve the same result.

Fig. 2.3 shows a basic system block diagram of the OFDM system. At the transmitter of the OFDM system, a sequence symbol stream is converted into size N parallel streams, where each stream can be drawn from any signal constellations as a conventional single carrier system. These N streams

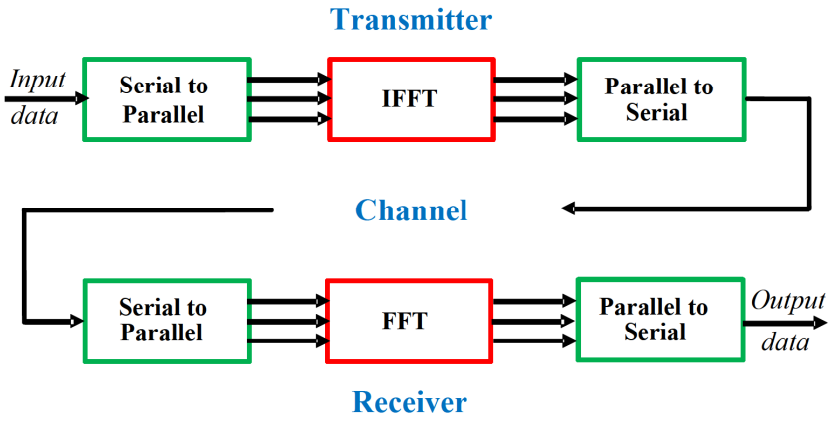

Figure 2.3. Basic block diagram of the conventional OFDM system, exploiting the FFT and serial to parallel and parallel to serial converters.

are then modulated onto N subcarriers via a size N IFFT.

$$x(n) = \frac{1}{N} \sum_{k=0}^{N-1} X(k) e^{j2\pi kn/N} \quad \text{for} \quad n = 0, ..., N-1 \tag{2.3.1}$$

where N denotes the duration of one OFDM symbol, k is the frequency index for IFFT and n is the index for the sample of $x(n)$.

That means, the IFFT converts the frequency-domain signal into a time-domain signal whilst maintaining the orthogonality. The N outputs of the IFFT are then converted to a serial data stream that can then be modulated by a single carrier. Although it would seem that combining the IFFT outputs at the transmitter would create interference between subcarriers, the orthogonal spacing allows the receiver to perfectly separate out each subcarrier provided the channel is static within the OFDM block. While at the receiver side, the received data are split into N parallel streams that are processed with a size N FFT.

$$X(k) = \sum_{n=0}^{N-1} x(n) e^{-j2\pi kn/N} \quad \text{for} \quad k = 0, ..., N-1 \tag{2.3.2}$$

That means, the FFT converts the time-domain signal into the frequency-domain to recover the information that was originally sent. The size N FFT efficiently implements a bank of filters each matched to the N possible subcarriers. The FFT output is then converted into a single serial data stream for decoding.

2.3.3 CP insertion

To mitigate the effects of ISI which is induced by the multipath channel during the signal propagation, each OFDM block after applying the IFFT process is typically preceded by a CP with length not less than the channel delay spread. At the receiver side, this extension of the CP is removed before applying the FFT process. Mathematically, a linear convolution of the transmitted OFDM signal and the channel is converted to a circular convolution in the case of applying the CP. So, the effects of the ISI are easily and completely eliminated.

The basic idea of the CP is to repeat a copy of the last part of the OFDM symbol from the back to the front to create a guard interval [2]. The duration of the guard interval T_{CP} should be longer than the worst-case delay spread of the target multipath environment, then all reflections of the previous symbol are removed and the orthogonality still exists. Therefore, the transmitted signal can completely be extracted at the receiver. Fig. 2.4

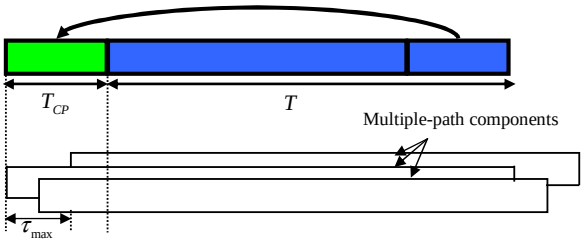

Figure 2.4. Illustration of cyclic prefix extension to the original OFDM symbol.

illustrates the idea of the CP. At the receiver, a certain position within the

cyclic prefix is chosen as the sampling starting point, which satisfies the criterion $\tau_{max} < T_{CP}$ where τ_{max} is the worst-case multi-path spread. As shown in Fig. 2.4, once the above condition is satisfied, there is no ISI since the previous symbol will only have effect over samples within $[0, \tau_{max}]$.

2.4 Summary

In this chapter, a background and literature survey on cooperative communications developments based on D-STBC schemes was presented. Also, the OFDM-based transmission in cooperative relay systems was briefly introduced. The D-Alamouti STBC transmission technique for cooperative relay systems was studied and compared with the classical relay model scheme. The D-Alamouti scheme significantly improves the BER performance over the classical relay model due to diversity gain of order two. This outstanding performance can be achieved without requiring extra transmit power or bandwidth so this technique can be considered as a bandwidth-efficient technique. In fact, the D-Alamouti code is the only D-STBC scheme that achieves full diversity and full rate at the same time. The important property within the D-Alamouti scheme is the orthogonality of the scheme code, which minimizes the computational complexity and leads to a very simple symbol-wise decoder. However, this scheme is limited to diversity of order two without any array gain which reduces its functionality in very heavy fade environments.

In the next chapter, a new D-STBC scheme for cooperative relay systems that can achieve double Alamouti diversity order with the same low order complexity will be proposed. This scheme can also provide an array gain which can considerably improve the system performance.

Chapter 3

DISTRIBUTED EXTENDED ORTHOGONAL SPACE-TIME BLOCK CODES IN WIRELESS COOPERATIVE RELAY NETWORKS

Exploiting cooperative spatial diversity within single-antenna relay nodes has gained considerable attention recently due to its potential remarkable improvements in reliability or capacity of a wireless cooperative network. The relay nodes in wireless relay networks are usually assumed to be available for cooperative operation. However, in the literature, full diversity and unity code rate[1] distributed space-time block codes generated from complex constellations for more than two relay nodes do not exist [49]. In this chapter, a complex design of distributed extended orthogonal space-time block code (D-EO-STBC) with feedback for wireless cooperative relay networks equipped with four or three relay nodes with the assumption of quasi-static flat fading channels is proposed. Full rate in each phase and full cooperative

[1]Since a half-duplex protocol is used, the code rate of the two-hop relay network is actually unity for each hop.

diversity for D-EO-STBCs are achieved by providing channel state information (CSI) at certain relay nodes. Three closed-loop schemes are proposed which employ simple partial feedback from the destination node to a particular number of relay nodes, not exceeding half of the total number of such relay nodes. Simulation results show that these three closed-loop D-EO-STBCs achieve full cooperative diversity in addition to array gain with linear processing. In particular, the proposed D-EO-STBC designs preserve low decoding complexity and save both transmission power and total transmit time between source and destination.

3.1 Introduction

Transmit diversity techniques in the form of space-time block codes (STBCs) pioneered by Alamouti [23] have been gaining popularity in the last decade due to their ability to exploit effectively the spatial diversity and because of their potential low computational complexity in decoding. STBCs can be divided into two main classes, namely, orthogonal such as the Alamouti code, and non-orthogonal, which includes quasi-orthogonal codes [5]. However, orthogonal STBCs are especially promising because full diversity is achieved while a very simple symbol-wise maximum-likelihood (ML) decoding algorithm can be used at the decoder. Originally, STBCs were designed for point-to-point multiple-input multiple-output (MIMO) systems which can efficiently exploit the benefits of MIMO channels. Fortunately, extending STBCs to cooperative relay systems in a distributed manner extracts essentially the same benefits as in point-to-point MIMO systems in addition to overcoming the limits of MIMO systems which include path loss, correlated channels and equipment size. The term distributed STBCs (D-STBCs) which has been recently proposed in several works [8], [53], [67], [110] is used to denote cooperation with STBCs. In fact, D-STBCs exploit effectively

spatial diversity within single-antenna terminals on network without the requirement of equipping any terminal with multiple antennas. As such, the terminals are less complex and smaller size and consequently less cost which make cooperative relay networks are more feasible and practical than point-to-point MIMO systems. In [67], Jing and Hassibi proposed distributed STBCs for wireless relay networks based on a two-step protocol. This scheme can achieve full cooperative diversity if the coherence time, which is equal at least to the number of symbol periods, is equal to or bigger than the number of relay nodes. Hence, the decoding delay for this scheme will be large if the number of employed relay nodes becomes large. Generally, extending complex designs of D-STBCs for more than two cooperative nodes in two-hop cooperative relay systems can not provide full diversity and full transmission rate at the same time [49]. In particular, D-OSTBCs for more than two cooperative nodes can achieve full diversity at the expense of transmission rate while distributed quasi O-STBCs (D-QO-STBCs) can achieve full transmission rate at the expense of loss in diversity gain and increasing the decoding complexity as in [49]. Likewise, STBC schemes in point-to-point MIMO systems for more than two transmit antennas which can not achieve full diversity and full rate at the same time have been presented in [26] and [27]. However, there are several STBC schemes based on closed-loop or constellation rotated methods in the literature which have been proposed for more than two transmit antennas that can attain together full diversity and full rate [29], [30], [31], [32] and [35]. In [31], the group-coherent STBC (GC-STBC) with one-bit feedback was proposed for more than two transmit antennas while in [29] the extended orthogonal STBC (EO-STBC) scheme with limited feedback was proposed for three and four transmit antennas. However, the two-hop cooperative relay system should consider all the channels in the two hops while in the MIMO system there are only one hop channels, between the transmitter and the receiver, which makes

the cooperative channel more complex than the MIMO channel. In fact, the distributed Alamouti (D-Alamouti) code [52], [111], [112] and [66] is the only proposed scheme for cooperative relay systems that can achieve full rate and full diversity at the same time for two cooperative nodes. The maximum possible diversity order for the D-Alamouti code is two. However, increasing the diversity order increases the transmission reliability and improves the system performance in terms of bit error rate (BER) and signal-to-noise ratio (SNR).

In this chapter, a novel D-EO-STBC scheme with simple partial feedback for cooperative relay networks equipped with four or three relay nodes is proposed where the relays perform simple operations to generate this code at the destination. This scheme can potentially achieve twice the D-Alamouti diversity order in addition to array gain.

3.2 D-EO-STBC Properties

In the literature, there are several types of codes which have been suggested for wireless cooperative relay systems in order to exploit the spatial diversity gain given by the relays. However, transmission based on a time-division protocol requires as many time slots as number of participating relays to send one information symbol which results in long decoding delay and low data rate. On the other hand, transmission based on orthogonal space-time block coding (STBC) is much more effective in exploiting the time slots and thereby results in increasing data rate with spatial diversity. One of the most attractive properties of STBCs is their potential low complexity in decoding. However, increasing the number of participating relays is contingent upon the selected orthogonal or non-orthogonal STBC codeword. Also, as the number of relays increases the computational complexity and decoding delay will consequently increase. So, on the basis of the issues above, EO-STBCs

employed in a distribution manner, which are basically multiple versions of the D-Alamouti code, are proposed here to avoid the aforementioned drawbacks and get benefit from their advantages which can be summarized as:

1. Low complexity in implementation.
2. Low decoding delay (just needs two time slots where each slot corresponds to two symbol periods) which might make them a potential candidate for real-time wireless applications.
3. Simple symbol-wise ML decoding algorithm can be used at the decoder.
4. High robustness where the code can work even if the number of relays is reduced.
5. High capability so the code can be extended to any arbitrary number of relays as compared with other STBCs which results in extra cooperative diversity.

3.3 System Model and Problem Statement

Consider a wireless relay system with one single-antenna source node, one single-antenna destination node, and four half-duplex relay nodes, as depicted in Fig. 3.1. Every relay node in the system has only one antenna which can be used for both transmission and reception. Relays are assumed to be located in the middle between the source and destination nodes, and operate with the amplify-and-forward (AF) strategy. They are within the coverage of the source node and assist the source in conveying the information to the destination which is not included in the source coverage or in deep fade due to pathloss or shadowing effects. So, there is no direct link between the source and destination nodes. Denote the fading coefficient from

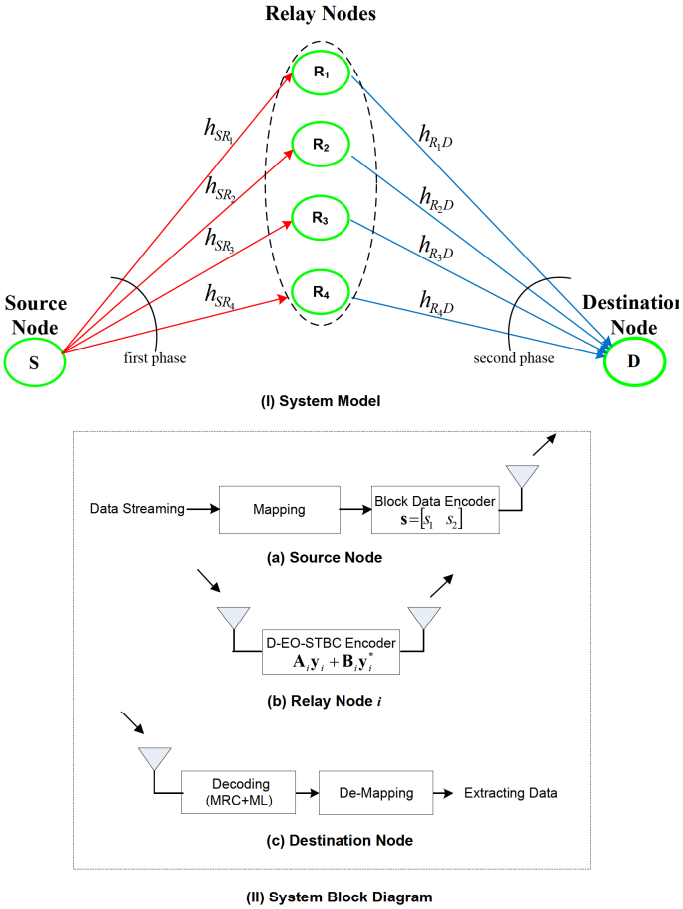

Figure 3.1. Wireless relay network with single source and destination together with a relay stage.

the source node to the ith relay as h_{SR_i}, and the fading coefficient from the ith relay to the destination node as h_{R_iD}. Assume the channel between any two terminals is quasi-static flat Rayleigh fading. Therefore, assume that h_{SR_i} and h_{R_iD} are independent complex Gaussian random variables with zero-mean and unit-variance, i.e. $\mathcal{CN}(0,1)$.

On the other hand, implementation of a two-hop multiple-relay is actually more difficult than implementing a multiple-antenna system due to the necessity of considering the two-hop channels and the multiple-relay additive noises in extracting the required information. Similarly, employing EO-STBCs in a distributed fashion has the same complexity since the multiple-

relays should perform the encoding process cooperatively using their received noisy signals instead of using directly the information signal as in the case of a multiple-antenna system. Moreover, the code construction of the D-EO-STBC implies that two of the relay nodes transmit the received noisy signals that involve the same information symbol while the remaining two relay nodes transmit the received noisy signals that involve the other information symbol after performing the encoding process. The similarity in transmission between each pair of relay nodes will induce interference to the received signals at the destination node which results in failing to achieve full cooperative spatial diversity. In this work, employing D-EO-STBCs over four relay nodes is investigated and analyzed, and then a novel simple partial feedback scheme based on phase rotation over just two relay nodes is proposed which can achieve full diversity in addition to array gain. As a result, a doubling in cooperative diversity order can be obtained as compared to the D-Alamouti code. Although the proposed scheme does use two more relay nodes as compared with the D-Alamouti scheme, in wireless relay networks these are likely to be available from the cooperative principle.

3.4 D-EO-STBCs Implementation

Constructing D-EO-STBCs at the destination node requires simple implementations to be performed at the source node and the AF type relay nodes. On the basis of system model, all system nodes are assumed to be in half-duplex mode and there is no direct link between the source node and destination node. So, to transmit the information from the source node to the destination node, they undergo two phases where each phase requires one time slot. The two phases are called in this thesis as broadcasting phase and relaying or cooperation phase. In the broadcasting phase, all signal operations at the source node until the two transmitted information signals arrive

at the relay nodes will be included. In the relaying phase, on the contrary, all signal operations on the received noisy signals at the AF type relay nodes until the forwarded signals arrive at the destination node will be included. Therefore, the whole transmission process takes just two time slots where each time slot corresponds to two symbol periods as shown in Table 3.1.

Table 3.1. Time slots required for a cooperative relay network with four relays where each time slot corresponds to two symbol periods

Broadcasting Phase				Relaying Phase			
$S \to R_1$	$S \to R_2$	$S \to R_3$	$S \to R_4$	$R_1 \to D$	$R_2 \to D$	$R_3 \to D$	$R_4 \to D$
1 time slot				1 time slot			

3.4.1 Broadcasting phase

In this phase, the source node broadcasts two information symbols $\mathbf{s} = [s_1 \ s_2]^T$ after modulation onto complex symbols to the relay nodes, where $(.)^T$ denotes vector transpose. During this phase, the relay nodes receive the transmitted information over two symbol periods. In fact, the received signal vector at the ith relay, which is denoted as $\mathbf{y}_i$, is corrupted by both the fading coefficient between the source node and the ith relay node h_{SR_i} and the noise vector at the ith relay $\mathbf{v}_i$. Therefore, the received noisy signals at the relay nodes can be expressed as

$$\mathbf{y}_i = \sqrt{P_s} h_{SR_i} \mathbf{s} + \mathbf{v}_i \tag{3.4.1}$$

where P_s denotes the average transmission power at the source node and the elements of the noise vector $\mathbf{v}_i = [v_{i1} \ v_{i2}]$ are assumed to be zero-mean and unit-variance complex additive white Gaussian noises (AWGN), i.e. $\mathcal{CN}(0, 1)$.

3.4.2 Relaying phase

In this phase, the source node stops the transmission process whilst the AF type relay nodes forward the received noisy signals to the destination node after performing simple signal operations. In particular, the signal operations in the form of complex conjugation and minus multiplication are required to construct the D-EO-STBC codeword at the destination node. Therefore, the relay nodes based on certain encoding strategy employ these signal operations on the received noisy signals before forwarding them towards the destination node. To implement these operations in practice, the four relay nodes are designed to employ unitary matrices $\mathbf{A}_i$ and $\mathbf{B}_i$ using the block coding strategy in Table 3.2. From Table 3.2, the forwarded signal at the ith relay is designed to be a linear function of its received signal and its conjugate before scaling by an amplification factor. To minimize the computational complexity, it is considered that two relay nodes are designed to employ only $\mathbf{A}_i$ and the remaining two relay nodes are designed to employ only $\mathbf{B}_i$ so the relay nodes that use $\mathbf{A}_i$ do not use $\mathbf{B}_i$ and vice versa. So, the system unitary matrices can be expressed as

Table 3.2. Block coding over the four relay nodes in the Relaying phase

Relay Nodes			
R_1	R_2	R_3	R_4
$\mathbf{A}_1\mathbf{y}_1 + \mathbf{B}_1\mathbf{y}_1^*$	$\mathbf{A}_2\mathbf{y}_2 + \mathbf{B}_2\mathbf{y}_2^*$	$\mathbf{A}_3\mathbf{y}_3 + \mathbf{B}_3\mathbf{y}_3^*$	$\mathbf{A}_4\mathbf{y}_4 + \mathbf{B}_4\mathbf{y}_4^*$

$$\mathbf{A}_1 = \mathbf{A}_2 = \begin{bmatrix} 1 & 0 \\ 0 & 1 \end{bmatrix}, \mathbf{A}_3 = \mathbf{A}_4 = \begin{bmatrix} 0 & 0 \\ 0 & 0 \end{bmatrix}$$

$$\mathbf{B}_1 = \mathbf{B}_2 = \begin{bmatrix} 0 & 0 \\ 0 & 0 \end{bmatrix}, \mathbf{B}_3 = \mathbf{B}_4 = \begin{bmatrix} 0 & -1 \\ 1 & 0 \end{bmatrix}$$

As shown from the matrices $\mathbf{A}_i$ and $\mathbf{B}_i$, it is clear that if the ith relay node employs $\mathbf{A}_i$, therefore $\mathbf{B}_i = \mathbf{0}_2$ while if the ith relay node employs $\mathbf{B}_i$, therefore $\mathbf{A}_i = \mathbf{0}_2$ where the matrix $\mathbf{0}_2$ denotes the 2×2 matrix with all zeros. In other words, the matrix $\mathbf{A}_i = \mathbf{0}_2$ means that the ith column of the code matrix contains the conjugate of the information $\mathbf{s}$ while the matrix $\mathbf{B}_i = \mathbf{0}_2$ means that the ith column contains the information $\mathbf{s}$.

On the other hand, the processed signals are then amplified by an amplification factor or a scalar relaying gain before forwarding them to the destination nodes. In this work, the relay nodes utilize a fixed amplification factor where the average values of the channel realizations between the source and relay nodes are exploited, i.e. $\mathrm{E}\{|h_{SR_i}|^2\}$ values, to satisfy the power constraints, where $\mathrm{E}\{.\}$ is the expected value. Due to the unit variance assumption of the fading channels between the source and relay nodes h_{SR_i} and the additive noise at relay nodes $\mathbf{v}_i$, the mean power of the signal $\mathbf{y}_i$ at a relay node then is equal to $P_s + 1$. Let P_r denotes the average transmission power at every relay node. Hence, the amplification factor is equal to $\sqrt{\frac{P_r}{P_s+1}}$. Moreover, the optimum power allocation in [67] is adopted in the proposed scheme as follows.

$$P_s = \frac{P}{2} \quad \text{and} \quad P_r = \frac{P}{2R} \tag{3.4.2}$$

where P denotes the total transmission power in the whole scheme and R is the total number of the relay nodes.

Then the scaled transmit signal at the ith relay can be expressed as

$$\begin{aligned} \mathbf{t}_i &= \sqrt{\frac{P_r}{P_s+1}}(\mathbf{A}_i\mathbf{y}_i + \mathbf{B}_i\mathbf{y}_i^*) \\ &= \sqrt{\frac{P_rP_s}{P_s+1}}(h_{SR_i}\mathbf{A}_i\mathbf{s}+h_{SR_i}^*\mathbf{B}_i\mathbf{s}^*)+\sqrt{\frac{P_r}{P_s+1}}(\mathbf{A}_i\mathbf{n}_i+\mathbf{B}_i\mathbf{n}_i^*) \end{aligned} \tag{3.4.3}$$

where $(.)^*$ denotes the complex conjugation.

Since the matrices $\mathbf{A}_1 = \mathbf{A}_2 = \mathbf{I}_2$ and the matrices $\mathbf{B}_1 = \mathbf{B}_2 = \mathbf{0}_2$, then the

two relays R_1 and R_2 perform pure AF protocol while the other two relays perform AF type protocol which also involves complex conjugation. Thus the proposed unitary matrices contribute in obtaining reduced computational complexity which results in a more practical and feasible system.
Equivalently, the transmitted signals at the ith relay can be written as

$$\mathbf{t}_i = \sqrt{\frac{P_r P_s}{P_s+1}}\hat{h}_{SR_i}\hat{\mathbf{A}}_i\mathbf{s}^{(i)} + \sqrt{\frac{P_r}{P_s+1}}\hat{\mathbf{A}}_i\hat{\mathbf{v}}_i$$

where

$$\begin{cases} \hat{\mathbf{A}}_i = \mathbf{A}_i, \quad \hat{h}_{SR_i} = h_{SR_i}, \quad \hat{\mathbf{v}}_i = \mathbf{v}_i, \quad \mathbf{s}^{(i)} = \mathbf{s}\ , \quad \text{if } \ \mathbf{B}_i = 0_2 \\ \hat{\mathbf{A}}_i = \mathbf{B}_i, \quad \hat{h}_{SR_i} = h^*_{SR_i}, \quad \hat{\mathbf{v}}_i = \mathbf{v}_i^*, \quad \mathbf{s}^{(i)} = \mathbf{s}^*, \quad \text{if } \ \mathbf{A}_i = 0_2 \end{cases}$$

During this phase, the destination node receives the relayed signals over two symbol durations. However, the received signals at the destination node can be written as

$$\mathbf{r} \ = \ \sqrt{\frac{P_r P_s}{P_s+1}}\mathbf{S}\mathbf{h} + \mathbf{n} \tag{3.4.4}$$

with

$$\begin{aligned} \mathbf{S} \ &= \ \begin{bmatrix} \hat{\mathbf{A}}_1\mathbf{s}^{(1)} & \ldots & \hat{\mathbf{A}}_4\mathbf{s}^{(4)} \end{bmatrix} \\ &= \ \begin{bmatrix} s_1^{(1)} & s_1^{(2)} & -s_2^{*(3)} & -s_2^{*(4)} \\ s_2^{(1)} & s_2^{(2)} & s_1^{*(3)} & s_1^{*(4)} \end{bmatrix} \\ \mathbf{h} \ &= \ \begin{bmatrix} \hat{h_{SR_1}}h_{R_1D} & \ldots & \hat{h_{SR_4}}h_{R_4D} \end{bmatrix}^T \\ \mathbf{n} \ &= \ \sqrt{\frac{P_r}{P_s+1}}\sum_{i=0}^{4} h_{R_iD}\hat{\mathbf{A}}_i\hat{\mathbf{v}}_i + \mathbf{w} \end{aligned}$$

where $\mathbf{S}$ is the codeword matrix, $\mathbf{h}$ is the equivalent channel vector, $\mathbf{n}$ is the equivalent noise vector and $\mathbf{w}$ is the noise vector at the destination node with zero-mean and unit variance AWGN elements.

The codeword matrix is called D-EO-STBC. Therefore, the four relay nodes construct the D-EO-STBC codeword distributively at the destination without decoding. As observed, the first two columns of the D-EO-STBC codeword contain s_1, s_2 and the remaining two columns contain their conjugates exclusively. In fact, the D-EO-STBC codeword is generated from the well known Alamouti code [23]. In particular, the first two columns of the D-EO-STBC code are a copy of the first column of the transposed of the Alamouti code while the remaining two columns of the D-EO-STBC code are a copy of the second column of the transposed of the Alamouti code since the Alamouti code originally has the following form [23]

$$\begin{bmatrix} s_1 & s_2 \\ -s_2^* & s_1^* \end{bmatrix}$$

Furthermore, it is noteworthy to mention that the D-EO-STBCs codeword $\mathbf{S}$ has the scale-free property [29], [49] which means by deleting one column of $\mathbf{S}$ (or in practice one of the relay nodes does not work), two D-EO-STBCs for three relay nodes are obtained as

$$\begin{bmatrix} s_1^{(1)} & s_1^{(2)} & -s_2^{*(3)} \\ s_2^{(1)} & s_2^{(2)} & s_1^{*(3)} \end{bmatrix} \quad \text{and} \quad \begin{bmatrix} s_1^{(2)} & -s_2^{*(3)} & -s_2^{*(4)} \\ s_2^{(2)} & s_1^{*(3)} & s_1^{*(4)} \end{bmatrix} \tag{3.4.5}$$

3.4.3 Implementation at the destination node

Initially, there is no channel information assumed at the relay nodes but full channel information at the destination node, i.e. an open-loop scheme. So, the received signals at the destination node can be expressed as

$$\mathbf{r} = \sum_{i=1}^{4} h_{R_i D} \mathbf{t}_i + \mathbf{w} \tag{3.4.6}$$

That is, the received signals at the destination node corresponding to two symbol durations. Also, the network channels are assumed to be quasi-static

with coherence interval equal at least to two symbol intervals, i.e. each time slot ≤ 2. Therefore, the received signal vector, $\mathbf{r}$, the relayed transmitted signal vector, $\mathbf{t_i}$, and the noise vector at the destination, $\mathbf{w}$, can be written as

$$\mathbf{r} = \begin{bmatrix} r_1 & r_2 \end{bmatrix}^T, \mathbf{t}_i = \begin{bmatrix} t_{i1} & t_{i2} \end{bmatrix}^T \text{ and } \mathbf{w} = \begin{bmatrix} w_1 & w_2 \end{bmatrix}^T$$

Consequently, the received signals r_1 and r_2 at the two independent symbol intervals can be found as

$$\begin{aligned} r_1 &= t_{11}h_{R_1D} + t_{21}h_{R_2D} + t_{31}h_{R_3D} + t_{41}h_{R_4D} + w_1 \\ &= \sqrt{\frac{P_rP_s}{P_s+1}}\left((h_{R_1D}h_{SR_1} + h_{R_2D}h_{SR_2})s_1 - (h_{R_3D}h^*_{SR_3} + h_{R_4D}h^*_{SR_4})s_2^*\right) + n_1 \\ r_2 &= t_{12}h_{R_1D} + t_{22}h_{R_2D} + t_{32}h_{R_3D} + t_{42}h_{R_4D} + w_2 \\ &= \sqrt{\frac{P_rP_s}{P_s+1}}\left((h_{R_1D}h_{SR_1} + h_{R_2D}h_{SR_2})s_2 + (h_{R_3D}h^*_{SR_3} + h_{R_4D}h^*_{SR_4})s_1^*\right) + n_2 \end{aligned}$$

where $n_1 = \sqrt{\frac{P_r}{P_s+1}}(h_{R_1D}v_{11} + h_{R_2D}v_{21} - h_{R_3D}v^*_{32} - h_{R_4D}v^*_{42})$ and $n_2 = \sqrt{\frac{P_r}{P_s+1}}(h_{R_1D}v_{12} + h_{R_2D}v_{22} + h_{R_3D}v^*_{31} + h_{R_4D}v^*_{41})$, i.e. $\mathbf{n} = [n_1\ n_2]^T$.
By taking the conjugate of r_2, the received signal vectors at the destination can be equivalently written as

$$\dot{\mathbf{r}} = \sqrt{\frac{P_rP_s}{P_s+1}} \underbrace{\begin{bmatrix} h_{SR_1}h_{R_1D} + h_{SR_2}h_{R_2D} & -(h^*_{SR_3}h_{R_3D} + h^*_{SR_4}h_{R_4D}) \\ h_{SR_3}h^*_{R_3D} + h_{SR_4}h^*_{R_4D} & h^*_{SR_1}h^*_{R_1D} + h^*_{SR_2}h^*_{R_2D} \end{bmatrix}}_{\mathbf{H}} \dot{\mathbf{s}} + \begin{bmatrix} n_1 \\ n_2^* \end{bmatrix} \tag{3.4.7}$$

where $\dot{\mathbf{r}} = [r_1\ r_2^*]$ and $\dot{\mathbf{s}} = [s_1\ s_2^*]$.
Therefore, the equivalent channel matrix corresponding to the codeword in (3.4.4) used over four relay nodes is given by

$$\mathbf{H} = \begin{bmatrix} h_{SR_1}h_{R_1D} + h_{SR_2}h_{R_2D} & -(h^*_{SR_3}h_{R_3D} + h^*_{SR_4}h_{R_4D}) \\ h_{SR_3}h^*_{R_3D} + h_{SR_4}h^*_{R_4D} & h^*_{SR_1}h^*_{R_1D} + h^*_{SR_2}h^*_{R_2D} \end{bmatrix} \tag{3.4.8}$$

Applying the matched filter (maximum ratio combining (MRC) technique) at the destination receiver with the equivalent channel matrix $\mathbf{H}$ in (3.4.8), the Gramian matrix $\mathbf{G}$ can be obtained as

$$\mathbf{G} = \mathbf{H}^H\mathbf{H} = \begin{bmatrix} \gamma & 0 \\ 0 & \gamma \end{bmatrix} \tag{3.4.9}$$

where $(.)^H$ denotes Hermitian transpose and γ represents the channel gain of the system.

The channel gain γ can be expressed as

$$\gamma = \alpha + \beta = \sum_{i=1}^{4} |h_{SR_i} h_{R_i D}|^2 + \beta_1 + \beta_2 \tag{3.4.10}$$

where α denotes the achievable cooperative diversity gain, i.e.

$$\alpha = \sum_{i=1}^{4} |h_{SR_i} h_{R_i D}|^2$$

and $\beta = \beta_1 + \beta_2$ denotes the overall interference factor where β_1 is related to the correlation interference for the received signals from the relay nodes R_1 and R_2 while β_2 is related to the interference for the received signals from the relay nodes R_3 and R_4 such that

$$\beta_1 = h^*_{SR_1} h^*_{R_1 D} h_{SR_2} h_{R_2 D} + h^*_{SR_2} h^*_{R_2 D} h_{SR_1} h_{R_1 D} = 2\mathrm{Re}\{h^*_{SR_2} h^*_{R_2 D} h_{SR_1} h_{R_1 D}\}$$

$$\beta_2 = h^*_{SR_3} h_{R_3 D} h_{SR_4} h^*_{R_4 D} + h^*_{SR_4} h_{R_4 D} h_{SR_3} h^*_{R_3 D} = 2\mathrm{Re}\{h^*_{SR_3} h_{R_3 D} h_{SR_4} h^*_{R_4 D}\}$$

where $|.|^2$ denotes the squared modulus of a complex number and $Re\{.\}$ its real part.

Actually, the interference factors β_1 and β_2 appear in the system implementation because each pair of relay nodes transmits the same information symbol after employing the same signal operation. On the other hand, from

the Gramian matrix in (3.4.9), it is evident that the D-EO-STBC code is orthogonal, which indicates that the information symbols can be extracted separately symbol by symbol with a simple ML decoder such that

$$\hat{\mathbf{s}} = \arg\min_{\mathbf{S}} \parallel \mathbf{r} - \sqrt{\frac{P_r P_s}{P_s+1}}\mathbf{Sh} \parallel = \arg\min_{\dot{\mathbf{s}}} \parallel \dot{\mathbf{r}} - \sqrt{\frac{P_r P_s}{P_s+1}}\mathbf{H}\dot{\mathbf{s}} \parallel$$

where $\parallel . \parallel$ indicates the Euclidean norm.

However, the end-to-end signal-to-noise ratio (SNR) of the system can be computed as

$$\text{SNR} = \gamma \ \frac{\sigma_s^2}{\sigma_n^2} = (\sum_{i=1}^{4} |h_{SR_i} h_{R_i D}|^2 + \beta)\frac{\sigma_s^2}{\sigma_n^2} \tag{3.4.11}$$

where σ_s^2/σ_n^2 is ratio of the total transmit power of the desired signal to the total noise power at the destination, which can be calculated as follows

$$\frac{\sigma_s^2}{\sigma_n^2} = \frac{\mathrm{E}\{|\sqrt{\frac{P_s P_r}{P_s+1}}\mathbf{s}|^2\}}{\mathrm{E}\{|n_j|^2\}} = \frac{P_s P_r}{P_s + 4P_r + 1} \quad \text{where} \quad j = 1, 2 \tag{3.4.12}$$

On the other hand, it can be seen from (3.4.10) that the β term may reduce the channel gain to below the full cooperative diversity, i.e. $\gamma < \alpha$, and correspondingly the SNR will be affected adversely. Thus to achieve full cooperative diversity, the β term should be always non-negative during the whole transmission. In the following section, a simple feedback scheme based on phase rotation is proposed. This novel scheme has the potential to overcome the correlation interference and hence ensure that both β_1 and β_2 terms are always non-negative during the whole transmission. Moreover, this scheme smartly exploits the interference to achieve array gain which results in further improvement on the end-to-end BER performance.

3.4.4 Closed-loop D-EO-STBCs for four relay nodes

Next consider there is partial channel information at the relay nodes and full CSI at the destination node, i.e. a closed-loop scheme. Specifically,

partial channel information is fed into only two particular relay nodes each having different encoding processing in terms of the construction of the D-EO-STBC codeword. In the considered system, the two selected relay nodes are R_1 and R_3 as shown in Fig. 3.2. Therefore, the two particular relay nodes exploit this information to modify accordingly their transmitted signals (or in practice rotate accordingly their antenna signals with an appropriate phase rotation) which results in overcoming the interference as explained below. In

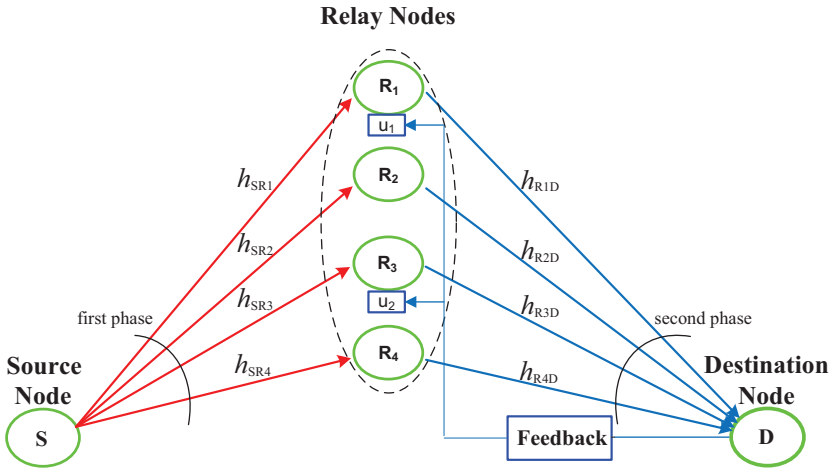

Figure 3.2. Schematic representation of the proposed closed-loop EO-STBC system for four relay nodes with feedback to two nodes.

particular, the relay transmitted signals $\mathbf{t}_1$ and $\mathbf{t}_3$ are multiplied by u_1 and u_2 before transmitting them from the first and third relay nodes, respectively, while the remaining two relay nodes are kept unchanged where u_1 and u_2 are the weighted rotation values. It is assumed that the feedback process occurs within the channel coherence time and the feedback channel is perfect. The phase rotation on the transmitted symbols is equivalent to rotating the phases of the corresponding channel coefficients. Then, the received signals r_1 and r_2 after applying the phase rotation process over R_1 and R_3 can be

expressed as

$$\begin{aligned} r_1 &= t_{11}u_1h_{R_1D} + t_{21}h_{R_2D} + t_{31}u_2h_{R_3D} + t_{41}h_{R_4D} + w_1 \\ r_2 &= t_{12}u_1h_{R_1D} + t_{22}h_{R_2D} + t_{32}u_2h_{R_3D} + t_{42}h_{R_4D} + w_2 \end{aligned}$$

By following the same procedures as in the open-loop scheme, the equivalent channel matrix $\dot{\mathbf{H}}$ can be found such that

$$\dot{\mathbf{H}} = \begin{bmatrix} u_1h_{SR_1}h_{R_1D} + h_{SR_2}h_{R_2D} & -(u_2h^*_{SR_3}h_{R_3D} + h^*_{SR_4}h_{R_4D}) \\ u_2^*h_{SR_3}h^*_{R_3D} + h_{SR_4}h^*_{R_4D} & u_1^*h^*_{SR_1}h^*_{R_1D} + h^*_{SR_2}h^*_{R_2D} \end{bmatrix} \tag{3.4.13}$$

Hence, the Gramian matrix $\mathbf{G}$ can be expressed as

$$\mathbf{G} = \dot{\mathbf{H}}^H\dot{\mathbf{H}} = \begin{bmatrix} \gamma_f & 0 \\ 0 & \gamma_f \end{bmatrix}$$

where γ_f is the channel gain of the system when the proposed partial feedback scheme is employed such that

$$\gamma_f = \alpha + \beta_f = \sum_{i=1}^{4} |h_{SR_i}h_{R_iD}|^2 + \beta_1^f + \beta_2^f \tag{3.4.14}$$

with

$$\beta_1^f = 2\mathrm{Re}\{u_1h^*_{SR_2}h^*_{R_2D}h_{SR_1}h_{R_1D}\}$$

$$\beta_2^f = 2\mathrm{Re}\{u_2h^*_{SR_3}h_{R_3D}h_{SR_4}h^*_{R_4D}\}$$

Therefore, the feedback performance gain β_f, i.e. array gain, is equal to

$$\beta_f = \beta_1^f + \beta_2^f$$

From (3.4.14), it is clear that if $\beta_f > 0$, the designed closed-loop system can obtain additional performance gain, which leads to an improved whole

channel gain, and correspondingly the SNR at the destination receiver. Also, it is clear that the weighted phase values u_1 and u_2 can control the values of β_1^f and β_2^f. Therefore, calculating the weighted phase values u_1 and u_2 is important to ensure that the values of β_1^f and β_2^f are always non-negative values. In a point-to-point MIMO system, calculating u_1 and u_2 as in [29] and [30] is much simpler than that in the case of a cooperative relay system because in the MIMO system only the channels between the transmitter and the receiver are considered in the analysis while here the channels in the two hops should be considered which makes the calculation more involved. However, in the following, three methods to calculate the weighted phase values u_1 and u_2 are suggested which are different in the way of exploiting the feedback information. In the first method, the closed-loop system is designed to employ the weighted phase values u_1 and u_2 only if the values of β_1 and β_2 are negative. Hence, u_1 and u_2 turn the negative sign(s) of the values of β_1 and β_2 to be positive. Mathematically [29],

$$u_1 = (-1)^{k_1} \quad \text{and} \quad u_2 = (-1)^{k_2}$$

where the values of k_1 and k_2 can be computed by using the following proposed design criterion:

$$k_1 = \begin{cases} 0 & \text{if } \mathrm{Re}\{h_{SR_2}^* h_{R_2D}^* h_{SR_1} h_{R_1D}\} \geq 0 \\ 1 & \text{otherwise} \end{cases} \tag{3.4.15}$$

$$k_2 = \begin{cases} 0 & \text{if } \mathrm{Re}\{h_{SR_3}^* h_{R_3D} h_{SR_4} h_{R_4D}^*\} \geq 0 \\ 1 & \text{otherwise} \end{cases} \tag{3.4.16}$$

Hence, this method requires only one-bit as a feedback which means the rotation angle for the signals is either 0 or π.

In the second method, the closed-loop system is designed to employ the

weighted phase values u_1 and u_2 all time whether the values of β_1 and β_2 are negative or positive in order to leverage the feedback gain to the maximum. Therefore, the weighted phase values u_1 and u_2 can be calculated as follows [30]

$$u_1 = e^{j\theta_1} \quad \text{and} \quad u_2 = e^{j\theta_2}$$

where the phase rotation angles θ_2 and θ_2 that depend on the two-hop channels of the cooperative relay system can be calculated based on the following proposed design criterion

$$\theta_1 = -\angle(h^*_{SR_2} h^*_{R_2D} h_{SR_1} h_{R_1D}) \tag{3.4.17}$$

$$\theta_2 = -\angle(h^*_{SR_3} h_{R_3D} h_{SR_4} h^*_{R_4D}) \tag{3.4.18}$$

where $\angle(.)$ denotes the angle operator.

Therefore, exact phase rotation angles are used for feedback which requires very large feedback overhead. In fact, this method can not be used in practical wireless application due to the limited feedback bandwidth but it can instead be used as a benchmark for other methods. However, this method can be represented as the general form of the first method.

To gain the same advantage of the exact phase feedback scheme (the second method) with limited feedback, a quantization scheme, which is the third method, is proposed. This method quantizes the perfect phases found in (3.4.17) and (3.4.18) to a number of bits for each phase. In the simulation results, very little degradation in end-to-end BER performance as compared with exact phase scheme will be shown in Section 3.5 which makes the quantization scheme a more practical and feasible solution.

3.4.5 Closed-loop D-EO-STBCs for three relay nodes

For wireless relay networks equipped with three relay nodes, the relay nodes process their received noisy signal according to Table 3.3 in order to con-

struct the specified codeword from the two D-EO-STBC codeword matrices mentioned in (3.4.5) at the destination node. From computational complexity viewpoint, the first codeword matrix is the best choice.

However, to achieve at least full spatial cooperative diversity, only one feedback link is required to ensure that the β is always non-negative as shown in Fig. 3.3. Therefore, the closed-loop system is designed to employ only one weighted phase value u_1 which can be determined by using any one of the proposed three methods mentioned in the previous section. In fact, by using the first method, only a single feedback bit is required to achieve at least full cooperative diversity.

Table 3.3. Block coding over the three relay nodes in the Relaying phase

Relay Nodes		
R_1	R_2	R_3
$A_1\mathbf{y}_1 + B_1\mathbf{y}_1^*$	$A_2\mathbf{y}_2 + B_2\mathbf{y}_2^*$	$A_3\mathbf{y}_3 + B_3\mathbf{y}_3^*$

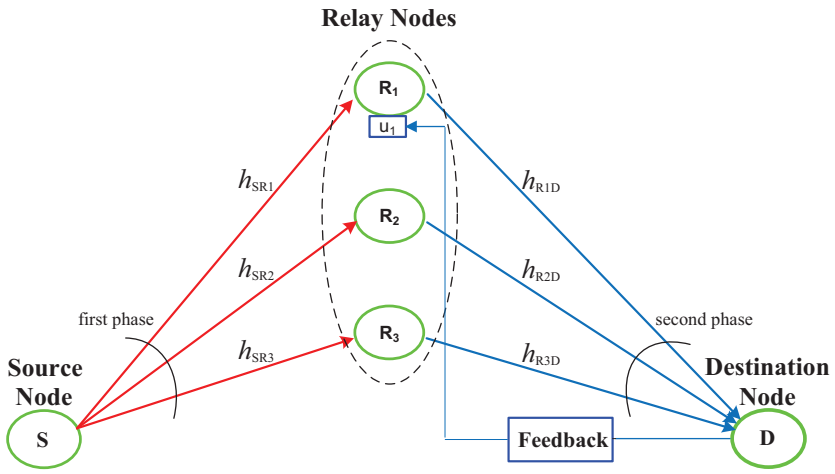

Figure 3.3. Schematic representation of the proposed closed-loop EO-STBC system for three relay nodes with one feedback link.

3.4.6 Concatenated D-EO-STBC with Viterbi-decoded convolutional codes

The original cooperative relay system with D-EO-STBC can achieve the maximum possible diversity order in addition to array gain with a simple ML decoding algorithm. However, in practice, D-EO-STBC should be concatenated with an outer channel code technique such as a convolutional code [113] to further improve the system performance. As a result, a significant coding gain can be provided but at the expense of a reduction in the data rate by a factor equal to the code rate. Convolutional codes represent one technique within the general class of error-correcting codes [113] and [114] which are used widely in many wireless applications such as mobile communications, and satellite communications in order to achieve reliable and efficient transmission over various channel conditions. Convolutional codes are commonly specified by three parameters which are required output data, current input data and the constraint length of the code where the ratio of the number of input data bits to the number of output data bits is the code rate. Therefore, the convolutional encoder depends on the current input data and the constraint length of the code to provide output coded data. On the other hand, one of the most attractive and efficient existing techniques for decoding convolutional codes especially for relatively small code constraint length is the Viterbi technique [115] and [114]. This decoding technique can provide ML performance.

In practice, the combination of convolutional encoder and Viterbi ML decoder is a very popular and robust technique to mitigate the effect of fading channels and improve the performance of communication thereby taking advantage of achieving a significant coding gain.

In the simulation result section, the improvement in system behaviour has been investigated when the proposed scheme is concatenated with a half rate

binary convolutional encoder at the source and the associated Viterbi ML decoder at the destination. Therefore, the incoming data are firstly encoded by a half-rate convolutional encoder and then fed into the signal mapper while at the destination side the received data are decoded by the Viterbi ML decoder before extracting the data.

3.5 Simulation Results

In this section, the end-to-end BER performance of the proposed D-EO-STBC schemes is compared with earlier proposed schemes in quasi-static flat fading channels. The fading is constant within a frame and changes independently from frame-to-frame. Each frame consists of two blocks of 64 symbols in the simulation. The source, relays and destination are considered to have only one half duplex antenna. All schemes use quadrature phase-shift keying (QPSK) modulation and have the same total power. The x-axis shows the average transmitted power from the source node in dB and the y-axis shows the end-to-end BER.

In Fig. 3.4, the performance of the proposed D-EO-STBC for four relay nodes is shown. It is seen that the closed-loop D-EO-STBCs for the three methods are better than the open-loop D-EO-STBC scheme. In particular, at a BER of 10^{-4}, the proposed D-EO-STBC scheme with one-bit feedback (method 1) provides approximately 6.1 dB improvement, the proposed scheme with exact phase feedback (method 2) provides approximately 6.8 dB improvement while the proposed scheme with 2-bit quantized phase feedback (method 3) provides approximately 6.7 dB improvement. It is clear that method 2 provides the best BER performance but at the expense of a very large number of feedback bits which is difficult or even impossible to achieve in a practical wireless application due to the very limited feedback bandwidth. However, method 3 performs very close to method 2 with a

very limited number of feedback bits (2-bits/transmission). The difference in performance between these two methods is less than 0.1 dB for the test environment. Moreover, the improvement increases as the average transmit-

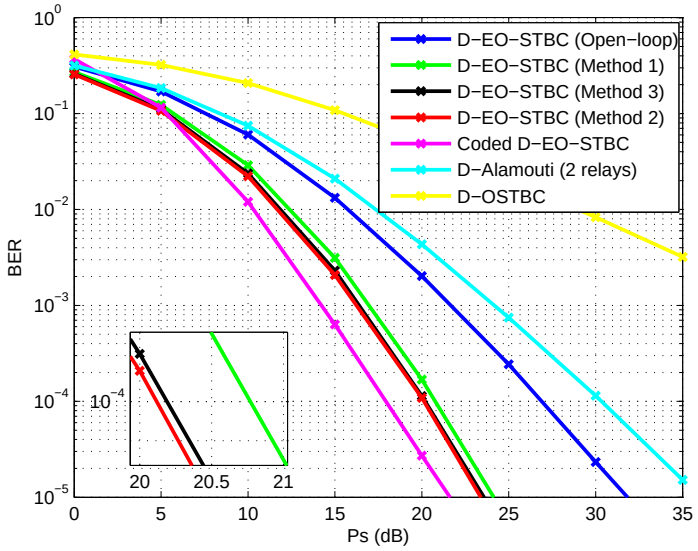

Figure 3.4. Performance comparison for various STBCs in a four relay wireless network.

ted power increases. This improvement of the proposed closed-loop schemes is because they achieve full cooperative diversity of order four combined with array gain. In fact, the difference between the three methods is in array gain quantity. The figure also provides a comparison of the proposed schemes with the distributed orthogonal STBC (D-OSTBC) [26], using the optimal power allocation protocol for distributed space-time codes with unequal time intervals as in [49], and the D-Alamouti scheme [23] and [52]. First, the design of the D-OSTBC is explained. It is a rate-3/4 complex O-STBC as mentioned in [26]. It was selected because of its orthogonality, its high transmission rate and its relatively low decoding delay (because fewer symbol periods are used) as compared to the other rate-1/2 complex O-STBCs. It is clear that the proposed D-EO-STBC scheme outperforms both of them. Specifically, when the BER is 10^{-4}, the proposed open-loop scheme can achieve more

than 3 dB gain over the D-Alamouti scheme and more than 19 dB gain (off plot) over D-OSTBC. Moreover, the proposed scheme achieves half full transmission rate (full rate at each hop) which is better than the D-OSTBC transmission rate where its actual end-to-end transmission rate is equal to 3/7 if the ratio of number of transmitted symbols to the number of channel uses is considered (unity code in the first hop and 3/4 code rate in the second hop) while achieving the same transmission rate as the D-Alamouti scheme. It is obvious that in the high average transmitted power region, the difference in improvement becomes bigger for the proposed schemes.

On the other hand, concatenation of the proposed D-EO-STBC scheme based on method 2 with a half rate convolutional code is studied as depicted in Fig. 3.4. As observed, approximately 2.1 dB additional gain has been achieved as compared to the proposed scheme based on method 2 when BER $= 10^{-4}$. This is because the coded scheme has achieved further coding gain.

In Fig. 3.5, the performance of the proposed D-EO-STBC scheme with

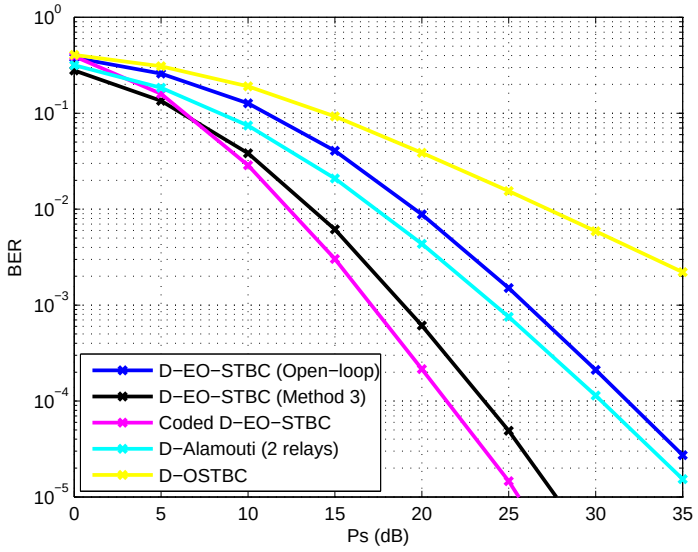

Figure 3.5. Performance comparison for various STBCs in a three relay wireless network.

2-bit quantized feedback (method 3) is shown for three relay nodes. Because method 3 is the most practical scheme as compared to the other two methods due to its ability to retain the advantage of the exact phase feedback scheme (method 2) with very limited number of feedback bits (2-bits/full transmission), this method is selected for this figure. However, similar results for the other methods can be concluded as in Fig. 3.4 so they are not repeated in this simulation. It can be seen that the closed-loop D-EO-STBCs based on method 3 is better than the D-EO-STBC without feedback. In particular, at BER of 10^{-4}, the proposed closed-loop D-EO-STBC scheme provides approximately 8.3 dB improvement. Furthermore, the improvement increases as the average transmitted power increases. In fact, the closed-loop scheme achieves full cooperative diversity of order three combined with array gain. The figure also provides a comparison of the proposed scheme with the D-OSTBC [26] and the D-Alamouti scheme. It is clear that the proposed closed-loop scheme outperforms both of them while the open-loop scheme provides better performance than the D-OSTBC but worse than the D-Alamouti scheme. For example, at BER = 10^{-4}, the proposed closed-loop scheme provides approximately 7 dB and 24 dB (off plot) improvements as compared to the D-Alamouti and D-OSTBC schemes, respectively, while the open-loop scheme provides approximately 15 dB (off plot) improvement as compared with D-OSTBC scheme and less than 2 dB reduction as compared with the D-Alamouti scheme. On the other hand, the performance of the coded D-EO-STBC scheme with 2-bit quantized feedback based on a half rate convolutional code is shown in the figure. It is clear that the closed-loop coded D-EO-STBC scheme provides better performance than the closed-loop uncoded D-EO-STBC scheme. For instant, 2 dB improvement can be achieved at BER = 10^{-4}.

On the other hand, the performance of the proposed closed-loop D-EO-STBC scheme for four relay nodes in the case of erroneous feedback channel

is investigated at Ps=20 dB as depicted in Fig. 3.6. The x-axis presents the probability of error in the feedback link P(e) which ranges from 0 to 1 and the y-axis presents the end-to-end BER. Interestingly, the proposed closed-

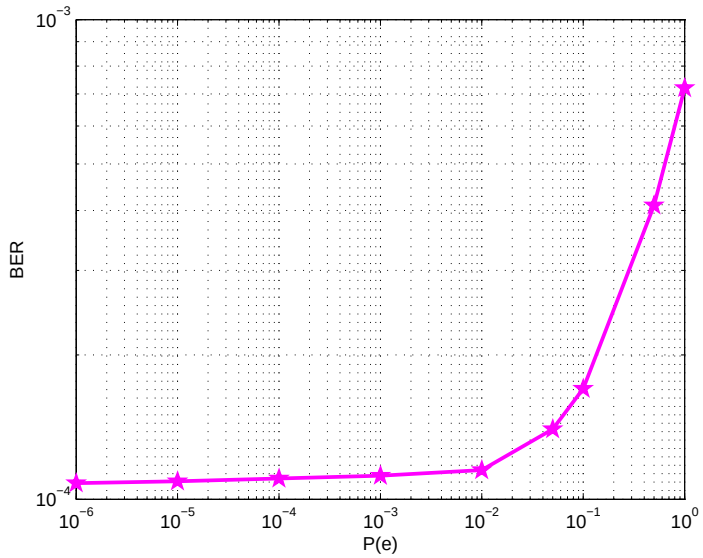

Figure 3.6. Performance comparison for various STBCs in a three relay wireless network.

loop D-EO-STBC scheme is relatively robust to the errors in the feedback channel. In particular, the BER performance remains relatively constant with increasing P(e) until P(e)=10^{-2} where the BER performance decreases sharply. However, the closed-loop scheme still provides better BER performance as compared to the open-loop scheme even with feedback errors. For example, at Ps = 20 dB and when feedback is fully erroneous, the BER performance of the proposed closed-loop scheme is approximately 7.2×10^{-4} as shown in Fig. 3.6 while the BER of the open-loop scheme is approximately 2×10^{-3} as shown in Fig. 3.4.

Finally, as shown from the simulations, the proposed D-EO-STBC schemes can be implemented over four relays and three relays which make these schemes flexible and feasible for different circumstances such as when one relay fails within a network equipped with four relays (due for example to

maintenance purpose or shadowing effects) or adding one relay to a network consisting of three relays.

3.6 Summary

In this chapter, a complex D-EO-STBC transmission scheme for wireless cooperative relay networks was proposed. Simulations showed that D-EO-STBC provides better performance than the D-Alamouti scheme and the D-OSTBC when both closed-loop and open-loop schemes are used in the case of four relays and when closed loop in the case of three relays is used. In terms of data rate, the open-loop D-EO-STBC provides half full rate which is equal to the data rate of the D-Alamouti scheme and outperforms the D-OSTBC. These results are very encouraging since the total transmission power is the same or constant in addition to the information symbols being decoded separately in a very simple manner at the receiver. The simulations also show that with partial channel knowledge at the relays, the D-EO-STBC achieves higher gain compared with no feedback because the closed-loop D-EO-STBC achieves full diversity gain in addition to array gain. For systems with three and four relay nodes, the amount of feedback information per block is as little as 1 bit and 2 bits, respectively. Finally, the main result is that the extended schemes in wireless relay networks potentially save a transmission time and power.

On the other hand, this scheme is introduced assuming an ideal environment with no synchronization problem which is theoretically valid. However, in practice synchronizing multiple relays with the destination maybe a problem. In the next chapter, this problem will be considered and addressed for both frequency flat and frequency-selective channels.

Chapter 4

COOPERATIVE D-EO-STBC SCHEME TOLERANT TO IMPERFECT SYNCHRONIZATION FOR NARROWBAND AND BROADBAND RELAY SYSTEMS

Employing multiple relay nodes between source and destination nodes can provide enhanced cooperative diversity in wireless relay systems as shown in Chapter 3. However, in practice, there is an effective problem of synchronization between these multiple relay nodes due to several factors such as different propagation delays, different relay locations, and different relay oscillators. As a result, the relay signals arrive at different time instants at the destination which may cause inter-symbol interference (ISI). In this chapter, a novel robust scheme for three and four relay nodes to employ in cooperative

relay networks without requirement of synchronization between relay nodes is proposed. Based on distributed extended orthogonal space-time block code (D-EO-STBC) type transmission coding, low-rate quantized feedback approaches that can achieve full cooperative diversity and array gain with unity code rate over each hop in the case of one-way systems, and end-to-end code rate of 2/3 for two-way systems, will be presented. In these schemes, orthogonal frequency division multiplexing (OFDM) type pre-coding has been employed with cyclic prefix (CP) insertion at the source node to combat the effects of random delays at the relay nodes, which operate in a simple amplify-and-forward (AF) mode. In this chapter, a one-way narrowband system, where the two-hop channels are assumed to be flat Rayleigh fading, is initially considered. A new low complexity quantized phase feedback scheme is proposed for narrowband systems which can retain the advantage of the perfect feedback scheme with substantial reduction in the feedback overhead. Next, a one-way broadband system, where the two-hop channels are assumed to be frequency-selective Rayleigh fading, is consider. To reduce the feedback overhead significantly, two types of quantized group feedback approaches are proposed which can enhance the system performance. Finally, this scheme is developed for a two-way broadband scenario where two terminals exchange their independent information via relay nodes located between them. The resultant closed-loop-based D-EO-STBC transmission scheme exploits a three-time slot framework which can achieve full cooperative diversity with array gain at each terminal and high end-to-end transmission rate of 2/3. Simulation results are included to confirm that these schemes provide better bit error performance as compared with previous schemes. Furthermore, a very simple fast symbol-wise maximum-likelihood (ML) decoder can be employed at the destination node to extract the information symbols.

4.1 Introduction

Wireless communication systems will require efficient and cost effective approaches to meet increased performance demands. One of the promising and potential candidate approaches for such systems is cooperative diversity schemes. Theses schemes have the ability to combine benefits of multi-antenna systems in terms of high reliability and throughput without the need for increasing the bandwidth, with the advantages of relaying systems in terms of power-efficiency, high coverage and avoiding shadow fading without employing multiple antennas at individual nodes [8], [116]. In these schemes, different nodes between the source and destination in the wireless relay network share their antennas and resources to create a virtual array. By cooperation between them, they forward the received data generated by the source to the destination after some processing at each relay node and thereby exploit cooperative diversity. In cooperative relay systems, there are two main relaying protocols used to help a source to communicate with its destination which are decode-and-forward (DF) and AF protocols. However, the AF protocol is more practical for its simplicity in implementation because there is no need for the decoding process at the relay nodes. Fortunately, space-time code transmission schemes which are efficient transmit diversity techniques that were originally proposed for multi antenna systems can be employed over cooperative relay network in a distributed framework which can effectively exploit the cooperative diversity gains offered by cooperative relay systems with very low decoder complexity. However, in most previously proposed cooperative diversity schemes, it has been assumed that perfect synchronization is achieved at the destination [8], [49], [53], [67], [68]. In practice, the relay nodes within cooperative systems are spread over different locations which makes synchronization between these nodes difficult to achieve. In this work, the asynchronism considered is for the former case and

is manifested in the variation of the frame delays from the different relays. Recently, there have been several studies on such asynchronous cooperative relay systems for DF and AF schemes [21], [73], [76], [77], [78], [82], [80] and [79]. Most of them are proposed for flat fading channels which limits their application to narrowband systems. To combat the timing errors from relay nodes, an OFDM-based transmission approach is proposed in [74], [75], [80], [83] for application over relay nodes which results in high computational complexity. In [81], at the source node for transmission, another scheme is suggested in which the OFDM pre-coding over relay nodes is avoided which results in reduced computational complexity. However, this scheme is limited to a distributed Alamouti (D-Alamouti) code which restricts its applications to a wireless system with only two relays and therefore the maximum achievable cooperative diversity is order two. This scheme has been developed for frequency-selective fading channels over wireless systems with two relays [21]. Utilizing more than two relay nodes for the cooperative relay system will result in improved diversity, and, hence, better mitigating the detrimental effects of fading channels. However, extracting full diversity and unity code form complex space-time code designs do not exist for more than two relays. In this chapter, an OFDM type pre-coding at the source node with a CP addition combined with closed-loop schemes based on D-EO-STBC transmission are proposed for asynchronous cooperative relay systems which are equipped with four relay nodes. Full cooperative diversity with unity code at each phase can be achieved and timing errors and fading can be effectively resolved.

Additionally, most previous cooperative schemes have considered only one-way communication. Recently, two-way relay network (TWRN) communications have gained much interest from researchers [86], [87], [88], [89]. In a TWRN, where two terminal nodes exchange their information with the assistance of the relay nodes located between them, in addition to exploiting the

cooperative diversity gains, the combined end-to-end transmission rate of the network can be improved [90]. In [86], the authors considered distributed space-time block coding (D-STBC) over flat fading channels while in [87] the authors considered D-STBC over frequency-selective channels. Asynchronous delay-tolerant D-STBCs for AF-TWRNs were proposed in [87] to achieve full cooperative diversity. Also, asynchronous coding schemes based on distributed orthogonal STBCs (D-OSTBCs) and distributed extended quasi-orthogonal STBCs (D-QO-STBCs) for a TWRN were proposed in [90] to achieve full diversity whilst utilizing an ML decoder.

In this chapter, robust closed-loop schemes based on D-EO-STBC transmission are proposed for one-way and two-way asynchronous cooperative relay systems which are equipped with four relay nodes. By applying limited partial feedback in the form of a phase rotation at two particular relay nodes, full cooperative diversity in addition to array gain can be achieved and a very simple symbol-wise ML decoder can be used. These contributions can effectively resolve the effects of multipaths and timing asynchronicity between the relay nodes by implementing OFDM type pre-coding at the source node and adding a CP. In particular, the proposed schemes for one-way communication is adapted for frequency-flat and frequency-selective fading channels and one timing error type which is asynchronicity at the destination node, while the proposed schemes for two-way communication consider frequency-selective fading channels and two timing error types which are the asynchronicity errors at the relay nodes and at the two terminals. To make these feedback schemes practical, feedback based quantization techniques have been proposed which can improve the overall system performance with significant reduction in feedback overhead. The temporal diversity available in the multipath links of the broadband systems can be exploited through using space-time-frequency block codes [117]. However, this issue is outside of the scope of this chapter.

4.2 One-Way Asynchronous Cooperative Relay Networks

In these networks, the source node transmits its information to the destination node via a collection of cooperative relay nodes. This section will consider narrowband and broadband communication systems where synchronization among the relays nodes is not required.

4.2.1 One-way system model and problem statement

Consider a wireless relay system with one source node, one destination node, and four half-duplex relay nodes, as shown in Fig. 4.1. Every node in the

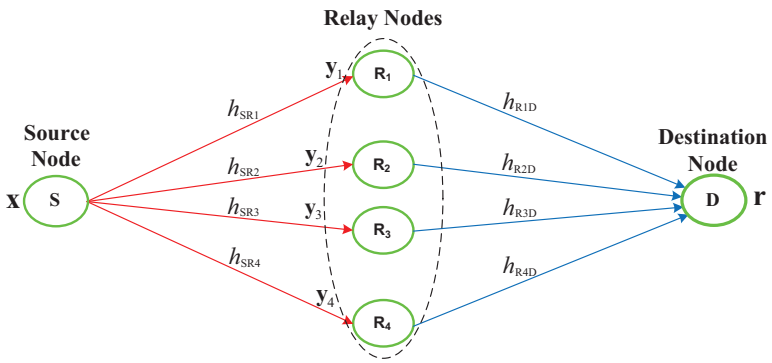

Figure 4.1. Wireless relay network with single source and destination together with a four relay stage.

system has only one antenna. The relay nodes are distributively located between the source and destination nodes. The source coverage extends to include the relay nodes but not the destination node due to deep fading, heavy path loss or shadowing effects, or the coverage design of the source. So, there is no direct path between the source and the destination nodes. The relay nodes assist the source in transmitting signals to the destination. Therefore, the system needs two phases to transmit the signals from the source node to the destination node. In the first phase, the source node

broadcasts the information symbols to the four relay nodes and then stops sending during the second phase. While in the second phase, the four relay nodes process the received signals and then retransmits them to the destination node. Denote the quasi-static fading coefficients from the source node to the ith relay as h_{SR_i} and from the ith relay to the destination node as h_{R_iD}, where $i = 1, 2, 3, 4$.

In real-life wireless applications, each relay node in a cooperative relay system is in a different location and has its own oscillator so the transmitted signals from relay nodes will most likely arrive at the destination receiver at different time instants causing the asynchronization problem. Therefore, there is normally a timing misalignment of τ_i between the received versions of these signals at the destination because exact synchronization in wireless networks is difficult if not impossible. Without loss of generality, it is assumed that the receiver at the destination is perfectly synchronized to R_1, i.e. $\tau_1 = 0$, and τ_i-sample misalignment as compared with the other three relay nodes R_2, R_3 and R_4 as shown in Fig. 4.2. Therefore, the signals received at the destination node from the relay nodes will be delayed by τ_i.

In particular, for applying the D-EO-STBC scheme over the cooperative

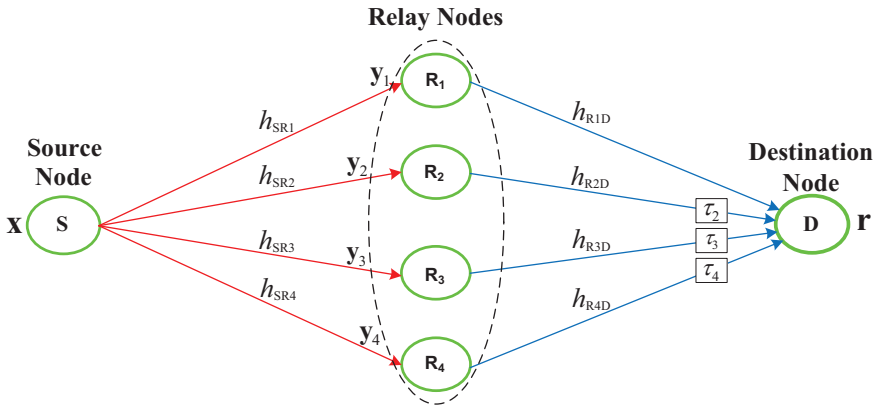

Figure 4.2. Wireless relay network with single source, destination and four relay nodes together with relative time delays.

four relay network as in Chapter 3, pairs of relay-to-destination paths will carry the same information symbols, but individual paths have their own delays which eventually causes a problem of multipath and timing errors. Such a problem will cause ISI between the received signals.

To solve this problem, a closed-loop D-EO-STBC scheme based on OFDM pre-coding with CP insertion is proposed in this chapter. To do so, simple implementations are performed at the source, relay, and destination nodes as explained later.

4.2.2 D-EO-STBC scheme for one-way narrowband systems

The term narrowband system is used here to refer to the type of the wireless channels in this section is assumed to be frequency-flat. Specifically, the channels between any two terminals are assumed to be quasi-static flat Rayleigh fading. Therefore, the channels h_{SR_i} and h_{R_iD} are assumed to be independent complex Gaussian random variables with zero-mean and unit-variance, i.e. $\mathcal{CN}(0,1)$.

Broadcasting phase

In this phase, the source node broadcasts sequentially two consecutive OFDM blocks $\mathbf{x} = [\mathbf{x}_1 \;\; \mathbf{x}_2^*]^T$ using the IDFT operation, where each of them is composed of a set of N modulated symbols, $\mathbf{x}_j = [x_{0,j}, x_{1,j}, ..., x_{N-1,j}]^T$ where $j = 1, 2$, considering that the elements of the second block are complex conjugated. The IDFT transform can be implemented using an IFFT operation which can significantly reduce the system computational complexity. So,

$$\mathbf{s} = \text{IFFT}(\mathbf{x}) = [\text{IFFT}(\mathbf{x}_1) \;\; \text{IFFT}(\mathbf{x}_2^*)]^T = [\mathbf{s}_1 \;\; \mathbf{s}_2]^T \tag{4.2.1}$$

Then before broadcasting them to the four relays, each OFDM symbol $\mathbf{s}_j$ is preceded by a CP with length l_{cp}. It is assumed that l_{cp} is not less than

the channel memory length L and the maximum of the possible relative timing errors τ_{max} of the signals arriving at the destination node, i.e. $L = 0$ due to flat fading assumption. Denote two OFDM symbols $\mathbf{s}_j$ with the corresponding CP as $\overline{\mathbf{s}}_j$.

Relaying phase

The received signals at relay i for two successive OFDM symbol durations can be written as

$$\mathbf{y}_{ij} = \sqrt{P_s}\overline{\mathbf{s}}_j h_{SR_i} + \mathbf{v}_{ij} \tag{4.2.2}$$

where $\mathbf{v}_{ij}$ is the corresponding additive white Gaussian noise (AWGN) vector terms at relay node i with elements having zero-mean and unit-variance, in two successive OFDM symbol durations, respectively. The channel coefficients are assumed constant during two OFDM symbol intervals.

Let P_s denotes the transmission power used at the source node. Then the mean power of the signal $\mathbf{y}_{ij}$ at a relay node is $P_s + 1$ due to the unit variance assumption of the fading channel from the source node to a relay node, h_{SR_i}, and the additive noise, $\mathbf{v}_{ij}$, at the relay node in (4.2.2). Let P_r denote the average transmission power at every relay node. The optimum power allocation proposed in [67] is used in this proposed scheme, which yields

$$P_s = RP_r = \frac{P}{2} \tag{4.2.3}$$

where P is the total transmission power in the whole scheme and R is the total number of the relay nodes.

An AF type relay mode is assumed. So, the four relay nodes will process and transmit the received noisy signals according to the ith column of the

relay encoding matrix of the narrowband system, $\mathbf{C}_N$,

$$\mathbf{C}_N = \rho \begin{bmatrix} \mathbf{y}_{11} & \mathbf{y}_{21} & -\zeta(\mathbf{y}_{32}^*) & -\zeta(\mathbf{y}_{42}^*) \\ \mathbf{y}_{12} & \mathbf{y}_{22} & \zeta(\mathbf{y}_{31}^*) & \zeta(\mathbf{y}_{41}^*) \end{bmatrix} \tag{4.2.4}$$

where $\rho = \sqrt{\frac{P_r}{P_s+1}}$ and $\zeta(.)$ represents the time-reversal of the signal, i.e. $\zeta(\mathbf{y}(k)) = \mathbf{y}(N-k), k = 0, 1, ..., N-1$, and $\mathbf{y}(N) = \mathbf{y}(0)$.

According to the simple relay encoding scheme (4.2.4), two relay nodes just perform pure AF operation while the other two relays perform an AF type operation after implementing very simple operations on their received noisy signal in the form of time reversal and complex conjugation. Moreover, the relay nodes do not need to perform a decoding process or a Fourier transform operation.

Implementation at the destination node

The relayed signals arrive at the destination at different time instants. However, timing synchronization is easily implemented for the shortest path from the source to destination. Without loss of generality, this will be assumed to be the path through relay 1. Hence, the delays for different relayed signals τ_i are measured relative to the received signal from relay 1. Such relative delays will cause ISI between subcarriers. However, because l_{cp} is not less than $L + \tau_{max}$, the receiver still can overcome the effect of ISI and the orthogonality between the subcarriers can still be maintained, where $\tau_{max} = \max\{\tau_i\}, i = 1, 2, 3, 4$ and $\tau_1 = 0$. On the other hand, the delay in the time domain can be interpreted in the frequency domain as phase changes

$$\mathbf{f}^{\tau_i} = \begin{bmatrix} f_0^{\tau_i}, f_1^{\tau_i}, ..., f_{N-1}^{\tau_i} \end{bmatrix}^T \tag{4.2.5}$$

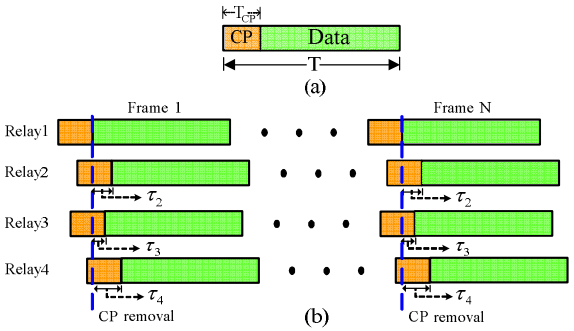

Figure 4.3. (a) OFDM frame structure after CP insertion. (b) CP removal with respect to relay 1 synchronization.

where $f_k^{\tau_i} = \exp(-j2\pi k\tau_i/N)$ and $k = 0, 1, ..., N-1$.

To process the data, the receiver performs the following operations:

1. It removes firstly the CP for each OFDM symbol as in a conventional OFDM system as shown in Fig. 4.3.

2. It then performs the reordering process on the second OFDM received frames to correct for the misalignment caused by the time reversal in (4.2.4). This can be performed by shifting the last l_{cp} samples of the N-point vector as the first l_{cp} samples.

3. It lastly applies the N-point DFT transformations process, i.e. N-point FFT, for the two received consecutive OFDM symbols $\mathbf{z}_j = [z_{0,j}, z_{1,j}, ..., z_{N-1,j}]^T$ taking into account the identities $\zeta(\text{DFT(x)}) = \text{IDFT(x)}$, $\zeta(\text{IDFT(x)}) = \text{DFT(x)}$, $(\text{DFT(x)})^* = \text{IDFT(x}^*)$ and $(\text{IDFT(x)})^* = \text{DFT(x}^*)$.

Therefore, the received data signals, $\mathbf{z}_j$, can be expressed as

$$\begin{aligned}\mathbf{z}_1 &= \sqrt{\frac{P_s P_r}{P_s+1}}\,(\mathbf{x}_1 \circ \mathbf{h}_1 + \mathbf{x}_1 \circ \mathbf{h}_2 - \mathbf{x}_2 \circ \mathbf{h}_3 - \mathbf{x}_2 \circ \mathbf{h}_4) + \mathbf{n}_1 \\ \mathbf{z}_2 &= \sqrt{\frac{P_s P_r}{P_s+1}}\,(\mathbf{x}_2^* \circ \mathbf{h}_1 + \mathbf{x}_2^* \circ \mathbf{h}_2 + \mathbf{x}_1^* \circ \mathbf{h}_3 + \mathbf{x}_1^* \circ \mathbf{h}_4) + \mathbf{n}_2 \end{aligned} \quad (4.2.6)$$

with

$$\mathbf{h}_i = \begin{cases} \mathbf{f}^{\tau_i} \circ \mathrm{FFT}(h_{SR_i}) \circ \mathrm{FFT}(h_{R_iD}) = \mathbf{f}^{\tau_i} h_{SR_i} h_{R_iD} & \text{if} \quad i = 1, 2 \\ \mathbf{f}^{\tau_i} \circ \mathrm{FFT}(h^*_{SR_i}) \circ \mathrm{FFT}(h_{R_iD}) = \mathbf{f}^{\tau_i} h^*_{SR_i} h_{R_iD} & \text{if} \quad i = 3, 4 \end{cases} \tag{4.2.7}$$

where the operation $\circ$ is the Hadamard product, i.e. element-wise product, and $\mathbf{n}_1 = \rho(\sum_{i=1}^{2} \mathbf{f}^{\tau_i} h_{R_iD} \circ \mathrm{FFT}(\mathbf{v}_{i1}) - \sum_{k=3}^{4} \mathbf{f}^{\tau_i} h_{R_iD} \circ \mathrm{FFT}(\mathbf{v}^*_{i2})) + \mathbf{w}_1$ and $\mathbf{n}_2 = \rho(\sum_{i=1}^{2} \mathbf{f}^{\tau_i} h_{R_iD} \circ \mathrm{FFT}(\mathbf{v}_{i2}) + \sum_{i=3}^{4} \mathbf{f}^{\tau_i} h_{R_iD} \circ \mathrm{FFT}(\mathbf{v}^*_{i1})) + \mathbf{w}_2$ where $\mathbf{w}_j$ is an AWGN vector at the destination node with elements having zero-mean and unit-variance.

The $\mathbf{z}_1$ and $\mathbf{z}_2$ in (4.2.6) can be written as in the following D-EO-STBC form at each subcarrier k

$$\begin{bmatrix} z_{k,1} \\ z_{k,2} \end{bmatrix} = \rho \underbrace{\begin{bmatrix} x_{k,1} & x_{k,1} & -x_{k,2} & -x_{k,2} \\ x^*_{k,2} & x^*_{k,2} & x^*_{k,1} & x^*_{k,1} \end{bmatrix}}_{\mathbf{X}_k} \begin{bmatrix} h_{k,1} \\ h_{k,2} \\ h_{k,3} \\ h_{k,4} \end{bmatrix} + \begin{bmatrix} v_{k,1} \\ v_{k,2} \end{bmatrix} \tag{4.2.8}$$

where $h_{k,i=1,2} = f_k^{\tau_i} h_{SR_i} h_{R_iD}$, $h_{k,i=3,4} = f_k^{\tau_i} h^*_{SR_i} h_{R_iD}$, $n_{k,1} = \rho(\sum_{i=1}^{2} f_k^{\tau_i}$ $h_{R_iD} v_{i,i1} - \sum_{i=3}^{4} f_k^{\tau_i} h_{R_iD} v^*_{k,i2}) + w_{k,1}$ and $n_{k,2} = \rho(\sum_{i=1}^{2} f_k^{\tau_i} h_{R_iD} v_{k,i2} +$ $\sum_{i=3}^{4} f_k^{\tau_i} h_{R_iD} v^*_{k,i1}) + w_{k,2}$.

Equivalently, the received data signals $\mathbf{z}_1$ and $\mathbf{z}_2$ at each subcarrier k, conjugated for convenience, can be expressed as follows

$$\begin{bmatrix} z_{k,1} \\ z^*_{k,2} \end{bmatrix} = \rho \underbrace{\begin{bmatrix} h_{k,1} + h_{k,2} & -(h_{k,3} + h_{k,4}) \\ (h_{k,3} + h_{k,4})^* & (h_{k,1} + h_{k,2})^* \end{bmatrix}}_{\mathbf{H}_k} \begin{bmatrix} x_{k,1} \\ x^*_{k,2} \end{bmatrix} + \begin{bmatrix} n_{k,1} \\ n^*_{k,2} \end{bmatrix} \tag{4.2.9}$$

4.2.3 Phase rotation schemes for asynchronous one-way narrow-band system

As shown in (4.2.9), it is clear that the equivalent channel matrix corresponding to the D-EO-STBC codeword $\mathbf{X}_k$ in (4.2.8) used over four relay nodes is given by

$$\mathbf{H}_k = \begin{bmatrix} h_{k,1} + h_{k,2} & -(h_{k,3} + h_{k,4}) \\ (h_{k,3} + h_{k,4})^* & (h_{k,1} + h_{k,2})^* \end{bmatrix} \tag{4.2.10}$$

Assuming that perfect channel state information (CSI) is available at the destination receiver and matched filtering is performed with the equivalent channel matrix in (4.2.10) so the Gramian matrix $\mathbf{G}_k$ for each of the k subcarriers can be obtained as follows

$$\mathbf{G}_k = \mathbf{H}_k^H \mathbf{H}_k = \begin{bmatrix} \gamma_k & 0 \\ 0 & \gamma_k \end{bmatrix} \tag{4.2.11}$$

where $(.)^H$ denotes Hermitian transpose and γ_k represents the channel gain such that $\gamma_k = \alpha_k + \beta_k$ where

$$\begin{aligned} \alpha_k &= \sum_{i=1}^{4} |h_{k,i}|^2 \\ \beta_k &= \beta_{k,1} + \beta_{k,2} = 2\mathrm{Re}\{h_{k,2}^* h_{k,1}\} + 2\mathrm{Re}\{h_{k,3} h_{k,4}^*\} \end{aligned}$$

where α_k is the cooperative diversity gain and β_k is an interference factor due to the correlation between channel coefficients where $\beta_{k,1}$ is the interference factor related to the channel correlation between the two paths passing through R_1 and R_2 and $\beta_{k,2}$ is the interference factor related to the channel correlation between the two paths passing through R_3 and R_4, the operator $|.|^2$ denotes the squared modulus of a complex number, and $\mathrm{Re}\{.\}$ its real part and $(f_k^{\tau_i})^* f_k^{\tau_i} = 1$.

As shown in (4.2.11), the off-diagonal elements are zeros which prove that the distributed STBC in (4.2.8) is orthogonal, which indicates that the code can be decoded with a simple ML receiver. The average value of the channel gain can therefore be expressed as

$$\mathrm{E}\{\gamma_k\} = \mathrm{E}\{\alpha_k + \beta_k\} = 4 + \mathrm{E}\{\beta_k\} \tag{4.2.12}$$

As such, the $\beta_{k,1}$ and $\beta_{k,2}$ terms may reduce channel gain, and correspondingly the SNR where the relation between channel gain γ_k and the SNR can be expressed as

$$SNR = \gamma_i \frac{\sigma_x^2}{\sigma_n^2} = (\sum_{k=1}^{4} |h_{i,k}|^2 + \beta_{i,1} + \beta_{i,2}) \frac{\sigma_x^2}{\sigma_n^2} \tag{4.2.13}$$

where $\sigma_x^2/\sigma_n^2 = \frac{P_s P_r}{P_s + 4P_r + 1}$ is the ratio of the total transmit power of the desired signal to the noise power at the destination receiver.

In order to leverage the system gain to the maximum, i.e. full cooperative diversity and array gain, a simple feedback scheme based on applying appropriate phase rotations, denoted by $u_{k,1}$ and $u_{k,2}$, at certain relay nodes each having different code processing in terms of codeword construction, $\mathbf{X}_k$, is proposed. So doing that, the $\beta_{k,1}$ and $\beta_{k,2}$ terms are maximized during the transmission period. The two relays selected in the system are R_1 and R_3 as shown in Fig. 4.4. So, before the signals are transmitted from the first and third relay nodes, they are multiplied by $\mathbf{u}_1$ and $\mathbf{u}_2$, respectively, while the other two are kept unchanged. Therefore, the process over relay nodes for the proposed closed-loop D-EO-STBC scheme can be summarized in Table 4.1. In fact, the feedback scheme which was originally designed for single-carrier implementation as in [118] is developed here and extended for multi-carrier implementation by applying the algorithm in [118] for each OFDM sub-carrier independently using the equivalent source to destination channel coefficients besides performing additional simple operations as shown

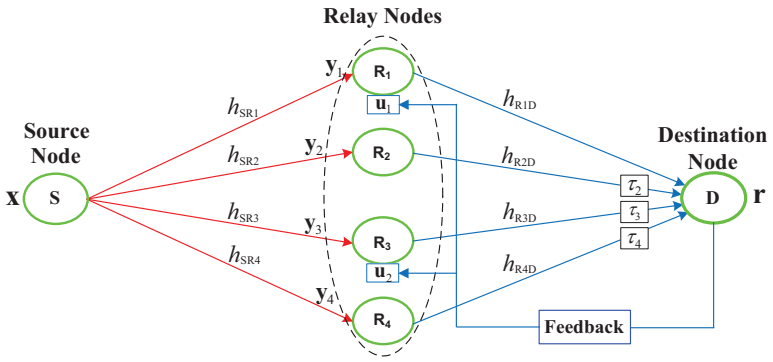

Figure 4.4. Schematic diagram for asynchronous wireless relay network with single source, destination and four relay nodes together with feedback links to two relays.

Table 4.1. D-EO-STBC over relay nodes for asynchronous narrowband system

	Relay Nodes			
Symbol duration	R_1	R_2	R_3	R_4
OFDM Symbol 1	$\mathbf{u}_1 \circ \mathbf{y}_{11}$	$\mathbf{y}_{21}$	$-\zeta(\mathbf{u}_2 \circ \mathbf{y}_{32}^*)$	$-\zeta(\mathbf{y}_{42}^*)$
OFDM Symbol 2	$\mathbf{u}_1 \circ \mathbf{y}_{12}$	$\mathbf{y}_{22}$	$\zeta(\mathbf{u}_2 \circ \mathbf{y}_{31}^*)$	$\zeta(\mathbf{y}_{41}^*)$

in Table 4.1. The equivalent channel matrix of the closed-loop scheme, $\dot{\mathbf{H}}_k$, is therefore given by

$$\dot{\mathbf{H}}_k = \begin{bmatrix} u_{k,1}h_{k,1} + h_{k,2} & -(u_{k,2}h_{k,3} + h_{k,4}) \\ (u_{k,2}h_{k,3} + h_{k,4})^* & (u_{k,1}h_{k,1} + h_{k,2})^* \end{bmatrix} \tag{4.2.14}$$

and consequently, $\gamma_k = \alpha_k + \beta_k^f = \sum_{k=1}^{4} |h_{k,i}h_{k,i}|^2 + \beta_{k,1} + \beta_{k,2}$ where $\beta_k^f = \beta_{k,1} + \beta_{k,2}$ is the array gain with $\beta_{k,1} = 2\mathrm{Re}\{u_{k,1}h_{k,2}^* h_{k,1}\}$ and $\beta_{k,2} = 2\mathrm{Re}\{u_{k,2}h_{k,3}h_{k,4}^*\}$ taking into account that $|u_{k,1}|^2 = |u_{k,2}|^2 = 1$. The values of $\beta_{k,1}$ and $\beta_{k,2}$ after applying the feedback will be positive $\beta_k^f \geq 0$ which means that the designed closed-loop system can obtain additional performance gain, which leads to an improved whole channel gain, and correspondingly the SNR at the destination receiver.

The weighted values $u_{k,1}$ and $u_{k,2}$ for each subcarrier k are computed as in the following $u_{k,1} = e^{j\theta_{k,1}}$ and $u_{k,2} = e^{j\theta_{k,2}}$. So, the following design criteria can be proposed:

$$\theta_{k,1} = -\angle(h^*_{k,2}h_{k,1}) \text{ and } \theta_{k,2} = -\angle(h_{k,3}h^*_{k,4}) \tag{4.2.15}$$

where the operation $\angle(.)$ is the angle value.
In this case, the values of the two phase rotations $\theta_{k,1}$ and $\theta_{k,2}$ are computed perfectly. However, feeding back the exact values of $\theta_{k,1}$ and $\theta_{k,2}$ requires very large feedback overhead which in practice may not be available due to the very limited feedback bandwidth. Therefore, the phase angles should be quantized to minimize the overhead of the feedback channel. In this work, two quantized phase feedback strategies have been proposed.

Direct quantization strategy

This strategy is based on applying quantization directly to $\theta_{k,1}$ and $\theta_{k,1}$ for each OFDM subcarrier with b-bits assigned as feedback for each sub-carrier phase. In this strategy, the overhead of the channel is proportional to the OFDM symbol length and the number of bits that are used for the quantization process. In simulation, 2-bit feedback per sub-carrier phase quantization (2-bit FB/SCPQ) with the overhead of 128 bits/feedback link and 1-bit FB/SCPQ with the overhead of 64 bits/feedback link have been used. The proposed scheme is designed to implement only two feedback links.

Sub-carrier quantized phase linear interpolation considering discontinuity (SCQPLI-CDC) strategy

The perfect phase angle for each OFDM symbol subcarrier k is represented diagrammatically in Fig. 4.5 (a) and (c) for two different sets of channel

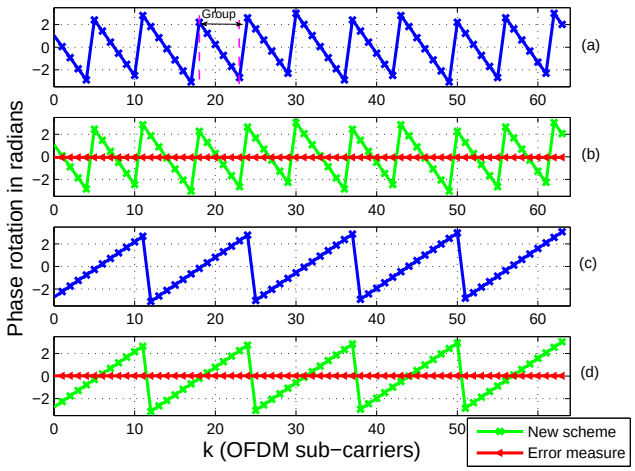

Figure 4.5. Instantaneous OFDM N=64 sub-carriers phase rotation based on: (a) Independent calculations (descending relation). (b) The proposed scheme with 6-bits quantized value for each of the first two angles together with error measure between the two scheme results. (c) Independent calculations (ascending relation). (d) The proposed scheme with 6-bits quantized value for each of the first two angles together with error measure between the two scheme results.

realizations. It is clear from these figures that the phase angles change linearly with k. In fact, the phase angles fluctuate between π and $-\pi$, i.e. the principal phase range, which make this relationship discontinuous at several points. As marked on Fig. 4.4(a), the carriers are divided into groups where all the subcarrier phases lie on a continuous linear phase portion. In other words, each group of consecutive subcarriers has a linear relationship and is in parallel with the others. Therefore, the relationship between the change in phase rotations is linear but discontinuous. However, these linear relationships may be ascending or descending. In the proposed scheme, both cases are considered. This process requires two stages. In the first stage at the destination receiver, the phase rotations of the first and second sub-carriers, $\theta_{0,j}$ and $\theta_{1,j}$, are calculated. In this case, the values of these two phase rotations are computed perfectly which requires many feedback bits which in practice may not be possible. So, these two phase rotation angles are quantized as; $\phi_{0,j}$ and $\phi_{1,j}$, to minimize the required feedback bits. The quantization bits

should be 6 bits or more to improve the interpolation process as shown in Fig. 4.5. After that, the two phase rotations are fed back to certain relay nodes. At the relay nodes, which is the second stage, the relay interpolates the remaining subcarriers phase rotations $[\phi_{2,j} \;\; \phi_{3,j} \; ... \; \phi_{N-1,j}]$ exploiting the linear relationships between them whilst considering the discontinuities and if these relations are ascending or descending. So,

$$\phi_{i,j} = \phi_{i-1,j} + D_j \tag{4.2.16}$$

where

$$D_j = \begin{cases} \phi_{1,j} - \phi_{0,j} & \text{if } \; |\phi_{1,\mathrm{j}} - \phi_{0,\mathrm{j}}| > |\phi_{1,\mathrm{j}} - \phi_{0,\mathrm{j}} - 2\pi| \\ \phi_{1,j} - \phi_{0,j} - 2\pi & \text{otherwise} \end{cases} \tag{4.2.17}$$

and if $\phi_{i,j} > \pi$ or $\phi_{i,j} < -\pi$, then

$$\phi_{i,j} = \begin{cases} \phi_{i,j} + 2\pi & \text{if } \; \mathrm{D_j} < 0 \\ \phi_{i,j} - 2\pi & \text{otherwise} \end{cases} \tag{4.2.18}$$

This simple phase relationship across subcarriers simplifies the calculation of sub carrier phase rotation angles. Therefore, the quantized CSIs for the first two subcarriers are only required to compute the phase rotation angles for the remaining subcarriers. This then reduces the feedback requirements for the proposed scheme to the quantized phase rotation of the first and second subcarriers. Therefore, the feedback overhead will be significantly reduced which makes this scheme very attractive for wireless communication systems.

4.2.4 Closed-loop asynchronous D-EO-STBCs for three relay nodes

For the wireless networks equipped with three relay nodes, one of the following encoding matrices is performed at the cooperative three relay nodes

exploiting the free-scale property of the D-EO-STBC codeword $\mathbf{X}_k$ in (4.2.8)

$$\begin{bmatrix} \mathbf{u} \circ \mathbf{y}_{11} & \mathbf{y}_{21} & -\zeta(\mathbf{y}_{32}^*) \\ \mathbf{u} \circ \mathbf{y}_{12} & \mathbf{y}_{22} & \zeta(\mathbf{y}_{31}^*) \end{bmatrix} \quad \text{or} \quad \begin{bmatrix} \mathbf{y}_{11} & -\zeta(\mathbf{u} \circ \mathbf{y}_{22}^*) & -\zeta(\mathbf{y}_{32}^*) \\ \mathbf{y}_{12} & \zeta(\mathbf{u} \circ \mathbf{y}_{21}^*) & \zeta(\mathbf{y}_{31}^*) \end{bmatrix} \tag{4.2.19}$$

In this case, only one feedback link, $\mathbf{u}$, is required to achieve full cooperative diversity with array gain in addition to unity code at each phase. It is clear that the left-hand encoding matrix is better in terms of low complexity where only one relay has to implement complex conjugation and time revision simple operations. However, the constructed codeword for each subcarrier k at the destination will be one of the following forms, respectively,

$$\begin{bmatrix} x_{k,1} & x_{k,1} & -x_{k,2} \\ x_{k,2}^* & x_{k,2}^* & x_{k,1}^* \end{bmatrix} \quad \text{or} \quad \begin{bmatrix} x_{k,1} & -x_{k,2} & -x_{k,2} \\ x_{k,2}^* & x_{k,1}^* & x_{k,1}^* \end{bmatrix} \tag{4.2.20}$$

Similarly, the quantized feedback schemes proposed for four relay nodes can be utilized for the case of three relay nodes with appropriate modifications.

4.2.5 D-EO-STBC scheme for one-way broadband systems

In a broadband two-hop wireless communication network, the channels during the two hops are usually assumed to be frequency-selective fading channels which implies that the transmitted signals via relays experience multi paths to arrive at the destination node [79]. Furthermore, the transmitted signals from relay nodes will most likely arrive at the destination receiver at different time instants due to different propagation delays, different relay locations, and different relay oscillators.

In the previous section, a D-EO-STBC scheme has been designed for multi-carrier system over quasi-static flat fading channels. In this section, the D-EO-STBC scheme will be extended to the quasi-static frequency-selective context using similar implementation processes at the source, relay, desti-

nation nodes with some significant differences. Specifically, there are two important differences in the open-loop scheme and one more in the closed-loop scheme as explained later. Mathematically, the multiplication process between the information symbols and the system channels in the case of narrowband systems is converted into a convolutional process in the case of the broadband systems. In the following, the open-loop and closed-loop D-EO-STBC schemes are presented.

Open-loop D-EO-STBC scheme for asynchronous one-way broadband relay networks

The system model in Fig. 4.2 is considered. The channels between the source node and relay nodes, $\mathbf{h_{SR_i}}$, and between the relay nodes and the destination node, $\mathbf{h_{R_iD}}$, are assumed to be quasi-static frequency-selective Rayleigh fading channels so that the vectors $\mathbf{h_{SR_i}}$ and $\mathbf{h_{R_iD}}$ have elements which are independent complex Gaussian random variables with elements having zero-mean and unit-variance. The half-duplex four relay nodes use AF relaying protocol. Similarly, as in one-way narrowband relay networks, in the first phase, the source node broadcasts sequentially two consecutive OFDM symbol blocks $\mathbf{s} = \text{IFFT}(\mathbf{x}) = [\text{IFFT}(\mathbf{x}_1) \;\; \text{IFFT}(\mathbf{x}_2^*)]^T = [\mathbf{s}_1 \;\; \mathbf{s}_2]^T$ where $\mathbf{x_j} = [x_{0,j}, x_{1,j}, ..., x_{N-1,j}]^T$ and each OFDM symbol is preceded by a CP with length l_{cp1} while in the second phase, the relay nodes firstly eliminate the CP before they apply simple linear operations, as in the previous section, over the received signals and then add a CP with length l_{cp2} before forwarding them to the destination node where the information extraction process is performed. In fact, there are two important differences as compared with the open-loop D-EO-STBC scheme for narrowband systems which are

1. CP insertion process occurs twice, the first one is performed at the source node just before broadcasting the information symbols while

the second one is performed at the relays just before forwarding their received noisy signals towards the destination. Consequently, the CP removal process occurs twice, the first one is performed at the relay nodes while the second one is performed at the destination.

2. At the destination node, a reordering process is not required, which results in minimizing the decoding complexity and delay.

Therefore, the received signals at relay node i, in two successive OFDM symbol durations j, after the CP removal process at the relay nodes can be written as

$$\mathbf{y}_{ij} = \mathbf{s}_j \otimes \mathbf{h}_{SR_i} + \mathbf{v}_{ij} \tag{4.2.21}$$

where $\otimes$ denotes a linear convolution operation and the vector $\mathbf{v}_{ij}$ contains the corresponding zero mean AWGN terms at the relay node i with zero-mean and unit-variance, respectively.

The received signals at the relays are then subject to the same process as in equation (4.2.4) considering the CP removal and insertion processes at the relay nodes. At the destination node, the same procedure as in the previous section is followed to decode the information symbols considering that the fading channels are quasi-static frequency-selective and the reordering process is avoided. Therefore, the channel gain for each subcarrier k, γ_k, can be calculated as

$$\gamma_k = \sum_{i=1}^{4} |h_{k,i}|^2 + \beta_{k,1} + \beta_{k,2} \tag{4.2.22}$$

with the interference factors $\beta_{k,1} = 2\mathrm{Re}\{h_{k,2}^* h_{k,1}\}$ and $\beta_{k,2} = 2\mathrm{Re}\{h_{k,3} h_{k,4}^*\}$.

Closed-loop D-EO-STBC scheme for asynchronous one-way broadband relay networks

From (4.2.22), it is clear that the $\beta_{k,1}$ and $\beta_{k,2}$ terms may reduce the performance of the system. In order to extract full cooperative diversity and array

gain, i.e. achieving maximized performance, a simple feedback scheme as in the previous section is proposed to modify the transmitted signals from certain two relay nodes each having different code processing by rotating with an appropriate phase angle, denoted by $u_{k,1}$ and $u_{k,2}$, to ensure that the $\beta_{k,1}$ and $\beta_{k,2}$ terms are maximized during the transmission period. The two selected relays to perform phase rotation which process their forwarded signals are R_1 and R_3 as shown in Fig. 4.3. So, before the signals are transmitted from the first and third relay nodes, they are multiplied by $\mathbf{u}_1$ and $\mathbf{u}_2$, respectively, while the other two relays are kept unchanged. To apply the weighted values $u_{k,1}$ and $u_{k,2}$ over each subcarrier k, the two selected relays require to perform an N-point OFDM transformation (FFT/IFFT) operation to be able to change the phase rotation of their signals to the proper phases. Therefore, the received signals at the two selected relays, R_1 and R_3, after CP removal process can be expressed as

$$\mathbf{y}_{ij} = \mathrm{FFT}(\mathbf{s}_j \otimes \mathbf{h}_{SR_i} + \mathbf{v}_{ij}), \text{where} \quad i = 1, 3 \tag{4.2.23}$$

According to that, the encoding relay matrix in equation (4.2.4) is changed to

$$\mathbf{C}_B = \begin{bmatrix} \mathrm{IFFT}(\mathbf{u}_1 \circ \mathbf{y}_{11}) & \mathbf{y}_{21} & -\mathrm{IFFT}(\mathbf{u}_2 \circ \mathbf{y}_{32}^*) & -\zeta(\mathbf{y}_{42}^*) \\ \mathrm{IFFT}(\mathbf{u}_1 \circ \mathbf{y}_{12}) & \mathbf{y}_{22} & \mathrm{IFFT}(\mathbf{u}_2 \circ \mathbf{y}_{31}^*) & \zeta(\mathbf{y}_{41}^*) \end{bmatrix} \tag{4.2.24}$$

where $\mathbf{C}_B$ denotes the encoding relay matrix for the broadband system. Therefore, the process over relay nodes will include FFT/IFFT operation over two particular relays in addition to time-reversal and complex conjugation operations. However, the time-reversal is discarded over the relays that perform the IFFT operation which result in a good compromise in terms of the computational complexity. The processes over the relay nodes before relaying their signals are summarized in Table 4.2. For the encoding matrix

for the four relay broadband system in equation (4.2.24), it is possible to derive two encoding matrices for use in the case of the three relay broadband system due to the free-scale property of the D-EO-STBC codeword which are

$$\begin{bmatrix} \text{IFFT}(\mathbf{u} \circ \mathbf{y}_{11}) & \mathbf{y}_{21} & -\zeta(\mathbf{y}_{32}^*) \\ \text{IFFT}(\mathbf{u} \circ \mathbf{y}_{12}) & \mathbf{y}_{22} & \zeta(\mathbf{y}_{31}^*) \end{bmatrix} \quad \text{or} \quad \begin{bmatrix} \mathbf{y}_{11} & -\text{IFFT}(\mathbf{u} \circ \mathbf{y}_{22}^*) & -\zeta(\mathbf{y}_{32}^*) \\ \mathbf{y}_{12} & \text{IFFT}(\mathbf{u} \circ \mathbf{y}_{21}^*) & \zeta(\mathbf{y}_{31}^*) \end{bmatrix} \tag{4.2.25}$$

Table 4.2. Closed-loop D-EO-STBC over relay nodes for asynchronous broadband system

	Relay Nodes			
Symbol duration	R_1	R_2	R_3	R_4
OFDM Symbol 1	$\text{IFFT}(\mathbf{u}_1 \circ \mathbf{y}_{11})$	$\mathbf{y}_{21}$	$-\text{IFFT}(\mathbf{u}_2 \circ \mathbf{y}_{32}^*)$	$-\zeta(\mathbf{y}_{42}^*)$
OFDM Symbol 2	$\text{IFFT}(\mathbf{u}_1 \circ \mathbf{y}_{12})$	$\mathbf{y}_{22}$	$\text{IFFT}(\mathbf{u}_2 \circ \mathbf{y}_{31}^*)$	$\zeta(\mathbf{y}_{41}^*)$

However, after the four relay nodes process their received signals according to Table 4.2, they forward them towards the destination node. At the destination node, the received signals are subjected to the same procedure as in the open-loop scheme which yields the following equivalent channel matrix, $\dot{\mathbf{H}}_k$,

$$\dot{\mathbf{H}}_k = \begin{bmatrix} u_{k,1}h_{k,1} + h_{k,2} & -(u_{k,2}h_{k,3} + h_{k,4}) \\ (u_{k,2}h_{k,3} + h_{k,4})^* & (u_{k,1}h_{k,1} + h_{k,2})^* \end{bmatrix} \tag{4.2.26}$$

and consequently, $\gamma_k = \sum_{i=1}^{4} |h_{k,i}h_{k,i}|^2 + \beta_{k,1} + \beta_{k,2}$ where $\beta_{k,1} = 2\text{Re}\{u_{k,1} h_{k,2}^* h_{k,1}\}$ and $\beta_{k,2} = 2\text{Re}\{u_{k,2}h_{k,3}h_{k,4}^*\}$ taking into account that $|u_{k,1}|^2 = |u_{k,2}|^2 = 1$. The values of $\beta_{k,1}$ and $\beta_{k,2}$ after applying the feedback will always be non-negative which means that the designed closed-loop system can obtain additional performance gain, which leads to an improved whole channel gain, and correspondingly the SNR at the destination receiver.

The two phase rotations $\theta_{k,1}$ and $\theta_{k,2}$ of the weighted values $u_{k,1}$ and $u_{k,2}$

for each subcarrier k are similarly computed as

$$\theta_{k,1} = -\angle(h_{k,2}^{*} h_{k,1}) \quad \text{and} \quad \theta_{k,2} = -\angle(h_{k,3} h_{k,4}^{*}) \tag{4.2.27}$$

Feeding back the exact values of the two phase rotations $\theta_{k,1}$ and $\theta_{k,2}$ requires very large feedback overhead which may not hold in practice. Therefore, the phase angles should be quantized to reduce the overhead of the feedback channel. Unfortunately, the SCQPLI-CDC strategy can not hold in the context of frequency-selective channels due to the non-linear phase relationships between the OFDM subcarriers. However, in this work, two quantized phase feedback strategies have been proposed as shown below.

Direct quantization strategy

This strategy is based on applying quantization directly to $\theta_{k,1}$ and $\theta_{k,1}$ for each OFDM subcarrier with b-bits assigned as feedback for each subcarrier phase. As noted, this strategy is similar to that in the context of flat fading channels. However, the required overhead feedback in the case of frequency-selective channels is relatively high due to the high correlation among OFDM subcarriers. In the simulation, $b = 1$ bit/phase and $b = 2$ bits/phase have been used.

Group quantization strategy

This strategy can exploit the high correlation that exists among OFDM subcarriers as in [119]. This strategy can be divided into two methods which are fixed-group quantization method and adaptive-group quantization method. For an arbitrary frequency-selective channel of length eleven, the two level quantized phase feedback required for a 64 point OFDM symbol are computed based on fixed and adaptive group feedback schemes and depicted in Fig. 4.6. In the following, the two methods will be explained.

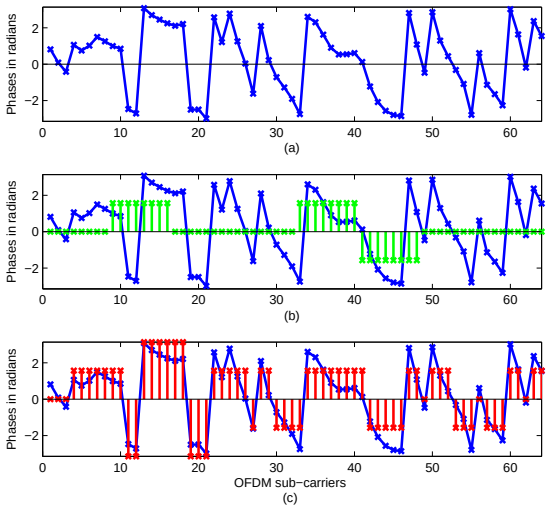

Figure 4.6. (a) Instantaneous OFDM N=64 sub-carriers phase rotation. (b) Group feedback scheme with fixed group size ($N_g = 8$ sub-carriers) using 2-bits/group.(c) Group feedback scheme with adaptive group size using 2-bits/group.

Fixed-group quantization method

This method is based on dividing the OFDM subcarriers into size N_g adjacent groups and hence one quantized phase is feedback for each group instead of for each subcarrier as shown in Fig. 4.6(b). The phase angles required are determined according to the majority of phase angles within each group. By this way, the feedback overhead can be reduced from Nb to $(N/N_g)b$. Also, this strategy can improve the bit error rate (BER) performance of the system compared with the system without feedback. However, at low quantization levels the system performance may not achieve full cooperative diversity. Furthermore, this strategy could provide better performance when the length of channels gets smaller as a result of the reduction in OFDM subcarrier phase fluctuations and therefore the reduction of quantization errors. From Fig. 4.6(b), the feedback overhead for the 64 OFDM subcarriers can be computed for the direct quantization strategy using 2-bits/subcarrier to be equal to 128 bits while for the fixed-group quantization strategy using

2-bits/group to be equal to 16 bits.

Adaptive-group quantization method

To improve the behaviour of the quantization strategy, an adaptive group feedback scheme is proposed. It is based on changing the group size according to the crossings over the zero phase line as shown in Fig. 4.6(c). This scheme can provide better BER performance but at the expense of increasing the total feedback overhead due to the requirement of feedback for both subcarriers groups and each crossover position.

4.3 Two-Way Asynchronous Cooperative Relay Networks

In two-way wireless relay networks, the two terminal nodes exchange their independent information with the assistance of the relay nodes located between them. Therefore, the transmission data rate can be enhanced as compared with one-way wireless relay networks. However, in practice, the relay nodes either receive the two terminals signals at separate time instants or at the same time instants, but this may cause signal collision problem at the relay nodes. Also, the relay nodes are located at different places which causes asynchronization problems at the relays and terminal nodes. In addition to that, the nature of the wireless environment might cause a multipath problem. In this section, robust D-EO-STBC schemes that consider the above mentioned problems are proposed which can effectively exploit the spatial diversity gain among the relay nodes and the available throughput data rate.

4.3.1 Two-way system model

Consider a wireless network with two terminal nodes, T_m, $m = 1, 2$, and four relay nodes, R_i, $i = 1, 2, 3, 4$, located between them as shown in Fig. 4.7. All system nodes are in half-duplex mode and equipped with one antenna which is used for both transmission and reception. So, each terminal can be

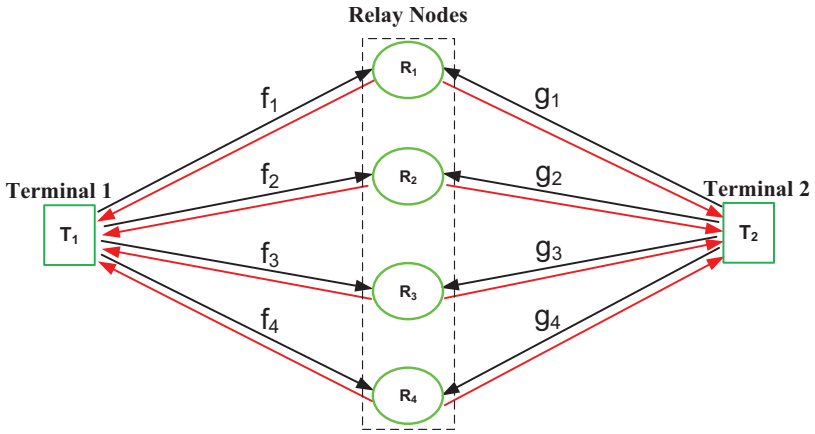

Figure 4.7. Wireless relay network for two-way broadband system where two terminals exchange their information via a relay stage.

considered as source node in the case of transmission and destination node in the case of reception. It is assumed that there is no direct path between the two terminals due to shadowing effects or path loss. The two terminals depend on the relay nodes, which exploit an AF type protocol, to exchange their information. So, the information needs two phases to reach its intended terminal. In the first phase, which is the broadcasting phase, each terminal node broadcasts the information to the relay nodes. In the second phase, which is the relaying phase (cooperation phase), the relay nodes process the received noisy signals before broadcasting them to the two terminals.

As shown in Fig. 4.7, the relay nodes are located randomly between the two terminals provided that they are all inside the coverage area of each terminal. In this network, the signal collisions are allowed at relay nodes. Due to the distributed nature of the nodes, the signals transmitted from the two terminals and the relay nodes experience different time delays and multipath to arrive at the relay nodes or the two terminals, respectively, as shown in Fig. 4.8. In fact, the timing errors in a two-way network can be divided into two types. The first one occurs at each terminal where the signals from

the four relays may arrive at each terminal node at different times which is similar to that which happens in the one-way scenario. The second type occurs at the four relays where the signals from the two terminals may arrive at one relay node at different times. The channels between the two terminal

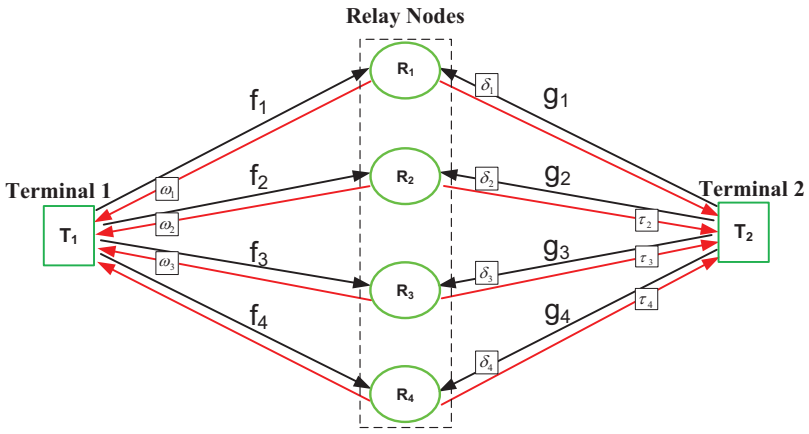

Figure 4.8. Two-way wireless relay network together with relative time delays for each path between the two terminals.

nodes T_m and relay nodes are assumed to be quasi-static frequency-selective Rayleigh fading with L independent paths. Denote the channel impulse response (CIR) from the terminal node T_1 to the ith relay as $\mathbf{f}_i$ and from the terminal node T_2 to the ith relay as $\mathbf{g}_i$, where $i = 1, 2, 3, 4$. Each path or element of $\mathbf{f}_i$ and $\mathbf{g}_i$ is modelled as an independent complex Gaussian random variable with zero-mean and unit-variance. Also, channel reciprocity [114] is assumed so the channel is the same for both direction from the terminal node T_m to the ith relay and vice versa.

4.3.2 Transmission process at terminals and relay nodes

The two terminals simultaneously broadcast sequentially two consecutive OFDM symbols $\mathbf{s}_j^m = \mathbf{Q}^* \mathbf{x}_j^m$, where $\mathbf{Q}^*$ is the normalized NxN IFFT matrix and j represents the two OFDM symbol durations, i.e. $j = 1, 2$,

taking into account that the two consecutive block information symbols $\mathbf{x}_j^m = [\mathbf{x}_1^m \quad (\mathbf{x}_2^m)^*]^T$ where the second symbol is complex conjugated and $\mathbf{x}_j^m = [x_{0,j}^m, x_{1,j}^m, ..., x_{N-1,j}^m]^T$ and N represents the OFDM symbol length. Each OFDM symbol is preceded by a CP with length l_{cp1} before broadcasting. Assume that l_{cp1} is not less than the maximum channel memory length, L, and the maximum relative time spread delay. The transmitted information signals from the two terminals will most likely arrive at the relay nodes at different time instants due to factors such as different relay locations, different oscillators in the terminals and relays and different signals propagations. Therefore, there is normally a timing misalignment of δ_i between the two received signals from the two terminals at each relay node. Without loss of generality, it is assumed that the relays R_i are perfectly synchronized to terminal T_1 and there is a δ_i-sample misalignment with the other terminal T_2, where $i = 1, 2, 3, 4$, as shown in Fig. 4.8. Such a relative delay will cause ISI between subcarriers. However, because l_{cp1} is not less than the maximum channel memory length and relative delay times, each relay can still overcome the effect of ISI as shown in Fig. 4.9(b).

The optimal power allocation in [67], which assumes that the relay nodes use half of the total network power, is adopted in the proposed TWRN scenario taking into account that the two terminal nodes consume half of the total transmit power. The total power for all the relays is denoted as P_R, so

$$P_R = P_{T_1} + P_{T_2} = \frac{P}{2} \tag{4.3.1}$$

where $P_{\mathrm{T}_1}, P_{\mathrm{T}_2}$ are the transmit powers of T_1 and T_2, respectively, and P is the total network transmit power. Each relay has a power equal to $P_r = P_R/R$ due to the symmetry where R is the total number of relays. It is also presumed that the two terminals are symmetric, i.e. $P_{\mathrm{T}_1} = P_{\mathrm{T}_2} = P_T$. The received signals at relay i for two successive OFDM symbol durations j

after CP removal can be written as

$$\mathbf{y}_j^i = \sqrt{P_T}\mathbf{F}^i\mathbf{s}_j^1 + \sqrt{P_T}\mathbf{D}_{\delta_i}\mathbf{G}^i\mathbf{s}_j^2 + \mathbf{v}_j^i \tag{4.3.2}$$

where $\mathbf{F}^i$ and $\mathbf{G}^i$ denote the NxN channel circulant matrices whose first column is equal to $\mathbf{f}^i$ and $\mathbf{g}^i$, respectively, and $\mathbf{D}_{\delta_i}$ denotes the NxN cyclic shift matrix at relay i (i.e. perform time delay at the relay nodes). The noise vector $\mathbf{v}_j^i$ corresponds to the zero-mean AWGN terms at relay node i with elements having zero-mean and unit-variance, in two successive OFDM symbol durations j. Due to the unit variance assumption of the system channels and the additive noises, $\mathbf{v}_j^i$, in (4.3.2), the mean power of the signal $\mathbf{y}_j^i$ at a relay node is $\sqrt{2P_T + 1}$. So, to ensure that the average transmission power at relay nodes is P_r, the relay scales the received signals by a factor $\sqrt{\frac{1}{2P_T+1}}$, i.e. the scalar amplification factor at the relay nodes is $\lambda = \sqrt{\frac{P_r}{2P_T+1}}$.
However, to obtain signals at each terminal receiver in the form of D-EO-STBC, the relay nodes implement very simple operations on their received noisy signals which are complex conjugation, reversed cyclic shift and minus multiplication. In fact, only two relay nodes are designed to perform these simple operations while the other two relays just perform pure AF type operation. Therefore, the relay nodes use the following distributed encoding matrix $\mathbf{C}$ for transmission process

$$\mathbf{C} = \lambda \begin{bmatrix} \mathbf{y}_1^1 & \mathbf{y}_1^2 & -\mathbf{P}(\mathbf{y}_2^3)^* & -\mathbf{P}(\mathbf{y}_2^4)^* \\ \mathbf{y}_2^1 & \mathbf{y}_2^2 & \mathbf{P}(\mathbf{y}_1^3)^* & \mathbf{P}(\mathbf{y}_1^4)^* \end{bmatrix} \tag{4.3.3}$$

where $\mathbf{P}(.)$ denotes the NxN reversed cyclic shift matrix (i.e. perform time-revision).

After that, each relay node appends each new symbol with a length-l_{cp2} CP and broadcasts it to the two terminals. Assume that l_{cp2} is not less than the maximum channel memory length between the four relay nodes and each

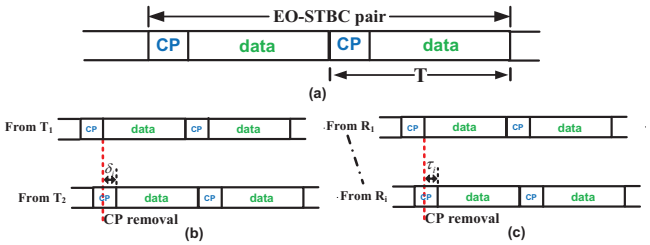

Figure 4.9. (a) D-EO-STBC pair structure. (b) CP removal at relay i with respect to terminal 1 synchronization. (c) CP removal at terminal 2 with respect to relay 1 synchronization (similarly the CP removal at terminal 1 but with respect to relay 4 synchronization).

terminal node and the maximum relative delay from the relay nodes to T_2, τ_i, or to T_1, ω_i.

4.3.3 Information extraction process

As mentioned earlier, exact synchronization is difficult or impossible to achieve at the two terminal receivers due to the distributed nature of the relay nodes. So, there is normally a timing misalignment between the received versions of these signals. Without loss of generality, it can be assumed that T_2 is perfectly synchronized to R_1 and τ_i-sample misalignment with the other R_i, where $i = 2, 3, 4$, while T_1 is perfectly synchronized to R_4 and ω_i-sample misalignment with the other R_i, where $i = 1, 2, 3$, as shown in Fig. 4.8. Such a relative delay will cause ISI between subcarriers. However, because l_{cp_2} is not less than the maximum channel memory length and relative delay times, i.e. τ_i or ω_i, each terminal still can overcome the effect of ISI as shown in Fig. 4.9(c). It is assumed that perfect CSI and all time delays are available at the two terminals. For extracting the desired data, each terminal T_m performs the following processes:

1. Removing the CP from its received signals as shown in Fig. 4.9(c).

2. Applying FFT transform (i.e. multiplying by $\mathbf{Q}$ where $\mathbf{Q}$ is defined as the normalized NxN FFT matrix).

3. Subtracting its own signals (i.e. $\mathbf{r}_j^m = \mathbf{Q}\mathbf{z}_j^m - \text{own terms}$).

So, the received signals at T_2, $\mathbf{z}_j^2$, after CP removal can be expressed as

$$\mathbf{z}_1^2 = \lambda\ [\mathbf{G}^1\mathbf{y}_1^1 + \mathbf{D}_{\tau_2}\mathbf{G}^2\mathbf{y}_1^2 - \mathbf{D}_{\tau_3}\mathbf{G}^3\mathbf{P}(\mathbf{y}_2^3)^* - \mathbf{D}_{\tau_4}\mathbf{G}^4\mathbf{P}(\mathbf{y}_2^4)^*] + \mathbf{w}_1^2 \quad (4.3.4)$$

$$\mathbf{z}_2^2 = \lambda\ [\mathbf{G}^1\mathbf{y}_2^1 + \mathbf{D}_{\tau_2}\mathbf{G}^2\mathbf{y}_2^2 + \mathbf{D}_{\tau_3}\mathbf{G}^3\mathbf{P}(\mathbf{y}_1^3)^* + \mathbf{D}_{\tau_4}\mathbf{G}^4\mathbf{P}(\mathbf{y}_1^4)^*] + \mathbf{w}_2^2 \quad (4.3.5)$$

where $\mathbf{D}_{\tau_i}$ is the NxN cyclic shift matrix at T_2 (i.e. perform time delay at T_2) and the noises vectors $\mathbf{w}_j^m$ are the AWGNs at T_m with zero-mean and unit-variance elements.

Similarly, the received signals $\mathbf{z}_j^1$ at T_1 after CP removal, taking into account the different relaying paths and signal experiences, can be expressed as

$$\mathbf{z}_1^1 = \lambda\ [\mathbf{D}_{\omega_1}\mathbf{G}^1\mathbf{y}_1^1 + \mathbf{D}_{\omega_2}\mathbf{G}^2\mathbf{y}_1^2 - \mathbf{D}_{\omega_3}\mathbf{G}^3\mathbf{P}(\mathbf{y}_2^3)^* - \mathbf{G}^4\mathbf{P}(\mathbf{y}_2^4)^*] + \mathbf{w}_1^1 \quad (4.3.6)$$

$$\mathbf{z}_2^1 = \lambda\ [\mathbf{D}_{\omega_1}\mathbf{G}^1\mathbf{y}_2^1 + \mathbf{D}_{\omega_2}\mathbf{G}^2\mathbf{y}_2^2 + \mathbf{D}_{\omega_3}\mathbf{G}^3\mathbf{P}(\mathbf{y}_1^3)^* + \mathbf{G}^4\mathbf{P}(\mathbf{y}_1^4)^*] + \mathbf{w}_2^1 \quad (4.3.7)$$

where $\mathbf{D}_{\omega_i}$ is the NxN cyclic shift matrix at T_1 (i.e. perform time delay at T_1).

Then, the two received OFDM symbols, $\mathbf{z}_j^m = [z_{0,j}^m, z_{1,j}^m, ..., z_{N-1,j}^m]^T$, pass through the FFT transform. To simplify calculations, the following identities are taken into account $\mathbf{Q}\mathbf{Q}^* = \mathbf{Q}\mathbf{P}\mathbf{Q} = \mathbf{I}_N$, $\mathbf{F}_i = \mathbf{Q}^H\Lambda_{\mathbf{F}_i}\mathbf{Q}$, $\mathbf{P}\mathbf{F}_i^*\mathbf{P} = \mathbf{F}_i^H$ and $\mathbf{F}_i^H = \mathbf{Q}^H\Lambda_{\mathbf{F}_i}^*\mathbf{Q}$ where $\Lambda_{\mathbf{F}_i}$ is defined as an NxN diagonal matrix whose (k,k)-th entry is equal to the kth FFT coefficient of the respective CIR, i.e. $\mathbf{f}_i$. Similar results will be concluded when the same operations have been performed for the following matrices $\mathbf{G}_i$, $\mathbf{D}_{\delta_i}$, $\mathbf{D}_{\tau_i}$ and $\mathbf{D}_{\omega_i}$. As a result, the received data at T_m, $\mathbf{r}_j^m$, after removing its own transmitted data $\mathbf{x}_j^m$ can be expressed as

$$\mathbf{r}_1^m = \rho\ [(\mathbf{A}_1^m + \mathbf{A}_2^m)\ \mathbf{x}_1^{\bar{m}} - (\mathbf{A}_3^m + \mathbf{A}_4^m)\ \mathbf{x}_2^{\bar{m}}] + \mathbf{n}_1^m \quad (4.3.8)$$

$$\mathbf{r}_2^m = \rho\ [(\mathbf{A}_3^m + \mathbf{A}_4^m)\ (\mathbf{x}_1^{\bar{m}})^* + (\mathbf{A}_1^m + \mathbf{A}_2^m)\ (\mathbf{x}_2^{\bar{m}})^*] + \mathbf{n}_2^m \quad (4.3.9)$$

where $\rho = \lambda \sqrt{P_T}$ and $\bar{m} \neq m$ where $\{m, \bar{m}\} \in \{1, 2\}$.

Thus, the two successively received samples, $(\mathbf{r}_j^m)_k$, $k = 0, 1, ..., N-1$, conjugated for convenience, can be expressed as follows

$$\begin{bmatrix} (\mathbf{r}_1^m)_k \\ (\mathbf{r}_2^m)_k^* \end{bmatrix} = \rho \underbrace{\begin{bmatrix} (\mathbf{A}_1^m + \mathbf{A}_2^m)_{k,k} & -(\mathbf{A}_3^m + \mathbf{A}_4^m)_{k,k} \\ (\mathbf{A}_3^m + \mathbf{A}_4^m)_{k,k}^* & (\mathbf{A}_1^m + \mathbf{A}_2^m)_{k,k}^* \end{bmatrix}}_{\mathbf{H}_k^m} \begin{bmatrix} x_{k,1}^m \\ x_{k,2}^m \end{bmatrix} + \begin{bmatrix} (\mathbf{n}_1^m)_k \\ (\mathbf{n}_2^m)_k^* \end{bmatrix} \tag{4.3.10}$$

where $\mathbf{H}_k^m$ are the equivalent channel coefficients at each terminal. They include all channel fading coefficients and timing delays. Since TWRN has two different relay paths, the equivalent channels elements of $\mathbf{H}_k^1$ and $\mathbf{H}_k^2$ are different. In the following, all elements of the two equivalent channels $\mathbf{H}^m$ are presented in addition to the related noise element vectors $\mathbf{n}_j^m$.

For the $\mathbf{H}^2$ elements, $\mathbf{A}_1^2 = \Lambda_{\mathbf{G}_1}\Lambda_{\mathbf{F}_1}$, $\mathbf{A}_2^2 = \Lambda_{\mathbf{D}_{\tau_2}}\Lambda_{\mathbf{G}_2}\Lambda_{\mathbf{F}_2}$, $\mathbf{A}_3^2 = \Lambda_{\mathbf{D}_{\tau_3}}\Lambda_{\mathbf{G}_3}\Lambda_{\mathbf{F}_3}^*$, $\mathbf{A}_4^2 = \Lambda_{\mathbf{D}_{\tau_4}}\Lambda_{\mathbf{G}_4}\Lambda_{\mathbf{F}_4}^*$ and the related noise vectors $\mathbf{n}_1^2 = \mathbf{Q}(\lambda\ [\mathbf{G}^1\mathbf{v}_1^1 + \mathbf{D}_{\tau_2}\mathbf{G}^2\mathbf{v}_1^2 - \mathbf{D}_{\tau_3}\mathbf{G}^3\mathbf{P}(\mathbf{v}_2^3)^* - \mathbf{D}_{\tau_4}\mathbf{G}^4\mathbf{P}(\mathbf{v}_2^4)^*] + \mathbf{w}_1^2)$ and $\mathbf{n}_2^2 = \mathbf{Q}(\lambda\ [\mathbf{G}^1\mathbf{v}_2^1 + \mathbf{D}_{\tau_2}\mathbf{G}^2\mathbf{v}_2^2 + \mathbf{D}_{\tau_3}\mathbf{G}^3\mathbf{P}(\mathbf{v}_1^3)^* + \mathbf{D}_{\tau_4}\mathbf{G}^4\mathbf{P}(\mathbf{v}_1^4)^*] + \mathbf{w}_2^2)$.

For the $\mathbf{H}^1$ elements, $\mathbf{A}_1^1 = \Lambda_{\mathbf{D}_{\omega_1}}\Lambda_{\mathbf{F}_1}\Lambda_{\mathbf{D}_{\delta_1}}\Lambda_{\mathbf{G}_1}$, $\mathbf{A}_2^1 = \Lambda_{\mathbf{D}_{\omega_2}}\Lambda_{\mathbf{F}_2}\Lambda_{\mathbf{D}_{\delta_2}}\Lambda_{\mathbf{G}_2}$, $\mathbf{A}_3^1 = \Lambda_{\mathbf{D}_{\omega_3}}\Lambda_{\mathbf{F}_3}\Lambda_{\mathbf{D}_{\delta_3}}^*\Lambda_{\mathbf{G}_3}^*$, $\mathbf{A}_4^1 = \Lambda_{\mathbf{F}_4}\Lambda_{\mathbf{D}_{\delta_4}}^*\Lambda_{\mathbf{G}_4}^*$ and the related noise vectors $\mathbf{n}_1^1 = \mathbf{Q}(\lambda\ [\mathbf{D}_{\omega_1}\mathbf{F}^1\mathbf{v}_1^1 + \mathbf{D}_{\omega_2}\mathbf{F}^2\mathbf{v}_1^2 - \mathbf{D}_{\omega_3}\mathbf{F}^3\mathbf{P}(\mathbf{v}_2^3)^* - \mathbf{F}^4\mathbf{P}(\mathbf{v}_2^4)^*] + \mathbf{w}_1^1)$ and $\mathbf{n}_2^1 = \mathbf{Q}(\lambda\ [\mathbf{D}_{\omega_1}\mathbf{F}^1\mathbf{v}_2^1 + \mathbf{D}_{\omega_2}\mathbf{F}^2\mathbf{v}_2^2 + \mathbf{D}_{\omega_3}\mathbf{F}^3\mathbf{P}(\mathbf{v}_1^3)^* + \mathbf{F}^4\mathbf{P}(\mathbf{v}_1^4)^*] + \mathbf{w}_2^1)$.

Also, it is noticeable that the equivalent channel coefficients of the asynchronous TWRN are different from those of the conventional asynchronous one-way relay network because the TWRN is affected by timing errors which never occur in a one-way network which are arriving of signals from the two terminals at one node at different time instants during the broadcasting phase as shown in Fig. 4.9(b).

Applying matched filter on each terminal T_m with the equivalent channel matrices $\mathbf{H}_k^m$ as in (4.3.10), the Gramian matrix $\mathbf{G}_k^m$ for each of the k sub-

carriers can be obtained as follows

$$\mathbf{G}_k^m = (\mathbf{H}_k^m)^H \mathbf{H}_k^m = \begin{bmatrix} \gamma_k^m & 0 \\ 0 & \gamma_k^m \end{bmatrix} \tag{4.3.11}$$

where γ_k^m is the channel gain such that $\gamma_k^m = \alpha_k^m + \beta_k^m$ with

$$\begin{aligned} \alpha_k^m &= \sum_{i=1}^{4} |(\mathbf{A}_i^m)_{k,k}|^2 \\ \beta_k^m &= 2\mathrm{Re}\{(\mathbf{A}_1^m)_{k,k}(\mathbf{A}_2^m)_{k,k}^*\} + 2\mathrm{Re}\{(\mathbf{A}_3^m)_{k,k}(\mathbf{A}_4^m)_{k,k}^*\} \end{aligned}$$

where α_k^m is the diversity gain and β_k^m is an interference factor due to the correlation between channel coefficients.

The average value of the channel gain can therefore be expressed as

$$\mathrm{E}\{\gamma_k^m\} = \mathrm{E}\{\alpha_k^m + \beta_k^m\} = 4 + \mathrm{E}\{\beta_k^m\} \tag{4.3.12}$$

As shown in (4.3.11), the diagonal matrix $\mathbf{G}_k^m$ proves the orthogonality for the extended STBC that we construct at each terminal, therefore the data can be extracted through using a simple fast ML decoder.

4.3.4 Feedback schemes for asynchronous two-way broadband networks

To ensure that the system performance achieves at least full cooperative diversity, the term β_k^m at each terminal T_m should be always positive. So, a simple feedback approach is proposed as in one-way scenario to achieve diversity gain in addition to the maximum possible of array gain without increasing the transmit power. It requires only two feedback links from each terminal to send back two phase shift angle vectors $\boldsymbol{\vartheta}_1^m$ and $\boldsymbol{\vartheta}_2^m$ to two particular relay nodes each transmitting different information signals, R_1 and R_3 in this case, where $\boldsymbol{\vartheta}_j^m = [(\boldsymbol{\vartheta}_1^m)_1\ (\boldsymbol{\vartheta}_1^m)_2\ ...\ (\boldsymbol{\vartheta}_1^m)_N]$ and $j = 1, 2$. So, the

transmitted signals from the first and third relay nodes are rotated by the appropriated phase angle vectors, i.e. $\mathbf{u}_1^m = e^{\boldsymbol{\vartheta}_1^m}$ and $\mathbf{u}_2^m = e^{\boldsymbol{\vartheta}_2^m}$, respectively, while the other two transmitted signals from the second and fourth relay nodes are kept unchanged. Although the original implementation was designed for a one-way network, this can be extended to a two-way network by applying the closed-loop D-EO-STBC approach for each terminal independently using the equivalent channel coefficients of each terminal $\mathbf{H}^m$. This is because in TWRN there are two different relaying paths each has different timing errors which result in different rotation angles. Specifically, the rotation angles for each subcarrier k, $(\boldsymbol{\vartheta}_1^m)_k$ and $(\boldsymbol{\vartheta}_2^m)_k$, at each terminal $m, m = 1, 2$ can be computed as

$$(\boldsymbol{\vartheta}_1^m)_k = -\angle(\mathbf{A}_1^m)_{k,k}(\mathbf{A}_2^m)_{k,k}^* \tag{4.3.13}$$

$$(\boldsymbol{\vartheta}_2^m)_k = -\angle(\mathbf{A}_3^m)_{k,k}(\mathbf{A}_4^m)_{k,k}^* \tag{4.3.14}$$

more specifically,

$$\begin{aligned}
(\boldsymbol{\vartheta}_1^2)_k &= -\angle(\Lambda_{\mathbf{G}_1}\Lambda_{\mathbf{F}_1})_{k,k}(\Lambda_{\mathbf{D}_{\tau_2}}\Lambda_{\mathbf{G}_2}\Lambda_{\mathbf{F}_2})_{k,k}^* \\
(\boldsymbol{\vartheta}_2^2)_k &= -\angle(\Lambda_{\mathbf{D}_{\tau_3}}\Lambda_{\mathbf{G}_3}\Lambda_{\mathbf{F}_3}^*)_{k,k}(\Lambda_{\mathbf{D}_{\tau_4}}\Lambda_{\mathbf{G}_4}\Lambda_{\mathbf{F}_4}^*)_{k,k}^* \\
(\boldsymbol{\vartheta}_1^1)_k &= -\angle(\Lambda_{\mathbf{D}_{\omega_1}}\Lambda_{\mathbf{F}_1}\Lambda_{\mathbf{D}_{\delta_1}}\Lambda_{\mathbf{G}_1})_{k,k}(\Lambda_{\mathbf{D}_{\omega_2}}\Lambda_{\mathbf{F}_2}\Lambda_{\mathbf{D}_{\delta_2}}\Lambda_{\mathbf{G}_2})_{k,k}^* \\
(\boldsymbol{\vartheta}_2^1)_k &= -\angle(\Lambda_{\mathbf{D}_{\omega_3}}\Lambda_{\mathbf{F}_3}\Lambda_{\mathbf{D}_{\delta_3}}^*\Lambda_{\mathbf{G}_3}^*)_{k,k}(\Lambda_{\mathbf{F}_4}\Lambda_{\mathbf{D}_{\delta_4}}^*\Lambda_{\mathbf{G}_4}^*)_{k,k}^*
\end{aligned}$$

From the above equations, it is clear that $(\boldsymbol{\vartheta}_1^2)_k \neq (\boldsymbol{\vartheta}_1^1)_k$ and $(\boldsymbol{\vartheta}_2^2)_k \neq (\boldsymbol{\vartheta}_2^1)_k$. Therefore, the rotation weighted values at each subcarrier k are different, i.e. $(\mathbf{u}_1^2)_k \neq (\mathbf{u}_1^1)_k$ and $(\mathbf{u}_2^2)_k \neq (\mathbf{u}_2^1)_k$. So, to achieve full diversity gain together with the maximum array gain at each terminal in the TWRN scenario, this new scheme proposes to apply the feedbacks independently during the cooperation phase which require two time slots to complete the two-way transmission process. So, the proposed system is designed to work on a three-time-slot basis as shown in Fig.4.10 where the first time slot is specified

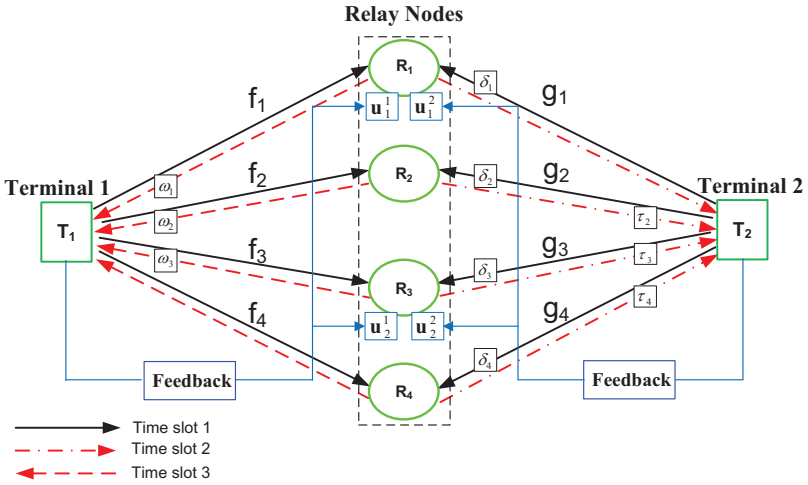

Figure 4.10. Two-way wireless relay network with feedback links from each terminal to certain two relay nodes.

for the broadcasting phase while the other two time slots are specified for the cooperation phase as depicted in Table 4.3. At the first time slot during the relaying phase, the relay nodes apply only the feedbacks received from T_2, i.e. the transmitted signals from the first and third relay nodes are rotated by $\mathbf{u}_1^2 = e^{\boldsymbol{\vartheta}_1^2}$ and $\mathbf{u}_2^2 = e^{\boldsymbol{\vartheta}_2^2}$, respectively. During this time, T_1 switches to off mode or does not receive these forward signals. In the second such time slot, the relay nodes apply only the feedbacks received from T_1, i.e. the transmitted signals from the first and third relay nodes are rotated by $\mathbf{u}_1^1 = e^{\boldsymbol{\vartheta}_1^1}$ and $\mathbf{u}_2^1 = e^{\boldsymbol{\vartheta}_2^1}$, respectively. During this time, T_2 switches to off mode. In so doing, it is ensured that the two terminals achieve maximum performance, i.e. full cooperative diversity and array gain. The processes performed over the four relay nodes during the relaying phase are summarized in Table 4.4.

Table 4.3. Time slots required for a two-way cooperative relay network equipped with four relays where each time slot corresponds to two symbol periods

Broadcasting Phase	Relaying Phase	
$T_1, T_2 \rightarrow R_1, R_2, R_3, R_4$	$R_1, R_2, R_3, R_4 \rightarrow T_2$	$R_1, R_2, R_3, R_4 \rightarrow T_1$
1 time slot	1 time slot	1 time slot

Table 4.4. Block coding over the four relay nodes during the Relaying phase for two-way broadband scenario

Relaying phase		Relay Nodes			
duration	Symbol	R_1	R_2	R_3	R_4
1 time slot	1	$\text{IFFT}(\mathbf{u}_1^2 \circ \mathbf{y}_{11})$	$\mathbf{y}_{21}$	$-\text{IFFT}(\mathbf{u}_2^2 \circ \mathbf{y}_{32}^*)$	$-\zeta(\mathbf{y}_{42}^*)$
	2	$\text{IFFT}(\mathbf{u}_1^2 \circ \mathbf{y}_{12})$	$\mathbf{y}_{22}$	$\text{IFFT}(\mathbf{u}_2^2 \circ \mathbf{y}_{31}^*)$	$\zeta(\mathbf{y}_{41}^*)$
1 time slot	1	$\text{IFFT}(\mathbf{u}_1^1 \circ \mathbf{y}_{11})$	$\mathbf{y}_{21}$	$-\text{IFFT}(\mathbf{u}_2^1 \circ \mathbf{y}_{32}^*)$	$-\zeta(\mathbf{y}_{42}^*)$
	2	$\text{IFFT}(\mathbf{u}_1^1 \circ \mathbf{y}_{12})$	$\mathbf{y}_{22}$	$\text{IFFT}(\mathbf{u}_2^1 \circ \mathbf{y}_{31}^*)$	$\zeta(\mathbf{y}_{41}^*)$

Therefore, the received signals $\mathbf{r}_j^m$ at each terminal T_m are given by

$$\mathbf{r}_j^m = \rho\, \mathbf{h}_j^m \mathbb{U}^m \mathbf{c}_j^m + \mathbf{n}_j^m \tag{4.3.15}$$

with

$$\begin{aligned}
\mathbf{h}_1^m &= [\ \mathbf{A}_1^m \quad \mathbf{A}_2^m \quad -\mathbf{A}_3^m \quad -\mathbf{A}_4^m\ ] \\
\mathbf{h}_2^m &= [\ \mathbf{A}_3^m \quad \mathbf{A}_4^m \quad \mathbf{A}_1^m \quad \mathbf{A}_2^m\ ] \\
\mathbf{c}_1^{\bar{m}} &= [\ \mathbf{x}_1^{\bar{m}} \quad \mathbf{x}_1^{\bar{m}} \quad \mathbf{x}_2^{\bar{m}} \quad \mathbf{x}_2^{\bar{m}}\ ]^T \\
\mathbf{c}_2^{\bar{m}} &= [\ (\mathbf{x}_1^{\bar{m}})^* \quad (\mathbf{x}_1^{\bar{m}})^* \quad (\mathbf{x}_2^{\bar{m}})^* \quad (\mathbf{x}_2^{\bar{m}})^*]^T \\
\mathbb{U}^m &= \begin{bmatrix} \mathbf{U}_1^m & & & \\ & \mathbf{I}_N & & \\ & & \mathbf{U}_2^m & \\ & & & \mathbf{I}_N \end{bmatrix}
\end{aligned}$$

The weighted array $\mathbb{U}^m$ is a diagonal array of diagonal matrices $\mathbf{U}_1^m, \mathbf{I}_N, \mathbf{U}_2^m$ and $\mathbf{I}_N$ where $\mathbf{U}_j^m = diag(\mathbf{u}_j^m)$ and $\mathbf{I}_N$ is the identity matrix of size $N \times N$. As shown, the diagonal weighted array $\mathbb{U}^m$ is applied on relay nodes to align two transmitted signals which result in achieving array gain. The equivalent channel at each terminal T_m, $\dot{\mathbf{H}}_k^m$, is therefore given by

$$\dot{\mathbf{H}}_k^m = \begin{bmatrix} (\mathbf{u}_1^m)_k (\mathbf{A}_1^m)_{k,k} + (\mathbf{A}_2^m)_{k,k} & -(\mathbf{u}_2^m)_k (\mathbf{A}_3^m)_{k,k} - (\mathbf{A}_4^m)_{k,k} \\ (\mathbf{u}_2^m)_k^* (\mathbf{A}_3^m)_{k,k}^* + (\mathbf{A}_4^m)_{k,k}^* & (\mathbf{u}_1^m)_k^* (\mathbf{A}_1^m)_{k,k}^* + (\mathbf{A}_2^m)_{k,k}^* \end{bmatrix} \tag{4.3.16}$$

where $(\mathbf{u}_1^m)_k = e^{j(\boldsymbol{\vartheta}_1^m)_k}$ and $(\mathbf{u}_2^m)_k = e^{j(\boldsymbol{\vartheta}_2^m)_k}$.

Consequently, $\alpha_k^m = \sum_{i=1}^4 |(\mathbf{u}_1^m)_k|^2 | (\mathbf{A}_i^m)_{k,k}|^2$ and $\beta_k^m = 2\ \mathrm{Re}\{(\mathbf{u}_1^m)_k (\mathbf{A}_1^m)_{k,k}(\mathbf{A}_2^m)_{k,k}^*\} + 2\mathrm{Re}\{(\mathbf{u}_2^m)_k(\mathbf{A}_3^m)_{k,k}(\mathbf{A}_4^m)_{k,k}^*\}$ taking into account that $|(\mathbf{u}_1^m)_k|^2 = |(\mathbf{u}_2^m)_k|^2 = 1$. This process ensures that the values of β_k^m are always non-negative which means that the system can obtain additional performance gain (i.e. array gain). The advantage of the exact phase feedback scheme can be retained by applying independently in two time slots the two quantization strategies as in one-way broadband scenario that can significantly reduce the feedback overhead thereby yielding a more practical scheme.

On the other hand, to obtain end-to-end unity code rate, the system can be designed to employ a two-time slot framework based on exploiting the feedback information of only one terminal, i.e. two feedback links from only one terminal are required. By this way, the system can achieve end-to-end full rate with full cooperative diversity at the exploited terminal while the end-to-end BER performance of the other terminal will be better than the open-loop scheme but the diversity order is not full.

Similarly, a closed-loop D-EO-STBC scheme for asynchronous two-way three relay broadband system can be designed where the two terminals apply the same implementations as mentioned in the case of using four relay nodes while the three relay nodes have the option to select any three columns from the four given below in the Relay Nodes section in Table 4.4 to process their received signals. By doing so, the design of the closed-loop system for three relay nodes equipped only with one feedback link from each terminal and that is adequate to achieve end-to-end transmission rate of 2/3 and full cooperative diversity with array gain at each terminal.

4.4 Simulation Results

The performances of the proposed schemes have been studied via numerical simulation and a comparison with previous schemes is provided. For the consistency within the thesis, end-to-end BER is used as the performance measure instead of end-to-end frame error rate (FER). In the simulation, the source transmits quadrature phase-shift keying (QPSK) symbols with power allocation following equation (4.2.2). The transmit power is fixed and identical for all schemes used in the comparisons. All CSIs are assumed to be perfectly known at the destination. The length of N-point OFDM is 64 and the length of CP is 16. The delay is chosen randomly from the range 0 to 15 with uniform distribution for the narrowband scenario, where the Rayleigh fading channels are assumed to be flat, while the delay is chosen randomly from 0 to 6 with uniform distribution for the broadband scenario, where the Rayleigh fading channels are assumed to be 11 tap frequency-selective channels. The length of the frequency-selective channels is chosen here to be the same as the previous works used in the simulation for fairness comparison.

4.4.1 Simulation results for one-way narrowband system scenario

In Fig. 4.11, the end-to-end BER performance of the proposed closed-loop D-EO-STBC for four relay nodes is shown. Also, the equivalent BER performances of the previous AF Alamouti-OFDM scheme [81] and DF OFDM scheme [75] are depicted on the same figure. The DF OFDM scheme either applies Alamouti-OFDM transmission over the two relays if they can successfully decode the information symbols or applies single-input single-output(SISO) OFDM scheme over one relay if only one relay can successfully decode the information symbols, otherwise the information symbols are not forwarded to the destination and the decoding process completely fails.

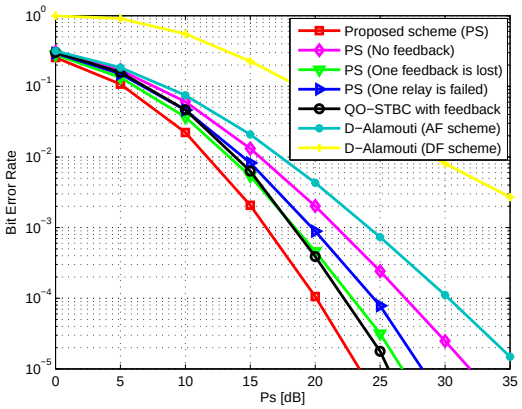

Figure 4.11. Comparison of end-to-end BER performance of the proposed AF asynchronous scheme for a four relay network using exact feedback channel information with previous asynchronous schemes in a wireless relay narrowband system.

The results are depicted in Fig. 4.11 and confirm that the robust proposed scheme significantly improves the BER performance over the previous schemes. For example, at a BER of 10^{-4}, the proposed scheme requires $P_s \approx 20$ dB while the AF Alamouti-OFDM and DF OFDM schemes require 30 dB and 48 dB (off plot), respectively. Also, it is clear that if one of the feedback channels, or all of them, are lost or one of the relay nodes fails completely, the proposed scheme improves the BER performance over the previously mentioned two schemes for the whole source transmit power range; thereby ensuring a more robust transmission scheme.

The figure also provides a comparison of the proposed scheme with the closed-loop distributed quasi-orthogonal STBC (D-QO-STBC) scheme [82] for four relays, where it is clearly noticed that the proposed scheme outperforms the closed-loop D-QO-STBC scheme. In particular, at a BER of 10^{-4}, the proposed scheme provides approximately 2 dB improvement. This improvement is because in the proposed scheme the limited feedback is used to leverage the channel gain to the maximum so there is full cooperative diversity gain of order four and array gain while in D-QO-STBC scheme it

was used to achieve the orthogonality of the transmission code so there is only full cooperative diversity. In addition to that, the proposed scheme requires only half that required in the D-QO-STBC scheme to decode the transmitted data. As such, it is more robust to changes in the wireless channel and also more suitable and appropriate for real-time communication applications. Moreover, the proposed scheme with only one feedback link provides better performance than the D-QO-STBC scheme at a lower transmit power range up to approximately 17 dB where the improvement is switched to the D-QO-STBC scheme.

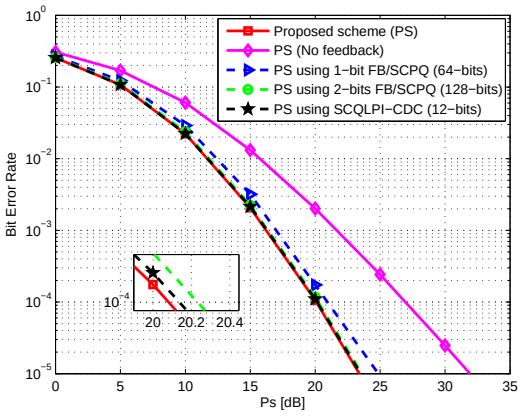

Figure 4.12. Comparison of end-to-end BER performance of the proposed AF asynchronous scheme using quantized channel information in a narrowband network.

The performances of the proposed scheme with the 2-bit FB/SCPQ, 1-bit FB/SCPQ, and the low-rate SCQLPI-CDC feedback schemes are depicted in Fig. 4.12. Very little degradation in BER performance in the case of using the low-rate SCQLPI-CDC scheme is shown as compared with the performance of the scheme when the un-quantized feedback is used, while a slight decrease in the performance is observed in the case of using the 2-bit FB/SCPQ and 1-bit FB/SCPQ schemes. Furthermore, it is seen that the performance of the new low-rate SCQLPI-CDC feedback scheme outperforms the 64-bits and 128-bits feedback schemes. For example, at a

BER of 10^{-4}, the low-rate feedback scheme requires 20.15 dB while the 64-bits/feedback link and 128-bits/feedback link schemes require 20.25 dB and 21 dB, respectively, although the new scheme only used a 12-bits/feedback link. So, the new low-rate SCQLPI-CDC scheme achieves both better BER performance and a substantial reduction in the feedback overhead, i.e. a saving of 90.6% as compared with 2-bit FB/SCPQ scheme. Moreover, the schemes with quantized feedback still provide significantly better performance than that of the previous schemes.

4.4.2 Simulation results for one-way broadband system scenario

In this section, the end-to-end BER performance of the proposed asynchronous D-EO-STBC scheme over frequency-selective Rayleigh fading channels for four relay nodes is presented. The results depicted in Fig. 4.13 confirm that the proposed robust scheme significantly improves the end-to-end BER performance over the previous scheme [21] proposed for two relays. For example, at a BER of 10^{-4}, the proposed scheme requires $P_s \approx 20$ dB while the previous two-relay scheme requires 30 dB. Furthermore, the proposed scheme outperforms the previous scheme even when the system lost one or both feedback links or one of the relays falls completely which means the proposed scheme adds more robustness for the transmission link. This improvement is because by using the feedback the proposed scheme can achieve full cooperative diversity gain of order four and array gain while the previous scheme [21] just achieves full cooperative diversity of order two.

The figure also provides a comparison of the proposed asynchronous scheme over frequency-selective fading channels with the proposed D-EO-STBC scheme over flat fading channels for four relays, where it is clearly noted that both schemes have almost the same BER performance which verifies that the the proposed asynchronous scheme can completely overcome the effects of timing errors and multipath fading for the test environment.

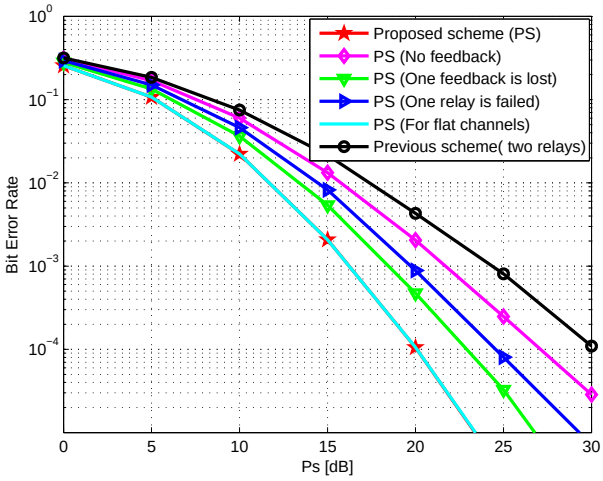

Figure 4.13. Comparison of end-to-end BER performance of the proposed AF asynchronous scheme over frequency-selective 11 tap channels using exact feedback channel information with previous asynchronous schemes in wireless relay broadband system.

The performances of the proposed scheme with direct (2-bits and 1-bit

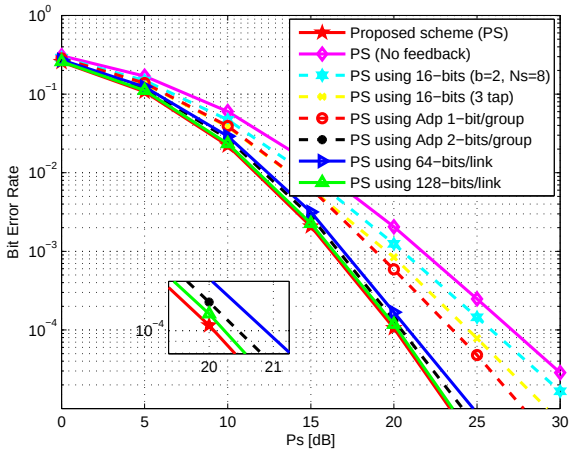

Figure 4.14. Comparison of end-to-end BER performance of the proposed AF asynchronous scheme over frequency-selective 11 tap channels using quantized channel information.

for each subcarrier phase) and group quantization schemes are depicted in Fig. 4.14. It is observed that for the 2-bits/subcarrier phase, there is very little degradation in BER performance as compared with the performance of

the scheme when the un-quantized feedback is used, while a slight decrease in the performance is observed in the case of using 1-bit/subcarrier phase. For example, at 10^{-4}, the scheme with un-quantized feedback provides approximately 0.25 dB improvement over 2-bits/subcarrier phase scheme and 1 dB over the 1-bit/subcarrier phase scheme. In fact, the difference between the un-quantized and the direct quantization schemes is in the array gain because the un-quantized scheme achieves the largest array gain while the higher quantization level in the direct quantization scheme provides higher array gain. Therefore, the direct quantization strategy ensures that full diversity is achieved with a more practical feedback scheme. On the other hand, the group feedback strategy improves the system BER performance as compared with the system with no feedback. In particular, at a BER of 10^{-4}, a fixed group feedback scheme with total feedback overhead of 16 bits/feedback link (2-bits/group) provides approximately 1.25 dB improvement as compared with the system without using feedback. In fact, the fixed group feedback scheme can achieve better performance when the channel length decreases. For example, the power required to achieve the BER of 10^{-4} with 11 tap channels is 26 dB while 24.5 dB is required when the channel length decreases to 3 taps; therefore saving 2.5 dB. On the other hand, the adaptive group scheme outperforms the system with fixed group feedback but at the expense of increasing the feedback overhead. In fact, the adaptive group feedback scheme provides substantially better performance when the quantization level increases. For example, for the adaptive group scheme with 2 bits/group, the system behaves close to the system performance with the 2-bits/subcarrier phase and better than the system performance with 1-bit/subcarrier phase with less requirement of feedback overhead than both of them. Finally, the schemes with quantized feedback provide significantly better performance than the system without feedback and the previous two-relays scheme [21].

4.4.3 Simulation results for two-way broadband system scenario

In this section, some simulation results for the asynchronous two-way D-EO-STBC proposed scheme are shown and a comparison with previous asynchronous schemes is provided. The two terminals transmit symbols with uncoded OFDM using a 64 point FFT. The data symbols are drawn from QPSK. The transmit power follows equation (4.3.1) and the CP lengths l_{cp_1} and l_{cp_2} are 16. The delay is chosen randomly from 0 to 8 with uniform distribution. Due to the symmetry, only the end-to-end BER performance of T_1 to T_2 is shown. However, the end-to-end BER performance of T_2 to T_1 is the same.

In Fig. 4.15, the end-to-end BER performance of the proposed scheme is compared with the previous asynchronous D-OSTBC scheme developed for four relay nodes in [90] over frequency-selective 2 tap channels. For fair comparison, the total average terminal and relays transmit power of the two schemes are the same. In fact, the two schemes need the same number of time slots to transmit the data symbols to the two terminals so they achieve the same data rate. The simulation results in Fig. 4.15 confirm that the proposed scheme significantly improves the BER performance over the previous scheme. For example, at BER of 10^{-4}, the proposed scheme provides approximately 0.7 dB improvement which means the proposed scheme adds more robustness for the transmission link. This improvement is because in the proposed scheme the feedback channels are used to leverage the channel gain to the maximum so there is full cooperative diversity gain of order four and array gain while in the previous scheme there is only full cooperative diversity. The figure also presents the BER performance for the proposed asynchronous two-way scheme for three relay nodes. This scheme is designed to utilize only one feedback link. It is clear that this scheme provides better BER performance than the two-way system with four relays but without feedback. For example, at BER of 10^{-4}, the proposed scheme for three relays

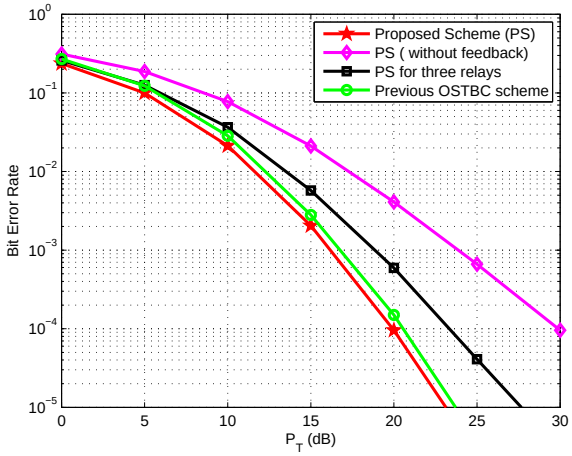

Figure 4.15. Comparison of end-to-end BER performance of the proposed D-EO-STBC scheme with the previous D-OSTBC scheme in TWRNs over frequency-selective two tap channels.

provides an improvement of approximately 7 dB over the four relay system without feedback.

In Fig. 4.16, the end-to-end BER performance of the proposed asyn-

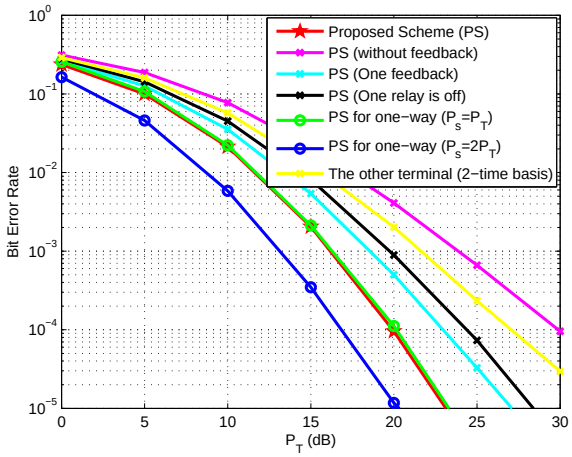

Figure 4.16. Comparison of end-to-end BER performance of the proposed two-way D-EO-STBC scheme with the proposed one-way scheme over frequency-selective 8 tap channels.

chronous two-way scheme is compared with the proposed asynchronous one-way scheme over frequency-selective 8 tap channels. The simulation of the

proposed one-way scheme was undertaken twice. At the beginning, the transmit power of the source node in the one-way system is set to equal to the transmit power for each terminal in the two-way system, i.e. $P_s = P_T$, and then repeated when the total transmit power for the one-way system is set to equal to the total power for the two-way system, i.e. $P_s = 2P_T$. As shown in Fig. 4.16, the proposed two-way scheme BER performance is almost the same as the proposed one-way scheme when $P_s = P_T$ while the proposed one-way scheme BER performance outperforms the proposed two-way scheme when $P_s = 2P_T$. For example, at BER of 10^{-4}, the proposed two-way scheme and the proposed one-way scheme require the same transmit power of 20 dB when $P_s = P_T$ while the proposed one-way scheme provides an improvement of 3 dB when $P_s = 2P_T$. From Fig. 4.16, it is clear that the slope of the BER curve of the proposed two-way scheme approaches the slope of the proposed one-way scheme when P_T increases. It implies that the proposed two-way system can achieve diversity order four when P_T is large. On the other hand, the proposed two-way scheme can achieve maximum end-to-end 2/3 data rate while the maximum end-to-end data rate that the proposed one-way scheme can achieve is half rate. In fact, the proposed two-way scheme can achieve maximum full data rate (i.e. unity rate) when a two-time slots basis is used, where two particular relay nodes apply only the feedback of terminal 1 or the feedback of terminal 2 before the relay nodes broadcast their signals to the two terminals at the same time. In this case, the BER performance at the two terminals will be different where the BER performance at the terminal where its feedback is exploited will be the same as in the case of using three-time slots framework which is better than the performance of the other terminal but the other terminal performance will be better than the performance of the open-loop scheme as depicted in Fig. 4.16.

The performance of the proposed two-way scheme if one of the relay nodes

fails completely or one of the feedback links is lost is also depicted in Fig. 4.16. It is clear that the scheme still extracts data; therefore ensuring a more robust transmission scheme. Furthermore, it improves the BER performance over that without feedback channels. For example, at BER of 10^{-4}, the proposed two-way scheme with one feedback link and with one relay off requires approximately 23 dB and 24 dB, respectively, while the two-way scheme without feedback requires 30 dB.

4.5 Summary

This work proposed distributed one-way and two-way systems for asynchronous cooperative networks that utilize distributed extended orthogonal space-time type block coding with partial low-rate feedback channels. The feedback schemes were based on phase rotation to certain relay nodes. The proposed schemes can achieve full cooperative diversity and array gain which results in improving the robustness of the wireless link between the transmitter and receiver sides in the presence of multipath fading and timing offset. In particular, the proposed scheme for two-way system requires an additional time-slot during the cooperation phase to extract full cooperative diversity and array gain at each terminal node. However, the proposed scheme for two-way scenario provided better end-to-end data rate, i.e. equal to 2/3, as compared to the one-way scenario, i.e. equal to 1/2. To minimize the feedback overhead, low-complexity based quantization feedback schemes which make these schemes more practical were suggested. Simulation results were used to show the performance improvements resulting from the proposed schemes. These result were very encouraging since there was no requirement to increase the transmit power or system bandwidth, and the information symbols can be decoded separately in a very simple manner.

On the other hand, the channel gains between the source and destina-

tion nodes are different from one link to another due to the random nature of the wireless environment which induces different attenuations into the signals received at the destination, thereby reducing the overall system performance. In fact, it is possible to exploit this variation in channels gain to add extra improvements to the system by using selection techniques. In the next chapter, relay selection techniques are exploited to enhance the system performance which can restrict the transmission process over only the best channel links.

Chapter 5

RELAY SELECTION IN COOPERATIVE RELAY NETWORKS BASED ON DISTRIBUTED SPACE-TIME BLOCK CODING

In this chapter, a two-hop relay network equipped with four half-duplex single antenna relay nodes is considered. More specifically, it is assumed that the relay nodes are able to operate with three power levels to exploit the available power effectively. In such a setting, a robust orthogonal space-time block coded (O-STBC) relay selection scheme is introduced. In particular, two different methods for use in the selection process have been proposed. In the first method, the four relays are grouped into two subsets of two relays, each having identical encoding process in terms of the construction of a distributed extended O-STBC (D-EO-STBC). The best two relays are selected based on the overall path gain and then Alamouti coding in a distributed manner is applied over the selected two relays. In the second method, the selection process deals with the four relays as one group and selects the best

three relay links based on the overall path gain. The selected three relays then construct the D-EO-STBC code form at the destination node. At the end of this chapter, the system performance for these two methods will be studied in terms of pairwise error probability (PEP) and end-to-end bit error rate (BER).

5.1 Introduction

Cooperative diversity approaches have been shown to provide substantial enhancement of the system data rate or reliability with extending coverage and avoiding shadow fading [8] and [49]. In fact, these approaches can achieve the same diversity benefits as in multi-input multi-output (MIMO) systems without needing multiple antennas at individual nodes by using distributed antennas [53] and [96]. In MIMO systems, the system hardware complexity and consequently the cost are challenges to practical application [120]. So, MIMO systems use transmit antenna selection (TAS) schemes to efficiently solve this problem and achieve high system performance [120] and [121]. Furthermore, TAS schemes combined with space-time coding (STC) have been proposed as in [122] and [123]. In particular, the authors in [122] proposed a scheme to combine TAS with space-time block coding (STBC), in which $N-1$ out of all N transmit antennas are selected to transmit data using an extended orthogonal STBC.

However, in cooperative wireless relay systems, the cooperative relay nodes have different locations so each transmitted signal from the source node to the destination node must pass through different paths causing different attenuations within the signals received at the destination which results in reducing the overall system performance. So, to minimize this effect and benefit from cooperative communication, certain paths should be avoided by using selection techniques. In fact, the selection techniques offer the

possibility to improve the system performance whilst reducing the system computational complexity. Recently, relay selection techniques for cooperative systems have been studied [91], [92], [93], [94], [95] and [97]. Most of the previous studies are based on selecting one relay to cooperate with the direct path between the source and the destination nodes.

In this work, two new robust relay selection methods for cooperative relay systems are proposed. The considered system is assumed to consist of four single antenna relay nodes and the relays are able to operate with three power levels. Also, the considered system is assumed to use an amplify-and-forward (AF) type relaying protocol and there is no direct path between the source and the destination. The optimum power allocation in [67] is adopted in the proposed methods as next described. The two methods use grouping criteria where the first method divides the relay nodes into two groups based on the relay encoding process while the second method considers the relay nodes as one group. The selected two relays based on the first method apply the distributed Alamouti (D-Alamouti) code [23], [52] while the selected three relays based on the second method apply the D-EO-STBC technique proposed in [118]. The proposed grouping criteria are designed to maximize the instantaneous received signal-to-noise ratio (SNR) for each transmitted symbol, and correspondingly to minimize the probability of bit error. It is shown by simulation that system gain benefits can be retained as if all the relay nodes were in use.

5.2 System Model and Problem Statement

Consider a wireless relay system with one source node, one destination node and four half-duplex single antenna relay nodes as shown in Fig. 5.1. All nodes are equipped with a single antenna. All channels are assumed to be quasi-static flat Rayleigh fading channels. The channel impulse responses

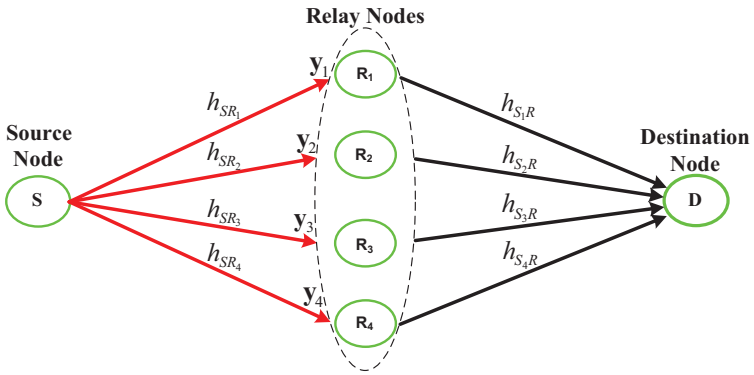

Figure 5.1. Wireless relay network with single source and destination together with four half-duplex relay nodes.

(CIRs) for $S \rightarrow R_i$ and $R_i \rightarrow D$ links are given by h_{SR_i} and h_{R_iD}. The CIRs are independent identically distributed (i.i.d.) zero mean circular Gaussian random variables with unit variances. All relays and destination node noises are modeled as i.i.d. additive white Gaussian noise (AWGN) with unity variance, i.e. $\mathcal{CN}(0, 1)$.

For each transmission, P_s is the power used at the source, P_r is the power used at each relay and P is the total average power such that $P_s = RP_r = \frac{P}{2}$ as in [67] where R is the number of relays. The STBC signals are generated over the relay nodes. The channel state information (CSI) is assumed to be perfectly known at the destination receiver through training. The receiver informs the relay nodes according to the latest CSI through a feedback channel with low complexity.

However, since the cooperative four relay nodes have different locations each transmitted signal from the source node to the destination node follows different paths which induce different attenuations into the signals received at the destination, thereby reducing the overall system performance. So, to tackle this challenging problem and benefit from cooperative communica-

tion, cooperation based on a relay selection technique is proposed. By using this effective scheme, certain paths which induce much attenuation are completely avoided. In fact, minimizing the number of paths, and consequently the number of relays, will minimize the computational complexity and consequently the cost which makes this scheme much more practically attractive. Moreover, cooperation based on a selection technique will save bandwidth and reduce the interference to other users as a result of reducing the number of operational relays.

5.3 Conventional D-EO-STBC Scheme for Wireless Relay Systems

The conventional D-EO-STBC scheme uses the available four relay nodes without employing feedback or relay selection techniques as follows. The source node broadcasts the information bits which are encoded into two symbols $\mathbf{s} = [s_1 \ s_2]^T$ over two time intervals, $j = 1, 2$, where $(.)^T$ denotes vector transpose. The received information signals at relay i and time interval j, y_{ij}, can be written as

$$y_{ij} = \sqrt{P_s} h_{SR_i} s_j + v_{ij} \quad \text{where} \quad i = 1, ..., 4 \tag{5.3.1}$$

where v_{ij} is the ith relay AWGN for the time instant j.

The relay nodes then process the received information signals, y_{ij}, according

Table 5.1. Coding process over the relay nodes for the conventional D-EO-STBC scheme during the relaying phase.

	Relay Nodes			
Symbol duration	R_1	R_2	R_3	R_4
Symbol 1	y_{11}	y_{21}	$-y_{32}^*$	$-y_{42}^*$
Symbol 2	y_{12}	y_{22}	y_{31}^*	y_{41}^*

to Table 5.1 to generate distributively the following D-EO-STBC codeword

at the destination receiver

$$\mathbf{S} = \begin{bmatrix} s_1 & s_1 & -s_2^* & -s_2^* \\ s_2 & s_2 & s_1^* & s_1^* \end{bmatrix} \tag{5.3.2}$$

where $(.)^*$ denotes the complex conjugation process.

At the destination node, the received signals over two time intervals, denoted by r_1 and r_2 respectively, can be written as

$$\begin{bmatrix} r_1 \\ r_2 \end{bmatrix} = \sqrt{\frac{P_s P_r}{P_s+1}} \underbrace{\begin{bmatrix} s_1 & s_1 & -s_2^* & -s_2^* \\ s_2 & s_2 & s_1^* & s_1^* \end{bmatrix}}_{\mathbf{S}} \begin{bmatrix} h_1 \\ h_2 \\ h_3 \\ h_4 \end{bmatrix} + \begin{bmatrix} n_1 \\ n_2 \end{bmatrix} \tag{5.3.3}$$

where $h_{(i=1,2)} = h_{SR_i} h_{R_i D}$ and $h_{(i=3,4)} = h_{SR_i}^* h_{R_i D}$. The noise components $n_1 = \sqrt{\frac{P_r}{P_s+1}}(\sum_{i=1}^{2} h_{R_i D} v_{i1} - \sum_{i=3}^{4} h_{R_i D} v_{i2}^*) + w_1$ and $n_2 = \sqrt{\frac{P_r}{P_s+1}}(\sum_{i=1}^{2} h_{R_i D} v_{i2} + \sum_{i=3}^{4} h_{R_i D} v_{i1}^*) + w_2$ where w_1 and w_2 are the receiver AWGN over two time instants, respectively. Equivalently, the received signals r_1 and r_2^* can be expressed as

$$\begin{bmatrix} r_1 \\ r_2^* \end{bmatrix} = \sqrt{\frac{P_s P_r}{P_s+1}} \underbrace{\begin{bmatrix} h_1+h_2 & -(h_3+h_4) \\ (h_3+h_4)^* & (h_1+h_2)^* \end{bmatrix}}_{\mathbf{H}} \begin{bmatrix} s_1 \\ s_2^* \end{bmatrix} + \begin{bmatrix} n_1 \\ n_2^* \end{bmatrix} \tag{5.3.4}$$

Therefore,

$$\mathbf{r} = \sqrt{\frac{P_s P_r}{P_s+1}} \mathbf{H}\mathbf{s} + \mathbf{n} \tag{5.3.5}$$

where $\mathbf{H}$ denotes the equivalent channel matrix. The maximum likelihood decision variables for symbols s_1 and s_2 are then computed as

$$\begin{bmatrix} \tilde{s}_1 \\ \tilde{s}_2^* \end{bmatrix} = \mathbf{H}^H \mathbf{H} \begin{bmatrix} s_1 \\ s_2^* \end{bmatrix} + \mathbf{H}^H \begin{bmatrix} n_1 \\ n_2^* \end{bmatrix} \tag{5.3.6}$$

where $(.)^H$ denotes Hermitian transpose.

The effective noise power calculated from the noise terms is equal to $\mathrm{E}\{|n_1|^2\}=$

$mathrmE\{|n_2^*|^2\} = \mathrm{E}\{\frac{P_r}{P_s+1}\sum_{i=1}^{4}|h_{R_iD}|^2+1\} = \frac{4P_r}{P_s+1}+1$. To aid in the later analysis, the signals within $\mathbf{r}$ are normalized so that their noise variance is unity.

$$\mathbf{r} = \sqrt{\frac{\sigma_{\mathbf{s}}^2}{\sigma_{\mathbf{n}}^2}}\mathbf{H}\mathbf{s} + \mathbf{n} \tag{5.3.7}$$

where $\frac{\sigma_{\mathbf{s}}^2}{\sigma_{\mathbf{n}}^2} = \frac{P_sP_r}{P_s+4P_r+1}$.

From (7.5.17), the Gramian matrix $\mathbf{G}$ which represents the term $\mathbf{H}^H\mathbf{H}$ is equal to

$$\mathbf{G} = \mathbf{H}^H\mathbf{H} = \begin{bmatrix} \gamma & 0 \\ 0 & \gamma \end{bmatrix} \tag{5.3.8}$$

where γ is the channel gain such that

$$\gamma = \alpha + \beta = \sum_{i=1}^{4}|h_i|^2 + \beta_1 + \beta_2 \tag{5.3.9}$$

where $\beta = \beta_1 + \beta_2$ which is composed of the interference factors due to channels correlation, $\beta_1 = h_1^*h_2 + h_2^*h_1 = 2\mathrm{Re}\{h_2^*h_1\}$ and $\beta_2 = h_3h_4^* + h_4h_3^* = 2\mathrm{Re}\{h_3h_4^*\}$. Therefore, β might take positive or negative values. The operator $|.|^2$ denotes the modulus squared of a complex number and $Re\{.\}$ its real part. The SNR for the system can be found as

$$SNR = \gamma\frac{\sigma_{\mathbf{s}}^2}{\sigma_{\mathbf{n}}^2} = (\sum_{i=1}^{4}|h_i|^2 + \beta_1 + \beta_2)\frac{\sigma_{\mathbf{s}}^2}{\sigma_{\mathbf{n}}^2} \tag{5.3.10}$$

Clearly, the channel realizations (h_1, h_2, h_3, h_4) for the system paths affect the SNR gain of the system. So, selecting the best relay paths from source to destination in such a way that also exploits the cooperative diversity offered by D-STBC will result in improving the SNR gain and consequently the system performance. In the following, two effective methods based on relay

selection techniques combined with simple three level power adaptation are proposed.

5.4 Relay Selection Technique for Wireless Relay Networks

Each relay has three power levels: zero, normal power value according to the optimal power allocation proposed in [67] and maximum power which is double the normal power. In the proposed schemes, the total system power, which is calculated based on normal power, should be constant. So, to switch one relay to use its maximum power means the status of one different relay is switched off. Two relay selection techniques are proposed to determine the best relays which can use their maximum power as follows:-

5.4.1 Two-groups method

In this method, the system relay nodes are divided into two groups each group consists of two relay nodes and each having the same encoding process in terms of the construction of D-EO-STBC (in this analysis, it is assumed that R_1 and R_2 are in one group while R_3 and R_4 are in the other group) as shown in Fig. 5.2. According to the CSI, the destination receiver can determine the best link which has the maximum path gain for each group so the system can use it for the transmitted data. After that, the receiver informs the relays to stop sending from the two worst relays that have the smallest path gains and switches the power of the best relays to the maximum (in other words, transferring the power of the worst relays to the best relays) to exploit efficiently the available power. Therefore, the wireless relay system will work with only two relay nodes and each of them performs the appropriate encoding process according to Table 5.1 taking into account that the transmit power of each of them has changed to the maximum power. As a result, a D-Alamouti code will be generated at the destination node. For ex-

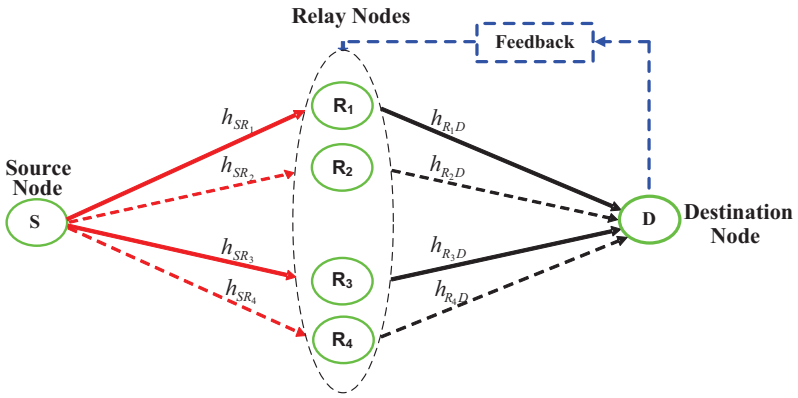

Figure 5.2. Wireless relay system with feedback links to select the suitable relays based on the two-groups method where the solid lines mean the selected paths.

ample, suppose the paths passing through relay 1 and 3 have the maximum path gains, i.e. $|h_1|^2 \geq |h_2|^2$ in group 1 and $|h_3|^2 \geq |h_4|^2$ in group 2. Therefore, the system stops transmitting from R_2 and R_4 while the relay nodes R_1 and R_3 are working with their maximum powers. The operational relays perform the encoding process as in Table 5.2 which is a modified version of Table 5.1 to generate the D-Alamouti code at the destination. The double

Table 5.2. D-Alamouti encoding process over the operational two relays.

	Working Relay Nodes			
Symbol duration	R_1	R_2	R_3	R_4
Symbol 1	$\sqrt{2}y_{11}$	0	$-\sqrt{2}y_{32}^*$	0
Symbol 2	$\sqrt{2}y_{12}$	0	$\sqrt{2}y_{31}^*$	0

power of the transmitted signals from R_1 and R_3 is equivalent to double path gain of the channels. Hence, the equivalent channel will be

$$\mathbf{H} = \begin{bmatrix} \sqrt{2}h_1 & \sqrt{2}h_3 \\ \sqrt{2}h_3^* & -\sqrt{2}h_1^* \end{bmatrix} \tag{5.4.1}$$

Applying the matched filtering at the destination receiver with the equivalent channel matrix in (5.4.1), the channel gain $\gamma_{(2)}$ can be obtained as

$$\gamma_{(2)} = \alpha_{(2)} + \beta_{(2)} = |\sqrt{2}h_1|^2 + |\sqrt{2}h_3|^2 + \beta_1 + \beta_2$$

where $\gamma_{(2)}$ denotes the channel gain for the system working with two selected relays, i.e. channel gain for the two-groups method.

Since there is no correlation between the channels, i.e. $\beta_1 = 0$ and $\beta_2 = 0$, so $\beta_{(2)} = 0$ as compared with the conventional D-EO-STBC scheme. Therefore, $\gamma_{(2)} = 2|h_1|^2 + 2|h_3|^2$, and consequently,

$$SNR = \gamma_{(2)} \frac{\sigma_S^2}{\sigma_N^2} = 2(|h_1|^2 + |h_3|^2) \frac{\sigma_S^2}{\sigma_N^2} \tag{5.4.2}$$

Furthermore, the scheme does not need feedback for aligning the forward signals because the system uses only two relays out of four and the selected two relays have different encoding processes as shown in Table 5.2. On the other hand, since the double squared values of the two maximum path gains give a bigger value than the summation of the squared gain of the four path gains with the interference factor β as in the conventional case, the system therefore yields better performance than that achieved by the conventional D-EO-STBC scheme as in (5.3.9), i.e. $\gamma_{(2)} \geq \gamma$.

However, this relay selection method can be generalized to select the best two out of R relays and the D-Alamouti code can be applied over the selected two relays or $R-2$ relays can be selected that include the best relay for each group and the D-EO-STBC scheme can be applied over the selected relays. In fact, when the number of relays increases, it is more likely to provide better performance but at the expense of computational complexity.

5.4.2 One-group method

In this method, all relay nodes are considered as one group to select the best relay among them and remove the worst one as depicted in Fig. 5.3. According to the CSI, the destination receiver can determine the link which

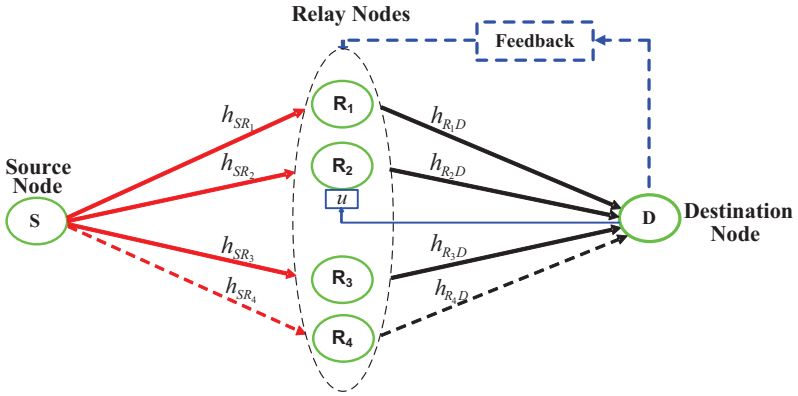

Figure 5.3. Wireless relay system with feedback links to select the suitable relays based on the one-group method with phase feedback u for signal alignments where the three solid lines mean the selected paths.

has the maximum path gain and the link which has the minimum path gain. After that, it informs the relays to stop sending from the worst relay and to switch the power of the best relay to the maximum. Hence, only three relays are working according to this method. Then, the three relays perform an appropriate encoding process according to Table 5.1 to generate a D-EO-STBC form at the destination node. Also, it is required to align the two signals that have the same relay encoding in terms of the construction of D-EO-STBC through using a feedback channel and multiplying one of them by the weighted feedback value, u. As a result, the system can achieve array gain which is not available in the two-groups method. This will leverage the system performance to the maximum. For example, suppose the best path passes through relay 1 and the worst path passes through relay 4. There-

fore, R_1 will work with its maximum power while R_4 will stop transmitting information signals. Then, the three working relays perform the encoding process as in Table 5.3 which is a modified version of Table 5.1 to implement the closed-loop D-EO-STBC scheme.

On the other hand, the best link and the worst link might have the same

Table 5.3. D-EO-STBC encoding process over the three working relays.

	Relay Nodes			
Symbol duration	R_1	R_2	R_3	R_4
Symbol 1	$\sqrt{2}y_{11}$	$u\ y_{21}$	$-y_{32}^*$	0
Symbol 2	$\sqrt{2}y_{12}$	$u\ y_{22}$	y_{31}^*	0

relay encoding process or not which leads to two different scenarios. In the following, each scenario will be explained individually in addition to a special scenario which combines between scenario 2 and a certain condition related to the second best link of the system.

Scenario 1

In this scenario, the best and the worst links have the same encoding process as in Table 5.1. According to the considered assumption in this work, R_1 and R_2 perform similar encoding process while R_3 and R_4 perform similar encoding process which is different from that of R_1 and R_2 as shown in Table 5.1. To clarify scenario 1, assume the best path passes through relay 1 and the worst path passes through relay 2. By using the appropriate encoding process over the three working relays, R_1, R_3 and R_4, the equivalent channel matrix can be written as

$$\mathbf{H} = \begin{bmatrix} \sqrt{2}h_1 & uh_3 + h_4 \\ u^*h_3^* + h_4^* & -\sqrt{2}h_1^* \end{bmatrix} \tag{5.4.3}$$

where u is the feedback weighted value.

After applying the matched filtering at the destination receiver with the

equivalent channel matrix in (5.4.3), the channel gain can be obtained such that

$$\gamma_{(3)}^1 = \alpha_{(3)}^1 + \beta_{(3)}^1 = |\sqrt{2}h_1|^2 + |u|^2|h_3|^2 + |h_4|^2 + \beta_1 + \beta_2$$

where $\gamma_{(3)}^1$ is the channel gain for the system working with three selected relays, i.e. the channel gain for the one-group method, and using scenario 1, $|u|^2 = 1$ and $\beta_1 = 0$ while $\beta_2 = uh_3h_4^* + u^*h_3^*h_4 = 2\text{Re}\{uh_3h_4^*\}$. Therefore, $\beta_{(3)}^1 = \beta_2$ and $\beta_{(3)}^1$ here represents the array gain for this scenario. Consequently,

$$SNR = \gamma_{(3)}^1 \frac{\sigma_x^2}{\sigma_n^2} = (2|h_1|^2 + |h_3|^2 + |h_4|^2 + \beta_{(3)}^1)\frac{\sigma_x^2}{\sigma_n^2} \tag{5.4.4}$$

Scenario 2

In this scenario, the best and the worst links have different relay encoding processes. Suppose the best path passes through relay 1 and the worst path passes through relay 4. By using the appropriate encoding process over the three working relays, R_1, R_2 and R_3, the equivalent channel matrix can be written as

$$\mathbf{H} = \begin{bmatrix} \sqrt{2}h_1 + uh_2 & h_3 \\ h_3^* & -\sqrt{2}h_1^* - u^*h_2^* \end{bmatrix} \tag{5.4.5}$$

After applying the matched filtering at the destination receiver with the equivalent channel matrix in (7.3.4), the channel gain can be obtained as

$$\gamma_{(3)}^2 = \alpha_{(3)}^2 + \beta_{(3)}^2 = |\sqrt{2}h_1|^2 + |u|^2|h_2|^2 + |h_3|^2 + \beta_1 + \beta_2$$

where $\beta_1 = \sqrt{2}h_1^*uh_2 + u^*h_2^*\sqrt{2}h_1 = 2\text{Re}\{\sqrt{2}h_1u^*h_2^*\}$ while $\beta_2 = 0$ so $\beta_{(3)}^2 = \beta_1$ which is the array gain of this scenario. Consequently, the SNR is

$$SNR = \gamma_{(3)}^2 \frac{\sigma_S^2}{\sigma_N^2} = (2|h_1|^2 + |h_2|^2 + |h_3|^2 + \beta_{(3)}^2)\frac{\sigma_S^2}{\sigma_N^2} \tag{5.4.6}$$

The system performance of this scenario is better that that of scenario 1 due to the improvement in array gain. The array gain in scenario 1 is equal to $\beta^1_{(3)} = 2\text{Re}\{uh_3h_4^*\}$ while the array gain in scenario 2 is equal to $\beta^2_{(3)} = 2\sqrt{2}\text{Re}\{h_1u^*h_2^*\}$. As observed, the array gain of scenario 2 includes the best path gain, $|h_1|^2$, while that was not available in scenario 1; so by performing a comparison between the two scenarios it is clear that the array gain of scenario 2 is the largest, i.e. $\beta^2_{(3)} > \beta^1_{(3)}$.

Scenario 3

In this scenario, the system is designed to permanently adopt the scenario 2 combination where the best link and the worst link use different relay encoding in addition to selecting the second best link to perform the same relay encoding as the best link. For example, assume $|h_1|^2$ is the best path gain and $|h_2|^2$ is the second best path gain. Hence, the channel gain of this scenario can be expressed as

$$\gamma^3_{(3)} = \alpha^3_{(3)} + \beta^3_{(3)} = |\sqrt{2}h_1|^2 + |u|^2|h_2|^2 + |h_3|^2 + \beta_1 + \beta_2$$

where $\beta_1 = 2\text{Re}\{\sqrt{2}h_1u^*h_2^*\}$ while $\beta_2 = 0$ so the array gain of this scenario will be $\beta^2_{(3)} = 2\sqrt{2}\text{Re}\{h_1u^*h_2^*\}$. The difference between the array gain of this scenario and that of scenario 2 is that the channel h_2 in this scenario always represents the second best link while in the case of scenario 2 this not always holds, which results in making the overall array gain of scenario 3 better that that of scenario 2, i.e. $\beta^3_{(3)} \geq \beta^2_{(3)}$. Therefore, the system with scenario 3 will give the best performance as compared to scenario 1 and scenario 2. However, it requires increased feedback overhead, delay and computational complexity.

As shown above, the one-group method and its different scenarios generally

achieve array gain but with different values. However, this method can be generalized to select the best $R-1$ out of R relays and then the D-EO-STBC can be applied over the selected relays.

5.4.3 Relay selection in the multi-carrier implementation

The implementation of the proposed relay selection schemes are designed for single-carrier implementation. However, these schemes can be extended to multi-carrier implementation by applying these schemes for each subcarrier independently using the equivalent channel coefficients. So, the relay selection is applied within a frequency selective channel context. In these schemes, where only spatial cooperative diversity is exploited, the signals, $\mathbf{s} = [\mathbf{s}_1 \ \ \mathbf{s}_2]$ where $\mathbf{s_1} = [s_{0,1}, s_{1,1}, ..., s_{N-1,1}]^T$ and $\mathbf{s_2} = [s_{0,2}, s_{1,2}, ..., s_{N-1,2}]^T$, are transmitted from the source towards the relay nodes and the received noisy signals at the relays are then transmitted towards the destination node. The transmitted signals from the source and relay nodes are propagated through frequency selective channels with asynchronous nature as shown in Fig. 5.4. The CIRs for $S \rightarrow R_i$ and $R_i \rightarrow D$ links are given by

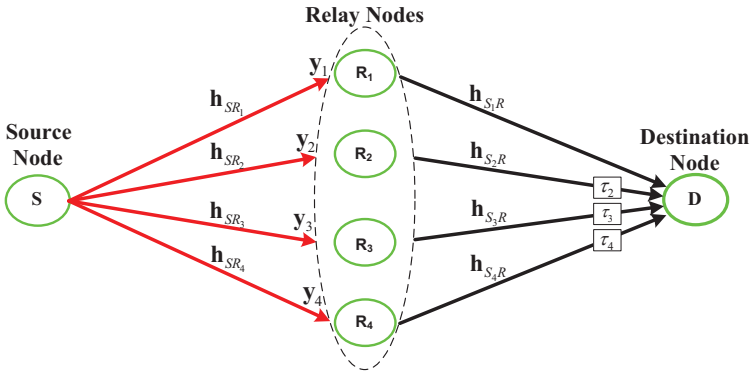

Figure 5.4. Wireless relay network with single source, destination and four relay nodes together with relative time delays, and frequency-selective links.

$\mathbf{h}_{SR_i} = [h_{SR_i}(0), h_{SR_i}(1), ..., h_{SR_i}(L_{SR_i})]$ and $\mathbf{h}_{R_iD}$ =$[h_{R_iD}(0), h_{R_iD}(1), ...,$ $h_{R_iD}(L_{R_iD})]$. The entries of the random vectors $\mathbf{h}_{SR_i}$ and $\mathbf{h}_{R_iD}$ are i.i.d. zero mean circular Gaussian random variables with variances of $1/(L_{SR_i}+1)$ and $1/(L_{R_iD}+1)$, respectively. The system implementations at source, relay nodes and destination follow the same steps as in Section 4.2.5. At the source node, the IFFT is performed on each input vectors $\mathbf{s}_1$ and $\mathbf{s}_2^*$, and a cyclic prefix, of length greater than the length of the channel memory and the relative spread delay, is added in order to preserve the orthogonality among the subcarriers of an OFDM symbol before broadcasting the two information OFDM symbols in two time intervals, i.e. $j = 1, 2$, to the relay nodes, R_i, where $i = 1, 2, 3, 4$. The AF type relay nodes then process the received noisy signals, $\mathbf{y}_{ij}$, according to Table 5.4 in order to generate D-EO-STBCs at the destination node where $\zeta(.)$ denotes reversal-time operation. As such, the received signals at the relays, $\mathbf{y}_{ij}$, can be expressed as

$$\mathbf{y}_{ij} = \sqrt{P_s}\mathbf{H}_{SR_i}\mathbf{s}_j + \mathbf{v}_{ij} \tag{5.4.7}$$

where $\mathbf{v}_{ij}$ is the corresponding zero mean AWGN terms at relay node i and time interval j with elements having zero-mean and unit-variance.

At the destination node, the received signals at two time intervals, $\mathbf{r}_j$, after

Table 5.4. Conventional D-EO-STBC encoding process over for frequency-selective channel system.

	Relay Nodes			
Symbol duration	R_1	R_2	R_3	R_4
OFDM Symbol 1	$\mathbf{y}_{11}$	$\mathbf{y}_{21}$	$-\zeta(\mathbf{y}_{32}^*)$	$-\zeta(\mathbf{y}_{42}^*)$
OFDM Symbol 2	$\mathbf{y}_{12}$	$\mathbf{y}_{22}$	$\zeta(\mathbf{y}_{31}^*)$	$\zeta(\mathbf{y}_{41}^*)$

removing the cyclic prefix and performing the FFT can be written as

$$\begin{bmatrix} (\mathbf{r}_1)^T \\ (\mathbf{r}_2)^T \end{bmatrix} = \sqrt{\frac{P_s P_r}{P_s+1}} \underbrace{\begin{bmatrix} (\mathbf{s}_1)^T & (\mathbf{s}_1)^T & (-\mathbf{s}_2^*)^T & (-\mathbf{s}_2^*)^T \\ (\mathbf{s}_2)^T & (\mathbf{s}_2)^T & (\mathbf{s}_1^*)^T & (\mathbf{s}_1^*)^T \end{bmatrix}}_{\mathrm{S}} \begin{bmatrix} \mathbf{H}_1 \\ \mathbf{H}_2 \\ \mathbf{H}_3 \\ \mathbf{H}_4 \end{bmatrix} + \begin{bmatrix} (\mathbf{n}_1)^T \\ (\mathbf{n}_2)^T \end{bmatrix} \tag{5.4.8}$$

where $\mathbf{H}_{(i=1,2)} = \mathbf{H}_{SR_i}\mathbf{H}_{R_iD}$ and $\mathbf{H}_{(i=3,4)} = \mathbf{H}^*_{SR_i}\mathbf{H}_{R_iD}$. The channel matrices $\mathbf{H}_{SR_i}$ and $\mathbf{H}_{R_iD}$ are $N \times N$ circulant channel matrices with entries of $\mathbf{H}_{SR_i}(a,b) = (h_{SR_i}(a-b)\mathrm{mod}N)$ and $\mathbf{H}_{R_iD}(a,b) = (h_{R_iD}(a-b)\mathrm{mod}N)$, respectively, with $a, b = 1, 2, ..., N$ and mod(.) represents modulo operation. The noise term $\mathbf{n}_1 = \sqrt{\frac{P_r}{P_s+1}}(\sum_{i=1}^{2}\mathbf{H}_{R_iD}\mathbf{v}_{i1} - \sum_{i=3}^{4}\mathbf{H}_{R_iD}\mathbf{v}^*_{i2}) + \mathbf{w}_1$ and $\mathbf{n}_2 = \sqrt{\frac{P_r}{P_s+1}}\ (\sum_{i=1}^{2}\mathbf{H}_{R_iD}\mathbf{v}_{i2} + \sum_{i=3}^{4}\mathbf{H}_{R_iD}\mathbf{v}^*_{i1}) + \mathbf{w}_2$ where $\mathbf{w}_1$ and $\mathbf{w}_2$ are AWGN vectors at the destination for the two time intervals, j. The received signal vectors $\mathbf{r}_1$ and $\mathbf{r}_2^*$ can equivalently be written as

$$\begin{bmatrix} \mathbf{r}_1 \\ \mathbf{r}_2^* \end{bmatrix} = \sqrt{\frac{P_s P_r}{P_s+1}} \underbrace{\begin{bmatrix} \mathbf{H}_1+\mathbf{H}_2 & -(\mathbf{H}_3+\mathbf{H}_4) \\ (\mathbf{H}_3+\mathbf{H}_4)^* & (\mathbf{H}_1+\mathbf{H}_2)^* \end{bmatrix}}_{\mathbf{H}} \begin{bmatrix} \mathbf{s}_1 \\ \mathbf{s}_2^* \end{bmatrix} + \begin{bmatrix} \mathbf{n}_1 \\ \mathbf{n}_2^* \end{bmatrix} \tag{5.4.9}$$

The effective noise power calculated from the noise terms is equal to $\mathrm{E}\{\|\mathbf{n}_1\|^2\} = \mathrm{E}\{\|\mathbf{n}_2^*\|^2\} = \mathrm{E}\{\frac{P_r}{P_s+1}\sum_{i=1}^{4}\sum_{l=0}^{L_{R_iD}}|h_{R_iD}(l)|^2+1\} = \frac{4P_r}{P_s+1}+1$ where the operator $\|.\|$ denotes Euclidean distance. To aid in the later analysis, the received signal vectors $\mathbf{r}_1$ and $\mathbf{r}_2^*$ are normalized so that the noise variance is unity. So,

$$\begin{bmatrix} \mathbf{r}_1 \\ \mathbf{r}_2^* \end{bmatrix} = \sqrt{\frac{\sigma^2_{\mathbf{s}}}{\sigma^2_{\mathbf{n}}}} \underbrace{\begin{bmatrix} \mathbf{H}_1+\mathbf{H}_2 & -(\mathbf{H}_3+\mathbf{H}_4) \\ (\mathbf{H}_3+\mathbf{H}_4)^* & (\mathbf{H}_1+\mathbf{H}_2)^* \end{bmatrix}}_{\mathbf{H}} \begin{bmatrix} \mathbf{s}_1 \\ \mathbf{s}_2^* \end{bmatrix} + \begin{bmatrix} \mathbf{n}_1 \\ \mathbf{n}_2^* \end{bmatrix} \tag{5.4.10}$$

where $\frac{\sigma_{\mathbf{s}}^2}{\sigma_{\mathbf{n}}^2} = \frac{P_s P_r}{P_s+4P_r+1}$.

Let $\mathbf{H}$ denote the $2N \times 2N$ equivalent channel matrix seen by the codeword (5.4.10) which is obtained by taking the conjugate of the second received signal, $\mathbf{r}_2$. So, the maximum likelihood decision variables for symbol vectors $\mathbf{s}_1$ and $\mathbf{s}_2$ are computed as

$$\begin{bmatrix} \tilde{\mathbf{s}}_1 \\ \tilde{\mathbf{s}}_2^* \end{bmatrix} = \sqrt{\frac{\sigma_{\mathbf{s}}^2}{\sigma_{\mathbf{n}}^2}} \mathbf{H}^H \mathbf{H} \begin{bmatrix} \mathbf{s}_1 \\ \mathbf{s}_2^* \end{bmatrix} + \mathbf{H}^H \begin{bmatrix} \mathbf{n}_1 \\ \mathbf{n}_2^* \end{bmatrix} \tag{5.4.11}$$

The proposed two relay selection methods are then employed independently at the level of a subcarrier. Therefore, these methods choose the best two or three relay nodes, according to which method is used, for each subcarrier depending on the channel gain indicator from the destination receiver. The D-Alamouti code or the D-EO-STBC is then applied to each subcarrier using the best relay nodes, hence improving the overall system performance as compared with the performance of the conventional D-EO-STBC scheme with no relay selection employed or feedback implemented.

5.5 Relay Selection Schemes Performance Based on PEP Expression

PEP is one of the common performance measure metrics used in a wireless communication system. It is simply referred to the probability of detecting one symbol when another symbol is transmitted. So, the system with the minimum PEP can be considered as the best system performance. In this section, the performance of the relay selection schemes based on PEP performance measure is evaluated. At the beginning, the PEP upper bound for the conventional D-EO-STBC scheme is analyzed. Then, based on this analysis, the comparison can be performed between the PEP upper bound of the relay selection schemes and the conventional scheme.

5.5.1 PEP upper bound for conventional D-EO-STBC scheme

The PEP upper bound is derived for the conventional D-EO-STBC scheme over a wireless relay system with frequency selective fading channels. For simplicity, it is assumed that the memory lengths for all channels are the same, i.e. $L_{SR_i} = L_{R_iD} = L$. From (5.4.10), the received information signals at the destination node are computed as

$$\begin{bmatrix} \mathbf{r}_1 \\ \mathbf{r}_2^* \end{bmatrix} = \sqrt{\frac{\sigma_{\mathbf{s}}^2}{\sigma_{\mathbf{n}}^2}} \underbrace{\begin{bmatrix} \mathbf{H}_1 + \mathbf{H}_2 & -(\mathbf{H}_3 + \mathbf{H}_4) \\ (\mathbf{H}_3 + \mathbf{H}_4)^* & (\mathbf{H}_1 + \mathbf{H}_2)^* \end{bmatrix}}_{\mathbf{H}} \begin{bmatrix} \mathbf{s}_1 \\ \mathbf{s}_2^* \end{bmatrix} + \begin{bmatrix} \mathbf{n}_1 \\ \mathbf{n}_2^* \end{bmatrix} \tag{5.5.1}$$

The conditional PEP with Chernoff bound for $\mathbf{s}_j$, where$\mathbf{s}_j = [s_{0,j}, s_{1,j}, ..., s_{N-1,j}]^T$ and $j = 1, 2$, is given by

$$P(\mathbf{s}_j \to \hat{\mathbf{s}}_j | \mathbf{h}_{SR_1}, ..., \mathbf{h}_{SR_4}, \mathbf{h}_{R_1D}, ..., \mathbf{h}_{R_4D}) \leq \exp(-\frac{d^2(\mathbf{s}_j, \hat{\mathbf{s}}_j)}{4N_0}) \tag{5.5.2}$$

where $d^2(\mathbf{s}_j, \hat{\mathbf{s}}_j)$ is the distance metric and taking into account that the noise variance N_0 can be replaced by unity according to the noise assumption. The distance metric $d^2(\mathbf{s}_j, \hat{\mathbf{s}}_j)$ can be calculated such as

$$d^2(\mathbf{s}_j, \hat{\mathbf{s}}_j) = \left\| \sqrt{\text{SNR}}(\mathbf{s}_j - \hat{\mathbf{s}}_j) \right\|^2 \tag{5.5.3}$$

where $\text{SNR} = \frac{\sigma_{\mathbf{s}}^2}{\sigma_{\mathbf{n}}^2}(\sum_{i=1}^{4} \|\mathbf{H}_i\|_{\mathcal{F}}^2 + \beta_1 + \beta_2)$ and $\|.\|_{\mathcal{F}}$ denotes the Frobenius norm. To facilitate analysis, it is assumed that $\beta_1 + \beta_2$ are replaced by their average value, i.e. $\beta_1 + \beta_2 \approx \text{E}\{\beta_1 + \beta_2\} = \beta$ where β might have positive or negative value. By substituting in (7.3.9),

$$\begin{aligned} d^2(\mathbf{s}_j, \hat{\mathbf{s}}_j) &\approx \left\| \left[\frac{\sigma_{\mathbf{s}}^2}{\sigma_{\mathbf{n}}^2} (\sum_{i=1}^{4} \|\mathbf{H}_i\|_{\mathcal{F}}^2 + \beta) \right]^{\frac{1}{2}} (\mathbf{s}_j - \hat{\mathbf{s}}_j) \right\|^2 \\ &= \frac{\sigma_{\mathbf{s}}^2}{\sigma_{\mathbf{n}}^2} \sum_{i=1}^{4} \|\mathbf{H}_i\|_{\mathcal{F}}^2 \|\mathbf{s}_j - \hat{\mathbf{s}}_j\|^2 + \frac{\sigma_{\mathbf{s}}^2}{\sigma_{\mathbf{n}}^2} \beta \|\mathbf{s}_j - \hat{\mathbf{s}}_j\|^2 \end{aligned} \tag{5.5.4}$$

Based on [91], the first term of $d^2(\mathbf{s}_j, \hat{\mathbf{s}}_j)$ in (7.3.10) can be replaced by $\frac{\sigma_{\mathbf{s}}^2}{\sigma_{\mathbf{n}}^2}\sum_{i=1}^{4}\|\mathbf{H}_i\|_{\mathcal{F}}^2\|\mathbf{s}_j-\hat{\mathbf{s}}_j\|^2 \approx \sum_{i=1}^{4}\frac{\sigma_{\mathbf{s}}^2}{\sigma_{\mathbf{n}}^2}\sum_{l=0}^{L}|h_{SR_i}(l)|^2\|(\mathbf{S}_j-\hat{\mathbf{S}}_j)\mathbf{h}_{R_iD}\|^2$ where $\mathbf{S}_j$ is a signal matrix of size $N\times(L+1)$ and is defined as

$$\mathbf{S}_j = \begin{bmatrix} s_{0,j} & s_{N-1,j} & \cdots & s_{N-L,j} \\ \vdots & \vdots & \ddots & \vdots \\ s_{N-1,j} & s_{N-2,j} & \cdots & s_{N-L-1,j} \end{bmatrix} \tag{5.5.5}$$

and $(\mathbf{S}_j-\hat{\mathbf{S}}_j)$ is the signal difference.

Suppose $\chi_j^i = \frac{\sigma_{\mathbf{s}}^2}{\sigma_{\mathbf{n}}^2}\sum_{l=0}^{L}|h_{SR_i}(l)|^2\left\|(\mathbf{S}_j-\hat{\mathbf{S}}_j)\mathbf{h}_{R_iD}\right\|^2$ and $\zeta_j = \frac{\sigma_{\mathbf{s}}^2}{\sigma_{\mathbf{n}}^2}\beta\|\mathbf{s}_j-\hat{\mathbf{s}}_j\|^2$. Therefore, the conditional PEP Chernoff bound can be expressed as

$$\begin{aligned} P(\mathbf{s}_j\to\hat{\mathbf{s}}_j|\mathbf{h}_{SR_1},...,\mathbf{h}_{R_1D},...) &\le \exp(-\frac{\zeta_j}{4N_0})\times\exp(-\frac{\sum_{i=1}^{4}\chi_j^i}{4N_0}) \\ &\le \exp(-\frac{\zeta_j}{4N_0})\times\prod_{i=1}^{4}\exp(-\frac{\chi_j^i}{4N_0}) \end{aligned} \tag{5.5.6}$$

The parameter χ_j^i is a random variable which depends on the complex Gaussian channel vectors $\mathbf{h}_{SR_i}$ and $\mathbf{h}_{R_iD}$. To obtain the conditional PEP upper bound it is therefore necessary to integrate over the random channel parameters as in [91]

$$P(\mathbf{s}_j\to\hat{\mathbf{s}}_j)\le\exp(-\frac{\zeta_j}{4N_0})\prod_{i=1}^{4}\int\int\exp(-\frac{\chi_j^i}{4N_0})d\mathbf{h}_{SR_i}d\mathbf{h}_{R_iD} \tag{5.5.7}$$

To solve the above integration following the approach in [91], χ_j^i can be represented as

$$\chi_j^i = \frac{\sigma_{\mathbf{s}}^2}{\sigma_{\mathbf{n}}^2}\sum_{l=0}^{L}|h_{SR_i}(l)|^2\,\mathbf{h}_{R_iD}^H(\mathbf{S}_j-\hat{\mathbf{S}}_j)^H(\mathbf{S}_j-\hat{\mathbf{S}}_j)\mathbf{h}_{R_iD} \tag{5.5.8}$$

and defining $\Delta_j = (\mathbf{S}_j-\hat{\mathbf{S}}_j)^H(\mathbf{S}_j-\hat{\mathbf{S}}_j)$ as the signal distance matrix. Since Δ_j is Hermitian, its singular value decomposition (SVD) can be found as $\Delta_j = \mathbf{V}_j^H\Lambda_j\mathbf{V}_j$. The matrix $\mathbf{V}_j$ is a unitary matrix and the Λ_j is a diagonal

matrix of non-negative eigenvalue elements, λ_j^l. By substituting in (5.5.8), χ_j^i will be

$$\begin{aligned}
\chi_j^i &= \frac{\sigma_{\mathbf{s}}^2}{\sigma_{\mathbf{n}}^2} \sum_{l=0}^{L} |h_{SR_i}(l)|^2 \, \mathbf{h}_{R_iD}^H \mathbf{V}_j^H \Lambda_j \mathbf{V}_j \mathbf{h}_{R_iD} \\
&= \frac{\sigma_{\mathbf{s}}^2}{\sigma_{\mathbf{n}}^2} \sum_{l=0}^{L} |h_{SR_i}(l)|^2 \, \hat{\mathbf{h}}_{R_iD}^H \Lambda_j \hat{\mathbf{h}}_{R_iD} \\
&= \frac{\sigma_{\mathbf{s}}^2}{\sigma_{\mathbf{n}}^2} \sum_{l=0}^{L} |h_{SR_i}(l)|^2 \sum_{l=0}^{L} \lambda_j^l \left| \hat{h}_{R_iD}(l) \right|^2 \\
&= \mu \cdot x_i \cdot y_i
\end{aligned} \tag{5.5.9}$$

where $\mu = \frac{\sigma_{\mathbf{s}}^2}{\sigma_{\mathbf{n}}^2}$ while $x_i = \sum_{l=0}^{L} |h_{SR_i}(l)|^2$ and $y_i = \sum_{l=0}^{L} \lambda_j^l \left| \hat{h}_{R_iD}(l) \right|^2$ are random variables. It is clear that the summation involves the channel elements $h_{SR_i}(l)$ and $\hat{h}_{R_iD}(l)$ which are assumed to be zero-mean complex Gaussian random variables with unit variance. Hence, the random variables x_i and y_i follow a Gamma distribution model. Following the same procedure as in [91], the PEP upper bound can be obtained as

$$\begin{aligned}
P(\mathbf{s}_j \to \hat{\mathbf{s}}_j) &\leq \exp(-\frac{\zeta_j}{4N_0}) \prod_{i=1}^{4} \int_0^{\infty} \int_0^{\infty} \exp\left(- \left(\frac{\mu x_i}{4N_0} \right) y_i \right) p_{y_i} dy_i p_{x_i} dx_i \\
&\leq \exp(-\frac{\zeta_j}{4N_0}) \prod_{i=1}^{4} \int_0^{\infty} \prod_{l=0}^{L} \frac{1}{(1 + \frac{\mu \lambda_j^l x_i}{4N_0})} p_{x_i} dx_i \\
&\leq \exp(-\frac{\zeta_j}{4N_0}) \prod_{i=1}^{4} \int_0^{\infty} \prod_{l=0}^{L} \frac{1}{(\frac{\mu \lambda_j^l x_i}{4N_0})} \frac{x_i^L e^{-x_i}}{\Gamma(L+1)} dx_i \\
&\leq \exp(-\frac{\zeta_j}{4N_0}) \prod_{i=1}^{4} \left(\frac{\Gamma(0)}{\Gamma(L+1)} \left(\frac{\mu}{4N_0} \right)^{-(L+1)} \prod_{l=0}^{L} (\lambda_j^l)^{-1} \right) \\
&\leq \exp(-\frac{\zeta_j}{4N_0}) \left(\frac{\mu}{4N_0} \right)^{-4(L+1)} \left(\frac{1}{\Gamma(L+1)} \right)^4 \prod_{l=0}^{L} (\lambda_j^l)^{-4}
\end{aligned} \tag{5.5.10}$$

For the flat fading channels case choose $L = 0$.

5.5.2 PEP comparison between conventional scheme and relay selection schemes

For the proposed relay selection methods, the overall system channel gains of the two methods $\gamma_{(2)}$ and $\gamma_{(3)}$ are greater than the overall system channel gain γ of the conventional D-EO-STBC scheme, and consequently the resultant SNRs for the two relay selection methods are greater than the resultant SNR for the conventional scheme. Therefore, based on (7.3.9), the relationship between the distance metrics of the two proposed relay selection methods, $d^2_{(2)}(\mathbf{s}_j, \hat{\mathbf{s}}_j)$ and $d^2_{(3)}(\mathbf{s}_j, \hat{\mathbf{s}}_j)$, and the distance metric of the conventional scheme, $d^2(\mathbf{s}_j, \hat{\mathbf{s}}_j)$, can be written as

$$\begin{aligned} d^2_{(2)}(\mathbf{s}_j, \hat{\mathbf{s}}_j) &\geq d^2(\mathbf{s}_j, \hat{\mathbf{s}}_j) \\ d^2_{(3)}(\mathbf{s}_j, \hat{\mathbf{s}}_j) &\geq d^2(\mathbf{s}_j, \hat{\mathbf{s}}_j) \end{aligned} \tag{5.5.11}$$

and consequently,

$$\begin{aligned} \exp(-\frac{d^2_{(2)}(\mathbf{s}_j, \hat{\mathbf{s}}_j)}{4N_0}) &\leq \exp(-\frac{d^2(\mathbf{s}_j, \hat{\mathbf{s}}_j)}{4N_0}) \\ \exp(-\frac{d^2_{(3)}(\mathbf{s}_j, \hat{\mathbf{s}}_j)}{4N_0}) &\leq \exp(-\frac{d^2(\mathbf{s}_j, \hat{\mathbf{s}}_j)}{4N_0}) \end{aligned} \tag{5.5.12}$$

Therefore, from the above two inequalities, the PEP upper bound for the two-groups and one-group selection methods can be found as,

$$P_{(2)}(\mathbf{s}_j \to \hat{\mathbf{s}}_j) \leq P(\mathbf{s}_j \to \hat{\mathbf{s}}_j) \tag{5.5.13}$$

$$P_{(3)}(\mathbf{s}_j \to \hat{\mathbf{s}}_j) \leq P(\mathbf{s}_j \to \hat{\mathbf{s}}_j) \tag{5.5.14}$$

It can observed that the two-groups method as well as the one-group method achieves the minimum PEP values as compared to the conventional D-EO-STBC scheme. Therefore, the two relay selection methods reduce the PEP

which result in enhancing the overall performance of the wireless relay system.

5.6 Simulation Results

The performance of the proposed relay selection schemes via numerical simulation including the two transmission implementations which are single-carrier and multi-carrier implementations have been studied. In the single-carrier case, the comparison with the distributed-Alamouti (D-Alamouti) scheme [23] for two relays and the conventional D-EO-STBC and closed-loop D-EO-STBC schemes proposed in [118] for four relays is provided where the channel has been assumed to be quasi-static flat Rayleigh fading. While in the multi-carrier case, where the channels are assumed to be quasi-static frequency-selective Rayleigh fading with 11 taps and the uncoded OFDM uses a 64 point FFT, the comparison with the asynchronous D-EO-STBC scheme proposed in [124] for four relay nodes is performed. The source transmits quadrature phase-shift keying (QPSK) symbols with optimal power allocation as in [67]. The transmit power is identical for all schemes used in the comparison. All CSI is assumed to be perfectly known at the destination node. For the consistency within the thesis end-to-end BER is used as the performance measure instead of end-to-end frame error rate (FER).

The performance of the proposed relay selection schemes for flat relay channel systems is depicted in Fig. 5.5. The results confirm that the proposed relay selection schemes significantly improves the BER performance over the the conventional open-loop D-EO-STBC with no relay selection employed and the D-Alamouti schemes. For example, at a BER of 10^{-4}, the proposed one-group method requires approximately 19.3 dB and the proposed two-groups method requires approximately 21.1 dB while the conventional open-loop D-EO-STBC scheme requires approximately 26.9 dB and the D-

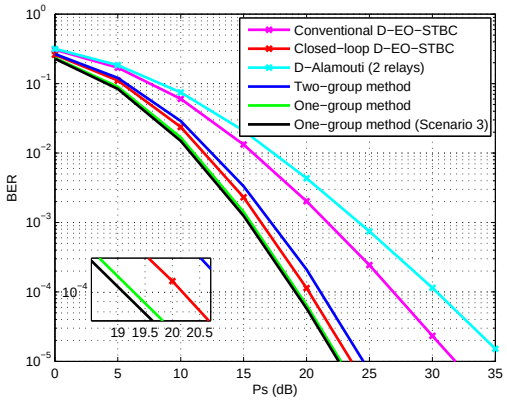

Figure 5.5. Comparison of BER performance of the proposed relay selection schemes over frequency-flat channels with previous schemes in wireless relay systems.

Alamouti scheme requires 30.3 dB. Furthermore, the one-group method provides 0.9 dB improvement over the closed-loop D-EO-STBC scheme with perfect phase feedback but the two-groups method provides a little degradation of 0.9 dB as compared with the closed-loop D-EO-STBC scheme. On the other hand, it is clear that the BER performance of the proposed one-group method is better than that of the proposed two-groups method. This better improvement in BER performance is because the one-group method can achieve array gain but at the expense of increased feedback overhead. Moreover, the performance of the one-group relay method can be enhanced more through implementing scenario 2 or scenario 3. In fact, scenario 3 gives the best BER performance. The performance difference between the various scenarios of one-group method arises from different amount of achieved array gain. The BER performance for one-group method using scenario 3 is also depicted in Fig. 5.5. It is clear that the one-group method using scenario 3 provides the best performance as compared with the previous ones. In particular, at a BER of 10^{-4}, this scheme provides improvement of approximately 2 dB as compared with the proposed two-groups method and an improvement of approximately 0.2 dB as compared with the proposed one-

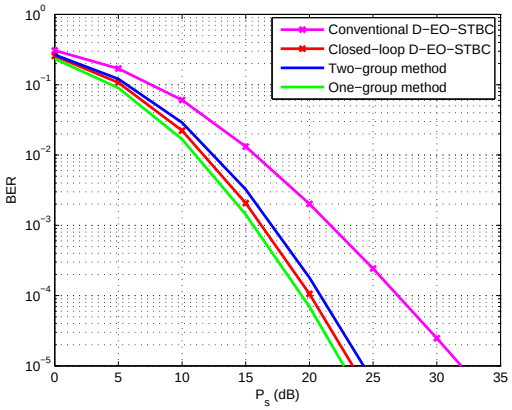

Figure 5.6. Comparison of BER performance of the proposed relay selection schemes over frequency-selective 11 tap channels with previous asynchronous scheme in wireless relay system.

group method. However, this scheme needs more feedback overhead and more complexity than the other proposed schemes.

The performance of the proposed relay selection schemes when frequency-selective channels are considered is depicted in Fig. 5.6. Similar results as in the case of flat fading channels can be observed. In particular, the proposed two-groups method substantially outperforms the conventional D-EO-STBC scheme and provides a little reduction as compared with the closed-loop D-EO-STBC scheme while the proposed one-group method provides much better performance than the previous ones. For example, at a BER of 10^{-4}, the proposed two-groups method provides approximately 6 dB improvement over the conventional D-EO-STBC scheme and approximately 0.9 dB reduction below the closed-loop D-EO-STBC scheme. More improvement in BER performance is shown in the case of the one-group relay selection method. For example, at a BER of 10^{-4}, the one-group selection method provides approximately 1.8 dB improvement over the two-group method and approximately 0.9 dB over the closed-loop D-EO-STBC scheme. The array gain achieved by the one-group method makes the positive difference in the BER performance for the one-group method over the two-groups method. How-

ever, the one-group method requires more feedback overhead as compared with the two-groups method.

5.7 Summary

In this chapter, two relay selection methods with simple three level power adaptation for cooperative AF type relaying systems combined with D-Alamouti code or D-EO-STBCs have been proposed. The investigations were performed for single and multi carriers transmissions for flat and frequency selective fading links. It has been shown through simulation results and PEP upper bound analysis that the proposed relay selection methods are effective in enhancing the system performance by selecting the best links for cooperative transmission together with exploiting the available power by transferring the power from the worst links to the best links.

However, the distributed approaches in this chapter and in the previous chapters focus on systems with four relays which limit the maximum possible order of the spatial cooperative diversity to four. In a practical situation, there will be a large number of relays available to the system network designers which can give extra spatial cooperative diversity performance due to increased in the available independent paths between the source and destination nodes. In the next chapter, the generalized closed-loop D-EO-STBC scheme for any arbitrary number of relay nodes will be presented and the related system improvement will be realized.

Chapter 6

A GENERALIZED DISTRIBUTED EXTENDED ORTHOGONAL SPACE-TIME BLOCK CODING SCHEME FOR COOPERATIVE RELAY NETWORKS

Increasing the number of independent paths between the source and the destination nodes in a wireless relay network can give extra diversity performance. This strategy can be realized through adding extra relay nodes to the network. In this chapter, a generalized distributed extended orthogonal space-time block code (D-EO-STBC) cooperative scheme is proposed to apply in wireless relay networks with an arbitrary number of relay nodes. By applying one-bit partial feedback over certain relays or subcarriers for certain relays, at least full spatial diversity of order equal to the number of relays can be achieved which can substantially improve the system reliability and robustness in the presence of fading effects and time asynchronicity.

In addition, two effective approaches are presented based on optimal partial feedback and relay selection, respectively, to further enhance the overall system performance. Moreover, the proposed low-complexity schemes utilize linear processing for encoding and a simple symbol-wise maximum likelihood (ML) process for decoding. Finally, numerical results are presented to show the performance improvements resulting from the proposed schemes.

6.1 Introduction

Recent developments in wireless communication have shown that a collection of single-antenna relay nodes in a wireless network can share their antennas to construct a virtual multi-input multi-output (MIMO) channel in a distributed manner. In this case, similar independent paths as in MIMO systems are also available, and this results in cooperative diversity gain [10], [53] and [54]. Several cooperation schemes based on different relaying protocols have been proposed [22] and [65]. Among different relaying protocols, there are two main protocols which are decode-and-forward (DF) and amplify-and-forward (AF). However, from a practical viewpoint, AF protocols are much more attractive because of their simplicity in installation and avoidance of digital processing at the relay nodes.

Implementation of cooperative schemes based on distributed space-time codes (D-STCs) has been proposed for relay networks [8], [67] and [110]. It has been shown that D-STCs potentially offer maximum diversity and data rate with low decoding complexity. In fact, the distributed Alamouti (D-Alamouti) scheme [23] for two relays is the only complex-symbol distributed orthogonal space-time block codes (D-OSTBCs) scheme that can achieve full diversity and full rate for each hop with simple linear ML decoding complexity. Recently, much effort has been undertaken into designing D-STC schemes for improving the diversity-multiplexing gain [63] for more than two relays. For

open-loop communication systems, the distributed orthogonal and quasi-orthogonal STBCs (D-OSTBCs and D-QO-STBCs) were proposed for more than two relay nodes [49]. However, they can not achieve full rate and full diversity at the same time and the decoding delay increases as the number of relays increases. In [51] and [72], distributed differential STCs (D-DSTCs) were proposed for any number of relay nodes. These schemes can achieve rate one with full diversity but at the expense of higher decoding delay and higher complexity in encoding and decoding especially for large number of relay nodes. For closed-loop communication systems, the channel state information (CSI) can be exploited to further enhance the system performance. In particular, providing all of the relay nodes with CSI through a separate feedback from the destination. However, in [49], a CSI at the relays has been utilized without resulting in improved diversity or coding. In [50], limited feedback beamforming combined with D-OSTBC considering multiple antennas at the receiver and a direct path between the source and receiver have been proposed for any number of relay nodes. Although this scheme achieves full rate and full diversity, this approach increases the computational complexity, decoding delay and the cost. Inspired by the idea of the Alamouti code, distributed extended OSTBCs (D-EO-STBCs) with partial feedback were presented in [118] for perfect synchronization and in [124] and [125] for imperfect synchronization. In those works, D-EO-STBCs using two feedback links exhibit full diversity order with coding gain and full rate while preserving low decoding complexity. However, they are applicable to scenarios with only three and four relays.

The performance of open-loop cooperative systems is worse than that of closed-loop cooperative systems due to the array gain penalty. In closed-loop systems, using partial feedback techniques is of particular practical interest because they exhibit high performance with significant reduced feedback overhead. There are two widely used techniques that use partial feedback

which are based on channel statistics [85] or quantized instantaneous channel values on which the work in this chapter is based. In fact, partial feedback is adopted for an increasing number of standards such as the wideband code division multiple access (WCDMA) standard [84]. Most cooperative schemes in the literature are based on D-OSTBCs due to their simplicity in detection and their maximum diversity advantages. However, the D-OSTBC designs exist only for a certain number of relay nodes [49] which limits their application. Furthermore, as the number of relays increases the linear ML decoding complexity is no longer achieved [49] and the decoding delay proportionally increases. So, the focus of this chapter is to use an extended version of the D-Alamouti code or in other words D-EO-STBCs for any number of relay nodes to address these problems. The use of such codes is shown to preserve low decoding delay as in the case of two relays without affecting the benefits of linear decoding and maximum diversity [118]. In addition, they are robust to relay node failure for any reason such as maintenance.
There are therefore three main contributions in this chapter.

1. A simple closed-loop AF type scheme for D-EO-STBCs is generalized to an arbitrary number of relay nodes considering the quasi-static flat fading channels. A simple partial feedback scheme in the form of one-bit feedback for only R-2 relay nodes is proposed for D-EO-STBCs, where R is the total number of relays. It is shown that the proposed scheme can achieve at least full spatial diversity and full rate over each hop with a simple linear ML detection. Moreover, the powerful property of this scheme is its ability in exploiting the increase in system relay nodes to proportionally increase the system reliability and robustness.

2. Two high performance approaches are proposed for the generalized closed-loop D-EO-STBCs which are based on optimal partial feedback

and relay selection, respectively. In the first approach, a full search is performed in order to select the optimal one-bit feedback for only R-2 relays which can result in full spatial diversity and maximum coding gain. In the second approach, relay selection is combined with the generalized closed-loop D-EO-STBCs. Based on the instantaneous fading coefficients, the destination chooses the best relay nodes to maximize the signal-to-noise ratio (SNR), which results in further performance improvement. Moreover, this relay selection based approach minimizes the computational complexity and the feedback overhead. On the other hand, the enhancement in system behavior has also been investigated when the proposed scheme is concatenated with a binary convolutional coding scheme at the source and the associated Viterbi decoding scheme at the destination [114].

3. As the synchronicity between the relay nodes is an important practical issue related to wireless relay networks [77] and [75], the proposed generalized scheme is extended to the case of imperfect synchronization in the presence of flat fading channels, as in narrowband communications, and for the case of imperfect synchronization in the presence of frequency-selective fading channels, as in broadband communications. An orthogonal frequency division multiplexing (OFDM) type pre-coding with cyclic prefix (CP) is applied over the transmitted signals to combat fading and the effects of timing asynchronicity between the relay nodes. Numerical results show that at least full spatial diversity can be achieved.

6.2 System Model and Problem Statement

Consider a wireless two-hop relay system with one source node, one destination node, and R relay nodes as shown in Fig. 6.1 where a two-hop relay

channel remains constant for coherence time N_c. Every node in the system has only a single half-duplex antenna. The relay nodes operate in AF type mode. There is no direct link between the source and destination nodes due to heavy fade, path loss, shadowing effects or source coverage design. Hence, the transmission process consists of two phases which are the broadcasting phase and relaying phase. Each phase has time slot interval $2N$, i.e. $2N \leq N_c$. The objective is to generate D-EO-STBCs at the destination node. Then, the information symbols, $\mathbf{s} = [s_1, ..., s_{2N}]^T$ selected from any

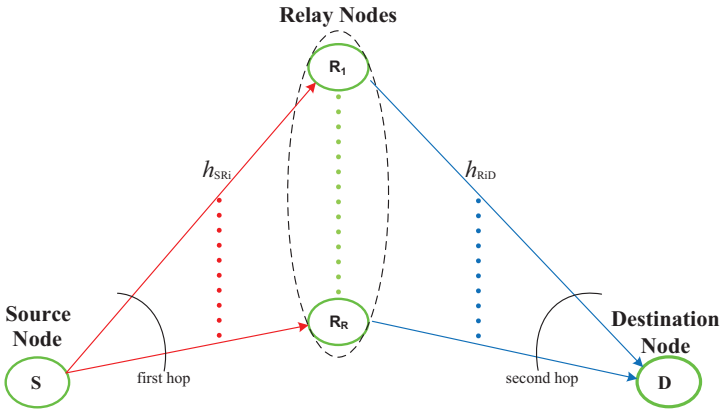

Figure 6.1. Wireless relay network with single source and destination together with multiple relay nodes; no direct path between source and destination is available.

signal constellation $\mathcal{S}$ where $(.)^T$ denotes vector transpose, are grouped into two symbol elements, i.e. $\mathbf{s} = [s_1 \ s_2]^T$, or two blocks, with each block of length N, i.e. $\mathbf{s} = [\mathbf{s}_1^T \ \mathbf{s}_2^T]^T$. Therefore, transmission occurs over two time slots, each with the interval of two symbol elements or block periods. Denote the fading coefficient from the source node to the ith relay as h_{SR_i}, and the fading coefficient from the ith relay to the destination node as h_{R_iD}. Assume the channel between any two terminals is quasi-static flat Rayleigh fading. Therefore, it is assumed that h_{SR_i} and h_{R_iD} are independent complex circular Gaussian random variables with zero-mean and unit-variance, i.e. $\mathcal{CN}(0, 1)$. The elements of the noise vectors at the relay nodes, $\mathbf{v}_i$, and at the destination node, $\mathbf{w}$, are also assumed to be independent identically

distributed (i.i.d.) zero-mean and unit-variance complex circular Gaussian random variables.

On the other hand, adding extra relay nodes to the wireless network will create more independent paths between the source and destination nodes which result in increased cooperative diversity gain. In practice, large numbers of relays will potentially be available for use in the wireless network. However, applying a feedback scheme based on D-EO-STBC over the relay nodes directly in a similar way as described in [118] cannot work well due to the correlation between channels and the dependency between them. So, in this chapter, a simple feedback scheme is designed to overcome these difficulties with limited feedback. By so doing, independent paths equal to the number of the deployed relay nodes will be realized which ensure that this system can achieve at least full cooperative diversity.

6.3 Generalized D-EO-STBC Scheme over Flat Fading Channels

6.3.1 Broadcasting phase

For the first time slot, the source node broadcasts two modulated information symbol elements $\mathbf{s} = [s_1 \ s_2]^T$ to the relay nodes, R_i, with the average transmit power per symbol $\mathcal{P}_s$. During the broadcasting phase, the received signal vector at the ith relay $\mathbf{y}_i$ which is corrupted by both the fading coefficient, h_{SR_i}, and the noise vector, $\mathbf{v}_i = [v_{i1} \ v_{i2}]^T$, can be expressed as

$$\mathbf{y}_i = \sqrt{\mathcal{P}_s} h_{SR_i} \mathbf{s} + \mathbf{v}_i \tag{6.3.1}$$

6.3.2 Relaying phase

In this work, the aim is to generate D-EO-STBCs at the destination node from the received two information symbols contained in $\mathbf{s}$, (s_1 and s_2). So, the network relay nodes are divided into two groups, named as group 1 and

group 2 as shown in Fig. 6.2. Each group of relay nodes should perform a complex conjugation over their received noisy signals from the source node. In practice, the network relay nodes are also designed to apply two different

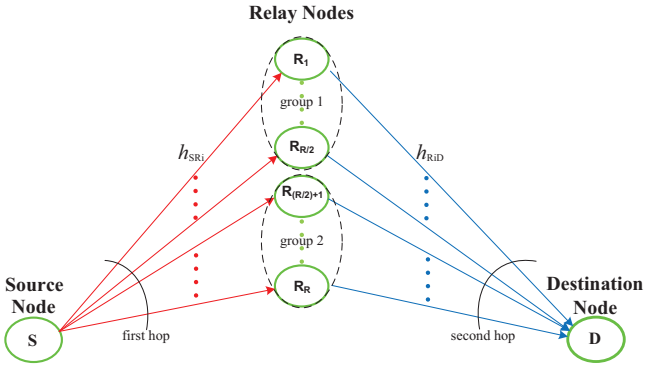

Figure 6.2. Wireless relay network where the relay nodes are equally divided into two groups.

unitary matrices denoted as $\mathbf{A}_i$ and $\mathbf{B}_i$ where $\mathbf{A}_i$ is applied to the received noisy signal $\mathbf{y}_i$ while $\mathbf{B}_i$ is applied to the conjugate $\mathbf{y}_i^*$ where $(.)^*$ denotes the complex conjugation. To minimize the computational complexity, the implementation of these two groups of relay nodes is designed to either implement $\mathbf{A}_i$ or $\mathbf{B}_i$. Therefore, only one group of relay nodes has to implement the complex conjugation operation. Without loss of generality, group 1 contains the first half of relay nodes, $i = 1, ..., \frac{R}{2}$ while group 2 contains the second half of the relay nodes, $i = \frac{R}{2} + 1, ..., R$, where R is the total number of the relay nodes. Mathematically, the transmit signal at the i-th relay can be described as a linear function of its received signal and its conjugate as follows

$$\mathbf{t}_i = \Omega(\mathbf{A}_i\mathbf{y}_i + \mathbf{B}_i\mathbf{y}_i^*) = \mathcal{P}_d(h_{SR_i}\mathbf{A}_i\mathbf{s} + h_{SR_i}^*\mathbf{B}_i\mathbf{s}^*) + \Omega(\mathbf{A}_i\mathbf{v}_i + \mathbf{B}_i\mathbf{v}_i^*) \tag{6.3.2}$$

where Ω is the relaying gain and the parameter $\mathcal{P}_d = \Omega\sqrt{\mathcal{P}_s}$.

The matrices $\mathbf{A}_i$ and $\mathbf{B}_i$ that are implemented at the i-th relays are con-

structed in the form of 2×2 matrices as follows

$$\mathbf{A}_1 = ... = \mathbf{A}_{\frac{R}{2}} = \begin{bmatrix} 1 & 0 \\ 0 & 1 \end{bmatrix}, \ \mathbf{A}_{\frac{R}{2}+1} = ... = \mathbf{A}_R = \begin{bmatrix} 0 & 0 \\ 0 & 0 \end{bmatrix}$$

$$\mathbf{B}_1 = ... = \mathbf{B}_{\frac{R}{2}} = \begin{bmatrix} 0 & 0 \\ 0 & 0 \end{bmatrix}, \ \mathbf{B}_{\frac{R}{2}+1} = ... = \mathbf{B}_R = \begin{bmatrix} 0 & -1 \\ 1 & 0 \end{bmatrix} \tag{6.3.3}$$

The relaying gain is computed as follows

$$\Omega = \sqrt{\frac{\mathcal{P}_r}{\mathcal{P}_s |h_{SR_i}|^2 + 1}} \tag{6.3.4}$$

where $\mathcal{P}_r$ is the average transmit power at every relay node per transmission and $|.|^2$ denotes the modulus squared of a complex number.

In order to simplify the analysis, only the channel variance is considered, $\mathrm{E}\{|h_{SR_i}|^2\} = 1$, to compute the relaying gain as follows

$$\Omega = \sqrt{\frac{\mathcal{P}_r}{\mathcal{P}_s + 1}} \tag{6.3.5}$$

The power allocation in [67] is adopted in this work where the total system power $\mathcal{P}_t$ is equally divided between the source node and the relay nodes to be $\mathcal{P}_s = R\mathcal{P}_r = \frac{\mathcal{P}_t}{2}$.

6.3.3 Processing at the destination node

The received signal vector $\mathbf{r}$ at the destination can be written as

$$\mathbf{r} = [r_1 \ r_2]^T = \sum_{i=1}^{R} h_{R_i D} \mathbf{t}_i + \mathbf{w} = \mathcal{P}_d \mathbf{S}\mathbf{h} + \mathbf{n} \tag{6.3.6}$$

with

$$\begin{aligned}
\mathbf{S} &= \begin{bmatrix} \mathbf{A}_1\mathbf{s} & \dots & \mathbf{A}_{\frac{R}{2}}\mathbf{s} & \mathbf{B}_{\frac{R}{2}+1}\mathbf{s}^* & \dots & \mathbf{B}_R\mathbf{s}^* \end{bmatrix} \\
&= \begin{bmatrix} s_1^{(1)} & \dots & s_1^{(\frac{R}{2})} & -s_2^{*(\frac{R}{2}+1)} & \dots & -s_2^{*(R)} \\ s_2^{(1)} & \dots & s_2^{(\frac{R}{2})} & s_1^{*(\frac{R}{2}+1)} & \dots & s_1^{*(R)} \end{bmatrix} \\
\mathbf{h} &= \begin{bmatrix} h_1^{g_1} & \dots & h_{\frac{R}{2}}^{g_1} & h_{\frac{R}{2}+1}^{g_2} & \dots & h_R^{g_2} \end{bmatrix}^T \\
\mathbf{n} &= [n_1\ n_2]^T = \Omega(\sum_{i=1}^{\frac{R}{2}} h_{R_iD}\mathbf{A}_i\mathbf{v}_i + \sum_{i=\frac{R}{2}+1}^{R} h_{R_iD}\mathbf{B}_i\mathbf{v}_i^*) + \mathbf{w}
\end{aligned} \tag{6.3.7}$$

where the matrix $\mathbf{S}$ denotes the D-EO-STBC codeword matrix, $\mathbf{h}$ is the equivalent channel vector whose elements are $h_i^{g1} = h_{SR_i}h_{R_iD}$ for group 1 and $h_i^{g2} = h_{SR_i}^* h_{R_iD}$ for group 2, $\mathbf{n}$ is the equivalent noise vector and the vector $\mathbf{w} = [w_1\ w_2]^T$ includes the noise elements at the destination node.

Therefore, without decoding, the relays distributively construct a space-time codeword $\mathbf{S}$ at the destination. As you can observe, the selected extended codeword is constructed from the well-known Alamouti code [23]. The D-EO-STBC codeword has the scale-free property which means that the code can continue working even if one column is ignored.

Equivalently, the received signal at the destination node, for convenience conjugated, can be written as follows

$$\dot{\mathbf{r}} = \begin{bmatrix} r_1 \\ r_2^* \end{bmatrix} = \mathcal{P}_d \underbrace{\begin{bmatrix} h_{g_1} & -h_{g_2} \\ h_{g_2}^* & h_{g_1}^* \end{bmatrix}}_{\mathcal{H}} \begin{bmatrix} s_1 \\ s_2^* \end{bmatrix} + \begin{bmatrix} n_1 \\ n_2^* \end{bmatrix}$$

where $h_{g_1} = \sum_{i=1}^{\frac{R}{2}} h_i^{g_1}$, $h_{g_2} = \sum_{i=\frac{R}{2}+1}^{R} h_i^{g_2}$ and the matrix $\mathcal{H}$ incorporates the equivalent source to destination channel fading coefficients.

To decode coherently the received signal, it is assumed that the equivalent channel $\mathcal{H}$ is available at the destination node. So, when matched filtering

is performed, the Gramian matrix $\mathbf{G}$ can be found as

$$\mathbf{G} = \mathcal{H}^H \mathcal{H} = \begin{bmatrix} \zeta & 0 \\ 0 & \zeta \end{bmatrix} \tag{6.3.8}$$

where $(.)^H$ denotes Hermitian transpose and ζ represents the channel gain such that

$$\zeta = \alpha + \beta = \sum_{i=1}^{\frac{R}{2}} |h_i^{g_1}|^2 + \sum_{i=\frac{R}{2}+1}^{R} |h_i^{g_2}|^2 + \beta_{g_1} + \beta_{g_2} \tag{6.3.9}$$

where $\beta = \beta_{g_1} + \beta_{g_2}$ with

$$\beta_{g_1} = \underbrace{\sum_{i_1=1}^{\frac{R}{2}} \sum_{i_2=1}^{\frac{R}{2}}}_{i_1 \neq i_2} h_{i_1}^{g_1} (h_{i_2}^{g_1})^*, \quad \beta_{g_2} = \underbrace{\sum_{i_1=\frac{R}{2}+1}^{R} \sum_{i_2=\frac{R}{2}+1}^{R}}_{i_1 \neq i_2} h_{i_1}^{g_2} (h_{i_2}^{g_1})^* \tag{6.3.10}$$

where β_{g_1} and β_{g_2} are the interference factors of the channel correlations at group 1 and group 2, respectively.

It is worth mentioning that the equivalent channel has the orthogonal structure property so the Gramian matrix is a diagonal matrix which indicates that the code can be decoded with a simple ML decoder. Also, it is clear that the ML decoding of the symbol vector $\mathbf{s}$ is very simple as two symbols in $\hat{\mathbf{s}} = [s_1 \; s_2^*]^T$ are independently decomposed from one another. Mathematically,

$$\hat{\mathbf{s}} = \arg \min_{\hat{\mathbf{s}} \in \mathcal{S}} \parallel \mathcal{H}^H \dot{\mathbf{r}} - \zeta \hat{\mathbf{s}} \parallel^2 \tag{6.3.11}$$

where $\|(.)\|$ denotes Euclidean norm.

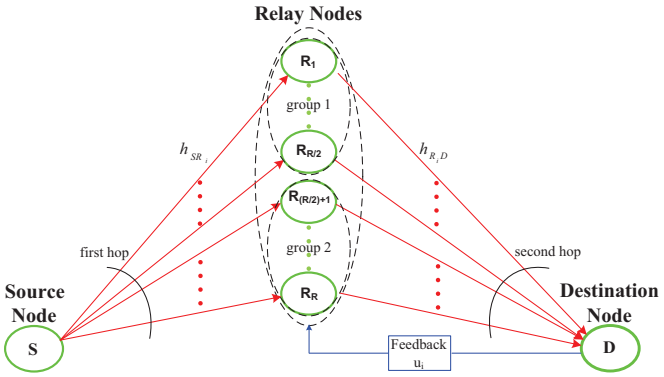

Figure 6.3. Schematic representation of the proposed closed-loop D-EO-STBC cooperative system for any number of relay nodes with partial feedback channels.

6.3.4 Closed-loop D-EO-STBCs using a one-bit partial feedback scheme

The objective is achieving at least full cooperative diversity, i.e. $\zeta \geq \alpha$. However, as in equation (6.3.9), it is clear that β_{g_1} and β_{g_2} may have negative values which may reduce the system gain below α. To ensure that β_{g_1} and β_{g_2} are always non-negative and consequently $\zeta \geq \alpha$, a new low complexity feedback scheme that can apply over any arbitrary number of relays is proposed. This scheme is based on implementing a phase rotation process over certain relay nodes. In particular, the proposed scheme requires $R-2$ feedback links between the destination and the relay nodes to achieve a diversity of order R. This means two relay nodes do not need to apply feedback so their forwarded signals remain unchanged. However, it is required that each relay of them should be from a different group. So, this scheme discards the worst link of each group to gain more system improvement. Without loss of generality, it is assumed that the relay nodes with the worst links in the considered system are $\frac{R}{2}$ and R, i.e. $u_{\frac{R}{2}} = 1$ and $u_R = 1$ where u_i is the relay feedback weighted value. The proposed

feedback scheme is designed to determine whether the $R-2$ relays require to rotate their forwarded signals by π radians or not based on analyzing the channel coefficients for each group so a single bit is enough for each rotation phase. Specifically, the feedback scheme calculates all β_{g_1} and β_{g_2} possible values, denoted as $\mathcal{L}_l^{g_1}$ and $\mathcal{L}_l^{g_2}$, respectively, and based on them it can determine the feedback coefficient for each link $c_i^{g_1}$ and $c_i^{g_2}$ which is either 1 or 0, where $l = 1, 2, ..., 2^m$ and $m = \binom{\frac{R}{2}}{2}$. The feedback coefficients of each group $c_i^{g_1}$ and $c_i^{g_2}$ are computed according to the channel coefficients of each group $h_i^{g_1}$ and $h_i^{g_2}$, respectively. The channel coefficients $h_i^{g_1}$ and $h_i^{g_2}$ can be positive or negative values, i.e. $\pm h_i^{g_1}$ and $\pm h_i^{g_2}$. In the following, the analysis process that occurs at the destination node will be explained in detail to find the feedback coefficients of group 1, $c_i^{g_1}$, for m links. In group 1, the channel coefficients are $h_i^{g_1} = h_{SR_i} h_{R_i D}$ where $i = 1, ..., \frac{R}{2}$. The channel related terms over group 1 can be calculated as follows

$$\begin{aligned} h^{g_1}_{\frac{R}{2}-1,\frac{R}{2}} &= 2\mathrm{Re}\{h^*_{\frac{R}{2}-1} h_{\frac{R}{2}}\} \\ h^{g_1}_{\frac{R}{2}-2,\pm\frac{R}{2}-1,\frac{R}{2}} &= 2\mathrm{Re}\{h^*_{\frac{R}{2}-2}(\pm h_{\frac{R}{2}-1} + h_{\frac{R}{2}})\} \\ h^{g_1}_{1,\pm...,\pm\frac{R}{2}-1,\frac{R}{2}} &= 2\mathrm{Re}\{h^*_1(\pm h_2 \pm ... \pm h_{\frac{R}{2}-1} + h_{\frac{R}{2}})\} \end{aligned}$$

Based on the channel related terms, $\mathcal{L}_l^{g_1}$ can be found as follows

$$\mathcal{L}_l^{g_1} = \pm h_{\frac{R}{2}-1,\frac{R}{2}} \pm h_{\frac{R}{2}-2,\pm\frac{R}{2}-1,\frac{R}{2}} \pm h_{\frac{R}{2}-3,\pm\frac{R}{2}-2,\pm\frac{R}{2}-1,\frac{R}{2}} \pm ... \pm h_{1,\pm...,\pm\frac{R}{2}-1,\frac{R}{2}}$$

Specifically,

$$\mathcal{L}_l^{g_1}=\begin{cases}\mathcal{L}_1^{g_1} & =h_{\frac{R}{2}-1,\frac{R}{2}}+h_{\frac{R}{2}-2,\frac{R}{2}-1,\frac{R}{2}}+h_{\frac{R}{2}-3,\frac{R}{2}-2,\frac{R}{2}-1,\frac{R}{2}}+...+h_{1,...,\frac{R}{2}-1,\frac{R}{2}}\\ \mathcal{L}_2^{g_1} & =h_{\frac{R}{2}-1,\frac{R}{2}}+h_{\frac{R}{2}-2,\frac{R}{2}-1,\frac{R}{2}}+h_{\frac{R}{2}-3,\frac{R}{2}-2,\frac{R}{2}-1,\frac{R}{2}}+...-h_{1,...,\frac{R}{2}-1,\frac{R}{2}}\\ ... & = ...\\ ... & = ...\\ \mathcal{L}_{2^{m-1}}^{g_1} & = h_{\frac{R}{2}-1,\frac{R}{2}}-h_{\frac{R}{2}-2,-\frac{R}{2}-1,\frac{R}{2}}-h_{\frac{R}{2}-3,-\frac{R}{2}-2,-\frac{R}{2}-1,\frac{R}{2}}-...\\ & \quad -h_{1,-...,-\frac{R}{2}-1,\frac{R}{2}}\\ \mathcal{L}_{2^{m-1}+1}^{g_1} & = -h_{\frac{R}{2}-1,\frac{R}{2}}+h_{\frac{R}{2}-2,\frac{R}{2}-1,\frac{R}{2}}+h_{\frac{R}{2}-3,\frac{R}{2}-2,\frac{R}{2}-1,\frac{R}{2}}+...+h_{1,...,\frac{R}{2}-1,\frac{R}{2}}\\ \mathcal{L}_{2^{m-1}+2}^{g_1} & = -h_{\frac{R}{2}-1,\frac{R}{2}}+h_{\frac{R}{2}-2,\frac{R}{2}-1,\frac{R}{2}}+h_{\frac{R}{2}-3,\frac{R}{2}-2,\frac{R}{2}-1,\frac{R}{2}}+...-h_{1,...,\frac{R}{2}-1,\frac{R}{2}}\\ ... & = ...\\ ... & = ...\\ \mathcal{L}_{2^m}^{g_1} & = -h_{\frac{R}{2}-1,\frac{R}{2}}-h_{\frac{R}{2}-2,-\frac{R}{2}-1,\frac{R}{2}}-h_{\frac{R}{2}-3,-\frac{R}{2}-2,-\frac{R}{2}-1,\frac{R}{2}}-...\\ & \quad -h_{1,-...,-\frac{R}{2}-1,\frac{R}{2}}\end{cases}$$

Based on that, the feedback coefficients can be determined as follows

$$c_i^{g_1}=\begin{cases}c_{\frac{R}{2}-1}^{g_1} & = \begin{cases}0 & \text{if } \mathcal{L}_l\geq 0 \text{ and } h_{\frac{R}{2}-1,\frac{R}{2}}\geq 0\\ 1 & \text{if } \mathcal{L}_l\geq 0 \text{ and } h_{\frac{R}{2}-1,\frac{R}{2}}<0\end{cases}\\ c_{\frac{R}{2}-2}^{g_1} & = \begin{cases}0 & \text{if } \mathcal{L}_l\geq 0 \text{ and } h_{\frac{R}{2}-2,\frac{R}{2}-1,\frac{R}{2}}\geq 0\\ 1 & \text{if } \mathcal{L}_l\geq 0 \text{ and } h_{\frac{R}{2}-2,\frac{R}{2}-1,\frac{R}{2}}<0\end{cases}\\ ... & = \begin{cases}...\end{cases}\\ ... & = \begin{cases}...\end{cases}\\ c_1^{g_1} & = \begin{cases}0 & \text{if } \mathcal{L}_l\geq 0 \text{ and } h_{1,...,\frac{R}{2}-1,\frac{R}{2}}\geq 0\\ 1 & \text{if } \mathcal{L}_l\geq 0 \text{ and } h_{1,...,\frac{R}{2}-1,\frac{R}{2}}<0\end{cases}\end{cases} \tag{6.3.12}$$

Similarly, the feedback coefficients of group 2, $c_i^{g_2}$, can be computed taking into consideration that $h_i^{g_2}=h_{SR_i}^{*}h_{R_iD}$ where $i=\frac{R}{2}+1,...,R$. Finally, the phase rotation factors u_i (feedback weighted values) can be calculated

according to the following equation

$$u_i = \begin{cases} (-1)^{c_i^{g_1}} & \text{if } i = 0, ..., \frac{R}{2} \\ (-1)^{c_i^{g_2}} & \text{if } i = \frac{R}{2}+1, ..., R \end{cases} \tag{6.3.13}$$

It is clear that the scheme only requires one bit for each rotation process. Therefore, the maximum overhead of the feedback channel in this scheme is $R-2$ bits.

It is assumed that the stationarity of the channel is sufficient to tolerate the feedback delay. By doing so, the relay transmitted signals $\mathbf{t}_i$ are multiplied by phase rotators u_i before they are transmitted from their relay nodes as shown in Fig. 6.3. The phase rotation on the transmitted symbols is equivalent to rotating the phases of the corresponding channel coefficients. The received signal vector $\mathbf{r}$ at the destination node can then be expressed as follows

$$\mathbf{r} = \sum_{i=1}^{R} \mathbf{t}_i u_i h_{R_i D} + \mathbf{w}$$

Consequently, the equivalent channel matrix $\hat{\mathcal{H}}$ is given by

$$\hat{\mathcal{H}} = \begin{bmatrix} \hat{h}_{g_1} & -\hat{h}_{g_2} \\ \hat{h}^*_{g_2} & \hat{h}^*_{g_1} \end{bmatrix} \tag{6.3.14}$$

where $\hat{h}_{g_1} = \sum_{i=1}^{\frac{R}{2}} u_i h_i^{g_1}$ and $\hat{h}_{g_2} = \sum_{i=\frac{R}{2}+1}^{R} u_i h_i^{g_2}$ taking into account that $u_{\frac{R}{2}} = u_R = 1$.

Consequently, $\zeta^f = \alpha^f + \beta^f = \sum_{i=1}^{\frac{R}{2}} |u_i h_i^{g_1}|^2 + \sum_{i=\frac{R}{2}+1}^{R} |u_i h_i^{g_2}|^2 + \beta_1^f + \beta_2^f$ where

$$\beta_{g_1}^f = \underbrace{\sum_{i_1=1}^{\frac{R}{2}} \sum_{i_2=1}^{\frac{R}{2}}}_{i_1 \neq i_2} u_{i_1} h_{i_1}^{g_1} (u_{i_2} h_{i_2}^{g_1})^*, \quad \beta_{g_2}^f = \underbrace{\sum_{i_1=\frac{R}{2}+1}^{R} \sum_{i_2=\frac{R}{2}+1}^{R}}_{i_1 \neq i_2} u_{i_1} h_{i_1}^{g_2} (u_{i_2} h_{i_2}^{g_2})^*$$

It is clear that $\alpha^f = \alpha$ taking into account that $|u_i|^2 = 1$.

The feedback gain (array gain) is $\beta_f = \beta_{g1}^f + \beta_{g2}^f$. As such, the feedback gain is equal to zero or a positive value, i.e. $\beta_f > 0$. Therefore, the designed closed-loop system can obtain additional performance gain, which leads to an improved channel gain, and correspondingly the SNR at the destination receiver. Also, as $\zeta^f \geq \sum_{i=1}^{R} |h_i|^2 = \alpha^f$, therefore the system can at least achieve full cooperative diversity of order R.

In the case of an arbitrary odd number of relay nodes, the relays are divided between the two groups where one group consists of $(R+1)/2$ while the other consists of $(R-1)/2$ relays. In fact, the proposed one-bit feedback scheme can be relaxed for any group size.

6.3.5 Optimal one-bit partial feedback approach for D-EO-STBCs

The feedback scheme can improve the system performance through increasing the feedback gain, β_f, without increasing the feedback bits. This will happen if the scheme optimally selects the one-bit feedback links for each group which results in maximizing $\beta_1^{g_1}$ and $\beta_1^{g_2}$. So, in the following, an optimal partial feedback approach that can leverage the system overall performance to the maximum using no more than $R-2$ bits is proposed. Then, based on a full search over all values of $\mathcal{L}_l^{g_1}$ and $\mathcal{L}_l^{g_2}$, this scheme will independently choose the maximum value of each. Therefore,

$$\mathcal{L}_{\max}^{g_1} = \max_l \{\mathcal{L}_l^{g_1}\} \quad \text{and} \quad \mathcal{L}_{\max}^{g_2} = \max_l \{\mathcal{L}_l^{g_2}\} \tag{6.3.15}$$

As a result, the corresponding feedback coefficients $c_i^{g_1}$ and $c_i^{g_2}$ can be found and consequently the phase rotation factors u_i. So, this method can achieve a significant improvement without needing to increase the transmit power or the feedback overhead.

6.3.6 Selection relay approach over closed-loop D-EO-STBCs and D-Alamouti

The relay selection approach for cooperative systems has been recently proposed as in [94], [97] and [126], to improve system reliability and reduce complexity. The key idea behind these approaches is to select the best relays between the source and destination nodes that have the best paths according to the channels conditions. However, most of the previous studies are based on selecting the best relay. In this section, two effective relay selection approaches combined with simple three level power adaptation are proposed. The relays are assumed to be able to operate with three power levels: zero, normal power value according to the optimal power allocation proposed in [67] and maximum power which is double the normal power. In the proposed approaches, the total system power, which is calculated based on normal power, should be constant. So, to switch one relay to use its maximum power that means the status of one different relay is switched off. In the following, the two relay selection approaches will be presented.

D-EO-STBC-based relay selection approach

In this approach, the system will work with $R-1$ relays instead of R relays where the worst relay, based on instantaneous channel conditions, is switched off. In particular, this approach determines the worst link and the best link for the whole system according to the instantaneous channel fading coefficients as follows.

$$\begin{aligned} h_{\max} &= \max\{\max_i\{|h_i^{g_1}|^2\}, \max_i\{|h_i^{g_2}|^2\}\} \\ h_{\min} &= \min\{\min_i\{|h_i^{g_1}|^2\}, \min_i\{|h_i^{g_2}|^2\}\} \end{aligned} \tag{6.3.16}$$

The approach then neglects the relay with the worst link, $h_{\min}$, by stopping its forwarding process and exploiting its transmit power $\mathcal{P}_r$ through

transferring it to the relay with the best link, $h_{\max}$, which result in doubling its transmit power to $2\mathcal{P}_r$. By so doing, the total transmit power remains unchanged. Mathematically, that means, in terms of channel coefficient h_i,

$$\begin{aligned} h_i &= 0 \qquad\quad \text{if} \quad h_i = h_{\min} \\ h_i &= \sqrt{2}h_{\max} \quad \text{if} \quad h_i = h_{\max} \end{aligned} \tag{6.3.17}$$

Finally, this approach performs the closed-loop D-EO-STBC over the selected relays with $(R-1)-2$ feedback links. Without loss of generality, it is assumed that R_1 has the best link while R_R has the worst link, the equivalent channel will consequently be

$$\dot{\mathcal{H}} = \begin{bmatrix} \dot{h}_{g_1} & -\dot{h}_{g_2} \\ \dot{h}^*_{g_2} & \dot{h}^*_{g_1} \end{bmatrix} \tag{6.3.18}$$

where

$$\dot{h}_{g_1} = \sqrt{2}u_1 h_{SR_1} h_{R_1 D} + \sum_{i=2}^{\frac{R}{2}} u_i h_{SR_i} h_{R_i D} \text{ and } \dot{h}_{g_2} = \sum_{i=\frac{R}{2}+1}^{R-1} u_i h^*_{SR_i} h_{R_i D}$$

and consequently, the channel gain of this approach , $\dot{\zeta}^f$, can be calculated as $\dot{\zeta}^f = \dot{\alpha}^f + \dot{\beta}^f = \dot{\alpha}^f_1 + \dot{\alpha}^f_2 + \dot{\beta}^f_1 + \dot{\beta}^f_2$ where

$$\dot{\alpha}^f_1 = |\sqrt{2}u_1 h^{g_1}_1|^2 + \sum_{i=2}^{\frac{R}{2}} |u_i h^{g_1}_i|^2 \text{ and } \dot{\alpha}^f_2 = \sum_{i=\frac{R}{2}+1}^{R-1} |u_i h^{g_2}_i|^2$$

$$\dot{\beta}^f_{g_1} = \sum_{i_2=2}^{\frac{R}{2}} \sqrt{2}u_1 h^{g_1}_1 (u_{i_2} h^{g_1}_{i_2})^* + \sum_{i_1=2}^{\frac{R}{2}} \sqrt{2}u_{i_1} h^{g_1}_{i_1} (2u_1 h^{g_1}_1)^* + \underbrace{\sum_{i_1=2}^{\frac{R}{2}} \sum_{i_2=2}^{\frac{R}{2}}}_{i_1 \neq i_2} u_{i_1} h^{g_1}_{i_1} (u_{i_2} h^{g_1}_{i_2})^*$$

$$\dot{\beta}^f_{g_2} = \underbrace{\sum_{i_1=\frac{R}{2}+1}^{R-1} \sum_{i_2=\frac{R}{2}+1}^{R-1}}_{i_1 \neq i_2} u_{i_1} h^{g_2}_{i_1} (u_{i_2} h^{g_2}_{i_2})^*$$

It is clear that this approach can effectively exploit the available total transmit power over the relay nodes to obtain better performance.

D-Alamouti-based relay selection approach

In this approach, the system will work with only two relays instead of R relays where the $R-2$ worst relays, based on instantaneous channel conditions, are switched off. Also, the approach does not require feedback for aligning the relay transmitted signals. In particular, according to the instantaneous channel fading coefficients, this approach selects the best link and the second best link to be employed within this system. So,

$$\begin{aligned} h_{\text{best}} &= \max\{\max_i\{|h_i^{g_1}|^2\}, \max_i\{|h_i^{g_2}|^2\}\} \\ h_{2^{\text{nd}}\ \text{best}} &= \max\{\max_i\{|h_i^{g_1}|^2\}, \max_i\{|h_i^{g_2}|^2\}\}(\text{except } h_{best}) \end{aligned} \quad (6.3.19)$$

The approach then neglects the remaining $R-2$ relays with the worst links by stopping their forwarding process and exploiting their transmit powers $(R-2)\mathcal{P}_r$ through transferring them to the best and second best relays, h_{best} and $h_{2^{\text{nd}}\ \text{best}}$, in equal quantities which results in increasing the transmit power for each of them to be $\frac{R}{2}\mathcal{P}_r$. Mathematically, that means, in terms of channel coefficient h_i,

$$\begin{aligned} h_i &= \sqrt{\tfrac{R}{2}}h_{\text{best}} && \text{if} \quad h_i = h_{\text{best}} \\ h_i &= \sqrt{\tfrac{R}{2}}h_{2^{\text{nd}}\ \text{best}} && \text{if} \quad h_i = h_{2^{\text{nd}}\ \text{best}} \\ h_i &= 0 && \text{if} \quad \text{elsewhere} \end{aligned} \quad (6.3.20)$$

Finally, the approach implements D-Alamouti code over the selected two relays. Therefore, the equivalent channel can be obtained as

$$\mathcal{H}_A = \begin{bmatrix} \sqrt{\frac{R}{2}}h_{\text{best}} & -\sqrt{\frac{R}{2}}h_{2^{\text{nd}}\ \text{best}} \\ \sqrt{\frac{R}{2}}h^*_{2^{\text{nd}}\ \text{best}} & \sqrt{\frac{R}{2}}h^*_{\text{best}} \end{bmatrix} \quad (6.3.21)$$

and consequently, the channel gain, ζ_A, based on this approach will be $\zeta_A = |\sqrt{\frac{R}{2}}h_{\text{best}}|^2 + |\sqrt{\frac{R}{2}}h_{2^{\text{nd}}\ \text{best}}|^2 = \frac{R}{2}(|h_{\text{best}}|^2 + |h_{2^{\text{nd}}\ \text{best}}|^2)$.
This approach will substantially minimize the computational complexity and

the feedback overhead as compared with the previous proposed relay selection approach.

6.4 Closed-Loop D-EO-STBC Scheme for Asynchronous Narrowband Networks

The term narrowband network is used here to refer to a network in which all channels between any two nodes are presumed as flat fading channels. In practical wireless narrowband communication, the transmitted signals through the relay nodes will most likely have different propagation delays and therefore arrive at the destination receiver at different time instants. That means the synchronization between the relay nodes is difficult or impossible due to several factors such as the relay nodes being spread out in different locations and each relay node having its own oscillator. Recently, there have been studies related to asynchronous cooperative relay systems; for example, [75]. In practice, the asynchronism represents frame delay shifts rather than carrier frequency offsets. Therefore, there is normally a timing misalignment of τ between the received versions of these signals. Without loss of generality, it is assumed that the receiver at the destination is perfectly synchronized to R_1 and τ_i-sample misalignment with the other relay nodes is present as shown in Fig. 6.4. Such a relative delay will cause inter-symbol interference (ISI) between subcarriers which will degrade the system performance. In the following section, a simple AF type scheme is proposed for an asynchronous cooperative system through the use of a feedback channel. This scheme can extract full spatial cooperative diversity from a complex orthogonal STBC design. Also, a very simple ML decoding algorithm can be used at the destination receiver.

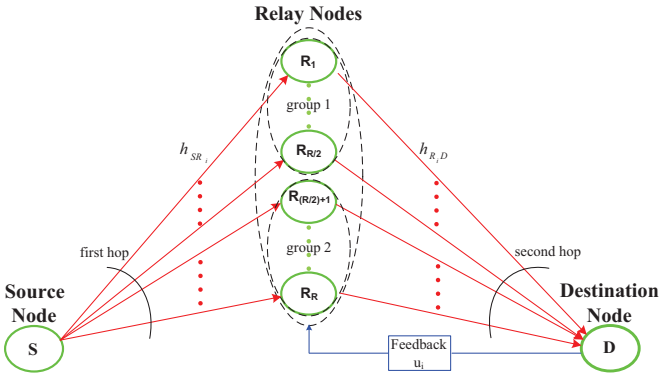

Figure 6.4. Schematic representation of the proposed asynchronous closed-loop D-EO-STBC cooperative system for any number of relay nodes with partial feedback channels.

6.4.1 Broadcasting and Relaying phases

In the broadcasting phase, the source node converts sequentially two consecutive symbol blocks $\mathbf{s} = [\mathbf{s}_1 \ \mathbf{s}_2^*]^T$ with complex conjugation for the second symbol into two OFDM symbols $\mathbf{x} = [\mathbf{x}_1 \ \mathbf{x}_2]$ by using the inverse discrete Fourier transform (IDFT) operation, i.e. $\mathbf{x} = \text{IDFT}(\mathbf{s})$, where $\mathbf{s}_j = [s_{0,j}, s_{1,j}, ..., s_{N-1,j}]^T$, $j = 1, 2$ and N represents the OFDM symbol length with a two-hop channel of $2N$ coherence time. Each OFDM symbol is preceded by a CP with length l_{cp} before broadcasting which makes each OFDM symbol length equal to $L_s = N + l_{cp}$. It is assumed that l_{cp} is not less than the maximum of the possible relative timing errors of the signals arriving at the destination node. The received signals at every relay $\mathbf{y}_i$ for two successive OFDM symbol periods can be written as

$$\mathbf{y}_i = \sqrt{\mathcal{P}_s}\mathbf{x}\, h_{SR_i} + \mathbf{v}_i \tag{6.4.1}$$

In the relaying phase, the relay nodes amplify and forward the OFDM signals using a similar way as described in the previous section where each relay is

designed to implement the matrices $\ddot{\mathbf{A}}_i$ and $\ddot{\mathbf{B}}_i$ of size $2N \times 2N$, where

$$\ddot{\mathbf{A}}_1 = ... = \ddot{\mathbf{A}}_{\frac{R}{2}} = \begin{bmatrix} \mathbf{I}_N & \mathbf{0}_N \\ \mathbf{0}_N & \mathbf{I}_N \end{bmatrix}, \quad \ddot{\mathbf{A}}_{\frac{R}{2}+1} = ... = \ddot{\mathbf{A}}_R = \begin{bmatrix} \mathbf{0}_N & \mathbf{0}_N \\ \mathbf{0}_N & \mathbf{0}_N \end{bmatrix}$$

$$\ddot{\mathbf{B}}_1 = ... = \ddot{\mathbf{B}}_{\frac{R}{2}} = \begin{bmatrix} \mathbf{0}_N & \mathbf{0}_N \\ \mathbf{0}_N & \mathbf{0}_N \end{bmatrix}, \quad \ddot{\mathbf{B}}_{\frac{R}{2}+1} = ... = \ddot{\mathbf{B}}_R = \begin{bmatrix} \mathbf{0}_N & -\mathbf{I}_N \\ \mathbf{I}_N & \mathbf{0}_N \end{bmatrix} \tag{6.4.2}$$

where $\mathbf{I}_N$ denotes the identity matrix of size $N \times N$ and $\mathbf{0}_N$ denotes the $N \times N$ matrix with all zeros.

However, to construct signals at the destination in the form of a D-EO-STBC codeword a simple reversed cyclic shift operation should be implemented on the received noisy signals, i.e. $\xi(\mathbf{y}_i)$, where $\xi(.)$ represents the time-reversal of the signal, defined as $\xi(\mathbf{a}(k)) = \mathbf{a}(N-k)$ where $k = 0, 1, ..., N-1$ and $\mathbf{a}(N) = \mathbf{a}(0)$. To minimize the computational complexity, the time-reversion operation is implemented over only one group, which is here group 2. Therefore, the transmit signal at the ith relay can be expressed as

$$\mathbf{t}_i = \Omega(\ddot{\mathbf{A}}_i \mathbf{y}_i + \ddot{\mathbf{B}}_i \xi(\mathbf{y}_i^*)) \tag{6.4.3}$$

In order to extract full spatial cooperative diversity, a simple feedback approach similar to that mentioned in the previous section is proposed to apply over $R-2$ relay nodes. Although the previous proposed feedback approach is designed for a single-carrier implementation, this approach is developed here for multi-carrier implementation by independently applying the same feedback algorithm for each OFDM sub-carrier using the equivalent channel coefficients for each sub-carrier. Therefore, it is adequate that the R-2 relay nodes rotate their signals according to the corresponding feedback vector $\mathbf{u}_i$ while the remaining two relays, in this case $\frac{R}{2}$ and R, keep their signals unchanged, i.e. $\mathbf{u}_i = \mathbf{1}_N$ where $\mathbf{1}_N$ is a vector of all elements equal to unity

and $i = \frac{R}{2}$ and R in this case.

6.4.2 Implementation at the destination node

The destination node receives the information symbols from the relay nodes in different relative time delay instants. The delay instants in the time domain are equivalent to phase changes in the frequency domain

$$\mathbf{f}^{\tau_i} = \left[\; f_0^{\tau_i}, \; f_1^{\tau_i}, ..., \; f_{N-1}^{\tau_i} \; \right]^T \tag{6.4.4}$$

where $f_k^{\tau_i} = \exp(-j2\pi k\tau_i/N)$ and $k = 0, 1, ..., N-1$.

However, to process the data at the destination node, the following steps are performed:

1. CP removal is performed for each received signal as shown in Fig. 6.5.

2. Shifting the last l_{cp} samples to be the first samples for the received signals during the second symbol period to correct the misalignment caused by the time reversal process.

3. Applying DFT transform operation taking into account the following identities $(\text{DFT}(\mathbf{x}))^* = \text{IDFT}(\mathbf{x}^*)$, $(\text{IDFT}(\mathbf{x}))^* = \text{DFT}(\mathbf{x}^*)$ and $\text{DFT}(\xi(\text{DFT}(\mathbf{x}))) = \text{IDFT}(\text{DFT}(\mathbf{x}))$.

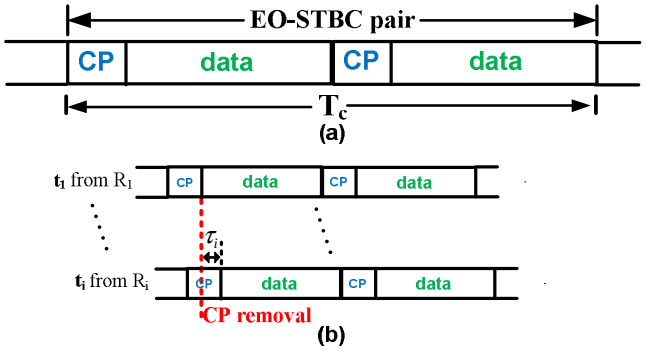

Figure 6.5. Relay synchronization with respect to relay 1 and CP removal.

The received signal vectors, $\mathbf{r}_1$ and $\mathbf{r}_2$, at the destination node therefore can be written as

$$\mathbf{r}_1 = \mathcal{P}_d(\sum_{i=1}^{\frac{R}{2}} \mathbf{s}_1 \circ \mathbf{f}^{\tau_i} \circ \mathbf{u}_i \mathrm{h}_i^{g_1} - \sum_{i=\frac{R}{2}+1}^{R} \mathbf{s}_2 \circ \mathbf{f}^{\tau_i} \circ \mathbf{u}_i \mathrm{h}_i^{g_2}) + \mathbf{n}_1 \qquad (6.4.5)$$

$$\mathbf{r}_2 = \mathcal{P}_d(\sum_{i=1}^{\frac{R}{2}} \mathbf{s}_2^* \circ \mathbf{f}^{\tau_i} \circ \mathbf{u}_i \mathrm{h}_i^{g_1} + \sum_{i=\frac{R}{2}+1}^{R} \mathbf{s}_1^* \circ \mathbf{f}^{\tau_i} \circ \mathbf{u}_i \mathrm{h}_i^{g_2}) + \mathbf{n}_2 \qquad (6.4.6)$$

where $\circ$ is the Hadamard product, $h_i^{g_1} = h_{SR_i} h_{R_iD}$, $h_i^{g_2} = h_{SR_i}^* h_{R_iD}$, $\mathbf{n}_1 = \Omega(\sum_{i=1}^{\frac{R}{2}} \mathbf{f}^{\tau_i} \circ \mathbf{u}_i h_{R_iD} \circ \mathrm{DFT}(\mathbf{v}_{i1}) - \sum_{i=\frac{R}{2}+1}^{R} \mathbf{f}^{\tau_i} \circ \mathbf{u}_i h_{R_iD} \circ \mathrm{DFT}(\mathbf{v}_{i2}^*)) + \mathbf{w}_1$, and $\mathbf{n}_2 = \Omega(\sum_{i=1}^{\frac{R}{2}} \mathbf{f}^{\tau_i} \circ \mathbf{u}_i h_{R_iD} \circ \mathrm{DFT}(\mathbf{v}_{i2}) + \sum_{i=\frac{R}{2}+1}^{R} \mathbf{f}^{\tau_i} \circ \mathbf{u}_i h_{R_iD} \circ \mathrm{DFT}(\mathbf{v}_{i1}^*)) + \mathbf{w}_2$. Hence, $\mathbf{r}_1$ and $\mathbf{r}_2$ in (6.4.5) and (6.4.6) can be written for each subcarrier k as follows

$$\begin{bmatrix} r_{k,1} \\ r_{k,2}^* \end{bmatrix} = \mathcal{P}_d \underbrace{\begin{bmatrix} h_k^{g_1} & -h_k^{g_2} \\ (h_k^{g_2})^* & (h_k^{g_1})^* \end{bmatrix}}_{\mathcal{H}_k} \begin{bmatrix} s_{k,1} \\ s_{k,2}^* \end{bmatrix} + \begin{bmatrix} n_{k,1} \\ n_{k,2}^* \end{bmatrix} \qquad (6.4.7)$$

where $h_k^{g_1} = \sum_{i=1}^{\frac{R}{2}} \mu_i^k h_{SR_i} h_{R_iD}$ and $h_k^{g_2} = \sum_{i=\frac{R}{2}+1}^{R} \mu_i^k h_{SR_i}^* h_{R_iD}$ where $\mu_i^k = f_k^{\tau_i} u_{k,i}$.

After applying the matched filtering process at the destination receiver with the equivalent channel matrix in (6.4.7) for each of the k sub-carriers, the Gramian matrix $\mathbf{G}_k$ can be obtained as follows.

$$\mathbf{G}_k = \mathcal{H}_k^H \mathcal{H}_k = \begin{bmatrix} \zeta_k & 0 \\ 0 & \zeta_k \end{bmatrix} \qquad (6.4.8)$$

where ζ_k represents the channel gain at each subcarrier k such that $\zeta_k = \alpha_k + \beta_k = \sum_{i=1}^{\frac{R}{2}} |\mu_i^k h_i^{g_1}|^2 + \sum_{i=\frac{R}{2}+1}^{R} |\mu_i^k h_i^{g_2}|^2 + \beta_k^{g_1} + \beta_k^{g_2}$ where

$$\beta_k^{g_1} = \underbrace{\sum_{i_1=1}^{\frac{R}{2}} \sum_{i_2=1}^{\frac{R}{2}}}_{i_1 \neq i_2} \mu_{i_1}^k h_{i_1}^{g_1} (\mu_{i_2}^k h_{i_2}^{g_1})^*, \quad \beta_k^{g_2} = \underbrace{\sum_{i_1=\frac{R}{2}+1}^{R} \sum_{i_2=\frac{R}{2}+1}^{R}}_{i_1 \neq i_2} \mu_{i_1}^k h_{i_1}^{g_2} (\mu_{i_2}^k h_{i_2}^{g_2})^*$$

taking into account that $|u_{k,1}|^2 = |u_{k,2}|^2 = 1$ and $(f_k^{\tau_i})^* f_k^{\tau_i} = 1$. The values of $\beta_k^{g_1}$ and $\beta_k^{g_2}$ after applying the feedback will be always non-negative which means the proposed scheme is able to achieve at least full spatial diversity.

6.5 Closed-Loop D-EO-STBC Scheme for Asynchronous Broadband Networks

The term broadband network is used because the channels in the wireless relay network are assumed to be frequency-selective fading channels. In the broadband network, the transmitted signals experience multiple paths to arrive at the destination node. Also, the transmitted signals experience different time delays to arrive at the destination node where the synchronization is difficult to achieve in this situation. In this section, a closed-loop one-bit feedback scheme is designed for a D-EO-STBC multi-carrier system over frequency-selective fading channels. In fact, it is an extension version of that proposed in the previous section. Hence, a similar procedure can be followed considering the differences that will be explained now. So, the source implements the same steps as in the previous section taking into account that all the system channels are assumed to be frequency-selective quasi-static fading channels. However, at the relay nodes, the system implements some different operations as follows. The relay nodes firstly remove the CP from their received information signals. Then, certain R-2 relays, which need to apply feedback over them, implement the DFT process in order to apply

the proper phase rotation while the remaining two relays, in this case $\frac{R}{2}$ and R, do not require this process. After applying feedback over the R-2 relays, these relays perform an IDFT process instead of a time-reversal process as in the previous section. However, the relay R should perform a time-reversal process over its received signals. Finally, all relays add a CP to their signals before transmitting them towards the destination node. Therefore, the transmit signals at certain $R-2$ relays can be expressed as

$$\mathbf{t}_i \;=\; \Omega(\ddot{\mathbf{A}}_i \;\mathrm{IDFT}(\mathbf{y}_i) + \ddot{\mathbf{B}}_i \;\mathrm{IDFT}((\mathbf{y}_i^*))) \tag{6.5.1}$$

As shown in equation (6.5.1), the group 2 does not require the time-reversion operations.

At the destination, only two steps are performed over the received signals in order to extract the information symbols which are the CP removal and DFT process. As is evident, a shifting step at the destination node as in the previous narrowband scenario is not needed in this scenario. It is noteworthy that the proposed scheme is focused on achieving spatial cooperative diversity. However, the temporal diversity available in the multipaths can be exploited by using complicated space-time-frequency block coding methods [117], but this is beyond the scope of this work.

6.6 Simulation Results

In this section, numerical simulation results for the AF cooperative system based on closed-loop D-EO-STBC schemes are presented to illustrate the end-to-end bit error rate (BER) performance of the proposed schemes over fading channels. The fading is assumed to be constant within a frame of two blocks each with 64 symbols and to change independently from frame-to-frame, i.e. quasi-static fading. The symbols are drawn from quadrature phase-shift keying (QPSK) modulation. The total transmit power is equally

divided between the source node and the relay nodes. The same total power is used for each simulation. One antenna at each node was considered. The x-axis shows the average transmitted power from the source node in dB and the y-axis shows the end-to-end BER.

In Fig. 6.6, the BER performance of the proposed closed-loop D-EO-STBC

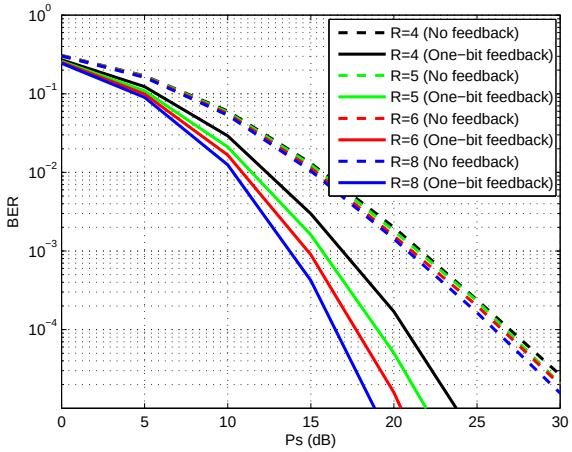

Figure 6.6. System performance for the proposed closed-loop scheme and a comparison in performance when the number of network relay nodes is increased from 4 to 8.

cooperative scheme for different numbers of relay nodes R over flat fading channels is shown. The BER curves show significant improvements on the system performance when the feedback channels are considered for the overall transmit power range. These improvements on the system performance are because the systems with feedback schemes can achieve at least full cooperative diversity while the systems without feedback schemes do not achieve full diversity. Another notable benefit is the increase in diversity as R increases so that AF type cooperation improves the BER performance significantly. It can be seen that a transition from $R = 4$ to $R = 8$ leads to a performance improvement greater than 4.25 dB for BER=10^{-4}. These plots demonstrate the effect of R on the cooperative diversity order, i.e. diversity order $= 1 \times R \times 1$. It is worth mentioning that as the number of R increases, the transmit power for each relay will decrease as a result of the adopted

power allocation so that will reflect on minimizing the interference to other users which is a great advantage.

Fig. 6.7, shows the result of the optimal one-bit feedback and the two relay

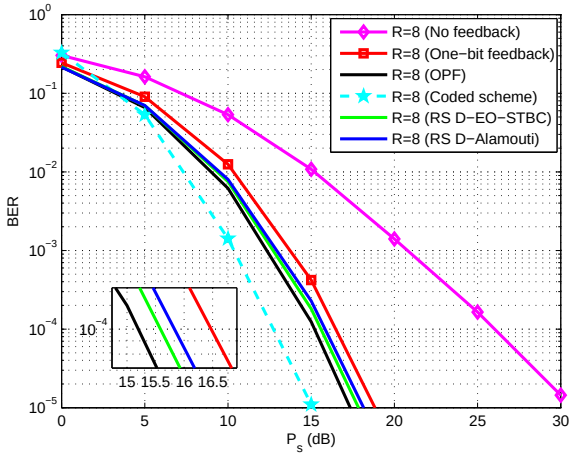

Figure 6.7. Performance comparison between the proposed closed-loop D-EO-STBCs combined with optimal partial feedback (OPF) and relay selection (RS) when the number of network relays equal to eight relays.

selection based approaches over flat fading channels on a wireless network with R=8 relay nodes. The optimal partial feedback system adds approximately 1.3 dB gain over the partial feedback system at an error rate of 10^{-4}. This is due to further improvement in array gain. On the other hand, the relay selection based on D-EO-STBC and D-Alamouti approaches provides approximately 0.95 dB and 0.70 dB gains, respectively, over the partial feedback system. This is due to exploiting the available power over relay nodes efficiently. In fact, the relay selection based D-EO-STBC approach outperforms the relay selection based D-Alamouti approach. However, from the curves, it is clear that the optimal feedback approach provides better performance than the relay selection based approaches. Specifically, at BER of 10^{-4}, the optimal feedback approach provides an improvement gain of approximately 0.35 dB over the relay selection based D-EO-STBC approach. On the other hand, in wireless applications it is desirable to use a channel

code to increase reliability. So, concatenation of the proposed scheme with a rate 1/2 convolutional code at the source and employing Viterbi decoding at the destination [114] is studied as shown in Fig. 6.7. As can be observed, approximately 3.75 dB additional gain has been achieved as compared to the proposed scheme with one-bit feedback when BER = 10^{-4}. This is because the coded scheme has achieved further coding gain.

In Fig. 6.8, the BER performance of the cooperative system over flat fading

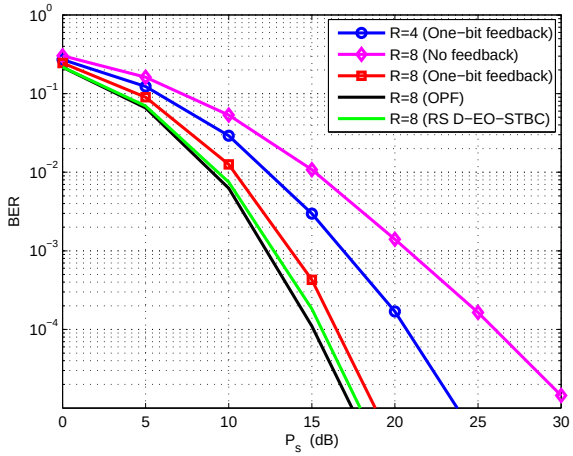

Figure 6.8. Performance comparison for the proposed closed-loop schemes over asynchronous narrowband network scenario.

channels for $R = 4$ and $R = 8$ when the synchronization is assumed to be imperfect is shown. It is clear that BER performance for the system with feedback is much better than that without feedback. Also, the positive effect of increasing R on the system performance can be noticed. In particular, at BER of 10^{-4}, the system when $R = 8$ requires approximately 16.5 dB while the system when $R = 4$ requires approximately 21 dB. Therefore, the increase of R will potentially improve the system performance. Also, the BER performance for the optimal feedback and relay selection based D-EO-STBC approaches when $R = 8$ relay nodes is depicted. It is clear that both approaches provide significant improvements as compared to the system with partial feedback. For example, at BER of 10^{-4}, performance improvements

of approximately 1.5 dB and 1 dB were achieved when the optimal feedback and relay selection based approaches are applied, respectively. It is also clear that the optimal feedback approach has achieved the best performance compared to others.

In Fig. 6.9, the effect of frequency-selective fading channels and imperfect synchronization on the system performance for the proposed closed-loop D-EO-STBC schemes is investigated. It is realized that the system can achieve at least full cooperative diversity when applying feedback channels which lead to substantially improved system performance as compared to the system with no feedback. Also, it is noticeable that the system diversity order increases as the number of relay nodes increases which reflects positively on the system performance. The figure also exhibits the advantages of using the optimal feedback and relay selection based D-EO-STBC approaches on the system performance. Also, you can recognize that the optimal feedback approach provides the best performance.

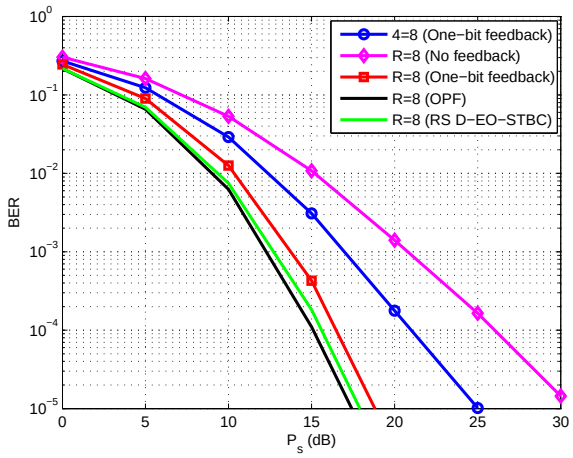

Figure 6.9. Performance comparison for the proposed closed-loop schemes over asynchronous broadband network scenario.

6.7 Summary

In this chapter, a generalized D-EO-STBC cooperative scheme for a wireless relay system over fading channels was proposed. The AF type relay nodes were equally divided into two groups with implementing simple and limited operations over only one group. A one-bit feedback from the destination node to certain relay nodes or subcarriers for certain relays was applied to combat the inter-channel correlation effects that might reduce the diversity below full orders. Numerical results show significant improvements of the proposed schemes over the open-loop schemes. Furthermore, increasing the number of relay nodes will lead to increased spatial diversity and therefore obtain further robustness for the system in the presence of fading. To improve the system performance more, two approaches which are based on optimal feedback and relay selection have been proposed. It has been shown that both schemes provide great improvements to the system performance. Different cooperative network scenarios have been presented. In terms of data rate, the proposed D-EO-STBC schemes provide full rate in each phase. On the other hand, the information symbols are being decoded separately in a very simple manner at the destination. Finally, the most importantly result can be concluded is the increase in the number of relay nodes can improve the system performance without requiring extra transmit power or bandwidth.

Chapter 7

COOPERATIVE COGNITIVE NETWORKS BASED ON DISTRIBUTED ORTHOGONAL SPACE-TIME BLOCK CODES

Cognitive radio is a novel paradigm that can substantially improve the efficiency of radio spectrum utilization. In this chapter, the performance analysis and evaluation of an amplify-and-forward (AF) type relay cooperative network where the relays operate as cognitive radios is investigated. A space-time-division (STD) protocol based on a distributed extended orthogonal space time block coded (D-EO-STBC) scheme is proposed and a closed-form expression for outage probability both with perfect and imperfect spectrum acquisition in Rayleigh fading channels is provided. Simulations show that the proposed scheme provides better outage performance than the conventional schemes based on a time-division (TD) protocol. The analytical outage probability expressions are finally validated through simulations. Also, the performance of a cognitive relay network when the cognitive user can

transmits its own information in addition to relaying the traffic of primary user is discussed and evaluated. A robust scheme based on the closed-loop D-EO-STBC has been proposed for the scenario where the cognitive user can utilize the spectrum when it is free or in other word opportunistically or it can transmit its own information simultaneously with the primary user. It is proved that the corrupted interference from the cognitive user to the primary user and vice versa can be completely eliminated which results in improved spectrum utilization efficiency without compromising on the primary transmission performance. In fact, the proposed cooperative schemes based on D-EO-STBC in the context of cognitive radio improve the transmission robustness of the primary communication and increase the probability of transmission opportunities of cognitive users which results ultimately in improving the spectrum utilization efficiency.

7.1 Introduction

Cooperative communications is an effective and promising solution for next-generation wireless systems which require high reliability and data rate [11], [12] and [127]. In fact, it is being considered in the standardization process of next-generation mobile broadband communication systems such as 3GPP LTE-Advanced and WiMAX standards (IEEE 802.16j and IEEE 802.16m) [12]. The key idea behind cooperative transmission is that the single antenna relays cooperatively assist the source node in transmitting information when the direct path from source to destination is in a deep fade and then the destination combines its received signals exploiting spatial diversity through the multiple receptions [8]. So, this new technology can overcome the limitations of other wireless technologies such as heavy shadowing effects, deep path loss and limited wireless terminal size whilst expanding network coverage and saving transmit power. In addition, it can

improve the efficiency of frequency spectrum. However, with huge growth in wireless services over the past decade, the spectrum becomes more congested. Specifically, the radio frequency spectrum is commonly divided into bands which are exclusively allocated to specific services without allowing unlicensed users to share them. Interestingly, most spectrum allocated for the primary licensed users is under-utilized at different time slots and location areas according to practical measurements and surveys; for example, in measurements performed by the Federal Communications Commission (FCC) [38] in the United States and Ofcom [39] in the United Kingdom. One of the key and innovative technologies in enhancing spectrum utilization is cognitive radio [41] and [98]. The main idea is allowing secondary unlicensed users to opportunistically or concurrently utilize licensed bands without causing harmful interference to the primary users operating in that band [128]. In fact, there are three main cognitive approaches which are interweave, overlay and underlay cognitive techniques [46]. However, only the interweave and overlay approaches are considered throughout this chapter.

Recently, there has been growing interest in the integration of cognitive radio capability into cooperative communications. In contrast to the conventional cooperative scenario, cognitive relays will only transmit if they are able to acquire spectrum. This combination can provide reliable transmission for both primary and secondary users. In [14], a cooperative cognitive relay network has been proposed to minimize interference to the primary users whilst ensuring reliable transmission for the secondary users. In [129], distributed power allocation schemes for wireless cognitive relay networks have been developed. In [100], cooperative cognitive relay schemes to improve spatial and spectrum diversities have been developed. In [14] and [99], both cooperative sensing and cooperative transmission among secondary cognitive relays are considered. In [101], a cognitive cooperation scheme to select the optimal cognitive relay among many moving relays has been proposed.

Outage probability is an important performance criterion that is widely used for characterizing the performance of communication systems [53], [130] and [131]. In [130], the outage probability of cooperative relay networks has been evaluated for arbitrary signal-to-noise ratio (SNR). The outage probability for a cooperative network equipped with multi AF relays has been obtained in [132]. In [104], the outage probability of a cognitive relay network has been derived to obtain diversity order. It was shown in [104] that the outage probability is valid in the high SNR regime. The outage performance analysis for decode-and-forward (DF) cooperative networks using a repetition-based relaying scheme or using the single best relay has been presented in [105] while the outage probability of a wireless two AF cognitive relay network has been investigated in [106]. The outage performance of a wireless cognitive relay network can be improved if cooperative spectrum sensing is used which can increase the probability of acquiring spectrum [104] and [133].

Most outage performance analyses for wireless cognitive relay networks in the literature have considered relaying schemes based on a TD arrangement. Although this type of scheme can facilitate orthogonal transmission, the required time for overall transmission will increase when the number of participant relays increases, and consequently this will maximize the outage threshold which will degrade the system performance. In this work, the outage performance of a wireless AF type cognitive relay network with a relaying scheme based on a STD arrangement in the form of D-EO-STBC is therefore investigated. This scheme requires only two time slots to complete the information transmission between the source and destination and can achieve a minimum outage threshold. Moreover, the gain exploited from the feedback process of the D-EO-STBC scheme for more than two relays will contribute in further minimizing the outage threshold. To derive the outage performance of an AF cognitive relaying scheme, a bound based approach

has been adopted and verified through simulations. Also, the outage probability of a wireless AF cognitive relay network based on selection cooperation has been proposed. Furthermore, the outage performance if the spectrum acquisition is not always perfect is discussed and evaluated.

On the other hand, secondary users can increase their transmission data rate by sharing the spectrum with the primary users concurrently or opportunistically and at the same time the primary users can exploit the concurrent secondary user to improve the transmission reliability by using cooperative diversity techniques. In [102] and [103], the primary and secondary transmission was studied where the primary user with the assistance of two secondary users that employs DF or AF relaying protocol, respectively, can communicate with its destination along with the direct path and one of the secondary users can simultaneously communicate with the other using the overlay approach. As a result, a reliable transmission for primary and secondary users was established. In this chapter, spectrum sharing based on an overlay approach and cooperative transmission is also investigated where the primary user depends on four cognitive relays in conveying its information to its destination, i.e. there is no direct link between the primary user and its destination. In this approach, an AF type relaying protocol is applied over the cognitive relays and the closed-loop D-EO-STBC cooperative scheme as in [118] is exploited. Simultaneously, any two cognitive relays can communicate with each other, i.e. the primary and secondary transmission can occur at the same time.

7.2 Wireless Cognitive Relay Network Model

Consider a dual-hop cognitive relay network which consists of a source, several clusters of relays and a destination, as shown in Fig. 7.1, where each cluster includes a primary (licensed) user and a secondary user (cognitive

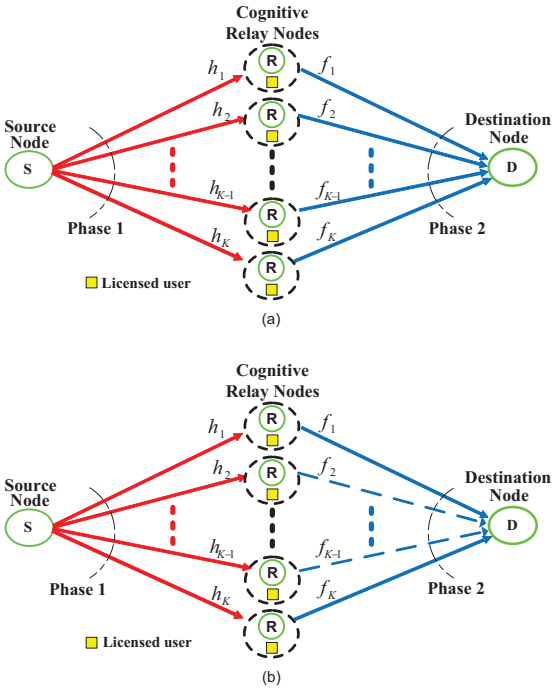

Figure 7.1. Wireless cognitive relay system where transmission occurs over two phases. (a) All cognitive relays participate in transmission during phase 2 based on D-EO-STBC scheme. (b) Only the best two cognitive relays based on selection cooperation scheme participant in transmission during phase 2 where the solid lines mean the selected paths.

relay). All nodes are equipped with only one antenna and are in half-duplex mode. There is no direct path between the source and destination due to heavy shadowing or deep path loss. Therefore, transmission occurs over two phases. In the first phase, the source transmits symbol vector $\mathbf{s} = [s_1 \ s_2]^T$ selected from any signal constellation $\mathcal{S}$, with average transmit power per symbol $\mathcal{P}_s$, where $[.]^T$ denotes vector transpose. During the first time slot, the received signal vector $\mathbf{y}_k$ at the kth relay is given by

$$\mathbf{y}_k = [y_{k1} \ y_{k2}]^T = \sqrt{P_s} h_k \mathbf{s} + \mathbf{v}_k \tag{7.2.1}$$

where $h_k \sim \mathcal{CN}(0, \lambda_{h_k})$ is the zero-mean Rayleigh-fading channel coefficient for the source-kth relay link of variance λ_{h_k} and the noise vector of the

kth relay $\mathbf{v}_k$ has elements that are complex additive white Gaussian noise (AWGN) of variance N_0 where $k = 1, ..., K$.

During the second phase, all cognitive relays participate to assist the source in conveying its information to the destination. If the cognitive relays employ a TD basis, the information transmission requires $1 + K$ time slots to be completed, where K is the total number of participant relays. So, in this section, it is proposed that all cognitive relays participate according to a STD protocol based on a closed-loop D-EO-STBC scheme as in [118] to minimize the required transmission time to be two time slots. In this case, the system can achieve the following advantages:

1. Completing the transmission process in a short time which is significant in the context of cognitive radio.

2. Minimizing the outage threshold which will reflect on improving the whole system outage performance.

3. Reducing the decoding delay which is required in real-time applications.

4. Reducing the cognitive transmit power which is essential to minimizing the interference (as a result of using cooperative transmission: transmit power savings can be provided due to path loss reduction and spatial cooperative diversity gain).

Therefore, the cognitive relays construct the D-EO-STBC scheme from the received signals, and then retransmit an amplified version to the destination with average power of $\mathcal{P}_r$ where $\mathcal{P}_r = \frac{\mathcal{P}_s}{K}$. In fact, the cognitive relays can only retransmit information if they are achieving the required conditions to be able to use the spectrum through the spectrum sensing process, i.e. an interweave cognitive approach is exploited. Therefore, in some cases, cognitive relay(s) might not be able to help in relaying due to the unavailability

of spectrum. So, with half-duplex AF relaying, the output signals $\mathbf{X}$ of the relays are presented in the form of a matrix of dimension $2 \times K$ as follows

$$\mathbf{X} = \mu\ \mathbf{C} \tag{7.2.2}$$

where $\mathbf{C}$ is the coded structure of the D-EO-STBC scheme, for which $K = 4$, and can be expressed as

$$\mathbf{C} = \begin{bmatrix} y_{11} & y_{21} & -y_{32}^* & -y_{42}^* \\ y_{12} & y_{22} & y_{31}^* & y_{41}^* \end{bmatrix} \tag{7.2.3}$$

and μ^2 is the relaying gain which can be presented as

$$\mu^2 = \frac{1}{K}\left(\frac{1}{\mathrm{E}\{|h_k|^2\} + (\mathrm{SNR}_0)^{-1}}\right) \tag{7.2.4}$$

where $\mathrm{SNR}_0 = \frac{\mathcal{P}_s}{N_0}$ is the SNR of each link without fading effects, $\mathrm{E}\{.\}$ is the statistical expectation value and $|.|^2$ denotes the modulus squared of a complex number.

The received signal vector $\mathbf{r}$ at the destination can be written as

$$\mathbf{r} = \sum_{k=1}^{K} f_k \mathbf{X} + \mathbf{w} = \sum_{k=1}^{K} \mu f_i \mathbf{C} + \mathbf{w} \tag{7.2.5}$$

where $f_k \sim \mathcal{CN}(0, \lambda_{f_k})$ is the zero-mean Rayleigh-fading channel coefficient for the kth relay-destination link of variance λ_{f_k} and $\mathbf{w}$ is the destination complex AWGN vector with elements of variance N_0. Note that, all the random variables h_k and f_k are statistically independent.

The received signal vector at the destination can be equivalently written as

$$\mathbf{r} = \mu\sqrt{\mathcal{P}_s}\mathbf{H}\ \mathbf{s} + \mathbf{n} \tag{7.2.6}$$

where $\mathbf{H}$ is the equivalent orthogonal complex channel, i.e.

$$\mathbf{H}^H\mathbf{H} = \left(\sum_{k=1}^{K}|h_k|^2|f_k|^2 + \beta_K\right)\mathbf{I}_2 \tag{7.2.7}$$

where $(.)^H$ denotes Hermitian transpose, $\mathbf{I}_2$ denotes the 2×2 identity matrix and $\mathbf{n}$ is a zero-mean AWGN vector with elements of variance $N_0(\mu^2\sum_{k=1}^{M}|f_k|^2 + 1)$.

With implementing a maximum-likelihood (ML) decoder at the destination, the symbol vector $\mathbf{s}$ can be decoded in a simple way where the two symbols in $\mathbf{s}$ are independently decomposed from one another. Therefore, the instantaneous end-to-end SNR at the destination is readily expressed as

$$\gamma = \mathrm{SNR}_0\left(\frac{\mu^2\left(\sum_{k=1}^{K}|h_k|^2|f_k|^2\right)}{\mu^2\sum_{k=1}^{K}|f_k|^2+1} + \frac{\mu^2\beta_K}{\mu^2\sum_{k=1}^{K}|f_k|^2+1}\right) \tag{7.2.8}$$

where β_K is the feedback gain of a network with $K = 4$ relays as in [118] taking into account that $\beta_K = 0$ if $K \leq 2$.

In the high SNR regime,

$$\gamma \leq \mathrm{SNR}_0\left(\frac{\left(\sum_{k=1}^{K}|h_k|^2|f_k|^2\right)}{\sum_{k=1}^{K}|f_k|^2} + \frac{\beta_K}{\sum_{k=1}^{K}|f_k|^2}\right) \tag{7.2.9}$$

To facilitate analysis, it is assumed that the second part of (7.2.9) is replaced by its average value, i.e. $\bar{\mathrm{G}} = \mathrm{E}\left\{\frac{\beta_K}{\sum_{k=1}^{K}|f_k|^2}\right\} \approx \frac{\mathrm{E}\{\beta_K\}}{\mathrm{E}\{\sum_{k=1}^{K}|f_k|^2\}}$. According to [134], $\mathrm{E}\{\mathcal{X}\} = \left(2^m\sigma^2\right)^{\frac{1}{2}}\left(\frac{\sqrt{\pi}}{2}\right)^m$ if $\mathcal{X}$ is the product of m independent Rayleigh distributed random variables with variance σ^2 and this can be applied in the case of calculating the average value of β_K, $\mathrm{E}\{\beta_K\}$. On the other hand, as $\sum_{k=1}^{K}|f_k|^2$ is the summation of non-identical independent exponentially distributed random variables each with expected value of λ_{f_k}, therefore, the expected value of the sum can be readily obtained as $\mathrm{E}\{\sum_{k=1}^{K}|f_k|^2\} = \mathrm{E}\{|f_1|^2\} + ... + \mathrm{E}\{|f_K|^2\}$.

7.3 Outage Probability of Cognitive Relay Network Based on D-EO-STBC Scheme

In this section, the outage probabilities for the proposed cooperative cognitive relay networks are derived. Outage probability is an important performance criterion of quasi-static systems. It is defined as the probability that the instantaneous capacity is lower than the required spectral efficiency threshold. Therefore, the outage probability can be defined as

$$\mathrm{P}_{out} = \mathrm{P}(R_K < R) \tag{7.3.1}$$

where R_K is the mutual information between the source and the destination and R is the target (threshold) rate at the destination.
To obtain outage probability, calculating mutual information between the source and the destination is required which is given by

$$R_K = \frac{1}{2}\log_2(1+\gamma) \tag{7.3.2}$$

where the factor $\frac{1}{2}$ accounts for the fact that information is conveyed to the destination over two time slots. It is clear that this factor is constant and not dependent on the number of participant relays as compared with systems based on TD protocol; and this as a result will reflect on improving the outage performance through minimizing the outage threshold. In outage analysis, it is important to examine the statistical characteristic of γ given in (7.2.9) such as via its probability density function (PDF) and cumulative distribution function (CDF). In fact, deriving these statistical characteristics (PDF and CDF) from the exact SNR is difficult. So, for the sake of simplicity, the upper-bound approximation is considered as follows

$$\gamma_K \leq \mathrm{SNR}_0(\Gamma_K + \bar{\mathrm{G}}) \tag{7.3.3}$$

where

$$\Gamma_K = \sum_{k=1}^{K} \gamma_k \quad \text{and} \quad \gamma_k = \min(|h_k|^2, |f_k|^2)$$

This approximation is adopted in many previous works [106] and [135] and it is shown to be sufficiently tight.

Therefore, the mutual information at the destination becomes

$$R_K = \frac{1}{2}\log_2\left(1 + \mathrm{SNR}_0\left(\sum_{k=1}^{K}\gamma_k + \bar{\mathrm{G}}\right)\right) \tag{7.3.4}$$

The SNR threshold at the destination can be then calculated as $\gamma_{th} = \frac{2^{2R}-1}{\mathrm{SNR}_0} - \bar{\mathrm{G}}$. It is obvious that the SNR threshold of the proposed scheme is much smaller as compared to that of the conventional TD scheme.

Since $h_k \sim \mathcal{CN}(0, \lambda_{h_k})$ where $k = 1, ..., K$, then $|h_k|^2$ obeys an exponential distribution with parameter $1/\lambda_{h_k}$. Therefore, the PDF of $|h_k|^2$ can be written as

$$p_{\gamma_{h_k}}(x) = \frac{1}{\lambda_{h_k}} \exp\left(-\frac{x}{\lambda_{h_k}}\right) \tag{7.3.5}$$

Similarly, the PDF of $|f_k|^2$ can be found.

When a single relay assists in the transmission, then $\Gamma_1 = \gamma_1$. The CDF of Γ_1, $F_{\Gamma_1}(\gamma)$, can be obtained as, taking into account that h_1 and f_1 are statistically independent from each other,

$$F_{\Gamma_1}(\gamma) = 1 - \int_{\gamma}^{\infty} p_{h_1}(\gamma)\, d\gamma \int_{\gamma}^{\infty} p_{f_1}(\gamma)\, d\gamma = 1 - e^{-(\frac{1}{\lambda_{h_1}}+\frac{1}{\lambda_{f_1}})\gamma} = 1 - e^{-\frac{\gamma}{\lambda_1}} \tag{7.3.6}$$

where $\frac{1}{\lambda_1} = \frac{1}{\lambda_{h_1}} + \frac{1}{\lambda_{f_1}}$.

7.3.1 Outage probability of D-Alamouti scheme

In this case, it is assumed that the number of available cognitive relays is two. When both of the two relays in the AF system simultaneously transmit,

then $\Gamma_2 = \gamma_1 + \gamma_2$. Therefore, the CDF of Γ_2 can be written as, taking into account that $\beta_K = 0$ in the case of the D-Alamouti scheme, i.e. $\bar{\mathrm{G}} = 0$,

$$F_{\Gamma_2}(\gamma) = \int_0^{\gamma} p_{\Gamma_2}(x) F_{\Gamma_1}(\gamma - x) dx \tag{7.3.7}$$

Finally, the $F_{\Gamma_2}(\gamma)$, after integrating (7.3.7) and simplifying the integral, can be obtained as

$$F_{\Gamma_2}(\gamma) = \frac{\frac{1}{\lambda_1}\left(1 - e^{-(\frac{1}{\lambda_2})\gamma}\right) - \frac{1}{\lambda_2}\left(1 - e^{-(\frac{1}{\lambda_1})\gamma}\right)}{\frac{1}{\lambda_1} - \frac{1}{\lambda_2}} \tag{7.3.8}$$

Therefore, the outage probability can be expressed as

$$P_{out}(\gamma_{th}) = F_{\Gamma_2}(\gamma_{th}) \tag{7.3.9}$$

where $\gamma_{th} = \frac{2^{2R}-1}{\mathrm{SNR}_0}$.

7.3.2 Outage probability of D-EO-STBC scheme

In this case, it is assumed that four cognitive relays are available. When the four relays transmit simultaneously, then $\Gamma_4 = \gamma_1 + \gamma_2 + \gamma_3 + \gamma_4$. The CDF of Γ_4 can be written as,

$$F_{\Gamma_4}(\gamma) = \int_0^{\gamma} p_{\Gamma_4}(x) F_{\Gamma_3}(\gamma - x) dx \tag{7.3.10}$$

The expression of CDF is evaluated by integrating (7.3.10). By evaluating (7.3.10), the final expression can be expressed as

$$F_{\Gamma_4}(\gamma) = \frac{1}{\lambda_4\lambda_3(\frac{1}{\lambda_1}-\frac{1}{\lambda_2})}\Bigg\{\left(\frac{1}{\frac{1}{\lambda_3}-\frac{1}{\lambda_2}}-\lambda_3\right)\frac{\left(e^{-\frac{\gamma}{\lambda_3}}-e^{-\frac{\gamma}{\lambda_4}}\right)}{\lambda_1(\frac{1}{\lambda_4}-\frac{1}{\lambda_3})}+\frac{\lambda_3\lambda_4\left(1-e^{-\frac{\gamma}{\lambda_4}}\right)}{\lambda_1} + \frac{\left(e^{-\frac{\gamma}{\lambda_4}}-e^{-\frac{\gamma}{\lambda_2}}\right)}{\lambda_1(\frac{1}{\lambda_3}-\frac{1}{\lambda_2})(\frac{1}{\lambda_4}-\frac{1}{\lambda_2})}-\Bigg[\left(\frac{1}{\frac{1}{\lambda_3}-\frac{1}{\lambda_1}}-\lambda_3\right)\frac{\left(e^{-\frac{\gamma}{\lambda_3}}-e^{-\frac{\gamma}{\lambda_4}}\right)}{\lambda_2\left(\frac{1}{\lambda_4}-\frac{1}{\lambda_3}\right)} + \frac{\lambda_3\lambda_4\left(1-e^{-\frac{\gamma}{\lambda_4}}\right)}{\lambda_2}+\frac{\left(e^{-\frac{\gamma}{\lambda_4}}-e^{-\frac{\gamma}{\lambda_1}}\right)}{\lambda_2\left(\frac{1}{\lambda_3}-\frac{1}{\lambda_1}\right)\left(\frac{1}{\lambda_4}-\frac{1}{\lambda_1}\right)}\Bigg]\Bigg\} \tag{7.3.11}$$

where $\frac{1}{\lambda_k} = \frac{1}{\lambda_{h_k}} + \frac{1}{\lambda_{f_k}}$.

Similarly, the outage probability can be found using equation (7.3.9) where $\gamma_{th} = \frac{2^{2R}-1}{\mathrm{SNR}_0} - \bar{\mathrm{G}}$.

7.3.3 Outage expressions in the case of imperfect spectrum acquisition scenario

In the above, the outage expressions are valid when the spectrum is always available for the cognitive relays. However, in a realistic scenario, the spectrum is not always guaranteed (imperfect spectrum acquisition scenario). In this case, the outage probability can be evaluated as

$$\mathrm{P}_{out}(k) = \mathrm{P}(R_k < R)\mathrm{P}(k) \tag{7.3.12}$$

where k is the number of cognitive relays that successfully acquire spectrum. The probability $P(k)$ is dependent on the average probability of detection, P_d, and is given by

$$\mathrm{P}(k) = \binom{K}{k}\mathrm{P}_d^k(1-\mathrm{P}_d)^{K-1} \tag{7.3.13}$$

The average probability of detection, P_d, in a Rayleigh fading environment [44] is given by

$$\mathrm{P}_d = e^{-\frac{\delta}{2}} \sum_{i=0}^{\nu-2} \frac{1}{i!} \left(\frac{\delta}{2}\right)^i + \left(\frac{1+\bar{\alpha}}{\bar{\alpha}}\right)^{\nu-1} \left[e^{-\frac{\delta}{2(1+\bar{\alpha})}} - e^{-\frac{\delta}{2}} \sum_{i=0}^{\nu-2} \frac{1}{i!} \left(\frac{\delta\bar{\alpha}}{2(1+\bar{\alpha})}\right)^i \right] \tag{7.3.14}$$

where (.)! denotes the factorial operator, δ is the threshold used for comparison to make a decision if the primary signal is present or not, ν is the time bandwidth product and $\bar{\alpha}$ is the average SNR.

7.4 Selection Cooperation Based on D-Alamouti Scheme

In the previous sections, the assumption was that all relays participate in the second phase in a STD protocol based on a D-EO-STBC scheme. In this section, it is proposed to implement a selection cooperation scheme as in [106], [136] and [137]. So, the best two cognitive relays based on their instantaneous channel gains are selected to forward information to the destination. Therefore, the two relays can construct the D-Alamouti scheme at the destination. So, based on full search over all values of $|h_k|^2$ and $|f_k|^2$, the best two relays can be determined

$$\begin{aligned} k_{best} &= \arg\max_k \{\min\{|h_k|^2, |f_k|^2\}\}, k=1,...,K \\ k_{2^{nd}best} &= \arg\max_k \{\min\{|h_k|^2, |f_k|^2\}\}, k=1,...,K(k \neq k_{best}) \end{aligned}$$

According to the optimal power allocation in [67], the source uses half of the total power and the relay nodes equally share the other half. So, selecting two relays out of K relays without changing their assigned powers will save the power of the non-selecting relays. This available power can be used to improve the outage performance of the system. In the following, the outage analysis in case of exploiting this available power or not is provided.

7.4.1 Selection cooperation without exploiting the available power

In this case, the mutual information of the selection cooperation scheme, i.e. selects 2 out of K, is given by

$$R_K = \frac{1}{2}\log_2\left(1 + \mathrm{SNR}_0(\gamma_{best} + \gamma_{2^{nd}best})\right) \tag{7.4.1}$$

Therefore, the outage probability can be written as

$$P\left(\gamma_{best} + \gamma_{2^{nd}best} < \gamma_{th}\right) \tag{7.4.2}$$

where $\gamma_{th} = \frac{2^{2R}-1}{\mathrm{SNR}_0}$. According to [138], if $\mathcal{X}$ and $\mathcal{Y}$ are exponential distributed random variables with parameters λ_x and λ_y, respectively, and $\mathcal{X} + \mathcal{Y} \leq \mathcal{Z}$, provided that $\mathcal{X} \geq \mathcal{Y} \geq 0$, therefore the CDF of $\mathcal{Z}$ can be expressed as

$$F_{\mathcal{Z}}(z) = \int_0^{\frac{z}{2}} \int_y^{z-y} f_{\mathcal{X},\mathcal{Y}}(x,y)\ \ dx\ dy \tag{7.4.3}$$

where

$$f_{\mathcal{X},\mathcal{Y}}(x,y) = K(K-1)(F_{\mathcal{Y}}(y))^{K-2} f_{\mathcal{X}}(x) f_{\mathcal{Y}}(y) \tag{7.4.4}$$

Therefore, the outage probability of selection cooperation can be expressed as

$$P_{out}(\gamma_{th}) = F_{\mathcal{Z}}(\gamma_{th}) \tag{7.4.5}$$

As explained in Section 7.3.3, the outage probability calculation for selection cooperation under imperfect spectrum acquisition is straightforward. In the following, the CDF expression of selecting two out of four and two out of three, respectively, will be presented.

The CDF expression for selecting two out of four

$$F_{\mathcal{Z}}(z)=\frac{12}{\lambda_y}\Bigg(\frac{1-e^{-(\frac{1}{\lambda_y}+\frac{1}{\lambda_x})\frac{z}{2}}}{\frac{1}{\lambda_y}+\frac{1}{\lambda_x}}+\frac{e^{-\frac{z}{\lambda_x}}\left(e^{-(\frac{1}{\lambda_y}-\frac{1}{\lambda_x})\frac{z}{2}}-1\right)}{\frac{1}{\lambda_y}-\frac{1}{\lambda_x}}+\frac{2\left(e^{-(\frac{2}{\lambda_y}+\frac{1}{\lambda_x})\frac{z}{2}}-1\right)}{\frac{2}{\lambda_y}+\frac{1}{\lambda_x}}$$
$$+\frac{2\ e^{-\frac{z}{\lambda_x}}\left(1-e^{-(\frac{2}{\lambda_y}-\frac{1}{\lambda_x})\frac{z}{2}}\right)}{\frac{2}{\lambda_y}-\frac{1}{\lambda_x}}+\frac{1-e^{-(\frac{3}{\lambda_y}+\frac{1}{\lambda_x})\frac{z}{2}}}{\frac{3}{\lambda_y}+\frac{1}{\lambda_x}}+\frac{e^{-\frac{z}{\lambda_x}}\left(e^{-(\frac{3}{\lambda_y}-\frac{1}{\lambda_x})\frac{z}{2}}\right)}{\frac{3}{\lambda_y}-\frac{1}{\lambda_x}}\Bigg) \tag{7.4.6}$$

where λ_x and λ_y are the parameters for the best and second best source-relay-destination links, respectively.

The CDF expression for selecting two out of three

$$F_{\mathcal{Z}}(z)=\frac{6}{\lambda_y}\left(\frac{1-e^{-(\frac{1}{\lambda_y}+\frac{1}{\lambda_x})\frac{z}{2}}}{\frac{1}{\lambda_y}+\frac{1}{\lambda_x}}+\frac{e^{-\frac{z}{\lambda_x}}\left(e^{-(\frac{1}{\lambda_y}-\frac{1}{\lambda_x})\frac{z}{2}}-1\right)}{\frac{1}{\lambda_y}-\frac{1}{\lambda_x}}+\frac{e^{-(\frac{2}{\lambda_y}+\frac{1}{\lambda_1})\frac{z}{2}}-1}{\frac{2}{\lambda_y}+\frac{1}{\lambda_1}}\right.$$
$$\left.+\frac{e^{-\frac{z}{\lambda_1}}(1-e^{-(\frac{2}{\lambda_y}-\frac{1}{\lambda_1})\frac{z}{2}})}{\frac{2}{\lambda_y}-\frac{1}{\lambda_1}}\right) \tag{7.4.7}$$

7.4.2 Selection cooperation with exploiting the available power

In this case, the available power is equally divided between the two selected relays, i.e. the resultant new relay power, P_c, at each relay will be $P_c = (1+\frac{K-2}{2})P_r$. Hence, the mutual information of the selection cooperation scheme, i.e. selects 2 out of K, is given by

$$R_K=\frac{1}{2}\log_2\left(1+\left(1+\frac{K-2}{2}\right)\mathrm{SNR}_0(\gamma_{best}+\gamma_{2^{nd}best})\right) \tag{7.4.8}$$

Therefore, the outage probability can be written as

$$P\left(\gamma_{best} + \gamma_{2^{nd}\ best} < \gamma_{th}\right) \tag{7.4.9}$$

where $\gamma_{th} = \frac{2^{2R}-1}{(1+\frac{K-2}{2})\mathrm{SNR}_0}$.

It is clear that the effect of exploiting the available power is in minimizing the outage threshold which consequently leads to improvement in the outage performance of the system. Therefore, the CDF expressions of selecting two out of four and selecting two out of three are still the same as in the case of not exploiting the available power.

7.5 Sharing Spectrum under Cooperative Cognitive Relay Network

Secondary (cognitive) transmission data rate can be increased through sharing spectrum opportunistically or concurrently with primary users while the the primary transmission robustness can be enhanced through exploiting the available concurrent cognitive users to cooperatively relay the primary traffic towards the intended destination, especially when there is no direct primary communication path. The primary and cognitive transmissions that represent the above situation can be realized in the network shown in Fig. 7.2. In this network, it is assumed that the cognitive users work as relays between the primary source and primary destination where four cognitive relays are used. Also, it is assumed that there is no direct path between the primary source and the primary destination due to heavy fade or shadowing effects. Therefore, the transmission process for the primary user requires an assistance of cognitive users. All nodes in this network are equipped with only one antenna and implement half-duplex mode. Thus, the primary information signals need two phases to arrive at the primary destination which are the broadcasting phase and relaying phase. Furthermore, there is the possibility

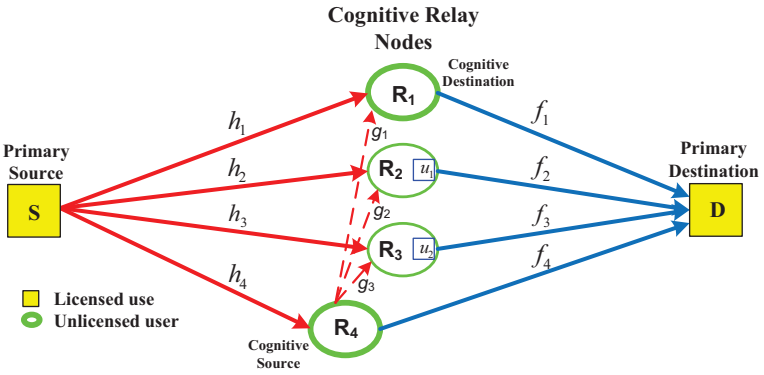

Figure 7.2. Wireless cognitive relay system where primary and cognitive transmissions occur opportunistically or simultaneously.

for cognitive (secondary) transmission between the cognitive relays R_4 and R_1 where R_4 is assumed to be the cognitive source and R_1 is assumed to be the cognitive destination. The cognitive user can either access the licensed spectrum opportunistically based on the interweave cognitive approach or concurrently with the primary user based on the overlay cognitive approach. However, the two different scenarios will be presented in the following two subsections.

Denote the fading coefficients from the primary source to the kth cognitive relay as h_k and from the kth cognitive relay to the primary destination as f_k, for $k = 1, 2, 3, 4$, while denote the fading coefficients from the cognitive source R_4 to the other cognitive relays as g_k, for $k = 1, 2, 3$. All the channels are assumed to be zero-mean quasi-static flat Rayleigh fading with variance of λ_{a_k} where $a_k \in \{h_k, f_k, g_k\}$.

7.5.1 Transmission scenario based on interweave approach

In this scenario, the cognitive (secondary) user can send its own information signals towards its intended destination opportunistically using the avail-

able white holes in the licensed frequency spectrum. In other words, the cognitive user is allowed to transmit only when the licensed spectrum is free from primary users through employing interweave cognitive approach. For applying this concept on the considered cognitive relay network shown in Fig. 7.2, the cognitive source R_4 sends its own information to the cognitive destination R_1 using the licensed spectrum during the periods where the primary user is not transmitting. In this case, it is assumed that there is no detection error. On the other hand, the primary user can utilize cognitive users as cooperative relays during its transmitting periods in a similar way as described in [118] while the cognitive user can implement either single-input single-output (SISO) communication or cooperative communication using the other remaining relays assistance. In fact, it is difficult in practice to adopt this scenario over wide area and time because the perfect spectrum acquisition might be not available and the detection process might be false. The system performance for this scenario can be evaluated in terms of outage probability and in terms of bit error rate (BER). The outage performance of the primary transmission can be found similarly as explained in the previous section for perfect spectrum acquisition scenario. Thus, the outage probability can be expressed as

$$
\begin{aligned}
P_{out}(\gamma_{th}) = \frac{1}{\lambda_4\lambda_3(\frac{1}{\lambda_1}-\frac{1}{\lambda_2})}\Bigg\{\Bigg(\frac{1}{\frac{1}{\lambda_3}-\frac{1}{\lambda_2}}-\lambda_3\Bigg)\frac{\left(e^{-\frac{\gamma_{th}}{\lambda_3}}-e^{-\frac{\gamma_{th}}{\lambda_4}}\right)}{\lambda_1(\frac{1}{\lambda_4}-\frac{1}{\lambda_3})}+\frac{\lambda_3\lambda_4\left(1-e^{-\frac{\gamma_{th}}{\lambda_4}}\right)}{\lambda_1} \\
+\frac{\left(e^{-\frac{\gamma_{th}}{\lambda_4}}-e^{-\frac{\gamma_{th}}{\lambda_2}}\right)}{\lambda_1(\frac{1}{\lambda_3}-\frac{1}{\lambda_2})(\frac{1}{\lambda_4}-\frac{1}{\lambda_2})}-\Bigg[\Bigg(\frac{1}{\frac{1}{\lambda_3}-\frac{1}{\lambda_1}}-\lambda_3\Bigg)\frac{\left(e^{-\frac{\gamma_{th}}{\lambda_3}}-e^{-\frac{\gamma_{th}}{\lambda_4}}\right)}{\lambda_2\left(\frac{1}{\lambda_4}-\frac{1}{\lambda_3}\right)} \\
+\frac{\lambda_3\lambda_4\left(1-e^{-\frac{\gamma_{th}}{\lambda_4}}\right)}{\lambda_2}+\frac{\left(e^{-\frac{\gamma_{th}}{\lambda_4}}-e^{-\frac{\gamma_{th}}{\lambda_1}}\right)}{\lambda_2\left(\frac{1}{\lambda_3}-\frac{1}{\lambda_1}\right)\left(\frac{1}{\lambda_4}-\frac{1}{\lambda_1}\right)}\Bigg]\Bigg\} \qquad (7.5.1)
\end{aligned}
$$

where $\frac{1}{\lambda_k}=\frac{1}{\lambda_{h_k}}+\frac{1}{\lambda_{f_k}}$.

Also, the BER performance of primary transmission in this scenario is the

same as that introduced in [118] so there is no need to repeat the analysis of BER performance of this scenario.

7.5.2 Transmission scenario based on overlay approach

In this scenario, the cognitive user can transmit simultaneously with primary user using the same spectrum where the cognitive user employs the overlay sharing spectrum approach. To realize this concept on the considered cognitive relay network shown in Fig. 7.2, the cognitive source R_4 transmits its own information towards the cognitive destination R_1 simultaneously with the primary source where the cognitive source R_4 and the cognitive destination R_1 are assumed in full-duplex mode which make them able to transmit and receive simultaneously. At the same time, the four cognitive relays can receive the primary source information signals and forward them towards the primary destination as shown in Fig. 7.2. So, in the broadcasting phase, the primary source broadcasts its information symbols $\mathbf{s}_p = [s_{p1}\ s_{p2}]^T$ to the cognitive relays and simultaneously the cognitive user R_4 transmits its information symbols $\mathbf{s}_c = [s_{c1}\ s_{c2}]^T$ towards the remaining cognitive relays and the primary destination. As a result, the received signals at a cognitive relay k, $\mathbf{y}_k$, and at the primary destination, $\mathbf{y}_d$, during two symbol durations can be written as

$$\begin{aligned}
\mathbf{y}_k &= [y_{k1}\ y_{k2}]^T = \sqrt{P_p}[s_{p1}\ s_{p2}]^T h_k + \sqrt{P_c}[s_{c1}\ s_{c2}]^T g_k + [v_{k1}\ v_{k2}]^T \text{ for } k = 1, 2, 3 \\
\mathbf{y}_4 &= [y_{41}\ y_{42}]^T = \sqrt{P_p}[s_{p1}\ s_{p2}]^T h_4 + [v_{41}\ v_{42}]^T \\
\mathbf{y_d} &= [y_{d1}\ y_{d2}]^T = \sqrt{P_c}[s_{c1}\ s_{c2}]^T f_4 + [v_{d1}\ v_{d2}]^T
\end{aligned} \tag{7.5.2}$$

where P_p denotes the transmit power at the primary source and P_c denotes the transmit power at the cognitive source R_4 while all the channels h_k, f_k and g_k are assumed to be zero-mean quasi-static flat Rayleigh fading with unit variance and v_{kj} and v_{dj} are the corresponding zero mean AWGN at

relay node k and the primary destination, respectively, with zero-mean and unit-variance where $j = 1, 2$.

The mean power of the signal y_{kj} at a cognitive relay k, for $k = 1, 2, 3$ is $P_p + P_c + 1$ due to the unit variance assumption of the fading channel from the primary source to the kth cognitive relay, h_k, and the additive noise, v_{kj}, at a cognitive relay in (7.5.2). However, the mean power of the signal y_{4j} at the cognitive relay R_4 is $P_p + 1$. The power allocation for the primary source and cognitive relays adopts the following relation

$$P_c = \frac{P_p}{K} \tag{7.5.3}$$

where K is the total number of the relay nodes and in this case $K = 4$.

The relaying mode of AF type is assumed. Also, the four cognitive relay nodes apply the closed-loop D-EO-STBC scheme described in [118] to exploit the cooperative diversity. Therefore, the cognitive relays will process the received noisy signals according to Table 7.1 before forwarding them towards the primary destination. The transmitted signals from the second and third cognitive relays are multiplied by u_1 and u_2, respectively, while the remaining two relays are kept unchanged, where u_1 and u_2 are the weighted feedback values which can be calculated using the following equations.

$$u_1 = e^{j\theta_1} \quad \text{and} \quad u_2 = e^{j\theta_2} \tag{7.5.4}$$

Based on the performance analysis which will presented later, the phase rotations, θ_1 and θ_2, can be found using the following proposed criteria

$$\theta_1 = -\angle(h_1^* f_1^* h_2 f_2) \quad \text{and} \quad \theta_2 = -\angle(h_3^* f_3 h_4 f_4^*) \tag{7.5.5}$$

where the operation $\angle(.)$ is the angle value.

As a result, the two received signals, y_{d3} and y_{d4}, at the primary destination

Table 7.1. Closed-loop D-EO-STBC scheme over cognitive relays for primary transmission

	Relay Nodes			
Symbol duration	R_1	R_2	R_3	R_4
Symbol 1	y_{11}	$u_1 y_{21}$	$-u_2 y_{32}^*$	$-y_{42}^*$
Symbol 2	y_{12}	$u_1 y_{22}$	$u_2 y_{31}^*$	y_{41}^*

during the relaying phase over two symbol duration can be expressed as

$$\begin{aligned} y_{d3} &= \mu_1 y_{11} f_1 + \mu_1 u_1 y_{21} f_2 - \mu_1 u_2 y_{32}^* f_3 - \mu_2 y_{42}^* f_4 + v_{d3} \\ &= \mu_3(h_1 f_1 + u_1 h_2 f_2) s_{p1} - \mu_3(u_2 h_3^* f_3 + \mu_4 h_4^* f_4) s_{p2}^* + \mu_4(g_1 f_1 + u_1 g_2 f_2) s_{c1} \\ &\quad - \mu_4 s_{c2}^* u_2 g_3^* f_3 + \mu_1(f_1 v_{11} + f_2 v_{21}) - \mu_1(f_3 v_{32}^* + \mu_5 f_4 v_{42}^*) + v_{d3} \\ y_{d4} &= \mu_1 y_{12} f_1 + \mu_1 u_1 y_{22} f_2 + \mu_1 u_2 y_{31}^* f_3 + \mu_2 y_{41}^* f_4 + v_{d4} \\ &= \mu_3(h_1 f_1 + u_1 h_2 f_2) s_{p2} + \mu_3(u_2 h_3^* f_3 + \mu_4 h_4^* f_4) s_{p1}^* + \mu_4(g_1 f_1 + u_1 g_2 f_2) s_{c2} \\ &\quad + \mu_4 u_2 s_{c1}^* g_3^* f_3 + \mu_1(f_1 v_{12} + f_2 v_{22}) + \mu_1(f_3 v_{31}^* + \mu_5 f_4 v_{41}^*) + v_{d4} \end{aligned} \tag{7.5.6}$$

where $\mu_1 = \sqrt{\frac{P_c}{P_p+P_c+1}}$, $\mu_2 = \sqrt{\frac{P_c}{P_p+1}}$, $\mu_3 = \sqrt{\frac{P_c P_p}{P_p+P_c+1}}$, $\mu_4 = \sqrt{\frac{P_c P_c}{P_p+P_c+1}}$ and $\mu_5 = \sqrt{\frac{P_p+P_c+1}{P_p+1}}$.

Thus, the received signals at the primary destination over the whole transmission, y_{d1}, y_{d2}, y_{d3} and y_{d4}, conjugated for convenience, can be expressed as

$$\begin{bmatrix} y_{d1} \\ y_{d2}^* \\ y_{d3} \\ y_{d4}^* \end{bmatrix} = \sqrt{P_c} \begin{bmatrix} f_4 & 0 & 0 & 0 \\ 0 & f_4^* & 0 & 0 \\ a_1 & -a_2 & a_3 & -a_4 \\ a_2^* & a_1^* & a_4^* & a_3^* \end{bmatrix} \begin{bmatrix} s_{c1} \\ s_{c2}^* \\ s_{p1} \\ s_{p2}^* \end{bmatrix} + \begin{bmatrix} v_{d1} \\ v_{d2}^* \\ \hat{v}_{d3} \\ \hat{v}_{d4}^* \end{bmatrix} \tag{7.5.7}$$

where $a_1 = \mu_1(g_1 f_1 + u_1 g_2 f_2)$, $a_2 = \mu_1 u_2 g_3^* f_3$, $a_3 = \mu_6(h_1 f_1 + u_1 h_2 f_2)$, $a_4 = \mu_6(u_2 h_3^* f_3 + \mu_5 h_4^* f_4)$ and $\mu_6 = \sqrt{\frac{P_p}{P_p+P_c+1}}$. The related noises $\hat{v}_{d3} = (\mu_1 f_1 v_{11} + \mu_1 u_1 f_2 v_{21}) - \mu_1 u_2 f_3 v_{32}^* - \mu_2 f_4 v_{42}^* + v_{d3}$ and $\hat{v}_{d4} = \mu_1 f_1 v_{12} +$

$\mu_1 u_1 f_2 v_{22} + \mu_1 u_2 f_3 v_{31}^* + \mu_2 f_4 v_{41}^* + v_{d4}$.

As observed, the received signals are corrupted by interference from the cognitive users. To cancel out this interference completely, the received signals therefore should be multiplied by the following proposed 2×4 matrix, $\mathbf{Z}_p$.

$$\mathbf{Z}_p = \begin{bmatrix} -a_1^* & a_2 & f_4^* & 0 \\ -a_2^* & -a_1 & 0 & f_4 \end{bmatrix} \tag{7.5.8}$$

The resultant two signals, r_1 and r_2, after multiplying the received signals by the matrix $\mathbf{Z}_p$ will be

$$\begin{bmatrix} r_1 \\ r_2 \end{bmatrix} = \begin{bmatrix} 0 & 0 & f_4^* a_3 & -f_4^* a_4 \\ 0 & 0 & f_4 a_4^* & f_4 a_3^* \end{bmatrix} \begin{bmatrix} s_{c1} \\ s_{c2}^* \\ s_{p1} \\ s_{p2}^* \end{bmatrix} + \begin{bmatrix} n_1 \\ n_2 \end{bmatrix} \tag{7.5.9}$$

where $n_1 = -a_1^* v_{d1} + a_2 v_{d2}^* + f_4^* \hat{v}_{d3}$ and $n_2 = -a_2^* v_{d1} - a_1 v_{d2}^* + f_4 \hat{v}_{d4}^*$.

It is clear that the cognitive signals s_{c1} and s_{c2} have been totally eliminated. Therefore, the primary destination can receive the primary signals with no interference from the cognitive user.

$$\begin{bmatrix} r_1 \\ r_2 \end{bmatrix} = \mu_3 \underbrace{\begin{bmatrix} f_4^*(h_1 f_1 + u_1 h_2 f_2) & -f_4^*(u_2 h_3^* f_3 + \mu_4 h_4^* f_4) \\ f_4(u_2^* h_3 f_3^* + \mu_4 h_4 f_4^*) & f_4(h_1 f_1 + u_1 h_2 f_2)^* \end{bmatrix}}_{\mathbf{H}_p} \begin{bmatrix} s_{p1} \\ s_{p2}^* \end{bmatrix} + \begin{bmatrix} n_1 \\ n_2 \end{bmatrix} \tag{7.5.10}$$

Finally, the primary information symbols can be decoded using matched filtering with the primary equivalent channel matrix $\mathbf{H}_p$ as follows

$$\begin{bmatrix} \tilde{s}_{p1} \\ \tilde{s}_{p2}^* \end{bmatrix} = \mu_3 \mathbf{H}_p^H \mathbf{H}_p \begin{bmatrix} s_{p1} \\ s_{p2}^* \end{bmatrix} + \mathbf{H}_p^H \begin{bmatrix} n_1 \\ n_2 \end{bmatrix} \tag{7.5.11}$$

The channel gain, γ_p, therefore can be found from the diagonal Gramian matrix, $\mathbf{G} = \mathbf{H}_p^H \mathbf{H}_p$, such that

$$\begin{aligned}
\gamma_p &= \alpha_p + \beta_p \\
\alpha_p &= |f_4|^2(|h_1|^2|f_1|^2 + |u_1|^2|h_2|^2|f_2|^2 + |u_2|^2|h_3|^2|f_3|^2 + |h_4|^2|f_4|^2) \\
\beta_p &= |f_4|^2(2\mathrm{Re}\{h_1^* f_1^* u_1 h_2 f_2\} + 2\mathrm{Re}\{u_2 h_3^* f_3 h_4 f_4^*\})
\end{aligned}$$

where α_p is the cooperative diversity gain and β_p is the array gain of the system while the operator $|.|^2$ denotes the modulus squared of a complex number and Re{.} its real part taking into account that $|u_1|^2 = |u_2|^2 = 1$. On the other hand, the cognitive information symbols, $[s_{c1} \quad s_{c2}]$, can be extracted at the cognitive destination R_1 using the same steps as followed at the primary destination. Hence, the two received signals, y_{13} and y_{14}, at the cognitive destination R_1 during the relaying phase over two symbol duration can be expressed as

$$\begin{aligned}
y_{13} &= -\mu_2\sqrt{P_p}s_{p2}^* h_4^* g_1 - \mu_2 g_1 v_{42}^* + v_{13} \\
y_{14} &= \mu_2\sqrt{P_p}s_{p1}^* h_4^* g_1 + \mu_2 g_1 v_{41}^* + v_{14}
\end{aligned} \tag{7.5.12}$$

Thus, the received signals at the cognitive destination R_1 over the whole transmission, y_{11}, y_{12}, y_{13} and y_{14}, conjugated for convenience, can be gathered as

$$\begin{bmatrix} y_{11} \\ y_{12} \\ y_{13}^* \\ y_{14}^* \end{bmatrix} = \begin{bmatrix} \sqrt{P_c}g_1 & 0 & \sqrt{P_p}h_1 & 0 \\ 0 & \sqrt{P_c}g_1 & 0 & \sqrt{P_p}h_1 \\ 0 & 0 & 0 & -\sqrt{\frac{P_c P_p}{P_p+1}}h_4 g_1^* \\ 0 & 0 & \sqrt{\frac{P_c P_p}{P_p+1}}h_4 g_1^* & 0 \end{bmatrix} \begin{bmatrix} s_{c1} \\ s_{c2} \\ s_{p1} \\ s_{p2} \end{bmatrix} + \begin{bmatrix} v_{11} \\ v_{12} \\ \hat{v}_{13} \\ \hat{v}_{14} \end{bmatrix} \tag{7.5.13}$$

where $\hat{v}_{13} = -\sqrt{\frac{P_c}{P_p+1}}v_{42}g_1^* + v_{13}^*$ and $\hat{v}_{14} = \sqrt{\frac{P_c}{P_p+1}}v_{41}g_1^* + v_{14}^*$.

After that, the received signals at R_1 should be multiplied by the following

proposed matrix, $\mathbf{Z}_c$ to be able to extract the cognitive information symbols.

$$\mathbf{Z}_s = \begin{bmatrix} \sqrt{\frac{P_c P_p}{P_p+1}} h_4 g_1^* & 0 & 0 & -\sqrt{P_p} h_1 \\ 0 & \sqrt{\frac{P_c P_p}{P_p+1}} h_4 g_1^* & -\sqrt{P_p} h_1 & 0 \end{bmatrix} \tag{7.5.14}$$

Multiplying the received signals by the matrix $\mathbf{Z}_c$ will result in the following two signals, q_1 and q_2, at the cognitive destination

$$\begin{bmatrix} q_1 \\ q_2 \end{bmatrix} = \begin{bmatrix} \sqrt{\frac{P_c^2 P_p}{P_p+1}} h_4 g_1^* g_1 & 0 & 0 & 0 \\ 0 & \sqrt{\frac{P_c^2 P_p}{P_p+1}} h_4 g_1^* g_1 & 0 & 0 \end{bmatrix} \begin{bmatrix} s_{c1} \\ s_{c2} \\ s_{p1} \\ s_{p2} \end{bmatrix} + \begin{bmatrix} w_1 \\ w_2 \end{bmatrix} \tag{7.5.15}$$

where $w_1 = \sqrt{\frac{P_c P_p}{P_p+1}} h_4 g_1^* v_{11} - \sqrt{P_p} h_1 \hat{v}_{14}$ and $w_2 = \sqrt{\frac{P_c P_p}{P_p+1}} h_4 g_1^* v_{12} - \sqrt{P_p} h_1 \hat{v}_{13}$. As a result, the cognitive destination can receive the cognitive signals with no interference from the primary user. Thus,

$$\begin{bmatrix} q_1 \\ q_2 \end{bmatrix} = \sqrt{\frac{P_c^2 P_p}{P_p+1}} \underbrace{\begin{bmatrix} h_4 g_1^* g_1 & 0 \\ 0 & h_4 g_1^* g_1 \end{bmatrix}}_{\mathbf{H}_c} \begin{bmatrix} s_{c1} \\ s_{c2} \end{bmatrix} + \begin{bmatrix} w_1 \\ w_2 \end{bmatrix} \tag{7.5.16}$$

Finally, the information symbols can be decoded using matched filtering with the cognitive equivalent channel matrix $\mathbf{H}_c$ as follows

$$\begin{bmatrix} \tilde{s}_{c1} \\ \tilde{s}_{c2} \end{bmatrix} = \sqrt{\frac{P_c^2 P_p}{P_p+1}}\ \mathbf{H}_c^H \mathbf{H}_c \begin{bmatrix} s_{c1} \\ s_{c2} \end{bmatrix} + \mathbf{H}_c^H \begin{bmatrix} w_1 \\ w_2 \end{bmatrix} \tag{7.5.17}$$

The channel gain for cognitive communication γ_c therefore can be found from the diagonal Gramian matrix, $\mathbf{G}_c = \mathbf{H}_c^H \mathbf{H}_c$, such that

$$\gamma_c = |g_1|^2 |h_4|^2$$

7.6 Simulation Results

In this section, simulation results are presented to support the considered system analyses. All curves shown in Figs. 7.3-7.11 correspond to λ_{h_1} =1.20, $\lambda_{f_1} = 0.35$ $\lambda_{h_2} = 1.40$, $\lambda_{f_2} = 0.40$, $\lambda_{h_3} = 1.60$, $\lambda_{f_3} = 0.45$, $\lambda_{h_4} = 1.75$ and $\lambda_{f_4} = 0.70$. In the simulations, the chosen target rate is R = 1 bit/sec/Hz and with setting $\bar{\mathrm{G}} = 0$ for simplicity. In Fig. 7.3, the outage probability of the proposed D-EO-STBC cognitive relay scheme for different number of relays, varying from one to four, with assumption of perfect spectrum acquisition is illustrated. Clearly, implementing more relays decreases the

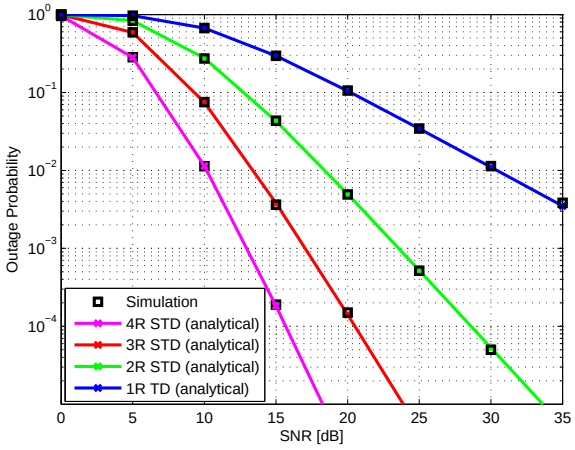

Figure 7.3. Outage probability for the proposed D-EO-STBC scheme versus SNR in dB (perfect spectrum acquisition).

probability of outage. The same result is deduced in the case of using selection cooperation as shown in Fig. 7.4. However, the outage performance of the selection cooperation with exploiting the available power at the relays is substantially better than that without changing the relaying power. For example, at an outage probability of 10^{-4}, the proposed selection cooperation scheme over three and four relays with exploiting the available power both provide approximately 3 dB improvement, respectively, over the proposed selection cooperation scheme without changing the relaying power. In Fig. 7.5, the outage performance comparison between the proposed D-EO-STBC

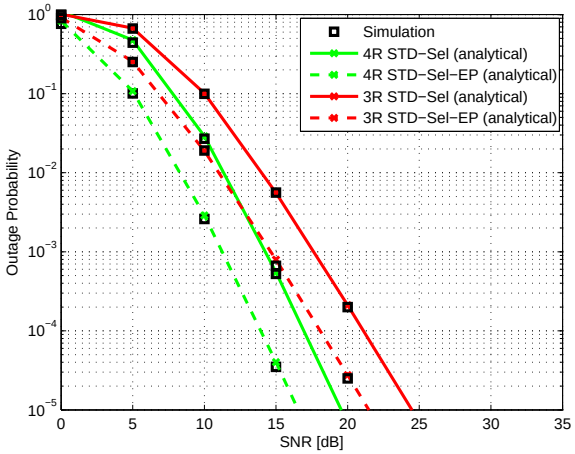

Figure 7.4. Outage probability for the proposed D-EO-STBC scheme based on selection cooperation versus SNR in dB (perfect spectrum acquisition).

cognitive relay network and the conventional TD cognitive relay network for two and four relays is shown. The results confirm that the proposed scheme significantly improves the outage performance over the conventional scheme. For example, at an outage probability of 10^{-4}, the proposed scheme for two and four relays provides approximately 10 dB and 3.7 dB improvements, respectively, over the conventional scheme. This improvement is because in the proposed scheme the outage threshold is much smaller as compared with that in the conventional TD scheme. On the other hand, a comparison between the proposed scheme when all cognitive relays participate in transmission and the proposed scheme based on selection cooperation when only the best two relays participate in transmission is provided as shown in Fig. 7.6. It is obvious that there is significant improvement in outage performance in the case of using the best two cognitive relays with exploiting the available relaying power as compared to the proposed scheme without selection while there is little degradation in outage performance in the case of using the best two cognitive relays without changing the relaying power. For example, at an outage probability of 10^{-4}, the proposed scheme based on selection

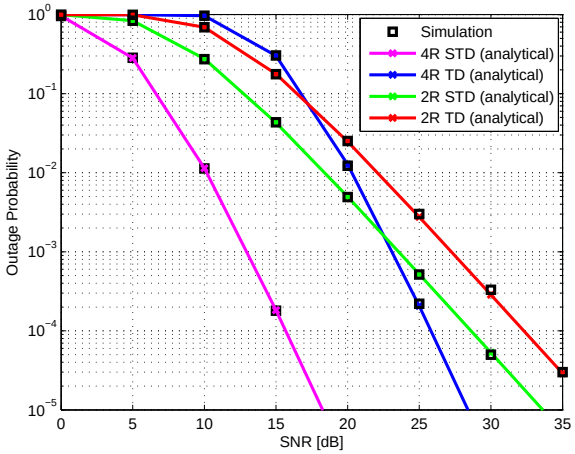

Figure 7.5. Outage performance comparison between the proposed D-EO-STBC scheme and the conventional TD scheme.

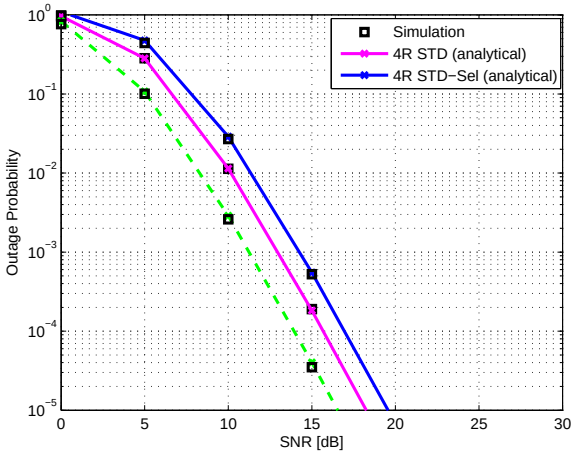

Figure 7.6. Comparison of outage performance of the proposed D-EO-STBC scheme with the proposed scheme based on selection cooperation.

cooperation over four relays provides approximately 1.7 dB improvement, respectively, in the case of exploiting the available power while providing approximately 1.3 dB degradation in the case of not changing the relaying power as compared to the proposed scheme without selection. Figs. 7.7-7.10 show the outage probability of the two proposed schemes with and without selection cooperation when spectrum acquisition is imperfect, i.e. $P_d < 1$. Clearly, the outage performance of both schemes is degraded when

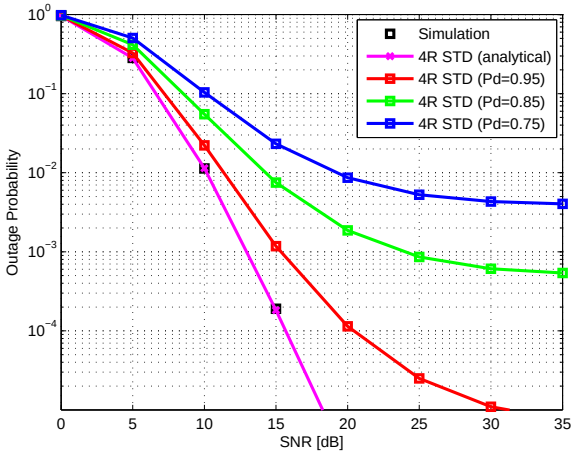

Figure 7.7. Outage probability for the proposed scheme when the spectrum acquisition is imperfect and K=4 relays.

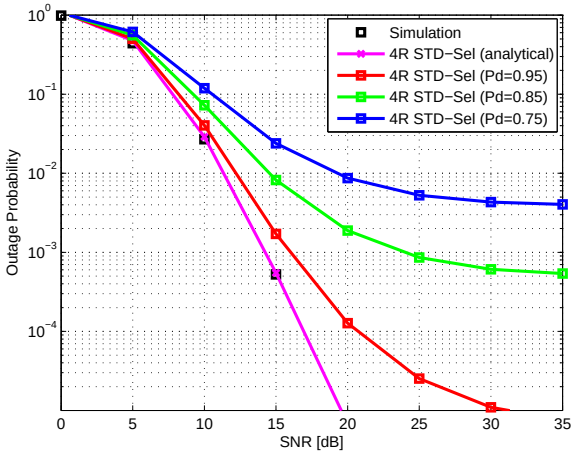

Figure 7.8. Outage probability for the proposed scheme based on selection cooperation when the spectrum acquisition is imperfect and K=4 relays.

the cognitive relays are likely to be unable to obtain spectrum. In general, it is observed that when the number of active relays increases, the probability of outage decreases. This is due to that increasing the number of relays leads to growth in the number of relays that are able to obtain spectrum. On the other hand, it is noticeable from these figures that the scheme implementing the best two cognitive relays out of the available four exploiting the available relaying power provides the best behavior as compared to the

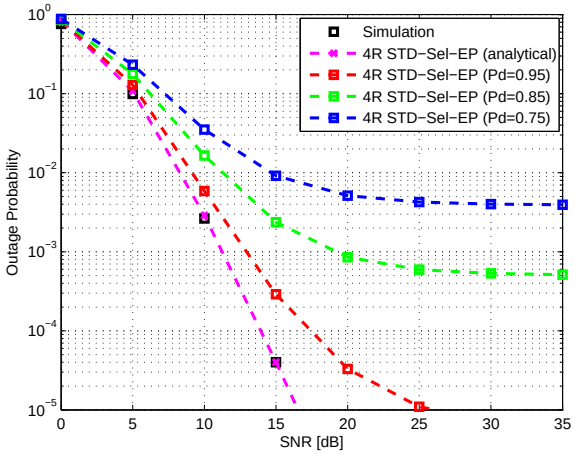

Figure 7.9. Outage probability for the proposed scheme based on selection cooperation with exploiting the available power when the spectrum acquisition is imperfect and K=4 relays.

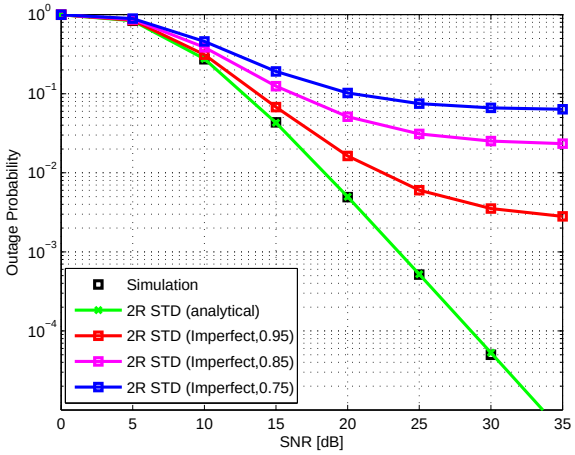

Figure 7.10. Outage probability for the proposed scheme when the spectrum acquisition is imperfect and K=2 relays.

others whether the spectrum acquisition is guaranteed or not always guaranteed. In Fig. 7.11 a comparison between the proposed two schemes with and without selection cooperation when four relays are available and $P_d = 0.85$ is depicted. As shown, the proposed selection cooperation scheme when the relaying power does not change has little degradation of outage performance at the low and medium SNR regimes with respect to the proposed scheme without selection while achieving the same outage performance in the high

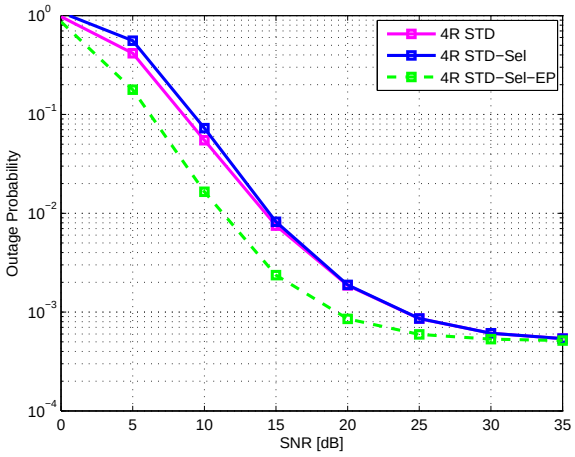

Figure 7.11. Comparison of the outage performance when $P_d = 0.85$.

SNR regime. On the other hand, the proposed selection cooperation scheme in the case of exploiting the available relaying power potentially outperforms the other two schemes for all SNR regimes.

Generally speaking, network design is based on the nature of the environment and the practical measurements can choose the most proper scheme to implement in a particular network.

7.7 Summary

In this chapter, a cooperative communications system based on the D-EO-STBC scheme was proposed in which transmission information is dependant on several AF type cognitive relays. The cognitive relays opportunistically access spectrum of the primary user to participate in transmitting information to the destination. Therefore, the system performance depends heavily on the spectrum acquisition of the cognitive relays. The performance of the system in terms of outage probability was evaluated and showed that the proposed scheme significantly outperforms the conventional TD schemes. However, it was found that the outage performance of the system degrades significantly when the spectrum acquisition is imperfect. The outage prob-

ability expressions were derived for both perfect and imperfect spectrum acquisition. The effectiveness of the derived outage expressions has been validated through simulations. On the other hand, the situation that the cognitive (secondary) user can transmit its own information in addition to relaying the primary user traffic was investigated. In fact, the performance of primary and cognitive transmissions were studied through two different scenarios where the cognitive user is allowed to opportunistically or concurrently access the spectrum allocated to the primary user. In both scenarios, the primary user enjoys a reliable transmission by exploiting the cooperative diversity among AF type cognitive relays while the cognitive user enjoys sharing spectrum to transmit its own information and maximize its data throughput. Finally, sharing spectrum with cooperative transmission will potentially improve the spectrum utilization and provide an effective reliable transmission which make the proposed schemes very attractive to cope with the spectrum scarcity and fading problems.

Chapter 8

SUMMARY, CONCLUSION AND FUTURE WORK

Explosive growth in wireless systems and applications has created a huge demand for reliable wireless technologies that promise high transmission robustness and data rate and effectively exploit the available resources. One of the new wireless communications paradigm that has drawn much attention from researchers in the last decade is a cooperative relay network. This new technology has the potential to enable effective solutions for different wireless challenging problems. Specifically, it is a promising approach for improving the range, system reliability and transmission data rate without the need for multiple antennas at individual nodes. More specifically, it is desirable for systems where it may not be practical or even feasible due to equipment size and cost to employ multiple antenna array elements on the nodes.

In particular, in this thesis it has been shown through the proposed distributed extended orthogonal space-time block coding (D-EO-STBC) scheme that worthwhile gains can be achieved in cooperative relay networks for different wireless challenges and scenarios. In this chapter, the contributions of this thesis will be summarized and concluded. Also, the potential open research directions are suggested and discussed.

8.1 Summary and Conclusions

This thesis focuses on cooperative communication via the proposed D-EO-STBC scheme as an effective cooperative diversity scheme that can fully exploit the benefit of diversity gains among a collection of single-antenna relays. In particular, this scheme can achieve full cooperative diversity and full rate in addition to array gain using a very low-complexity linear decoder at the destination. This scheme is based on a limited feedback channel so low-complexity partial feedback approaches have been proposed to make the proposed D-EO-STBC scheme more practical and feasible. Throughout this thesis, different network scenarios and challenges have been investigated and effectively addressed. To further enhance the system performance, effective relay selection approaches have been proposed. Finally, the proposed scheme has been applied over a cognitive radio application which results in significant performance improvements in the primary and secondary transmissions. In the following, the summary and conclusion for each chapter will be presented.

In Chapter 1, a general introduction to cooperative relay systems including the basic concept, system features and network architectures was provided. In addition, a brief introduction to cognitive radio systems was presented highlighting the main functions of cognitive radio and the feature of the cooperative cognitive networks. Finally, the outline of the thesis was briefly discussed. In Chapter 2, a historical background and literature survey of distributed space-time block coding (D-EO-STBC) summarizing the main challenges and the solutions that were introduced in the literature. This covered the works in the perfect and imperfect synchronization scenarios as well as in the flat and frequency-selective fading channel scenarios. Additionally, the literature survey included the latest works on cooperative cognitive relay networks. On the other hand, the distributed Alamouti (D-Alamouti) work for cooperative relay networks was studied and evaluated as the simplest

and most attractive example in this field. Finally, an orthogonal frequency division multiplexing (OFDM) precoding transmission in the context of cooperative communication was also presented briefly in this chapter clarifying the basic concept of OFDM and its implementation.

In Chapter 3, a D-EO-STBC transmission technique in a wireless amplify-and forward (AF) type relay system was proposed for four cooperative relays. The proposed scheme can be relaxed to employ over three cooperative relays. The important concept within the D-EO-STBC scheme is the orthogonality of the scheme code, which results in reduced computational complexity and leads to a very simple symbol-wise maximum-likelihood (ML) decoder. In fact, the closed-loop D-EO-STBC scheme achieves full data rate in each hop and full diversity at the same time for complex digital communication signals in addition to array gain. In particular, the performance of the D-EO-STBC cooperative diversity scheme in terms of cooperative diversity gain and the end-to-end bit error rate (BER) have been studied over four relay nodes and compared with the BER performance of the D-Alamouti and the distributed orthogonal STBC (D-OSTBC) schemes for perfect synchronization and flat Rayleigh fading. The main conclusion is that the closed-loop D-EO-STBC scheme over four cooperative relays provides twice the diversity order as that for the D-Alamouti scheme without increasing the transmit power, the channel bandwidth or the decoder complexity. With respect to the other orthogonal cooperative diversity schemes for the same number of relay nodes, the proposed closed-loop D-EO-STBC scheme and the previous D-OSTBC scheme can achieve the same cooperative diversity order which is equal to four. However, the closed-loop D-EO-STBC scheme provides array gain which is not available in the D-Alamouti and D-OSTBC schemes. In terms of the end-to-end BER, simulations showed that the D-EO-STBC provides better performance than the D-Alamouti and the D-OSTBC schemes when both the open-loop and closed-loop operations were employed. For

example, at BER of 10^{-4}, the proposed open-loop scheme achieved improvements of approximately 3.5 dB gain over the D-Alamouti scheme and 19 dB gain over D-OSTBC. Furthermore, the closed-loop D-EO-STBC scheme has an advantage over the D-OSTBC scheme in terms of decoding delay, where the proposed scheme requires less time than the D-OSTBC scheme to complete the whole transmission thereby extracting the information faster. In rapid varying channel environments and real-time implementations, it is preferable to employ lower decoding delay systems. In terms of data rate, the D-EO-STBC scheme provides the same data rate as that of the D-Alamouti scheme and outperforms the D-OSTBC scheme, where the D-EO-STBC scheme achieves unity data rate for each hop while the D-OSTBC scheme achieves unity data rate for the first hop and 3/4 data rate for the second hop. These results are very encouraging since the total transmission power is the same and the information symbols being decoded separately in a very simple manner at the receiver. The end-to-end BER performance of the D-EO-STBC scheme over three relay nodes was studied and compared with the BER performance of the the D-Alamouti scheme and the D-OSTBC over three relays scheme. The proposed closed-loop D-EO-STBC scheme provided for example approximately 7 dB and 24 dB at BER of 10^{-4} improvements as compared to the D-Alamouti and D-OSTBC schemes, respectively. On the other hand, the proposed closed-loop scheme has been studied through three proposed promising partial feedback schemes, one-bit feedback scheme, exact phase feedback scheme and quantized phase feedback scheme, where all of them can achieve full diversity and array gain thereby they provide better end-to-end BER performance than the open-loop scheme for the whole transmit power range. However, the three feedback schemes are different in the amount of achieved array gain where the achievable array gain by the exact phase feedback scheme is the largest but at the expense of a very large number of feedback bits. From practical viewpoint, the quan-

tized phase feedback scheme is more suitable due to its ability to retain the advantage of the exact phase feedback scheme with substantial reduction in feedback overhead. For example, at BER of 10^{-4}, the 2-bit quantized phase feedback provided approximately 0.6 dB gain improvement over that of the one-bit feedback scheme and approximately 0.1 dB gain reduction as compared to the exact phase feedback scheme.

Chapter 4 focused on the synchronization issue in a wireless cooperative relay network. In this chapter, robust schemes over four cooperative relays based on the closed-loop D-EO-STBC scheme for both frequency-flat and frequency-selective fading channels were proposed considering the asynchronization problem. These schemes exploited cooperative communication OFDM-based transmission to mitigate timing errors between relay nodes. In particular, the proposed AF type schemes implement an OFDM type precoding technique with cyclic prefix only at the source node for the flat fading channel scenario while also at two particular relays for the frequency-selective channel scenario. The proposed scheme for each scenario was studied through two proposed feedback approaches. In the flat fading channel scenario, the proposed partial feedback schemes can achieve full diversity in addition to array gain where the difference is in the amount of achieved array gain. In fact, the proposed sub-carrier quantized phase linear interpolation considering discontinuity (SCQPLI-CDC) feedback scheme can retain the same performance of exact phase feedback scheme with substantial reduction in the feedback overhead bandwidth. For example, at BER of 10^{-4}, the exact phase feedback scheme required 20.1 dB while the low-rate SCQPLI-CDC (12-bits/feedback link), the 64-bits/feedback link and 128-bits/feedback link schemes required 20.15 dB, 20.25 dB and 21 dB, respectively. Therefore, the low-rate SCQLPI-CDC scheme exhibits very little degradation in BER performance as compared to the exact phase feedback scheme while achieving both better BER performance and a substantial reduction in the feedback

overhead as compared to the 64-bits and 128-bits feedback schemes, i.e. a saving of 90.6% as compared with 128-bits feedback scheme.

In the frequency-selective fading channel scenario, the group quantization feedback schemes can achieve high performance with high reduction in the feedback channel bandwidth. They always provided better performance than that of the open-loop scheme. For example, at BER of 10^{-4}, a fixed group feedback scheme with total feedback overhead of 16 bits/feedback link (2-bits/group) provided approximately 1.25 dB improvement as compared with the system without using feedback. On the other hand, a comparison of the proposed asynchronous closed-loop D-EO-STBC schemes with previous schemes for flat and frequency-selective Rayleigh fading channels was provided. The simulation results confirmed that the proposed schemes over four relays significantly improve the end-to-end BER performance over the previous schemes which are designed for two relays or four relays. The achieved improvements are because in the proposed schemes the limited feedback was exploited to maximize the channel gain so there is full cooperative diversity gain of order four and array gain while the other scheme only achieved full diversity of order equal to the number of deployed relay nodes without array gain. For example, at BER of 10^{-4}, the proposed asynchronous narrowband scheme provided approximately 2 dB and 10 dB gain improvements as compared to the closed-loop quasi-orthogonal STBC scheme [82] for four relays and the AF D-Alamouti-OFDM scheme [81] for two relays in the case of flat fading scenario while the proposed asynchronous broadband scheme provided approximately 10 dB gain improvement as compared to the AF D-Alamouti-OFDM scheme [21] for two relays in the case of frequency-selective fading scenario.

At the end of this chapter, a two-way scenario was investigated and an extended version of closed-loop D-EO-STBC scheme was proposed which can achieve full diversity and array gain at each terminal. Also, an increased

data rate was achieved as compared to a one-way D-EO-STBC scheme scenario. On the other hand, simulation results for the proposed asynchronous D-EO-STBC scheme three-time slot framework was shown which presented clearly its performance and clarified the BER performance improvement as compared with the previous asynchronous OSTBC scheme developed for four relay nodes in [90]. For example, at BER of 10^{-4}, the proposed scheme provided approximately 0.7 dB improvement which means the proposed scheme adds more robustness for the transmission link.
However, the main conclusion of this chapter is that the closed-loop D-EO-STBC scheme with OFDM type precoding can effectively mitigate timing errors between relay nodes and channel fading effects in addition to achieving full cooperative diversity and array gain with potential reduction in feedback overhead bandwidth.

Chapter 5 provided a solution based on relay selection techniques to further enhance the system performance of the cooperative relay networks. The system complexity and the limited bandwidth may become a hindrance to exploit all available cooperative relay nodes. Also, heavy faded paths may reduce the overall system performance to be below a satisfactory level. To avoid these issues, some of the relay nodes should be dropped from the network. Hence, this chapter proposed relay selection approaches based on D-STBC schemes to select the best relay routes between the source and destination nodes and then apply the D-STBC scheme over the selected relays. In particular, two relay selection approaches, which are one-group and two-group approaches, based on the closed-loop D-EO-STBC and D-Alamouti schemes, respectively, with three level power adaptation were proposed. Three different scenarios based on one-group selection approach were provided. The system performance in terms of pairwise error probability (PEP) and the end-to-end BER were studied. Both of them confirmed that the two relay selection approaches can provide better system performance

as compared with the original open-loop network. Specifically, the two selection approaches reduced the PEP values as compared to the open-loop D-EO-STBC scheme which results in enhancing the overall performance of the wireless relay system. Simulation results were presented to show the BER performance enhancement of the proposed selection approaches over flat and frequency-selective channels. For example, at BER of 10^{-4} in the case of flat fading channels, the proposed one-group approach provided approximately 7.6 dB and 0.9 dB gain improvements over the open-loop D-EO-STBC and closed-loop D-EO-STBC schemes, respectively, while the proposed two-groups approach provided approximately 5.8 dB gain improvement over the open-loop D-EO-STBC scheme and a little degradation of 0.9 dB as compared with the closed-loop D-EO-STBC scheme. In the case of frequency-selective channels, similar results as in the case of flat fading channels were attained. However, the relay selection approach based on the closed-loop D-EO-STBC achieved better overall system performance than that of the approach based on the D-Alamouti code, but this provided a lower system complexity. The main conclusion is the available relay nodes can be fully exploited even if there are constraints on the system bandwidth or design by exploiting the relay selection approaches.

In Chapter 6, a generalized approach for the closed-loop D-EO-STBC scheme to employ over any arbitrary number of relay nodes was proposed. In this approach, the correlations introduced between the nodal channels are totally resolved by applying one-bit partial feedback which results in achieving at least full cooperative diversity. To further performance improvement, an optimal one-bit partial feedback scheme and relay selection scheme was proposed. In fact, the optimal feedback scheme can achieve the best system performance due to its ability to achieve the highest amount of array gain in addition to full cooperative diversity. For example, the optimal one-bit partial feedback scheme for a wireless network with R=8 relay nodes added

approximately 1.3 dB gain over the one-bit partial feedback scheme at the end-to-end BER of 10^{-4}. In terms of diversity order, the generalized closed-loop D-EO-STBC approach with more relay nodes gave extra cooperative diversity in the order of the number of the deployed relay nodes which positively reflects on the end-to-end BER performance as simulation results were confirmed. For example, a transition from $R = 4$ to $R = 8$ leads to a performance improvement greater than 4.25 dB for BER=10^{-4}. Moreover, the powerful property of the generalized approach is that the increase in diversity order is not at the expense of increased decoding delay as in previous schemes [49], [69] where the obtained decoding delay is fixed to two time slots each corresponding to two symbol intervals.

The synchronization problem among relay nodes was also discussed and addressed in two different fading channel assumptions which are flat fading channels and frequency-selective fading channels. The generalized approach combined with the OFDM type precoding can resolve the asynchronization effects and the fading problems in addition to obtaining at least full cooperative diversity. Numerical simulation results for the generalized approach based on closed-loop D-EO-STBC schemes were presented to illustrate the end-to-end BER performance of the proposed schemes over fading channels, in the presence of synchronization errors and different network scenarios. Based on these results, the generalized approach for the case of imperfect synchronization and frequency-selective channels can attain the same BER results as in the case of perfect synchronization and flat fading channels which means that the asynchronous version of the generalized approach can completely combat the timing errors effect and the multipath fading problem on the test environment.

The main conclusion is the ability to relax the closed-loop D-EO-STBC scheme to employ them over any arbitrary number of relay nodes where the cooperative spatial diversity among the single-antenna relay nodes can fully

be exploited.

Chapter 7 provided cooperation transmission based on the closed-loop D-EO-STBC scheme in the context of cognitive radio where the relay nodes are equipped with cognitive radios. By enabling a set of cognitive relay nodes to forward the received information based on the closed-loop D-EO-STBC scheme, the performance advantages achievable from using the D-EO-STBC can be realized and the spectrum utilization can be significantly improved. Two different cooperative transmission scenarios were considered and evaluated. In the first scenario, the cognitive users can only relay the traffic of another cognitive user or primary user to its intended destination which results in improving the robustness of the communication link, or increasing the probability of transmission opportunities in addition to increasing the throughput for a given spectrum hole. For example, implementing more relays reduced the probability of outage as proved by the simulation results. In this scenario, selection cooperation based on the D-Alamouti scheme was also proposed. The system performance in terms of outage probability was analyzed and validated for both perfect and imperfect spectrum acquisition cases through numerical simulations. The results confirmed that the cooperative cognitive relay network based on the proposed closed-loop D-EO-STBC scheme significantly improved the outage performance over the conventional time-division (TD) scheme. For example, at an outage probability of 10^{-4}, the proposed scheme for four relays provided approximately 3.7 dB improvements over the conventional scheme.

In the second scenario where the cognitive user can relay and transmit opportunistically or simultaneously, free interference spectrum sharing based on interweave and overlay cognitive approaches were proposed. In this scenario, the cognitive user can exploit the transmission opportunity and maximize their transmission rate without interfering with the primary user. The important conclusion for this chapter is that the closed-loop D-EO-STBC

scheme is an alluring and efficient transmission coding technique which can offer significant performance advantages for many practical wireless applications.

8.2 Future Work

In this thesis, the system reliability and transmission link robustness were the main objective where the final result was very encouraging because the proposed schemes were able to enhance significantly the system reliability and transmission robustness through achieving full spatial diversity and array gain which ensure the receiver capability to extract the desired data using very simple symbol-wise ML decoder. Thus, in future work, it would be very interesting to improve the system transmission rate. This potential area of future research will be investigated from two aspects which are improving the current proposed D-EO-STBC scheme and designing new optimal distributed codes as follows.

8.2.1 Potential data rate enhancement for the D-EO-STBC scheme

The group quantization feedback strategy discussed in Chapter 4 including quantized fixed and adaptive approaches for utilizing in the context of frequency-selective fading channels requires relatively high number of feedback bits as compared to that proposed feedback approaches for using in flat fading channels context which results in consuming more bandwidth for the feedback overhead. So, it would be very interesting to reduce the feedback overhead bandwidth of the proposed group quantization feedback strategy which will result in saving the available bandwidth. This saving can be exploited to send more data and consequently increasing the transmission data rate. This problem might be solved through studying carefully the correlation among the OFDM subcarriers above and below the zero phase

line as shown in Fig 4.6 and then determine only one proper phase for all subcarriers according to averaging approach.

Also, in Chapter 4, a closed-loop D-EO-STBC scheme for two-way communication scenario was proposed considering three-time-slot framework to ensure that each terminal has full cooperative diversity and array gain. However, the maximum end-to-end data rate that can be attained was 2/3. So, it would be very interesting to develop this scheme to use a two time-slots framework which preserves the diversity advantage of the proposed three-time slots framework which will result in increasing the transmission data rate to unity. The solution of this problem might come from studying the effect of timing errors on the rotation angles for each terminal by comparing them with the available best rotation angles. The objective is to find the best common rotation angles for the two terminals that can ensure achieving full diversity at each terminal.

8.2.2 Constructing new optimal distributed codes

The proposed D-EO-STBC scheme is optimal in diversity gain but it is not optimal in multiplexing gain, so constructing new optimal codes that can achieve the optimal diversity-multiplexing tradeoff (DMT) of the AF type cooperative relay channel considered in this thesis would be very interesting. In fact, designing brand new optimal codes for cooperative relay channels would be novel and distinguished. However, constructing new optimal distributed codes could be also attained in the following two ways:

1. Extending optimal codes that were originally designed for multi-input multi-output (MIMO) systems such as so-called perfect codes [139] and [140], which are a family of optimal STBCs. In this case, the optimal codes for certain number of transmit antennas more that two could be extended to cooperative relay networks equipped with single-antenna relay nodes equal to the number of transmit antennas in the

original MIMO systems. Furthermore, the optimal codes that are originally designed for a MIMO system with two transmit antennas could be combined with relay selection techniques to exploit them in cooperative relay networks. For example, combining in a distribution fashion the Golden code [141] or the Silver code [142], which are the best and second best Perfect codes in terms of DMT, with appropriate relay selection technique would be very interesting.

2. Developing optimal distributed codes that were originally proposed for certain system models such as in [143] and [144] to be valid for the considered system model. For example, a new construction of distributed space-time codes (D-STCs) that can achieve the optimal DMT of the MIMO cooperative channel based on a non-orthogonal AF protocol was presented in [143] while new optimal D-STCs for the multi-access AF relay channel were constructed in [144].

References

[1] A. Paulraj, R. Nabar, and D. Gore, *Introduction to Space Time Wireless Communications*. Cambridge University Press, 2003.

[2] M. Jankiraman, *Space-Time Codes and MIMO Systems*. Artech House, 2004.

[3] G. J. Foschini and M. J. Gans, "On the limits of wireless communication in a fading environment when using multiple antennas," *Wireless Pers. Commun.*, vol. 6, pp. 311–335, March 1998.

[4] I. E. Telatar, "Capacity of multi-antenna Gaussian channels," *Euro. Trans. Telecommun.*, vol. 10, pp. 585–596, Nov./Dec. 1999.

[5] B. Badic, *Space-Time Block Coding for Multiple Antenna Systems*. Vienna University of Technology, Austria: PhD Thesis, Nov. 2005.

[6] H. Jafarkhani, *Space-Time Coding Theory and Practice*. Cambridge University Press, 2005.

[7] D. Tse and P. Viswanath, *Fundamentals of Wireless Communication*. Cambridge University Press, 2005.

[8] J. N. Laneman and G. W. Wornell, "Distributed space-time coded protocols for exploiting cooperative diversity in wireless networks," *IEEE Trans. Inf. Theory*, vol. 49, pp. 2415–2425, Oct. 2003.

[9] A. Nosratinia, T. E. Hunter, and A. Hedayat, "Cooperative communication in wireless networks," *IEEE Commun. Mag.*, vol. 42, pp. 74–80, Oct. 2004.

[10] A. Sendonaris, E. Erkip, and B. Aazhang, "User cooperation diversity-part I: System description," *IEEE Trans. on Commu.*, vol. 51, pp. 1927–1938, Nov. 2003.

[11] R. Pabst, B. H. Walke, D. C. Schultz, P. Herhold, H. Yanikomeroglu, S. Mukherjee, H. Viswanathan, M. Lott, W. Zirwas, M. Dohler, H. Aghvami, D. D. Falconer, and G. P. Fettweis, "Relay-based deployment concepts for wireless and mobile broadband radio," *IEEE Commun. Mag.*, vol. 42, pp. 80–89, Sep. 2004.

[12] Y. Yang, H. Hu, J. Xu, and G. Mao, "Relay technologies for WiMAX and LTE-advanced mobile systems," *IEEE Commun. Mag.*, vol. 47, pp. 100–105, Oct. 2009.

[13] O. Oyman, J. N. Laneman, and S. Sandhu, "Multihop relaying for broadband wireless mesh networks: From theory to practice," *IEEE Commun. Mag.*, vol. 45, pp. 116–122, Nov. 2007.

[14] K. Letaief and W. Zhang, "Cooperative communications for cognitive radio networks," *IEEE Commun. Mag.*, vol. 97, pp. 878–893, May 2009.

[15] J. N. Laneman, *Cooperative Diversity in Wireless Networks: Algorithms and Architectures.* Massachusetts Institute of Technology, Cambridge, MA, USA: PhD dissertation, Aug. 2002.

[16] M. Dohler and Y. Li, *Cooperative Communications.* Chichester, United Kingdom: John Wiley and Sons Ltd, 2010.

[17] B. Sklar, "Rayleigh fading channels in mobile digital communication sys-

tems. I. Characterization," *IEEE Commun. Mag.*, vol. 35, pp. 90–100, Jul. 1997.

[18] N. A. Surobhi, *Outage Performance of Cooperative Cognitive Relay Networks*. Victoria University, Melbourne, Australia: M. Eng. thesis, Sep. 2009.

[19] K. J. Liu, A. K. Sadek, W. Su, and A. Kwasinski, *Cooperative Communications and Networking*. Leiden: Cambridge University Press, 2008.

[20] M. O. Hasna and M. S. Alouini, "A performance study of dual-hop transmissions with fixed gain relays," *IEEE Trans. Wireless Commun.*, vol. 3, pp. 1963–1968, Nov. 2004.

[21] K. Yan, S. Ding, Y. Qiu, Y. Wang, and H. Liu, "A simple Alamouti space-time transmission scheme for asynchronous cooperative communications over frequency-selective channels," *in Proc. 10th ICACT 2008*, vol. 4, pp. 1569–1572, Feb. 2008.

[22] V. Tarokh, N. Seshadri, and A. R. Calderbank, "Space-time codes for high data rate wireless communication: performance analysis and code construction," *IEEE Trans. Inf. Theory*, vol. 44, pp. 744–765, Mar. 1998.

[23] S. M. Alamouti, "A simple transmit diversity technique for wireless communications," *IEEE J. Select. Areas Commun.*, vol. 16, pp. 1451–1458, Oct. 1998.

[24] V. Tarokh, A. Naguib, N. Seshadri, and A. R. Calderbank, "Combined array processing and space time coding," *IEEE Trans. Inf. Theory*, vol. 45, pp. 1121–1128, May 1999.

[25] P. W. Wolniansky, G. J. Foschini, G. D. Golden, and R. A. Valenzuela, "V-BLAST: an architecture for realizing very high data rates over the rich-scattering wireless channel," *Bell Laboratories, Lucent Technologies, Crawford Hill Laboratory 791 Holmdel-Keyport RD., Holmdel, NJ07733.*

[26] V. Tarokh, H. Jafarkhani, and A. R. Calderbank, "Space-time block codes from orthogonal designs," *IEEE Trans. Inf. Theory*, vol. 45, pp. 1456–1467, Jul. 1999.

[27] H. Jafarkhani, "A quasi-orthogonal space-time block code," *IEEE Trans. Commun.*, vol. 49, pp. 1–4, Jan 2001.

[28] I.-M. Kim and V. Tarokh, "Variable rate spacetime block codes in m-ary psk systems," *IEEE J. Select. Areas Commun.*, vol. 45, pp. 362–373, Apr. 2003.

[29] Y. Yu, S. Keroueden, and J. Yuan, "Closed-loop extended orthogonal space-time block codes for three and four transmit antennas," *IEEE Sig. Process. lett.*, vol. 13, pp. 273–276, May 2006.

[30] N. M. Eltayeb, S. Lambotharan, and J. A. Chambers, "A phase feedback based extended space-time block code for enhancement of diversity," *in Proc. IEEE VTC 2007-Spring*, pp. 2296–2299, April 2007.

[31] J. Akhtar and D. Gesbert, "Extended orthogonal block codes with partial feedback," *IEEE Trans. Wireless Commun.*, vol. 3, pp. 1959–1962, Nov 2004.

[32] C. Toker, S. Lambotharan, and J. A. Chambers, "Closed-loop quasi-orthogonal STBCs and their performance in multipath fading environments and when combined with turbo codes," *IEEE Trans. Wireless Commun.*, vol. 3, pp. 1890–1896, Nov. 2004.

[33] C. Toker, S. Lambotharan, and J. A. Chambers, "Space-time block coding for four transmit antennas with closed loop feedback over frequency selective fading channel," *IEEE Inf. Theory Workshop*, Paris, France, Mar./Apr. 2003.

[34] G. Abreu, "GABBA codes: Generalized full-rate orthogonally decod-

able space-time block codes," *in Proc. IEEE 39th Asilomar*, pp. 1284–1286, Monterey, CA, Nov. 2005.

[35] W. Su and X. G. Xia, "Signal constellations for quasi-orthogonal space-time block codes with full diversity," *IEEE Trans. Inf. Theory*, vol. 50, pp. 2331–2347, Oct 2004.

[36] J. K. Milleth, K. Giridhar, and D. Jalihal, "Closed-loop transmit diversity schemes for five and six transmit antennas," *IEEE Signal Process. Lett.*, vol. 12, pp. 130–133, Feb. 2005.

[37] Z. Li and X. G. Xia, "An Alamouti coded OFDM transmission for cooperative systems robust to both timing errors and frequency offsets," *IEEE Trans. Wireless Commun.*, vol. 7, pp. 1839–1844, May 2008.

[38] F. C. Commission, "Facilitating opportunities for flexible, efficient, and reliable spectrum use employing cognitive radio technologies," ET Docket No., 03-108, Mar. 2005.

[39] Cognitive Radio Technology, [Online] Available: http://www.ofcom.org.uk/research/technology/overview/emertech/cograd/cogradmain.pdf.

[40] J. Mitola and G. Q. Maguire, "Cognitive radio: Making software radios more personal," *IEEE Pers. Commun.*, vol. 6, pp. 13–18, Aug. 1999.

[41] S. Haykin, "Cognitive radio: Brain-empowered wireless communications," *IEEE J. Sel. Areas Commun.*, vol. 23, pp. 201–220, Feb. 2005.

[42] C. Cordeiro, K. Challapali, and D. Birru, "IEEE 802.22: An introduction to the first wireless standard based on cognitive radios," *J. Commun.*, vol. 1, pp. 38–47, Apr. 2006.

[43] C. R. Sevension, *In Reply to Comments of IEEE 802.18.* 2004, [Online] Available: http://ieee802.org/18.

[44] A. Ghasemi and E. S. Sousa, "Collaborative spectrum sensing for opportunistic access in fading environments," *in Proc. IEEE DySPAN 2005*, pp. 131–136, Baltimore, USA, Nov. 2005.

[45] J. Lundn, V. Koivunen, A. Huttunen, and H. V. Poor, "Collaborative cyclostationary spectrum sensing for cognitive radio systems," *IEEE Trans. Signal Process.*, vol. 57, pp. 4182–4195, Nov. 2009.

[46] A. Goldsmith, S. A. Jafar, I. Maric, and S. Srinivasa, "Breaking spectrum gridlock with cognitive radios: an information theoretic perspective," *in Proc. of the IEEE*, vol. 97, pp. 894–914, May 2009.

[47] D. Chen and J. N. Laneman, "Modulation and demodulation for cooperative diversity in wireless systems," *IEEE Trans. Wireless Commun.*, vol. 5, pp. 1785–1794, Jul. 2006.

[48] I. Krikidis, Z. Sun, J. N. Laneman, and J. Thompson, "Cognitive legacy networks via cooperative diversity," *IEEE Commun. Lett.*, vol. 13, pp. 106–109, Feb. 2009.

[49] Y. Jing and H. Jafarkhani, "Using orthogonal and quasi-orthogonal designs in wireless relay networks," *IEEE Trans. Inf. Theory*, vol. 53, pp. 4106–4118, Nov. 2007.

[50] S. Ganesan, W. Liu, and M. Sellathurai, "Limited feedback precoding for distributed space-time coding in wireless relay networks," *in Proc.IEEE WCSP 2009*, pp. 1–5, Nanjing, Nov. 2009.

[51] G. S. Rajan and B. S. Rajan, "Distributed space-time codes for cooperative networks with partial CSI," *in Proc. IEEE WCNC*, pp. 902–906, Hong Kong, Mar. 2007.

[52] Y. Hua, Y. Mei, and Y. Chang, "Wireless antennasmaking wireless com-

munications perform like wireline communications," *in Proc. IEEE Topical Conf. Wireless Commun. Tech.*, pp. 47–73, Honolulu, USA, Oct. 2003.

[53] J. N. Laneman, D. N. Tse, and G. W. Wornell, "Cooperative diversity in wireless networks: efficient protocols and outage behavior," *IEEE Trans. Inf. Theory*, vol. 49, pp. 3062–3080, Dec. 2004.

[54] A. Sendonaris, E. Erkip, and B. Aazhang, "User cooperation diversity-part II: Implementation aspects and performance analysis," *IEEE Trans. on Commu.*, vol. 51, pp. 1939–1948, Nov. 2003.

[55] E. C. Van der Meulen, "Three-terminal communication channels," *Adv. Appl. Probab.*, vol. 3, pp. 120–154, 1971.

[56] T. M. Cover and A. A. E. Gamal, "Three-terminal communication channels," *IEEE Trans. Inf. Theory*, vol. IT-25, pp. 572–584, Sep. 1979.

[57] B. Schein and R. G. Gallager, "The Gaussian parallel relay network," *in Proc. IEEE ISIT 2000*, p. 22, Sorrento, Italy, Jun. 2000.

[58] M. Gastpar and M. Vetterli, "On the capacity of wireless networks: the relay case," *in Proc. IEEE INFOCOM 2002*, vol. 3, pp. 1577–1586, New York, USA, Jun. 2002.

[59] M. Gastpar and M. Vetterli, "On the capacity of large gaussian relay networks," *IEEE Trans. Inf. Theory*, vol. 51, pp. 765–779, Mar. 2005.

[60] H. Wang and X. G. Xia, "Upper bounds of rates of space-time block codes from complex orthogonal designs," *IEEE Trans. Inf. Theory*, vol. 49, pp. 2788–2796, Oct. 2003.

[61] G. Kramer, M. Gastpar, and P. Gupta, "Cooperative strategies and capacity theorems for relay networks," *IEEE Trans. Inf. Theory*, vol. 51, pp. 3037–3063, Sep. 2005.

[62] Y. Fan, J. S. Thompson, A. B. Adinoyi, and H. Yanikomeroglu, "Space diversity for multi-antenna multi-relay channels," *in Proc. Euro. Wireless Conf.*, pp. 1–5, Athens, Greece, Apr. 2006.

[63] K. Azarian, H. E. Gamal, and P. Schniter, "On the achievable diversity-multiplexing tradeoff in half-duplex cooperative channels," *IEEE Trans. Inf. Theory*, vol. 51, pp. 4152–4172, Dec. 2005.

[64] S. Yang and J.-C. Belfiore, "Towards the optimal amplify-and-forward cooperative diversity scheme," *IEEE Trans. Inf. Theory*, vol. 53, pp. 3114–3126, Sep. 2007.

[65] H. Kim, N. Kim, J. Kim, and H. Park, "Cooperative diversity system achieving full-rate and full-diversity by constellation rotation," *in Proc. IEEE VTC-2007 Fall.*, pp. 1177–1181, Baltimore, USA, Sep./Oct. 2007.

[66] R. U. Nabar, H. Bolcskei, and F. W. Kneubuhler, "Fading relay channels: Performance limits and space-time signal design," *IEEE J. Sel. Areas Commun.*, vol. 22, pp. 1099–1109, Aug. 2004.

[67] Y. Jing and B. Hassibi, "Distributed space-time coding in wireless relay networks," *IEEE Trans. Wireless Commun.*, vol. 5, pp. 3524–3536, Dec. 2006.

[68] Kiran T. and B. S. Rajan, "Distributed space-time codes with reduced decoding complexity," *in Proc. IEEE ISIT 2006*, pp. 542–546, Seattle, USA, Jul. 2006.

[69] B. Maham, A. Hjrungnes, and G. Abreu, "Distributed GABBA space-time codes in amplify-and-forward relay networks," *IEEE Trans. Wireless Commun.*, vol. 8, pp. 2036–2045, Apr. 2009.

[70] Kiran T. and B. S. Rajan, "Partially-coherent distributed space-time

codes with differential encoder and decoder," *IEEE J. Sel. Areas Commun.*, vol. 25, pp. 426–433, Feb. 2007.

[71] Y. Jing and H. Jafarkhani, "Distributed differential space-time coding for wireless relay networks," *IEEE Trans. Commun.*, vol. 56, pp. 1092–1100, Jul. 2008.

[72] G. S. Rajan and B. S. Rajan, "Multi-group ML decodable collocated and distributed space-time block codes," *IEEE Trans. Inf. Theory*, vol. 56, pp. 3221–3247, Jul. 2010.

[73] Y. Shang and X. G. Xia, "Shift-full-rank matrices and applications in space-time trellis codes for relay networks with asynchronous cooperative diversity," *IEEE Trans. Inf. Theory*, vol. 52, pp. 3153–3167, July 2006.

[74] Y. Li, W. Zhang, and X. G. Xia, "Distributive high-rate full-diversity space-frequency codes for asynchronous cooperative communications," *in Proc. IEEE ISIT 2006*, Seattle, USA, Jul. 2006.

[75] Y. Mei, Y. Hua, A. Swami, and B. Daneshrad, "Combating synchronization errors in cooperative relays," *in Proc. IEEE ICASSP 2005*, vol. 3, pp. 369–372, Mar. 2005.

[76] Y. Li and X. G. Xia, "A family of distributed space-time trellis codes with asynchronous cooperative diversity," *IEEE Trans. Commun.*, vol. 55, pp. 790–800, April 2007.

[77] S. Wei, D. L. Goeckel, and M. C. Valenti, "Asynchronous cooperative diversity," *IEEE Trans. Wireless Commun.*, vol. 5, pp. 1547–1557, Jun. 2006.

[78] X. Li, "Space-time coded multi-transmission among distributed transmitters without perfect synchronization," *IEEE Sig. Process. Lett.*, vol. 11, pp. 948–951, Dec. 2004.

[79] Z. Zhong, S. Zhu, and A. Nallanathan, "Distributed space-time trellis code for asynchronous cooperative communications under frequency-selective channels," *IEEE Trans. on Wireless Commun.*, vol. 8, pp. 796–805, Feb. 2009.

[80] X. Guo and X. G. Xia, "A distributed space-time coding in asynchronous wireless relay networks," *IEEE Trans. Wireless Commun.*, vol. 7, pp. 1812–1816, May 2008.

[81] Z. Li and X. G. Xia, "A simple Alamouti space-time transmission scheme for asynchronous cooperative systems," *IEEE Sig. Process. lett.*, vol. 14, pp. 804–807, Nov. 2007.

[82] M. Hayes, J. A. Chambers, and M. D. Macleod, "A simple quasi-orthogonal space-time scheme for use in asynchronous virtual antenna array enabled cooperative networks," *in Proc. EPSRC 2008*, Lausanne, Swizerland, Aug. 2008.

[83] O.-S. Shin, A. M. Chan, H. T. Kung, and V. Tarokh, "Design of an OFDM cooperative space-time diversity system," *IEEE Trans. Veh. Tec.*, vol. 56, pp. 2203–2216, Jul. 2007.

[84] R. T. Derryberry, S. D. Gray, D. M. Ionescu, G. Mandyam, and B. Raghothaman, "Transmit diversity in 3G CDMA systems," *IEEE Commun. Mag.*, vol. 40, pp. 68–75, Apr. 2002.

[85] V. Havary-Nassab, S. Shahbazpanahi, A. Grami, and Z. Q. Luo, "Network beamforming based on second-order statistics of the channel state information," *in Proc. IEEE ICASSP 2008*, pp. 2605–2608, Las Vegas, USA, Apr. 2008.

[86] T. Cui, F. Gao, T. Ho, and A. Nallanathan, "Distributed space-time coding for two-way wireless relay networks," *IEEE Trans. Signal process.*, vol. 57, pp. 658–671, Feb. 2009.

[87] Z. Zhong, S. Zhu, and G. Lv, "Distributed space-time code for asynchronous two-way wireless relay networks under frequency-selective channels," *in Proc. IEEE ICC 2009*, pp. 1–5, Dresden, Germany, Jun. 2009.

[88] B. Rankov and A. Wittneben, "Achievable rate regions for the two-way relay channel," *in Proc. IEEE ISIT 2006*, pp. 1668–1672, Seattle, USA, Jul. 2006.

[89] B. Rankov and A. Wittneben, "Spectral efficient protocols for half-duplex fading relay channels," *IEEE J. Sel. Areas Commun.*, vol. 25, pp. 379–389, Feb. 2007.

[90] Z. Li, X.-G. Xia, and B. Li, "Achieving full diversity and fast ML decoding via simple analog network coding for asynchronous two-way relay networks," *IEEE Trans. on Commun.*, vol. 57, pp. 3672–3681, Dec. 2009.

[91] S. Ganesan and M. Sellathurai, "Distributed STBC with relay subset selection for single carrier relay assisted transmissions," *in Proc. BROADNETS 2008*, pp. 8–15, London, UK, Sep. 2008.

[92] Y. Zhao, R. Adve, and T. J. Lim, "Improving amplify-and-forward relay networks: optimal power allocation versus selection," *IEEE Trans. Wireless Comm.*, vol. 6, pp. 3114–3122, Aug. 2007.

[93] Z. Lin, E. Erkip, and A. Stefanov, "Cooperative regions and partner choice in coded cooperative systems," *IEEE Trans. on Comm.*, vol. 54, pp. 1323–1334, Jul. 2006.

[94] A. Bletsas, D. P. Reed, and A. Lippman, "A simple cooperative diversity method based on network path selection," *IEEE Trans. on Sel. Areas in Comm.*, vol. 24, pp. 659–672, Mar. 2006.

[95] A. S. Ibrahim, A. Sadek, W. Su, and K. J. R. Liu, "Relay selection in multi-node cooperative communications: when to cooperate and whom to

cooperate with?," *in Proc. IEEE Globecom 2006*, San Francisco, USA, 27 Nov./Dec. 2006.

[96] Y. Ding and M. Uysal, "Amplify-and-forward cooperative OFDM with multiple-relays: performance analysis and relay selection methods," *IEEE Trans. on Wireless Comm.*, vol. 8, pp. 4963–4968, Oct. 2009.

[97] Y. Jing and H. Jafarkhani, "Single and multiple relay selection schemes and their diversity orders," *in Proc. IEEE ICC 2008*, pp. 349–353, Beijing, China, May 2008.

[98] J. Mitola III and G. Q. Maguire, "Cognitive radio: making software radios more personal," *IEEE Pers. Commun.*, pp. 13–18, Aug. 1999.

[99] O. Simeone, J. Gambini, U. Spagnolini, and Y. Bar-Ness, "Cooperation and cognitive radio," *in Proc. ICC 2007*, pp. 6511–6515, Glasgow, Aug. 2007.

[100] Z. Qian, J. Juncheng, and Z. Jin, "Cooperative relay to improve diversity in cognitive radio networks," *IEEE Commun. Mag.*, vol. 47, pp. 111–117, Feb. 2009.

[101] L. Yu, W. Hu, C. Liu, and H. Chen, "Cognitive partners in wireless networks," *2nd ICSPS 2010*, vol. 2, pp. 367–371, Dalian, China, 5-7 Jul. 2010.

[102] V. A. Bohara, S. H. Ting, Y. Han, and A. Pandharipande, "Interference-free overlay cognitive radio network based on cooperative space time coding," *in Proc. CrownCom 2010*, pp. 1–5, Cannes, France, Jun. 2010.

[103] L. Jun, H. Bo, W. Xiaofang, L. Fei, and L. Qinghua, "Performance evaluation for cognitive radio networks with cooperative diversity," *in Proc. WiCOM 2010*, pp. 1–4, Chengdu, China, Sep. 2010.

[104] K. Lee and A. Yener, "Outage performance of cognitive wireless relay

networks," *in Proc. IEEE Globecom 2006*, pp. 1–5, San Francisco, CA, Nov. 2006.

[105] H. A. Suraweera, P. J. Smith, and N. A. Surobhi, "Exact outage probability of cooperative diversity with opportunistic spectrum access," *in Proc. IEEE ICC 2008*, pp. 79–84, Beijing, China, May 2008.

[106] N. A. Surobhi and M. Faulkner, "Exact outage probability analysis of a diamond relay network with opportunistic spectrum access," *in Proc. ACoRN workshop on cooperative commun.*, pp. 79–84, Sydney, Australia, Jul. 2009.

[107] M. Engels, *Wireless OFDM System: How to make them.* USA: Springer Science, 2002.

[108] G. Stuber, J. Barry, S. Mclaughin, M. Ingram, Y. Le, and T. Pratt, "Broadband MIMO-OFDM wireless communication," *Proc. of the IEEE*, vol. 92, pp. 271–294, Feb. 2004.

[109] L. Li and G. Stuber, *Orthogonal Frequency Division Multiplexing for Wireless Communication.* USA: Springer Science, 2006.

[110] S. Yiu, R. Schober, and L. Lampe, "Distributed space-time block coding," *IEEE Trans. Commun.*, vol. 54, pp. 1195–1206, Jul. 2006.

[111] Y. Hua, Y. Mei, and Y. Chang, "Parallel wireless mobile relays with space time modulations," *IEEE SSP 2003*, pp. 375–378, St. Louis, USA, Oct. 2003.

[112] Y. Chang and Y. Hua, "Diversity analysis of orthogonal space-time modulation for distributed wireless relays," *IEEE ICASSP 2004*, pp. 561–564, Montreal, Canada, May 2004.

[113] T. Liew and L. Hanzo, "Space-time codes and concatenated channel

codes for wireless communications," *Proc. of the IEEE*, vol. 90, pp. 187–219, Feb. 2002.

[114] J. G. Proakis, *Digital Communications*. McGraw-Hill, 4th ed., 2001.

[115] A. Viterbi, "Error bounds for convolutional codes and an asymptotically optimum decoding algorithm," *IEEE Trans. Inf. Theory*, vol. IT-13, pp. 260–269, Apr. 1967.

[116] L. Hanzo, O. R. Alamri, M. El-Hajjar, and N. Wu, *Near-Capacity Multi-Functional MIMO Systems: Sphere-Packing, Iterative Detection and Cooperation*. UK: John Wiley and IEEE Press, 2009.

[117] W. Zhang, X.-G. Xia, and P. C. Ching, "Full-diversity and fast ML decoding properties of general orthogonal space-time block codes for MIMO-OFDM," *IEEE Trans. Wireless Commun.*, vol. 6, pp. 1647–1653, May 2007.

[118] F. T. Alotaibi and J. A. Chambers, "Extended orthogonal space time block codes in wireless relay networks," *in Proc. IEEE Workshop SSP*, pp. 745–748, Cardiff, UK, Aug. 2009.

[119] S. Lambotharan and C. Toker, "Closed-loop space time block coding techniques for OFDM based broadband wireless access systems," *IEEE Trans. Consumer Elect.*, vol. 51, pp. 765–769, Aug. 2005.

[120] D. Gore and A. Paulraj, "MIMO antenna subset selection with space-time coding," *IEEE Trans. on Sig. Process.*, vol. 50, pp. 2580–2588, Oct. 2002.

[121] M. Tao, Q. Li, and H. K. Garg, "Extended space-time block coding with transmit antenna selection over correlated fading channels," *IEEE Trans. on Wireless Commun.*, vol. 6, pp. 3137–3141, Oct. 2007.

[122] A. Eksim, "Extended balanced space-time block coding with transmit antenna selection," *European Trans. on Telecommun., Tech. Review*, 2010.

[123] D. Gore and A. Paulraj, "Space-time block coding with optimal antenna selection," *IEEE ICASSP 2001*, vol. 4, pp. 2441–2444, May 2001.

[124] F. T. Alotaibi and J. A. Chambers, "Full-rate and full-diversity extended orthogonal space-time block coding in cooperative relay networks with imperfect asynchronization," *in Proc. IEEE ICASSP*, pp. 2882–2885, Dallas, USA, Mar. 2010.

[125] F. T. Alotaibi and J. A. Chambers, "Extended orthogonal space-time block coding scheme for asynchronous cooperative relay networks over frequency-selective channels," *in Proc. IEEE SPAWC*, pp. 1–5, Marrakech, Morocco, Jun. 2010.

[126] F. T. Alotaibi and J. A. Chambers, "Relay selection scheme for cooperative relay networks with distributed orthogonal space-time block coding," *in Proc. IEEE UKIWCWS*, pp. 1–5, Delhi, India, Des. 2010.

[127] V. Genc, S. Murphy, Y. Yang, and J. Murphy, "IEEE 802.16J relay-based wireless access networks: An overview," *IEEE Commun. Mag.*, vol. 15, pp. 56–63, Oct. 2008.

[128] Q. Zhao and B. M. Sadler, "A survey of dynamic spectrum access," *IEEE Sig. Proc. Mag.*, vol. 24, pp. 79–89, May 2007.

[129] J. Mietzner, L. Lampe, and R. Schober, "Distributed transmit power allocation for relay-assisted cognitive-radio systems," *in Proc. Asilomar Conf. on Sig., Syst., and Comput.*, pp. 792–796, Pacific Grove, USA, Nov. 2007.

[130] Y. Zhao, R. S. Adve, and T. J. Lim, "Outage probability at arbitrary SNR in cooperative diversity networks," *IEEE Commun. Lett.*, vol. 9, pp. 700–702, Aug. 2005.

[131] H. A. Suraweera, P. J. Smith, and J. Armstrong, "Outage probabil-

ity of cooperative relay networks in Nakagami-m fading channels," *IEEE Commun. Lett.*, vol. 10, pp. 834–836, Dec. 2006.

[132] Y. Zhao, R. S. Adve, and T. J. Lim, "Improving amplify-and-forward relay networks: optimal power allocation versus selection," *IEEE Trans. Wireless Commun.*, vol. 6, pp. 3114–3123, Aug. 2007.

[133] Q. Chen, F. Gao, A. Nallanathan, and Y. Xin, "Improved cooperative spectrum sensing in cognitive radio," *in Proc. IEEE VTC 2008*, pp. 1418–1422, Marina Bay, Singapore, May 2008.

[134] J. Salo, H. M. El-Sallabi, and P. Vainikainen, "The distribution of the product of Rayleigh distributed random variables," *IEEE Trans. on Anten. and Prop.*, vol. 54, pp. 639–643, Feb. 2006.

[135] S. Ikki and M. H. Ahmed, "Performance analysis of dual-hop relaying communications over generalized Gamma fading channels," *in Proc. IEEE Globecom 2007*, pp. 3888–3893, Washington, DC, USA, Nov. 2007.

[136] A. Bletsas, A. Khisti, D. Reed, and A. Lippman, "A simple cooperative diversity method based on network path selection," *IEEE J. Sel. Areas Commun.*, vol. 24, pp. 659–672, Mar. 2006.

[137] E. Beres and R. S. Adve, "Outage probability of selection cooperation in the low to medium SNR regime," *IEEE Commun. Lett.*, vol. 11, pp. 589–597, Jul. 2007.

[138] A. Papoulis and S. U. Pillai, *Probability, Random Variables and Stochastic Processes.* Fourth Edition, New York: McGraw-Hill Companies, 2002.

[139] F. Oggier, G. Rekaya, J.-C. Belfiore, and E. Viterbo, "Perfect space-time block codes," *IEEE Trans. Inf. Theory*, vol. 52, pp. 3885–3902, Sep. 2006.

[140] P. Elia, B. A. Sethuraman, and P. V. Kumar, "Perfect space-time codes with minimum and non-minimum delay for any number of antennas," Dec. 2005. [Online]. Available: http://arxiv.org/pdf/cs/0512023v1.pdf.

[141] J.-C. Belfiore, G. Rekaya, and E. Viterbo, "The Golden code: a 2x2 full rate space-time code with non-vanishing determinants," *IEEE Trans. Inf. Theory,*, vol. 51, pp. 1596–1600, Nov. 2004.

[142] C. Hollanti, K. R. J. Lahtonen, R. Vehkalahti, and E. Viterbo, "On the algebraic structure of the Silver code," *IEEE Inf. Theory Workshop*, pp. 91–94, Porto, Portugal, May 2008.

[143] S. Yang and J.-C. Belfiore, "Optimal space-time codes for the MIMO amplify-and-forward cooperative channel," *IEEE Trans. Inf. Theory*, vol. 53, pp. 647–663, Feb. 2007.

[144] M. Badr and J.-C. Belfiore, "Distributed space time codes for the amplify-and-forward multiple-access relay channel," *in Proc IEEE ISIT 2008*, pp. 2543–2547, Toronto, Canada, Jul. 2008.